ABSTRACT

Title of Dissertation: PHOTOLYTIC STUDIES OF ARYL AND HETEROARYL NITRENIUM IONS: LASER FLASH PHOTOLYSIS STUDIES

Selina Ivan Thomas, Doctor of Philosophy, 2006

Dissertation directed by: Professor Daniel E. Falvey
Department of Chemistry and Biochemistry

The objective of the thesis was to understand the chemical and kinetic behavior of arylnitrenium ions and a heteroaromatic nitrenium ion through photolytic studies. *N*-(4,4'-dichlorodiphenyl) nitrenium ion and *N*-(4,4'-dibromodiphenyl) nitrenium ion are the halogenated counterparts of diphenylnitrenium ions and are generated photochemically from their respective *N*-(4,4'-dihalogenated diphenylamino)-2,4,6-trimethylpyridinium tetrafluoroborate salts. The halogenated diarylnitrenium ions are ground state singlets that live for more than 100 μs in CH_3CN. In the absence of nucleophiles, these ions decay to form a dimerized hydrazine.

These ions react with nucleophiles such as H_2O and alcohol at a rate constant of 10^4-10^5 $M^{-1}s^{-1}$ and at diffusion limit with chlorides. With arenes, these ions react via electron transfer mechanism and nucleophilic addition process. The rate constants for the electron transfer mechanisms are between 10^5-10^9 $M^{-1}s^{-1}$ and depend on the E_{ox} of the arenes. Arenes with E_{ox} above 1.78 V showed no reactivity towards the ion.

Unlike other diarylnitrenium ions, the halogenated diarylnitrenium ions react with hydrogen atom donors via a hydrogen atom transfer mechanism. The triplet behavior of these ions is attributed to singlet-triplet intersystem crossing facilitated by the lower singlet-triplet energy gap. Therefore, it has been concluded that substituting halogens in diphenylnitrenium ion lowers the singlet-triplet energy gap and increases the lifetime of these ions.

(*N*-Methyl-*N*-4-biphenylyl) nitrenium ion generated by photolysis was reacted with amino acids and proteins to determine their reactivity with these ions. Of the twenty amino acids studied, eight of them were observed to react with the ion at a rate constant of 10^7-10^9 $M^{-1}s^{-1}$. The rate constants depend on the nucleophilicity of the side chains of the amino acids. In addition, this ion also reacts rapidly with proteins with a rate constant of 10^8 $M^{-1}s^{-1}$, comparable to their reactions with ss-DNA.

Investigations on generating the quinoline *N*-oxide nitrenium ions showed that the transient species from the photolysis of 4-azidoquinoline *N*-oxide (4-AzQO) shows more characteristics of a nitrenium ion. The formation of 4-aminoquinoline *N*-oxide upon photolysis of 4-AzQO in CH_3CN with 10% H_2SO_4 and the electron transfer reactions observed with arenes, indicate that the transient species generated

could be a heteroaromatic nitrenium ion. However, more experiments are needed to confirm the assignment.

PHOTOLYTIC STUDIES OF ARYL AND HETEROAROMATIC NITRENIUM IONS: LASER FLASH PHOTOLYSIS STUDIES

by

Selina Ivan Thomas

Dissertation submitted to the Faculty of the Graduate School of the
University of Maryland, College Park, in partial fulfillment
of the requirements for the degree of
Doctor of Philosophy
2006

Advisory Committee:

Professor Daniel E. Falvey, Chair
Professor Jeffery Davis
Professor Lyle Isaacs
Professor Neil Blough
Professor David C. Straney

DEDICATION

I dedicate this work to my parents, David Thomas and Nirmala Thomas, and my brother, Samson Thomas, for their unconditional love and support.

ACKNOWLEDGMENTS

During the course of my years as a graduate student, I came across a lot of people who assisted me in various aspects. I would like to take a moment and thank them all for their assistance, guidance and friendship. First and foremost, I would like to render my heartfelt gratitude to my advisor, Dr. Daniel E. Falvey, for his guidance and intellect in my course work as well as lab work. Being his student, I gained an enormous amount of knowledge in chemistry and learned to apply that knowledge to solving scientific problems. Therefore, I am grateful to Dr. Falvey for giving me the opportunity to finish my higher studies and hope that many students in future would be able to have the same rewarding experience as I did. Next, I would like to thank the professors in my committee, Dr. Jeffery Davis, Dr. Lyle Isaac, Dr. Neil Blough and Dr. David Straney, for accepting my request and being in my dissertation committee.

Graduate school would not have been rewarding, if not for the friendship and help from fellow colleagues. I have made a lot of friends during my years at the department and I would like to acknowledge all of them, Mr. Arthur Winter, Dr.Andy Kung, Ms. Becky Vieira, Mr. Brian Borak, Dr. Serpil Gonen, Dr. Zhiyun Chen, Dr.Yu Tang, Ms. Rebecca Pease, Dr. Sean McIlroy, Dr.Peter Vath and Dr. Chitra Sundararajan. One way or another, I have required your assistance and you have all been willing to go up and beyond than that is required to help me. Especially, I would like to extend my sincere thanks to Arthur and Serpil. Art, you have been a tremendous help to me and a wonderful friend. Thank you for doing the calculations required for my research again and again, for editing parts of my thesis, listening to

my complaints and teaching me about different things (such as golf, birds, football etc - which I don't remember). Serpil, thank you for being my friend and for all your help. Thank you for editing my thesis and most of all, for the words of encouragement you gave me whenever I needed them.

Next, I would like to extend my appreciation to all the faculty and staff of the chemistry department. The department has a wonderful team of staff who renders excellent service to everyone. I especially like to thank Dr. Yui-Fai Lam, Dr. Yinde Wang and Mr. Noel Whittaker for their services and guidances in deciphering the chemical structures of the compounds generated in my research by NMR and mass spectroscopy, Dr. Hermon Ammon, for the diversed TA assignments, which gave me experience in teaching undergraduate courses both lab and discussions in general and organic chemistry, Dr. Daniel Steffeck, for being lenient about my TA duties while I was preparing for my dissertation and Mr. Bob Harper, for all the assistance with the computer and audio/visual services.

Finally, I thank my family – my dad, mom and brother – for their unconditional support in all the decisions I have made in my life. They have always stood by me and supported and encouraged me all the way to where I am today. I could not have accomplished anything without their help and guidance. Thank you so much, everyone. Graduate school is tough but having family and friends like you all made it more pleasant and a worthwhile experience.

TABLE OF CONTENTS

LIST OF TABLES

LIST OF FIGURES

SCHEMES

Chapter 1. Introduction

Nitrenium ions have been known since the late 1800's, but are extensively studied only in the recent decades. These ions are involved in the synthesis of complex molecules and are also looked upon as potential intermediates in the formation of electrically conducting polyaniline polymers. However, these ions first gained attention for their role in the carcinogenicity of anilines.

Nitrenium ions are a divalent nitrogen species with a lone pair of electrons and a positive charge. These species are formed as transient intermediates and typically exist in solution from several nanoseconds to a few microseconds. These species are highly electrophilic and are isoelectronic to other common intermediates such as carbenes, nitrenes and carbenium ions. (Figure 1.1) Nitrenes and nitrenium ions are both similar in that they are nitrogen analogs with six valence electrons. However, unlike nitrenium ions, nitrenes are monovalent and neutral.

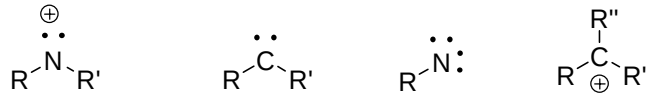

Figure 1.1 General structures of nitrenium ion, carbene, nitrene and carbenium ion

Carbenium ions and nitrenium ions differ in that carbenium ions are trivalent carbon-based compound while nitrenium ions are nitrogen-base and divalent; however, both species have six valence electrons and a positive charge.[1] As a result, nitrenium ions and carbenium ions have similar reactivities. Nitrenium ions also possess similar characteristics with carbenes. Both carbenes and nitrenium ions are divalent with six valence electrons. In addition, due to the differences in the electronic distribution of the lone pair electrons, both carbene and nitrenium ion have

two low energy electronic states: the singlet state and the triplet state which each have distinct chemical reactivities.

Nitrenium ions were first observed in the 1800's by Bamberger but it was Gassman that paved the way for today's research. Gassman conducted experiments to show that a positively charged nitrogen species could exist as a discrete intermediate in solution. Gassman's studies of nitrenium ions were followed by the work of several groups. However, due to the short lifetime of nitrenium ions, progress was slow. The development of laser flash photolysis (LFP) made it possible to detect these ions and learn more about their chemical and kinetic behaviors.

Nitrenium ions are mostly studied because of their ability to cause cancer. It was observed in the late 1800s that certain aromatic amines caused cancer such as bladder or colon cancers. Studies done in vivo and vitro showed that the aromatic amines are not carcinogenic themselves but are converted to carcinogenic arylnitrenium ions by enzymatic reactions. Even though nitrenium ions are known to react with proteins and nucleic acids, most research has focused on its DNA damaging reactions.

This thesis is comprised of three different projects based on the photolytical studies conducted on aryl and heteroaromatic nitrenium ions. The goal of the projects was to investigate the chemical and kinetic behavior of certain aromatic nitrenium ions such as dihalogenated diphenylnitrenium, biphenylylnitrenium and quinoline n-oxide nitrenium ion. Chapter 3 and 4 focuses on the chemical reactivity of the chemical and kinetic characterization of *N*-(4,4'-dichlorodiphenyl) and *N*-(4,4'-dibromodiphenyl) nitrenium ion. These ions are the halogenated counterparts of

diphenylnitrenium ion and are studied in order to understand the substituent effects of halogens on the ground state chemical reactivity of these ions. Diphenylnitrenium ions are ground state singlet due to the stabilization of the empty p orbital of the nitrogen by the π donation of the phenyl group. Since halogens are electron-withdrawing through sigma bonds and electron donors via π donation, the goal was to determine as to how this behavior of the halogens would alter the ground state reactivity of the diphenylnitrenium ions.

The work in chapter 5 is the continuation of an ongoing project in our lab on *N*-4-biphenylyl-*N*-methylnitrenium ion. This ion is a known carcinogen and many studies have been done on its effects on DNA. However, only few studies have been recorded on its reactivity with proteins. The goal of the study was to obtain kinetic evidence on the reaction of 4-biphenylylnitrenium with various amino acids and proteins, to test if their reactions with these biomolecules could also play a role in their carcinogenicity.

Chapter 6 discusses the preliminary LFP work done to generate quinoline *N*-oxide nitrenium ion photochemically. The long term goal of the project is to determine if quinoline *N*-oxide nitrenium ions are involved as intermediates in the carcinogenicity of 4-nitroquinoline *N*-oxide (4-NQO). From studies conducted in in vivo and in vitro, it was observed that 4-NQO covalently binds to the nucleophilic component of the DNA and protein that lead to the formation of tumors. However, the reaction mechanism by which the compound reacts with nucleophiles is not yet known. Based on the similaries between the carcinogenic behavior of 4-NQO and arylamines, the assumption is that 4-NQO reacts with the nucleophiles in the cell via

a nitrenium ion intermediate. The work described in the chapter serves as a foundation for future studies.

References

(1) McClelland, R. A. *Tetrahedron* **1996**, *52*, 6823 - 6858.

Chapter 2. Background Information on Nitrenium ions

2.1 Early Work

Nitrenium ions, referred to as imidonium ions in the earlier days, were first proposed as early as the 1800s by Bamberger as an intermediate which forms during the acid-catalyzed rearrangements of arylhydroxyamines. He observed that in aqueous sulfuric acid, *N*-hydroxyaniline (**1)** rearranges to yield 4-aminophenol (**3**).[1] (Scheme 2.1) Since the product was an isomer of **1**, he proposed that the reaction was a rearrangement process. As a result, he believed that the reaction occurred through an iminocyclohexadienyl cation (**2**) intermediate formed as a result of the protonation and elimination of the hydroxyl group. Even though the iminocyclohexadienyl cation is a resonance form of the arylnitrenium ion, Bamberger did not recognize that since divalent nitrogen species were not known at that time.

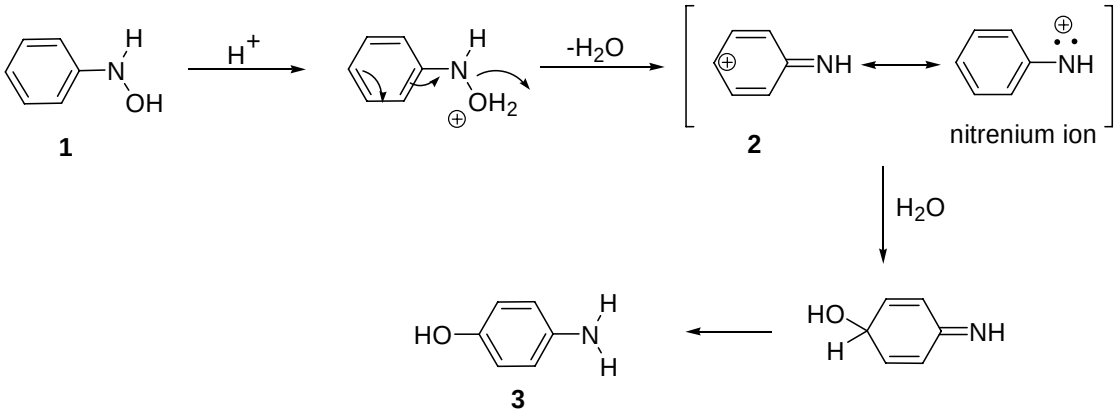

Scheme 2.1 Bamberger rearrangement of *N*-hydroxyamine

Bamberger studied several acid catalyzed reactions of *N*-arylhydroxylamine in the presence of various nucleophiles and observed that they all yielded nucleophilic addition products.[2] For example phenylhydroxylamines (**1**) in ethanol or methanol with aqueous sulphuric acid yields *ortho* and *para* phenetidines or anisidines

respectively. These products result from the addition of the alcohol to the phenyl ring. (Scheme 2.2) Also when **4** was refluxed in hydrochloric acid, *ortho* and *para*-chloroanilines were produced. From these nucleophilic addition products, Bamberger was convinced that during the reaction, the arylhydroxylamine was being converted to an electrophilic species such as **2** causing the nucleophiles to add to it. The hypothesis of an electrophilic intermediate was further confirmed by kinetic studies. Heller et. al. observed that the rearrangement depends on the formation of the cation and not on the concentration of the nucleophile.[2]

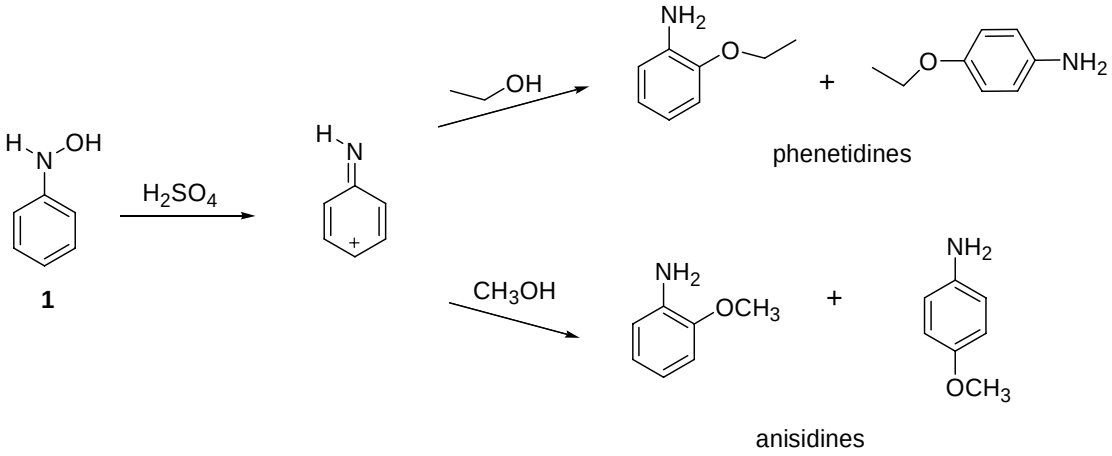

Scheme 2.2 Reaction of **1** with methanol and ethanol

Abramovitch, in his work with P-diphenyl-N-tosylphosphazine azide (**4**) reported evidence on the formation of a divalent nitrogen species as a possible intermediate.[3] He noticed that an unstable intermediate formed upon the loss of N_2 resonates between an univalent (nitrene) and a divalent nitrogen (nitrenium ion). (Scheme 2.3) He trapped this two intermediates by reacting with dicyclopentadiene to yield 1:1 adduct of **5** and **6** which appear to have originated from the two resonance forms of the intermediate. Compound **5** results from the addition of the diene to the nitrene and compound **6** results from the addition of the diene to the positively and

negative charged nitrogen centers. Since he succeeded in trapping the intermediate, he claimed the nitrogen atom could exist in its divalent form and that the intermediate Bamberger observed was indeed the nitrenium ion.

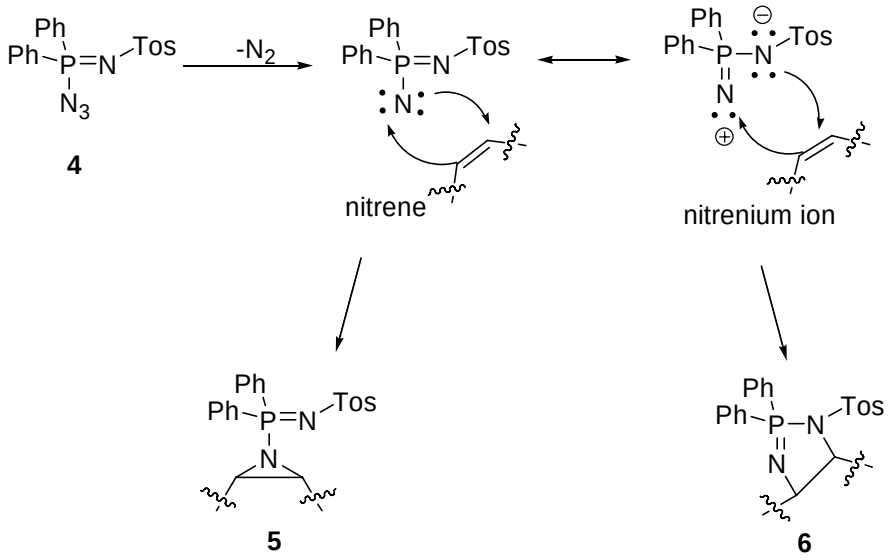

Scheme 2.3 Reaction of **4** with dienes

The concept of a divalent nitrogen species was investigated by several groups. Stieglitz et. al. studied the Bamberger rearrangement using tritylhydroxylamines.[4,5] They found that reacting triphenylmethyl hydroxylamine (**7**) with phosphorus pentachloride yields benzophenone (**8**) and aniline (**9**). (Scheme 2.4) Stieglitz proposed that the reaction proceeds via a univalent nitrogen species generated upon the concerted loss of H_2O. This was followed by the phenyl shift to the nitrogen and hydrolysis of the iminium ion (**10**) to yield the products. However, he observed that the reaction of *N*-methyl triphenyl methylhydroxyamine (**11**) with phosphorus pentachloride produced trace amounts of *N*-methyl aniline (**12**). (Scheme 2.5) In order to form **12**, compound **11** has to lose the hydroxyl group and undergo phenyl shift without the loss of the methyl group on the nitrogen. To him, this indicated that

a second pathway involving divalent nitrogen intermediate was possible. He argued that it was possible for the nitrogen to lose a pair of electrons and exist in a divalent form because similar process had been observed for oxygen. Wieland's rearrangement of triphenyl methylperoxide was explained to proceed via univalent oxygen intermediate species; hence he believed that nitrogen could also lose a pair of electron and exist as a discrete intermediate for a short period of time.

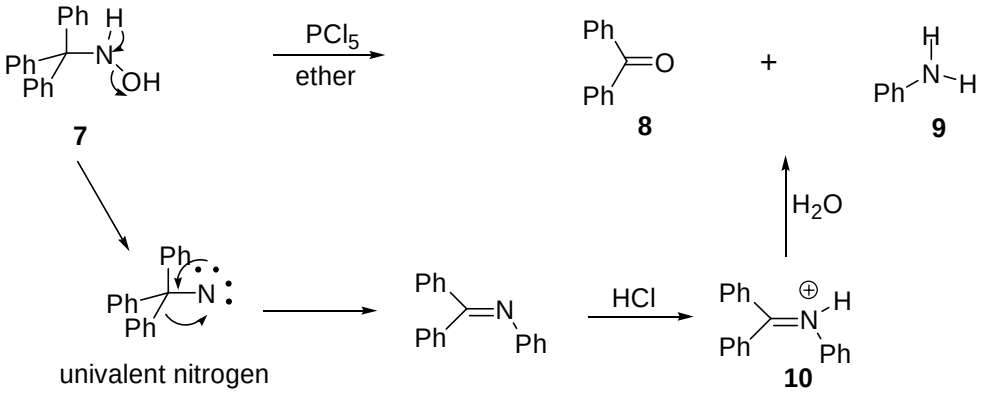

Scheme 2.4 Reaction of triphenylmethyl hydroxylamine with phosphorus pentachloride

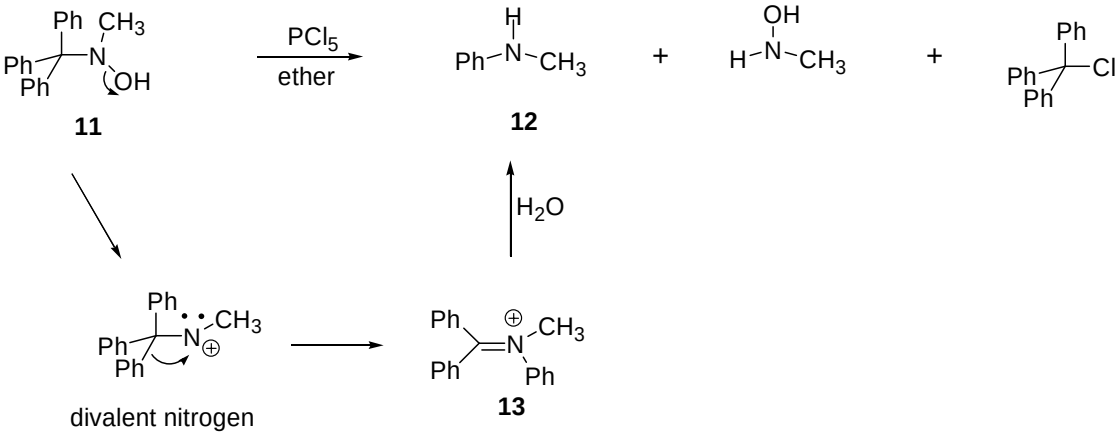

Scheme 2.5 Reaction of *N*-methyl triphenyl methylhydroxyamine with phosphorus pentachloride

Stieglitz's work was pursued by Gassman who set out to prove that nitrenium ions are formed as discrete intermediates during reactions similar to carbenium ions. Gassman argued that the rearrangement of tritylhydroxylamines observed by Stieglitz occurs through a divalent nitrogen species and the reason it was difficult to accurately predict the mechanism for **7** was because one of the substituents on the nitrogen was a hydrogen which could be deprotonated easily.[5] Hence in order to provide evidence that nitrenium ions do exist as discrete intermediates, he studied a series of bicyclic *N*-chloroamines by forcing the compounds to undergo alkyl migration to a nitrogen center.[5]

Even though Gassman's approach in proving the existence of nitrenium ions was flawed, he paved the way for today's work. He used alkyl migration as a method to prove the existence of nitrenium ion based on the argument that alkyl groups generally migrate only to a cationic center.[5] Therefore, his hypothesis was that if electron deficient nitrogen can be created adjacent to a tertiary carbon, then an alkyl group should migrate to that nitrogen. This would support the presence of a cationic intermediate. He tested this hypothesis by conducting solvolysis studies of *N*-halogenated isoquinuclidine compounds in methanol because these compounds generally rearranged via alkyl migration.

In order to test his hypothesis, he refluxed *N*-chloroisoquinuclidines (**14**) with silver nitrate in methanol. Silver nitrate was added to aid the removal of chloride by the cationic silver ion. As predicted refluxing *N*-chloroisoquinuclidines (**14**) with silver nitrate in methanol yields 2-methoxy-1-azabicyclo[3.2.1]-octane (**15**) in 65 %, a nucleophilic addition product.[5] (Scheme 2.6) From the product it was apparent that

the compound does undergo alkyl migration to nitrogen. However, it does not prove that the nitrenium ion exists as a discrete intermediate. This is because **15** could be obtained either by a S_N1 or S_N2 pathway as shown in scheme 2.6. In the S_N1 pathway, a positively charged divalent nitrogen intermediate is initially formed upon elimination of the chloride, which causes the alkyl group to migrate to the nitrogen generating a carbocation center. This carbocation is then subjected to nucleophilic attack by methanol. In the S_N2 pathway, a concerted elimination of chloride along with alkyl migration would lead directly to the carbocation. Addition of methanol to the ring confirms that a carbocation center was present during the reaction, further showing that the alkyl group migrates to the nitrogen with a pair of electrons. This implies that the nitrogen had to be electron deficient at some point of the reaction but it fails to show that the nitrenium ion exists as a distinct species.

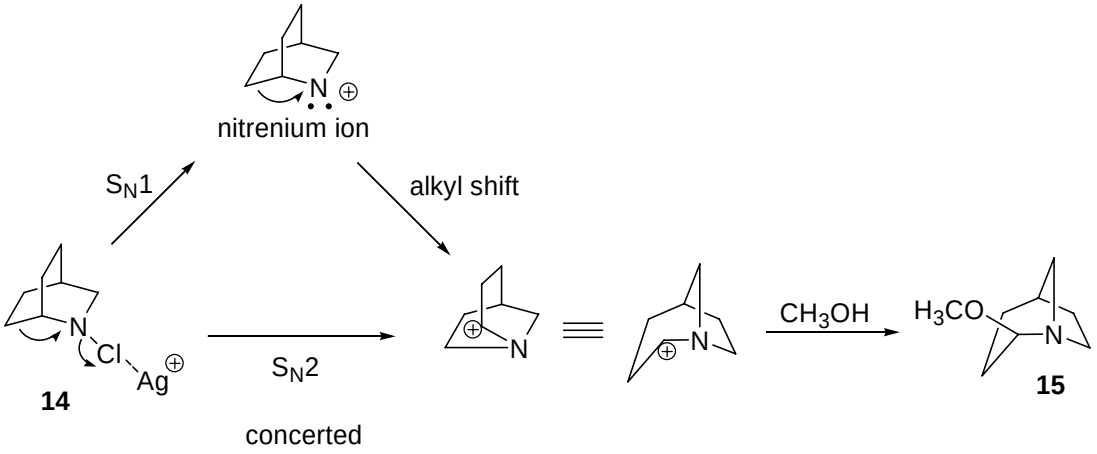

Scheme 2.6 Solvolysis of *N*-chloroisoquinuclidines with silver nitrate

Additional kinetic studies were preformed on series of *N*-chloroaziridines (**16**) and para substituted *N*-*tert*-butyl-*N*-chloroanilines (**18**) to show that nitrenium ion was an entirely distinct species.[5,6] Gassman measured the relative rate of ring

opening of a series of **16** and observed that the rates depended on the substitutents on carbon. *N*-chloroaziridines (**16**) with methyl groups on the carbons in the cis configuration yield an allylic cation (**17**) much faster than those derivatives with a methyl group or hydrogens on the carbon. (Scheme 2.7) It was claimed that the reaction was faster due to the relief of the methyl-methyl interactions with was aided by the heterolytical cleavage of the N-Cl bond to generate an electron deficient nitrogen center. Also by conducting experiments on series of *para* substituted *N-tert*-butyl-*N*-chloroanilines (**18**), it was shown that as the electron withdrawing properties of the *para* substitutent decreased, the rate of nucleophilic adduct formation on the phenyl ring increased.[6] (Scheme 2.8) A ρ value of -6.35 obtained from the Hammet plot upon fitting the log of rate of reaction of the various para substituted **18** as a function of the Brown σ^+ substitutent constant proved that there was considerable charge delocalization into the phenyl ring. Therefore, as the electron withdrawing characteristics of the substituents decrease, there is more charge delocalization of the positive charge on the nitrogen into the ring indicating the presence of a cationic species. This further supports the argument that the rearrangement occurs via electrophilic cation intermediate which in this case was a nitrenium ion.

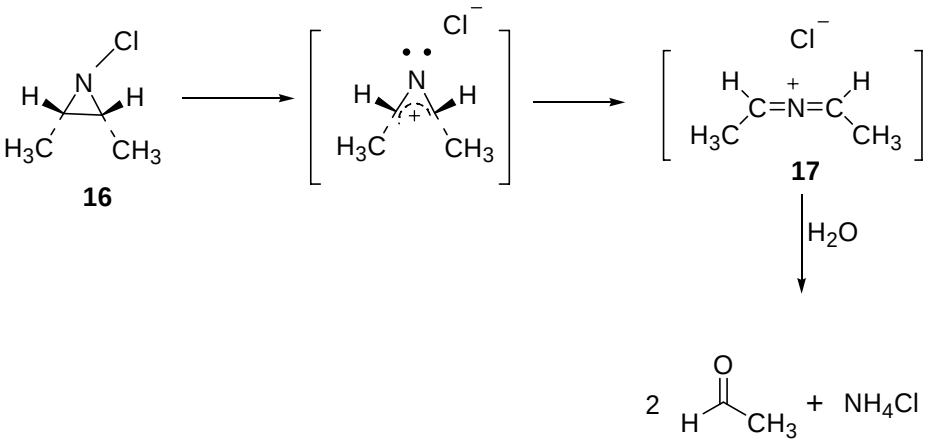

Scheme 2.7 Ring opening of *N*-chloroaziridines

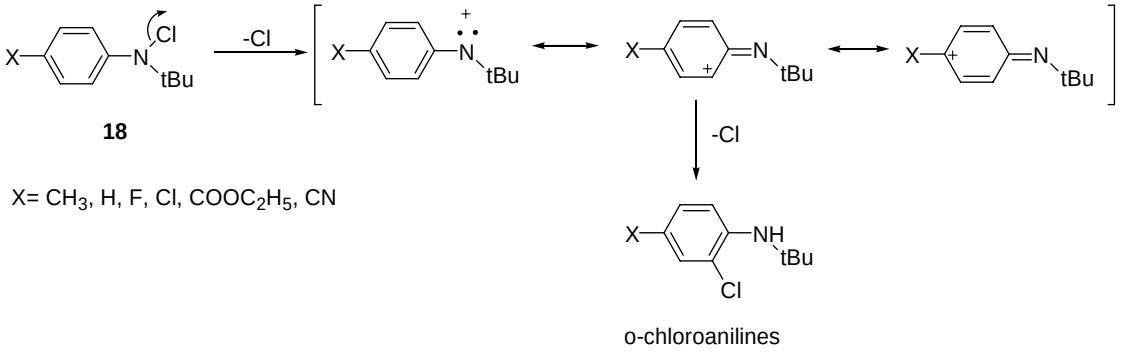

Scheme 2.8 Rearrangement of *N*-*tert*-butyl-*N*-chloroanilines

Gassman thought that he found the solution to his problem when he conducted solvolysis studies with *N*-chloro-4,7,7,-trimethyl-2-azabicyclo-[2.2.1] heptane (**19**).[7] He observed that heating **19** in methanol yields nucleophilic addition products, **20** and **21**, and reduction product **23** in 59, 20 and 7% respectively. (Scheme 2.9) Compound **23** appears to be the result of a hydrogen atom abstraction process and since hydrogen atom abstraction reactions are radical reactions, Gassman argued that **23** was the result of a triplet nitrenium ion because the latter undergoes radical chemistry.

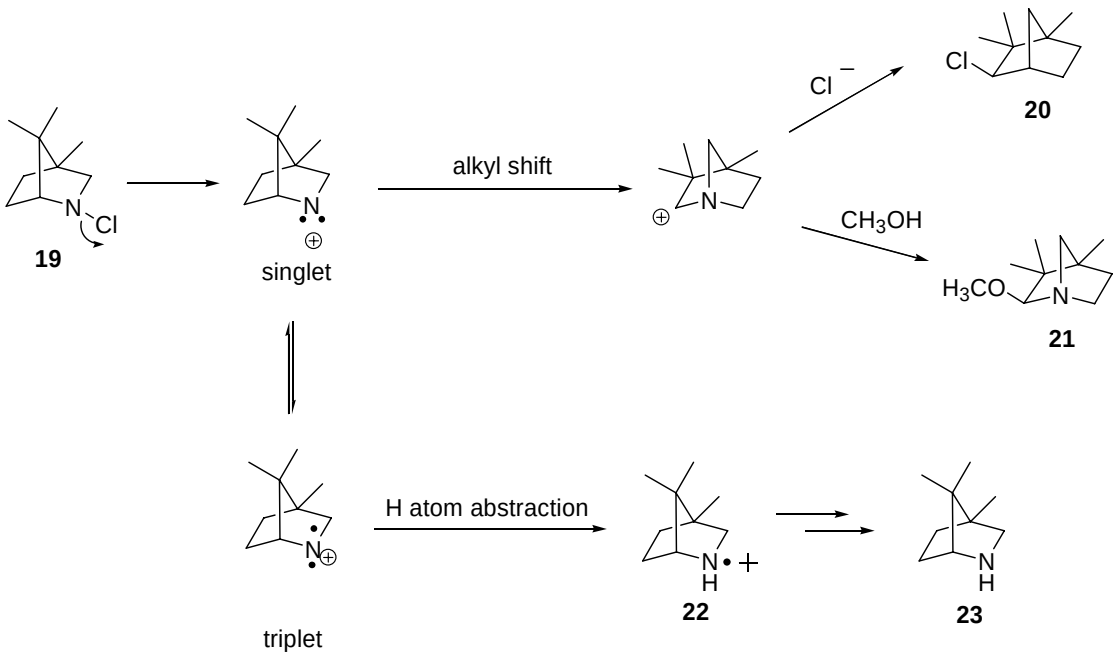

Scheme 2.9 Solvolysis of *N*-chloro-4,7,7,-trimethyl-2-azabicyclo-[2.2.1] heptane

Gassman recognized that the nitrenium ions could exist in the singlet and triplet state and that these two electronic states have different chemical properties. Based on this assumption, he proposed that upon refluxing in methanol, the N-Cl bond of the *N*-chloroamine cleaves heterolytically to eliminate chloride and form the singlet nitrenium ion intermediate. The singlet nitrenium ion then decays via an alkyl migration to form the carbocation intermediate or intersystem crosses to the higher energy triplet state. For the most part, the nitrenium ion rearranges to form the carbocation which then undergoes nucleophilic attack by the chloride or the solvent. However some fraction of the nitrenium ions intersystem crosses to the triplet state. The latter then carry out hydrogen atom abstraction and deprotonation to give the reduction product.

Gassman argued that the energies of the singlet and triplet states of the nitrenium ion from **19** must be close that they are in equilibrium. Hence the parent

amine (**23)** arises from the triplet that results from the singlet-triplet equilibrium. Solvolysis studies of **19** in methanol-heavy atom solvent were performed to test the assumption because heavy-atoms were generally known in photochemical studies to promote spin inversion. His hypothesis was that if a triplet state nitrenium ion was involved in the reaction mechanism, then the presence of a heavy-atom should promote spin inversion of the singlet to the triplet state by colliding with it. This should be observed by increased production of the parent amine (**23)**. Hence, refluxing **19** in varying amounts of heavy atom solvents such as $CHCl_3$, $CHBr_3$, *p*-dibromobenzene, CCl_4, results in a higher yield of the parent amine (**23**). Gassman was convinced that this indicates that the presence of the heavy-atom promoted spin inversion of singlet nitrenium ion leading to more triplet states. He dismissed the possibility of homolysis of N-Cl bond by arguing that the increased production of parent amine in CCl_4 and *p*-dibromobenzene. He argued that if homolysis was the initial step of the reaction, then carrying out the solvolysis in heavy-atom solvent should not affect the yield of the parent amine. He claimed that the production of the parent amine should remain the same both in heavy-atom solvents and non-heavy atom solvents.

Based on these results, Gassman concluded that the two states of the nitrenium ion are in equilibrium leading to the formation of the parent amine (**23**) from the triplet nitrenium ion. He argued that since reactions from both states were observed, it proved that the nitrenium ions exists as discrete intermediates like any other intermediates such as carbocation or nitrene. However, Gassman's assumption was challenged by many others especially Hoffmann.[8] Hoffmann et. al. argued that it

was unlikely for the nitrenium ion to intersystem cross to the triplet state due to its higher energy.[8,9] He felt that even if the nitrenium ion was generated, it would be in competition between two pathways: rearrangement or intersystem crossing. Therefore, the species would choose to decay via rearrangement rather than follow the higher energy pathway to form the triplet. The second argument posed by Hoffmann was that the reduction product observed by Gassman could be attained by a different pathway. Since the reaction was conducted in protic solvent, protonation or hydrogen bonding of the nitrogen atom of **19** could lead to the homolysis of N-Cl bond to give a radical cation of **23** which after a series of protonation and deprotonation would generate **23**. Even though, Gassman's methods and conclusions have been disproved by others, he is credited for proposing that the two states of the nitrenium could be distinguished based on their chemical reactivity.

Gassman's work triggered additional investigations of nitrenium ions and since these species were generated as intermediates that lived for few microsecond, several groups took this as a challenge to learn more about these species. Earlier work reported on nitrenium ions were solvolysis studies where the projected mechanism of the reaction was determined from the products isolated.

The photolytical methods for studying nitrenium ions were first introduced by Doppler et. al during their study with benzisoxazoles.[10] For example irradiation of benzisoxazoles (**24**) in concentrated sulphuric acid results in the formation of *ortho* and *para* substituted hydroxylated products.(Scheme 2.10) Based on Gassman's observation, it was postulated that the products form via the nitrenium ion.

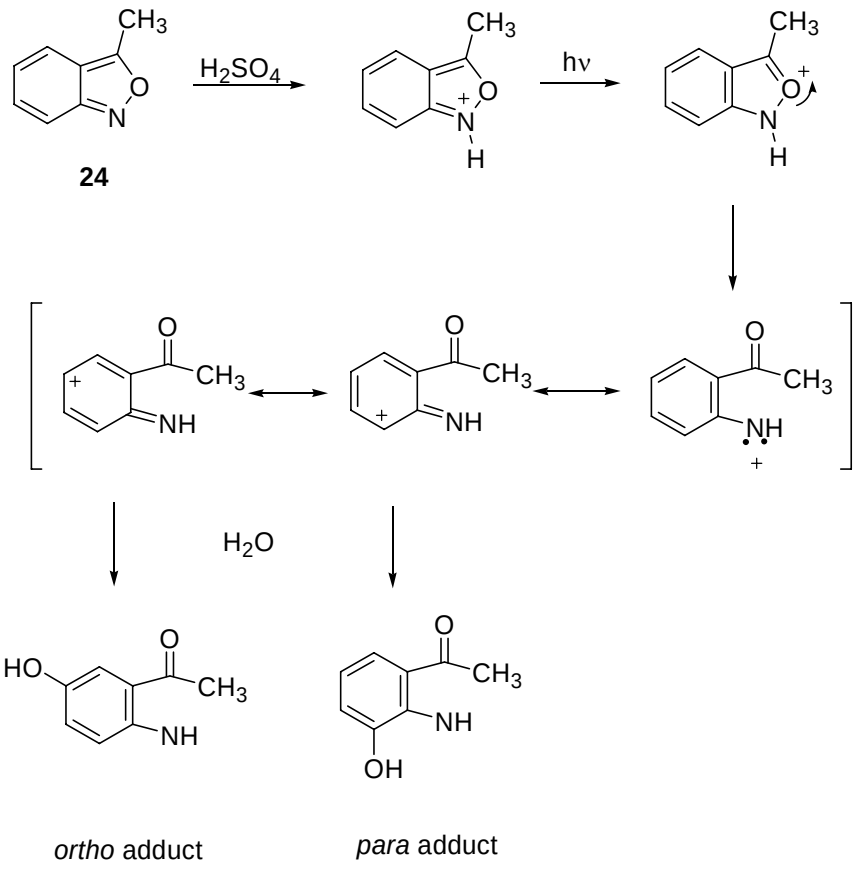

Scheme 2.10 Photolysis of benzisoxazoles in H_2SO_4

Haley's group also used photochemistry to provide evidence of nitrenium ions. They observed that irradiation of *N*-alkylated 2,1-benzisoxazolium salts (**25**) in the presence of inorganic salts (NaCl, NaBr, KSCN) decomposed to yield 4 and 6-substituted-2-acylanilines.[11] (Scheme 2.11). He proposed that these products were formed via a nitrenium ion intermediate resulting from the heterolytic cleavage of the N-O bond of benzisoxazolium salt. This intermediate is then subject to nucleophilic attack at the 4 or 6-position to yield the nucleophilic adducts. He followed the photolysis of 1,3-dimethyl-2,1-benzisoxazolium perchlorate in water using UV-Vis spectroscopy hoping to be able to detect the intermediate that was been formed during the reaction. However, only the absorbance band of the starting material and the end

product was observed; no intermediates were observed. He believed that this indicated that the reaction happened fast to be detected by the UV and that the intermediate formed during the reaction had a very short lifetime (<10s).

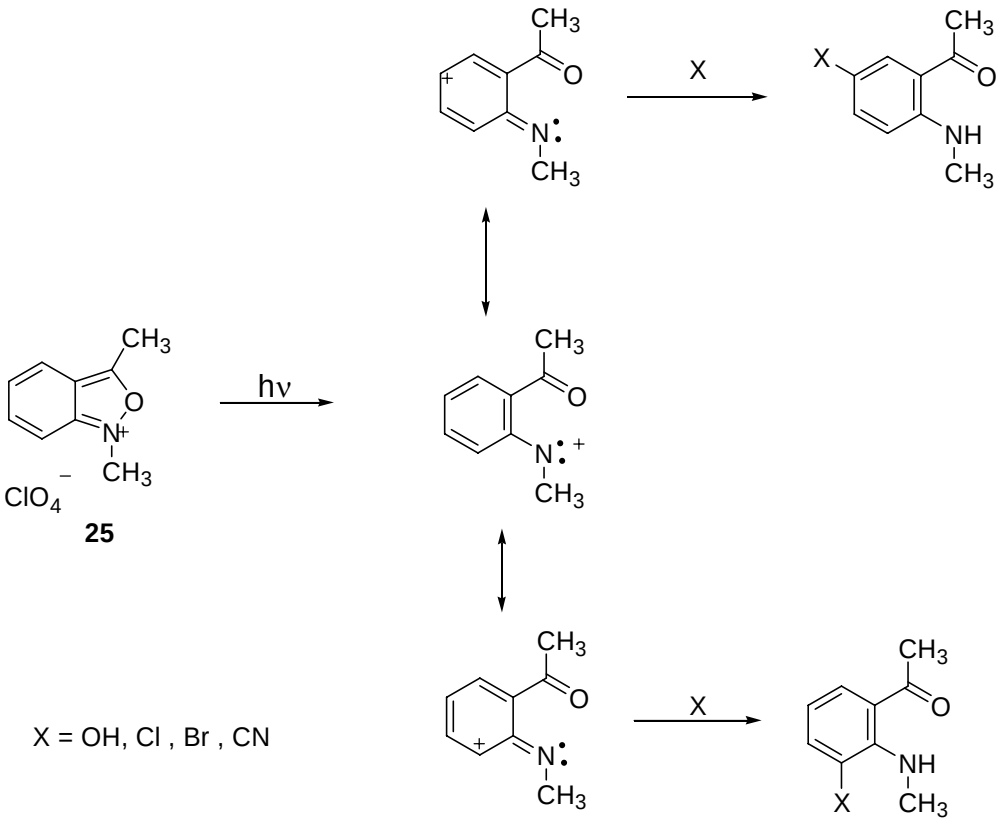

Scheme 2.11 Photolysis of 1,3-dimethyl-2,1-benzisoxazolium perchlorate

Haley provided further evidence for the intermediacy of nitrenium ion by trapping azahomoadamantane carbenium ion (**29**), an isomer of nitrenium ion (**27**), formed during the photolysis of *N*-adamantyl-substituted benzisoxazolium salts (**26**). Photolysis of **26** yielded **28** and **30** in 9:1 ratio. Both products are proposed to originate from the nitrenium ion intermediate. (Scheme 2.12) The latter then undergoes rearrangement or nucleophilic substitution depending on the reaction solvent. In methanol higher yield of **28** was obtained via a nucleophilic addition of solvent to the 4-position. The minor product **30** was suggested to occur through the

ring expansion of **27** to form **29** which was isolated and characterized. Hydrolysis of **29** led to the formation of **30**. Haley argued that isolation of **29** was concrete evidence that the nitrenium ion was formed during the reaction.

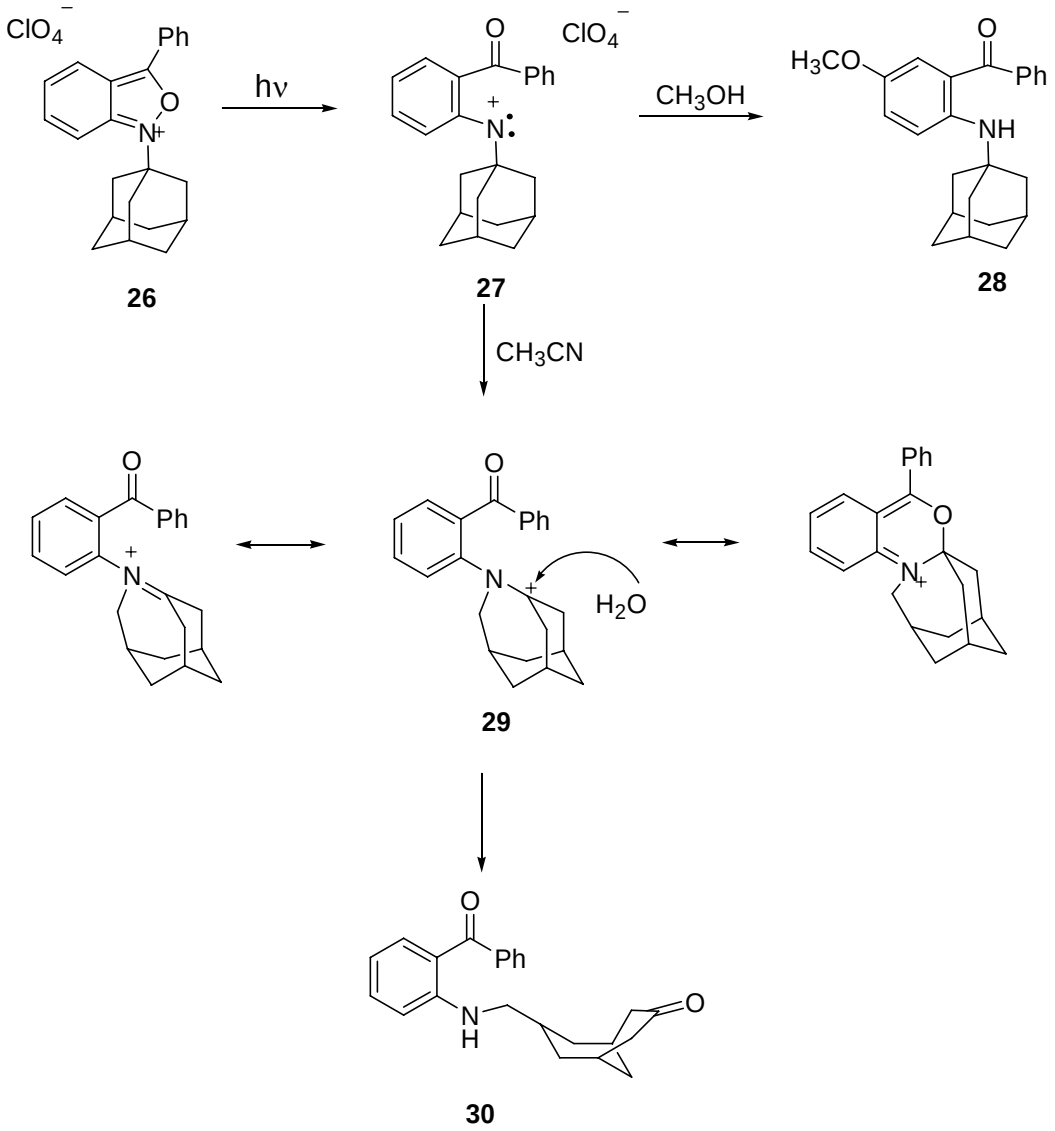

Scheme 2.12 Photolysis of *N*-adamantyl-substituted benzisoxazolium salts

Many groups used photolysis to study nitrenium ions generated from various aromatic amines. Photolysis of anthranils, indazoles and arylazides were conducted in concentrated acids and were assumed to yield nucleophilic adduct products via a nitrenium ion intermediate.[12-17] Takeuchi et. al. conducted direct amination of

aromatic compounds using photolysis to generate nitrenium ions from 1-aminopyridinium salts.[18]

2.2 Nitrenium ions as Discrete Intermediates

More concrete evidence of nitrenium ion existing as a discrete electrophilic intermediate was provided by the Novak and McClelland groups. In their pursuit of establishing that nitrenium ions are the ultimate metabolite in causing DNA damage leading to cancer, they proved that these species exist as cationic intermediates in aqueous media and were capable of selectively reacting with nucleophiles.

The evidence that nitrenium ions exist as a discrete cationic intermediates was proved by trapping the latter with various nucleophiles. Since nitrenium ions are cations, it was speculated that these species could be trapped by the solvent molecule or a nucleophile. This was observed in the photolysis of 4-biphenylylazide in H_2O. Since photolysis of arylazides in weakly acidic solvents generate nitrenium ions due to the protonation of nitrenes, arylazides were chosen to generate these ions.[19-21] As expected, photolysis of 4-biphenylylazide (**31**) in H_2O yields 4-hydroxy-4-phenyl-2,5-cyclohexadienone (**35**) as the major product along with nitrene (**32**) products. (Scheme 2.13) The ketone, **35** was clearly a nucleophilic addition product resulting from the addition of H_2O to the nitrenium ion (**33**) which was eventually hydrolyzed. Nitrenes do not undergo nucleophilic substitution reactions, instead decompose to yield ring expansion products and azo compounds.[19,22] In addition, they are electron deficient but basic, hence are easily protonated by weakly acidic media to give nitrenium ion.[20,23] Hence **35** that resulted did not originate from **32** but from **33**. Therefore, the addition of H_2O to the intermediate indicated that a distinct positively

charged species existed for a short period of time because H_2O being a weak nucleophile generally adds only to a strongly electrophilic site. This nucleophilic addition of H_2O to the intermediate showed that nitrenium ions existed as free cationic intermediates in solution.

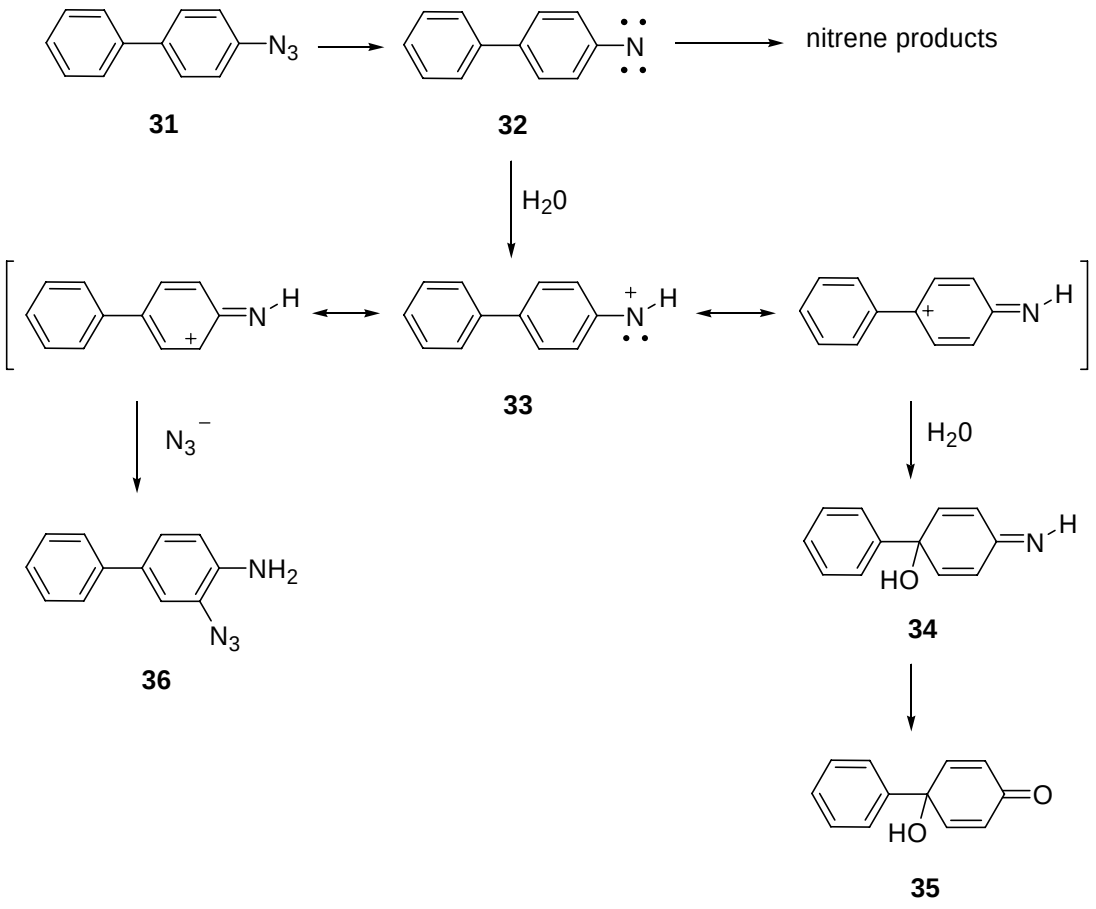

Scheme 2.13 Decomposition of 4-biphenylazide in H_2O

In addition to quenching by H_2O, nitrenium ions were also quenched by azide confirming that these species did exist in solution. In the presence of azide ions, photolysis of **31** yields **35** and azide adducts **36**.[23] (Scheme 2.13) The isolation of **36** supports the conclusion that **33** is generated during the reaction. Similar results were obtained from the competitive trapping studies of *N*-(2,6-dimethylphenyl)-hydroxyamine (**37**).[24,25] Under mildly acidic conditions, **37** decomposes in H_2O,

giving 4-hydroxy-2,6-dimethylaniline **39** in 96 % yield and in azide buffer (NH_3/N_3^-), the major product was 4-azido-2,6-dimethylaniline (**40**). (Scheme 2.14) However, in both cases, it was observed that the azide adduct was formed at the expense of the solvent adduct because increasing the concentration of azide, increases the yield of the azide adduct and lowers the yield of the solvent adduct while keeping the total yield of products constant.[23] This indicates that the both products originate from a common intermediate species. It also shows that the azide adduct results from the addition of azide to the nitrenium ion because photolysis of **31** in protic solvent generated nitrenium ions. Therefore, in order to be subjected to nucleophilic attack by both nucleophiles, the nitrenium ion had to exist as a distinct entity.

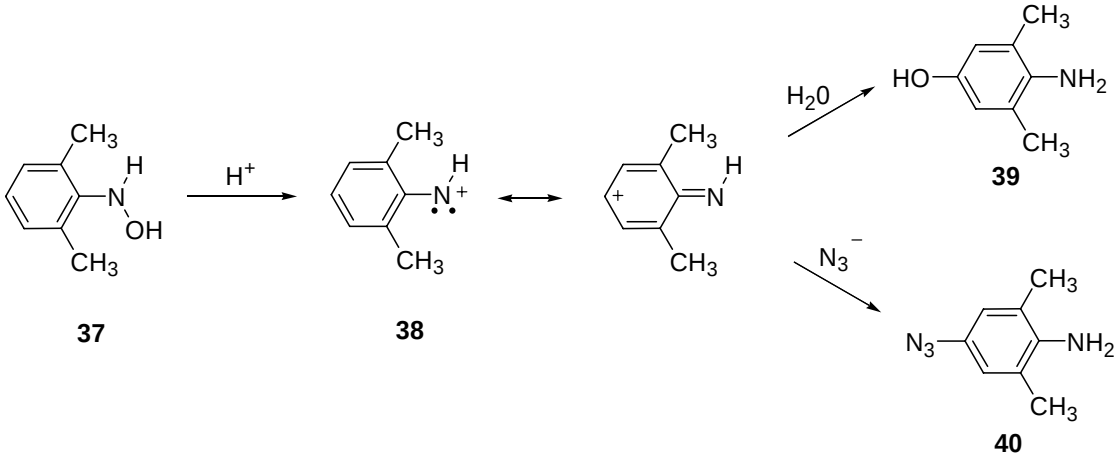

Scheme 2.14 Reaction of *N*-(2,6-dimethylphenyl)-hydroxyamine in acidic media

Based on the results from the photolysis of **37**, it was confirmed that the Bamberger rearrangement of *N*-hydroxyaniline also occurs via a nitrenium ion. The reaction mechanism was further verified by labeling experiments.[21] It was observed that the decomposition of N-hydroxyaniline in O^{18}-labelled H_2O, yields 4-aminophenol with $O^{18}H$ group. The incorporation of $O^{18}H$ in 4-aminophenol shows

that the reaction is intermolecular with the solvent adding to the electrophilic intermediate. This proved the hydroxyl group of *N*-hydroxyaniline was initially protonated and then eliminated to generate nitrenium ion which then underwent nucleophilic substitution by the solvent. Since no O^{18} labelled *N*-hydroxyaniline was observed, the reaction was assumed to be irreversible. Hence, once the positively charged nitrogen was formed, the charge is delocalized on to the para carbon and was quenched immediately by the solvent.

The presence of nitrenium ion as a discrete intermediate was additionally proved by kinetic studies. Competitive trapping studies showed that nitrenium ions generated by photolysis of aromatic compounds were trapped much more effectively by azides than H_2O. The nitrenium ions, *N*-acetyl-*N*-(4-biphenylyl) (**41**) and *N*-acetyl-*N*-(2-fluorenyl) (**42**) were quenched by azides at the diffusion limit at a rate constant of 5.0 x 10^9 $M^{-1}s^{-1}$ and 4.0 x 10^9 $M^{-1}s^{-1}$ respectively (k_{diff} CH_3CN = 1.9 x 10^9 $M^{-1}s^{-1}$).[23-25] (Figure 2.1) Azides are extremely electrophilic; hence they react readily with cationic sites at the diffusion limit. Therefore, the diffusion limited quenching by the azide supports the view that the species being generated in these conditions are cationic. Moreover, increasing the concentration of azide, only increases the amount of azide adduct but does not affect the rate of decomposition of the nitrenium ion precursor signifying a S_N1 mechanism which again proved the existence of a distinct cationic intermediate.

41 **42**

Figure 2.1*N*-acetyl-4-biphenylyl and *N*-acetyl-2-fluorenyl nitrenium ions

Additional proof for the existence of nitrenium ions was obtained by laser flash photolysis (LFP) studies. For example, 4-biphenylylnitrenium ion (**33**) and *N*-acetyl-4-biphenylylnitrenium ion photochemically generated from 4-biphenylazide (**31**) or *N*-acetoxy-*N*-acetyl-4-biphenylylamine respectively were observed to have an absorbance bands with λ_{max} at 460 nm.[20,26] (Scheme 2.15) In H_2O, these transients decay exponentially, characteristics of an S_N1 mechanism. The transients are also unaffected by O_2 but decay rapidly when nucleophiles such as azides or chlorides are added, indicating that the species responsible for these transients is a cation. The results obtained from the photolytic studies agree with the results obtained by solvolysis studies. The ratio of the azide quenching rate constant to the decay rate constant in H_2O measured by LFP give a value of $(2.8 \pm 0.2) \times 10^3\ M^{-1}$ which is in good agreement with the value obtained by solvolysis studies $(2.9 \pm 0.2) \times 10^3\ M^{-1}$.[23,27,28] Also, the photoproducts isolated from the quenching studies of *N*-acetoxy-*N*-acetyl-4-biphenylylamine in the presence of chloride yields **43**, **44**, **45** and **46** which are also obtained by solvolysis studies.[26] (Scheme 2.16) These indicate that the electrophilic intermediate generated in the solvolysis as well as LFP were the same. These evidence clearly showed that just like other intermediate species such as nitrenes, carbenes and carbenium ions, nitrenium ions also exist as free intermediates.

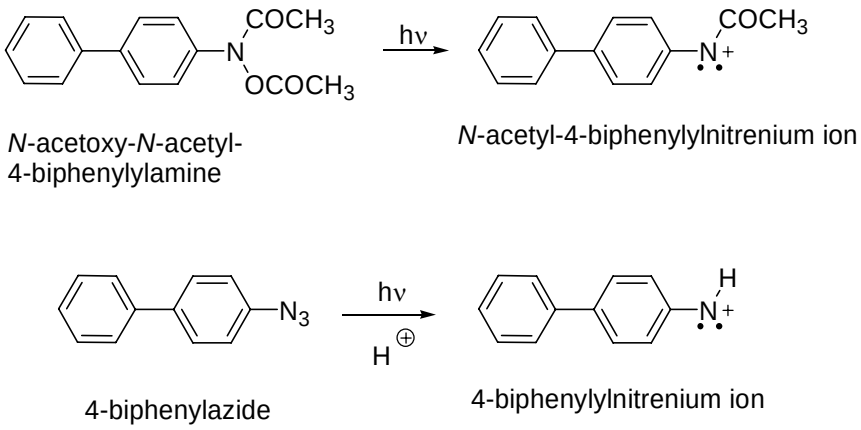

Scheme 2.15 Arylnitrenium ions photochemically generated from 4-biphenylylazide and *N*-acetoxy-*N*-acetyl-4-biphenylylamine.

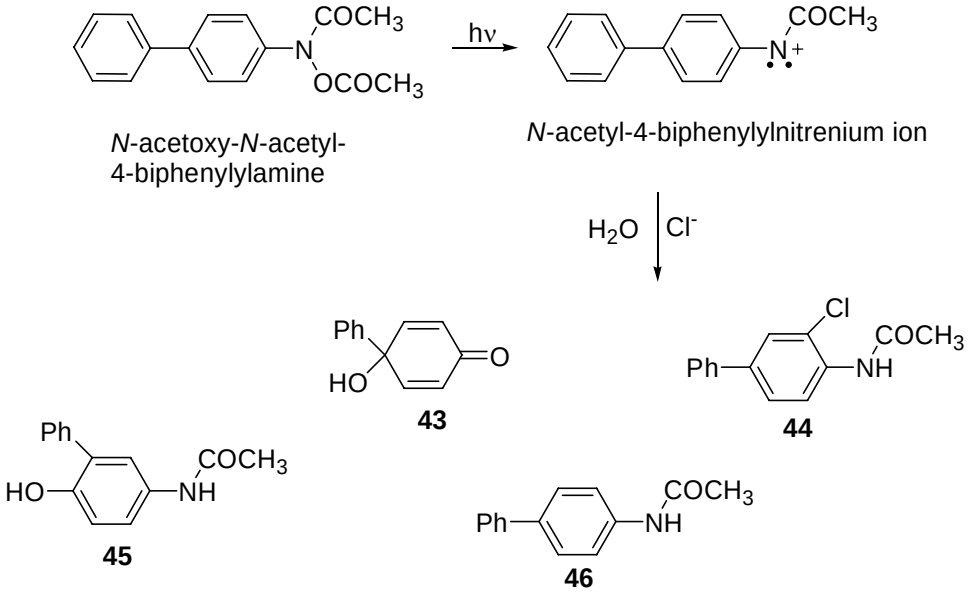

Scheme 2.16 Photoproducts obtained in the presence of chloride.

2.3 Laser Flash Photolysis

The introduction of laser flash photolysis (LFP) has contributed tremendously to the study of nitrenium ion in recent decades. The major obstacle to the advancement in the study of these ions was that they existed in solution only for a limited amount of time; hence it was difficult to obtain any direct information on its existence. However, with the advent of LFP techniques these problems were resolved

because using this technique one could photochemically generate and observe transient species that live for few nanoseconds to microseconds. The transient species are generated or chemically modified using short laser pulses and their existences are observed by UV absorption spectroscopy.[27] Before its application to nitrenium ions, LFP was used in the study of other transient intermediates such as carbenium ions and nitrenes.

In the study of nitrenium ions, LFP is used to cleave a specific nitrogen containing bond of a precursor heterolytically to yield nitrenium ion. The latter is then detected via its time-resolved absorption of the UV-visible light from a probe beam. In order to successfully study these species, it is necessary that the nitrenium ions be generated photochemically, and that their lifetime be longer than the laser pulse. Using LFP, it is possible to specifically generate a nitrenium ion and observe its chemical decay process. Thus it is possible to obtain a thorough understanding of the chemical and kinetic characteristics of the nitrenium ion as well as predict the reaction mechanism of its decomposition.

Shown in Figure 2.2 is the basic schematic of the Nd:YAG laser setup used in our LFP experiments described in this thesis. The reaction sample is illuminated with a short laser pulse (4-6 ns), which is focused at the center of a quartz cuvette via mirrors and a focusing lens. The probe beam from a lamp source is passed through the sample in such a way that it is perpendicular to the laser pulse and is focused on the edge of the cuvette. After exiting the sample, the probe beam is focused on the monochromator. The latter is connected to a photomultiplier tube (PMT) and an

oscilloscope. The probe beam is focused perpendicular to the laser pulse in order to minimize light scattering into the monochromator.

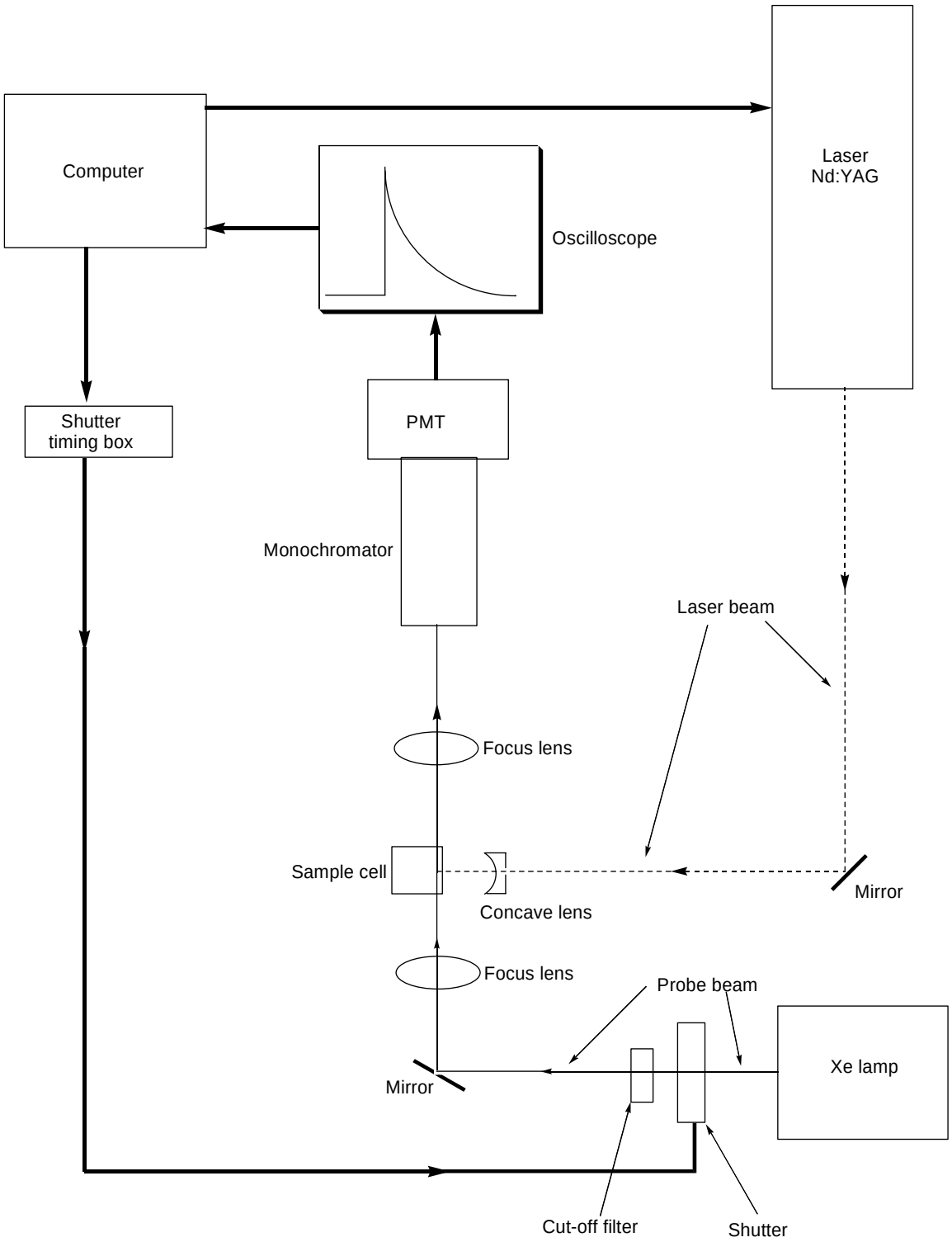

Figure 2.2 Schematic of Nd:YAG laser

The photosubstrate is excited by either 355 nm or 266 nm wavelength laser beams. The Nd:YAG laser emits a 1064 nm fundamental wavelength which is converted into shorter wavelengths using harmonic generator crystals. The second harmonic that is generated is the 532 nm wavelength that is obtained by combining 2 photons of 1064 nm wavelength. Similarly, 355 nm wavelength is generated by combining one 532 nm photon and one 1064 nm photon. Combining two 532 nm photon outputs the 266 nm wavelength.

Upon irradiation of the sample, the chemically transformed species that is generated absorbs UV light emitted from the probe beam. The probe beam used in the experiments discussed in thesis is a continuous light source from a 350 W Xe arc lamp (wavelength 260-850 nm). The UV light, after passing through the sample, enters the monochromator which is capable of selecting a single wavelength and hence allows the light of that particular wavelength to enter the detector, which is the PMT.

The PMT magnifies the intensity of the light from the monochromator and records the intensity as the current. The intensity of light recorded by the PMT is actually the change in absorbances of the UV light by the absorbing species and is detected within nanoseconds. The current is then fed to the oscilloscope where the current is recorded as voltage as a function of time, which is eventually converted to change in optical density (ΔOD) by the Labview software. Matlab and Labview are the two programs used to interpret the data obtained in our experiments.

Waveforms and time-resolved transient absorption spectrum are the two forms of data output that is obtained from LFP. The kinetic behavior of a new species is

initially observed on the oscilloscope as a waveform. A waveform is an exponential decay or growth curve where the ΔOD of an absorbing species is plotted as a function of time at a particular wavelength. At the irradiation by the laser pulse, photosubstrates are excited or chemically modified. As time passes, these species decay to the ground state or are transformed to a new species. The concentration of the observed intermediates decay or grow in exponentially with time and is measured by their ΔOD. The ΔOD of the absorbing species at a certain time can be related as shown in equation (1) where 'ε' is the molar absorptivity of the species at a certain wavelength, 'C' is the concentration of the species in molarity and 'l' is the length of the sample cell in cm.

$$\Delta OD(t) = \varepsilon C(t)l \qquad \text{equation 2.1}$$

There are mainly two types of waveforms: exponential decay curve or exponential growth curves. An exponential decay curve indicates loss of a species that is generated at the initial impact of the laser. (Figure 2.3) An exponential growth waveform indicates the accumulation or growth of a new species. (Figure 2.4) As the new species accumulates in the sample, the ΔOD increases until it eventually saturates. The lifetimes of the species and their change in concentration at a particular wavelength can be obtained from the waveform.

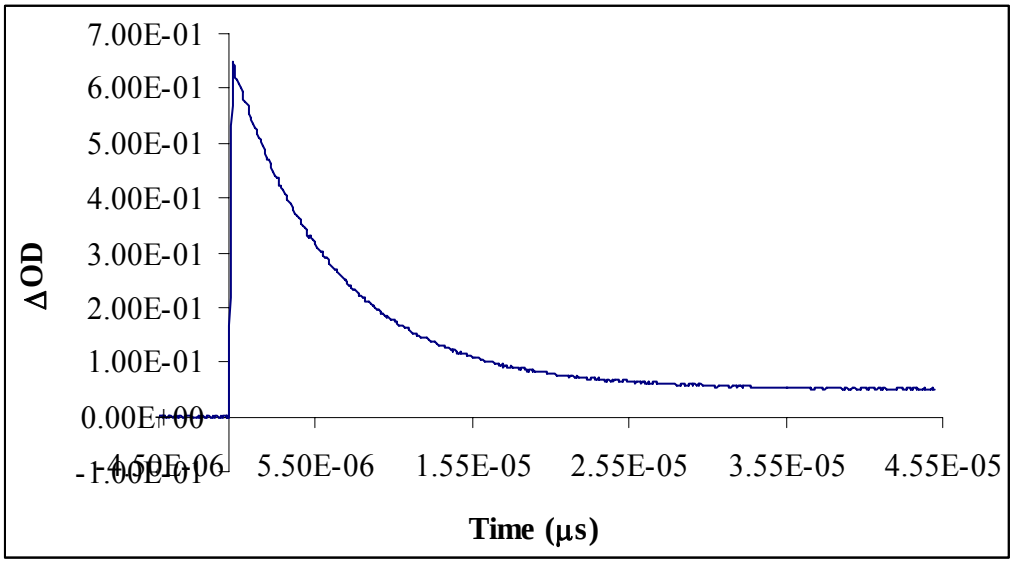

Figure 2.3 Exponential decay waveform of *N*-(4,4'-dibromodiphenyl) nitrenium ion (**78c**) in 9:1 buffer/CH_3CN at 690 nm

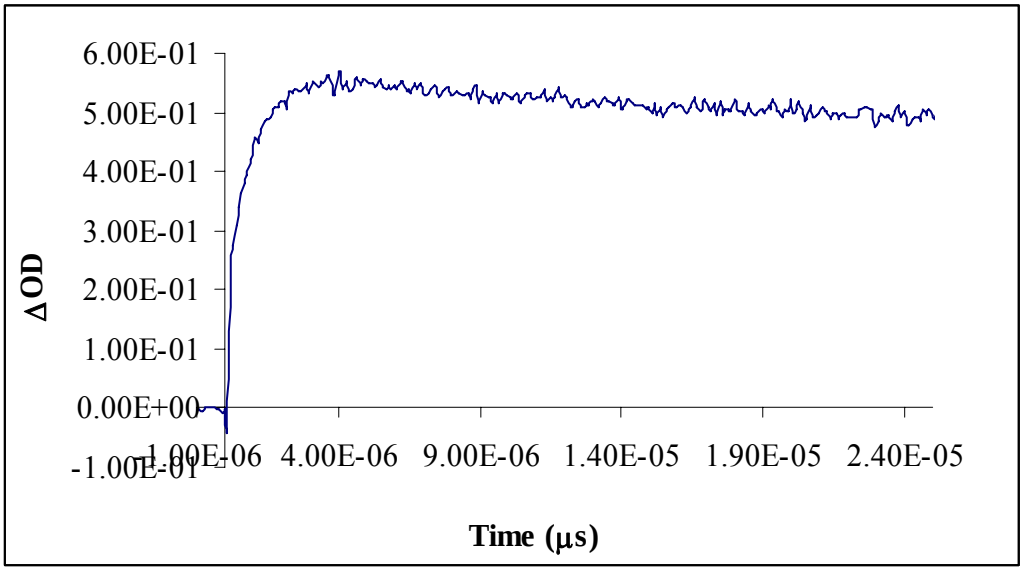

Figure 2.4 Exponential growth waveform of the radical cation (**85**) of *N*-(4,4'-dichlorodiphenyl) amine in CH_3CN and HBF_4 at 650 nm

A time-resolved transient absorption spectrum is basically the UV absorption spectrum of the different species generated during photolysis. (Figure 2.5) It is

basically a 3 dimensional graphical representation of the absorbences at different wavelengths at various time intervals following the laser pulse. It is obtained by compiling a series of waveforms over a range of wavelengths. The various species present during the course of the photolysis is indicated by their absorbance band in the spectrum; additionally their absorbencies at particular time following the laser pulse can also be observed. Hence the decay of an absorption band over a period of time indicates loss of a species and the growth of a new band signifies the formation of a new species. This spectroscopic data allow one to follow the chemical and kinetic behavior of any species during the course of the reaction. This method is useful because the laser is capable of detecting the absorbance of species that exists briefly in solutions.

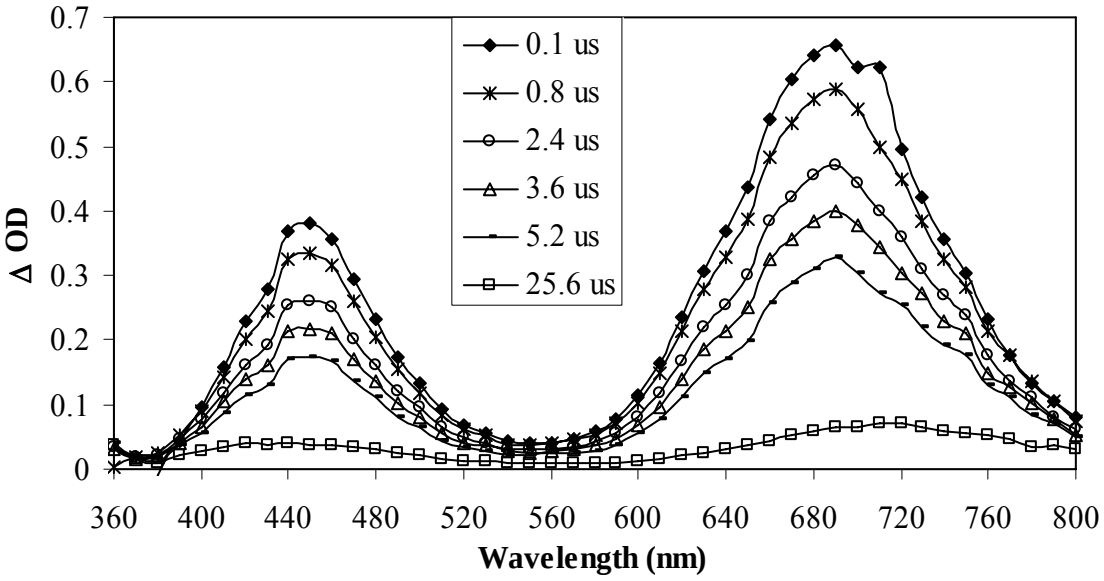

Figure 2.5 Transient absorption spectra of the photolysis of *N*-(4,4'-dibromodiphenylamino)-2,4,6-trimethypyridinium BF_4 salt (**77c**) in 9:1 buffer (25 mM PO_4^{-3}, 7.5 pH)/ CH_3CN

Information on the kinetic behavior of a transient species can be obtained from its waveform. The relative reactivity of the species of interest with various nucleophiles is measured by the rate of decay or growth of its waveform. Since the waveform represents the behavior of a single species, its reactivity with another species is indicated by the increase or decrease of the rate of decay or growth of the waveform. For example a typical decay waveform is represented by the equation 2.2

$$\Delta OD = A \exp(-k_{obs})t + b \qquad \text{equation 2.2}$$

ΔOD reflects the concentration of the species at time 't' of the decay process where k_{obs} is the decay rate constant of the curve. A is the collection constant and b is the baseline; these parameters are fitted by the kinetic analysis program of the computer. If the transient species reacts with a nucleophile, the waveform decays faster thus increasing k_{obs}. Therefore, in order to measure the bimolecular second order reaction rate constant of the nucleophile with the species, the k_{obs} at different nucleophile concentration is obtained. As the nucleophile concentration increases, the k_{obs} also increases. The kobs is then plotted as a function of the nucleophile concentration to produce a linear regression plot with a slope, k_q, as shown in equation 2.3.

$$k_{obs} = k_o + k_q[Q] \qquad \text{equation 2.3}$$

k_{obs} is the decay rate constant of the species at various quencher or nucleophile concentration [Q], k_o is the decay rate constant of the species in the absence of any quencher, and k_q is the bimolecular reaction rate constant between the quencher and the transient species. Even though the reaction between the nucleophile and the nitrenium ion is a bimolecular reaction, the k_{obs} is fitted to a pseudo-first order decay analysis based on the assumption that the effect of the nucleophile concentration on

the k_{obs} of nitrenium ion is negligible. Since the nucleophile is in large excess, the change in nucleophile concentration is negligible compared to the change in nitrenium ion concentration; hence would have least effect on the k_{obs}. The rate constants reported in this thesis is based on this assumption.

Spectroscopy data on the nitrenium ion was first obtained by Baetzold et. al in their oxidation study of *p*-phenylenediamine.[30] However, the species observed by UV spectroscopy was not recognized then as being a nitrenium ion rather an iminium ion. More spectroscopic data on nitrenium ions began emerging only in the early 1990s after the introduction of LFP which provided direct information on the kinetic behavior of the nitrenium ions. It is also easier to follow the chemical decay process of the nitrenium ions using LFP.

2.4 Singlet and Triplet States of Nitrenium Ions

In order to understand the kinetic and chemical characteristics of nitrenium ion, a thorough understanding of its electronic configuration is necessary. Similar to carbenes, nitrenium ions can exist in either one of the energy states, singlet or triplet, which arises from the difference in distribution of the non-bonding electrons within the non-bonding orbitals.[31-34] Along with the two covalent bonds, nitrenium ions have two non-bonding electrons and two non-bonding orbitals (σ and p). In the singlet state, the two non-bonding electrons may occupy either one of the non-bonding orbitals or both non-bonding orbital with anti-parallel spins giving rise to either one of the electronic configuration of σ^2, p^2 or σp. (Figure 2.6) Most singlet nitrenium ions exist in the lower energy σ^2 state. The other two states, p^2 and σp, are higher in energy. The triplet state is formed when the two non-bonding electrons occupy the

non-bonding orbitals separately with parallel spins to give an electronic configuration of σp.

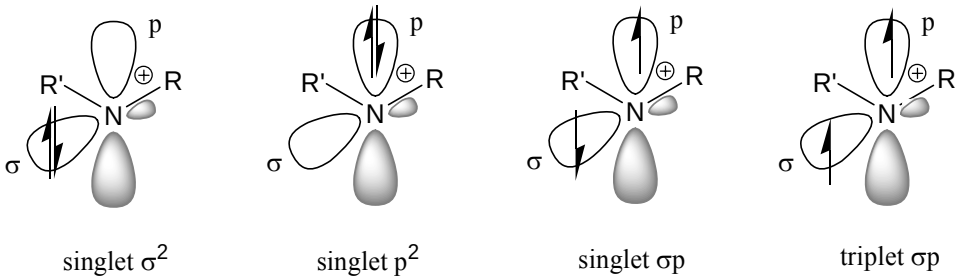

Figure 2.6 Schematic diagram of singlet and triplet energy states of nitrenium ion.

The population of the non-bonding electrons in the orbitals generally depends on the orbital energy spacing between the σ and p orbitals. The two orbitals are of different energies with σ being the lowest; therefore the population of the electrons in these orbitals depends upon the energy gap between these two orbitals. (Figure 2.7) Electrons generally occupy orbitals based on Hund's rule.[33] According to the Hund's rule, the electrons would prefer to occupy separate orbitals due to electron-electron repulsion. In addition, the separate occupancy of the electrons is favored by parallel spins due to the electron exchange interactions. Since the two orbitals in the triplet state are almost degenerate, the orbital energy spacing is smaller than the exchange and coulombic forces, thus allowing the electrons to assume a σp electronic configuration with parallel spin. Hence the triplet state would be favored over the singlet.[34] However, the energies of the two orbitals can vary such that they are not degenerate anymore, forcing the electrons to occupy the lowest energy orbital giving rise to the singlet state.

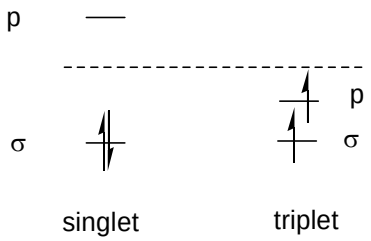

Figure 2.7 Orbital energy spacing

The singlet and triplet state have different energies and the difference in energy between the two states is known as the singlet-triplet energy gap, ΔE_{ST}. The lower energy configuration of the nitrenium ions depend on the orbital energy spacing of the σ and p orbitals. Any factor that destabilizes the p orbital or stabilize the σ orbital can increase the orbital energy spacing, thus causing the non-bonding electrons to occupy the lower energy σ orbital, thus favoring the singlet state. Likewise, any factor that stabilizes the p orbital or destabilizes the σ orbital brings the two orbital closer in energy, thus favoring the triplet state. Thus, factors that affect the σ and p orbitals affect the energies of the singlet and triplet state which in turn affects the ΔE_{ST}.

Factors that mainly influence the energies of σ and p orbitals are electron delocalization and bond angle of the nitrenium ion. These depend on the physical properties of the substituents on the nitrogen atom.[31,33] The parent nitrenium ion, NH_2^+ is a ground state triplet with a ΔE_{ST} of +29.9 kcal/mol and a bent geometry with a bond angle of 153°. Since the substituents on the nitrogen are hydrogens, the positive charge of NH_2^+ is localized on the nitrogen. This causes the two non-bonding orbitals to be degenerate, thus allowing the electrons to occupy the orbitals separately with parallel spins leading to the triplet state.

As substituents other than hydrogens are substituted on the nitrogen atom, their effects on the ΔE_{ST} are pronounced. The electron donating and withdrawing properties seems to have a significant effect in determining the ground state of the nitrenium ion. Electron donating groups generally stabilize the singlet state by electron delocalization. Thus substituting alkyl and phenyl group in nitrenium ion stabilize the singlet state relative to triplet state.[35] For example, phenylnitrenium is a ground state singlet by 18.8 kcal/mol.[33] As the positive charge on the nitrogen is delocalized by the π donation from the phenyl to the empty p orbital, the p orbital is destabilized, thus increasing its energy.[36] This increases the energy difference between the σ and p orbital causing the non-bonding electrons to occupy the σ orbital thus favoring the singlet state by lowering its energy.

The delocalization of the positive charge on to the phenyl carbon has been supported by LFP-TRIR studies conducted on *N*-methyl-*N*-phenylnitrenium ion. (time-resolved infrared spectroscopy).[36-38] TRIR uses infrared absorption to detect transient species formed during the reaction. Due to delocalization, singlet phenylnitrenium ion generally resembles 'iminocyclohexadienyl cation-like' intermediate and was confirmed by TRIR. (Scheme 2.17) Experimental data obtained by TRIR for *N*-methyl-*N*-phenylnitrenium ions showed IR bands in the region of 1628-1584 cm^{-1} corresponding to the aromatic C-C and C=C bond stretches. From these IR stretch, the average bond length of C-N of the nitrenium ion is calculated to be 1.320 + 0.003^{o}A. This bond length is in-between the bond length of a typical C=N or C-N bond which are 1.28 and 1.40^{o}A respectively. This indicates that the C-N

bond has partial characteristic of a double bond and a single bond. This proves that the iminocyclohexadienyl structure is in resonance with the arylnitrenium ion.

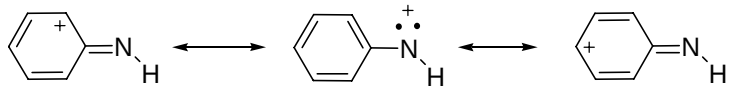

Scheme 2.17 Charge delocalization in phenylnitrenium ion

Like aryl rings, alkyl groups also stabilize the singlet state through hyperconjugation. The ΔE_{ST} for methylnitrenium ion has been calculated to be +7.8 kcal/mol.[31] Even though, it is a ground state triplet, the ΔE_{ST} is lower than NH_2^+ due to its relative stability of the singlet state.

Electron withdrawing groups generally favor the triplet state. *N*-tert-butyl-*N*-(2-acetyl-4-nitrophenyl)nitrenium ion is an example of a triplet nitrenium ion due to electron withdrawing properties of the nitro and acetyl groups.[39] (Figure 2.8) Arylnitrenium ions are generally ground state singlets; however the nitro group, being electron withdrawing, localizes the charge on the nitrogen thus decreasing the orbital energy spacing leading to a triplet state.

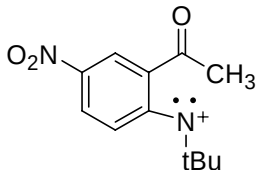

Figure 2.8 *N*-tert-butyl-*N*-(2-acetyl-4-nitrophenyl)nitrenium ion

However, halogens and nitrile on nitrogen atom of the nitrenium ion were observed to stabilize singlet state relative to the triplet state. Ab initio calculations conducted by Gonzalez et. al showed that nitrenium ions with chlorines, fluorines and cyano groups are ground state singlets.[40] Even though, these substituents are established as electron withdrawing groups, they are unique in that they are electron

acceptors through sigma bond and electron donors through π bond. Through π donation, these substituents donate electron density to the empty p orbital on nitrogen, thus destabilizing the p orbital and favoring the singlet state.

In addition to chemical properties of the substituents, the size of the substituents on the nitrogen atom can also influence the two energy states by decreasing the orbital energy spacing. ΔE_{ST} calculated for a series of nitrenium ions with electron donating groups show that substituting additional electron donating groups on nitrogen lowered the ΔE_{ST} of that nitrenium ion. The ΔE_{ST} for phenylnitrenium is predicted to be -18.8 kcal/mol but replacing the hydrogen with a methyl group or another phenyl group gives a ΔE_{ST} of -14.1 and -11.6 kcal/mol.[31] This is due to the fact that as substituents get bulkier, the steric interactions between the substituents begin to have an effect on the bond angle of the nitrenium ion.

Singlet nitrenium ions are generally have a bent geometry with a bond angle (R'-N-R) between 110 – 130°. As a result, the nitrogen in singlet is sp^2 hybridized with σ orbital having more of sp^2 characteristics.[31,36] However, as the size of the substituents get larger, the bond angle of the nitrenium ion increases by becoming more linear. This causes the hybridization to change from sp^2 to sp, thus imparting more p character to the σ non-bonding molecular orbital. Due to this effect, the σ orbital is destabilized, raising its energy, thus leading to smaller orbital energy spacing eventually stabilizing the triplet state. 2,6-di-tert-butylphenylnitrenium ion is an example of a ground state triplet nitrenium ion due to steric effects.[31,41] Its triplet state is lower in energy than the singlet by 7.3 kcal/mol and a R'-N-R bond angle of 180.0°.[34] Typically, the bond angles for triplets are between 150 – 160° but this ion

has a linear geometry.[34] The bond angle for the singlet state of 2,6-tert-butylphenylnitrenium ion is 141.0^{o} which is higher than expected for a typically singlet nitrenium ion (typical bond angle for single are 110 – 130^{o}). Hence the chemical and physical properties of the functional groups on nitrogen control the different energy states of the nitrenium ion which in turn are responsible for the chemical reactivities of these ions.

2.5 Chemical Behavior of Singlet and Triplet Nitrenium Ions

Due to the differences in the electronic configuration, singlet and triplet nitrenium ions have different chemical properties and hence react differently with nucleophiles. Singlets generally undergo carbocation type reaction, while triplets undergo radical-like reactions. As a result of different reaction mechanism, singlets and triplets give rise to different products. Gassman was the first to recognize this difference in reactivities and interpret product data based on it which were later discredited.

2.5.1 Reactivity of Singlet Nitrenium Ion

Singlet nitrenium ions are cationic intermediate that undergo electrophilic substitution reactions. Due to the empty p orbital, singlets are capable of accepting one or two electrons; therefore, they behave as Lewis acids. Hence these ions generally react with nucleophiles to form covalent bond to yield σ-adducts. In addition, these ions undergo rearrangement and electron abstraction processes.

Simple nucleophiles such as halides, H_2O and alcohols generally react with nitrenium ions to form nucleophilic addition products. NH_2^+ is the simplest form of nitrenium ions and is a ground state triplet. However, the singlet state of NH_2^+ can be

trapped by nucleophiles before it intersystem crosses to the lower energy triplet state. Srivastava et. al. showed that the singlet NH_2^+ generated from 1-amino-2,4,6-triphenylpyridinium ClO_4^- salt (**47**) reacts with H_2O and methanol to yield NH_2OH and NH_2OCH_3 respectively.[42] (Scheme 2.18) These products resulted from the addition of the nucleophile to the cation center on the nitrogen. NH_2^+ typically undergoes triplet-like chemistry, but in the presence of singlet traps, it is capable of undergoing singlet chemistry.

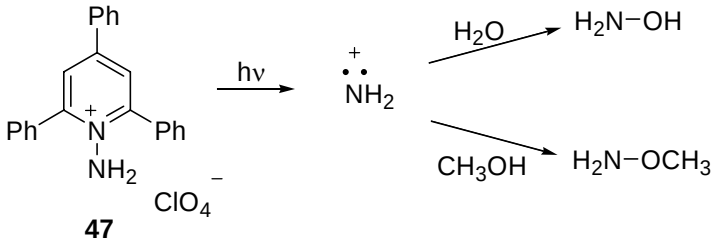

Scheme 2.18 Reaction of NH_2^+ with simple nucleophiles

Arylnitrenium ions are the most widely studied ground state singlet nitrenium ions. These ions generally react with halide or alcohols yield *para* or *ortho* adducts. The positive charge of the nitrogen in arylnitrenium ions can be delocalized to the *ortho* and *para* carbon of the phenyl ring; hence the nucleophiles add to those electron deficient sites. Anionic nucleophiles generally add to both the *ortho* and *para* carbons of the ion, however, weak nucleophiles preferentially add only to the para carbon.[29,35,37,43] For example, *N*-methyl-*N*-phenylnitrenium ion (**48**), photochemically generated from *N*-(methyl-*N*-phenylamino) BF_4^- salt reacts with chloride ions to yield *ortho* and *para* chloro-adducts, with *para* adduct being the major product.[44] (Scheme 2.19) But in the presence of methanol, only *para* adduct was observed. This was due to the fact that methanol, being a weak nucleophile, adds to the site that has the most positive charge density. The *para* carbon has the most positive charge density and is

more stable than the other resonance structures because the positive charge further away from the electronegative nitrogen. As a result, weak nucleophiles such as alcohols and H_2O, add to the *para* carbon and the strong nucleophiles such as azides and halides add to both the *ortho* and *para* carbocation sites.

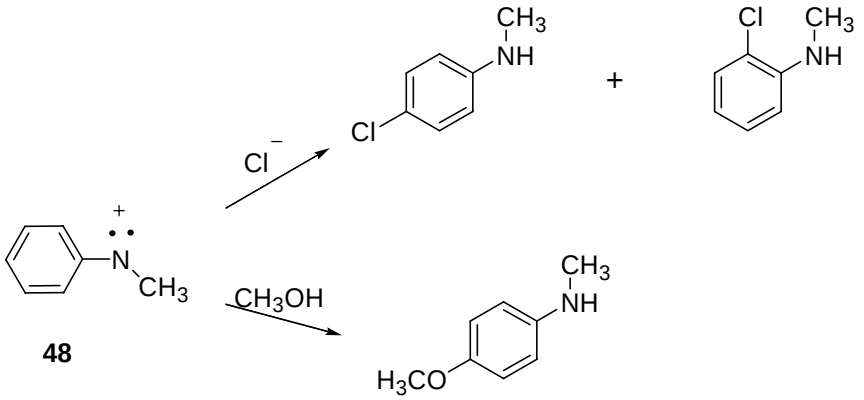

48

Scheme 2.19 Reaction of *N*-methyl-*N*-phenylnitrenium ion with chloride and methanol

Similar σ-adducts were observed for other arylnitrenium ions. *N*-tert-butyl-(2-acetylphenyl) nitrenium ions react with H_2O or methanol to yield photoproducts which result from the addition of the nucleophiles to the 4-position of the arylnitrenium ion.[45] In cases, where the *para* position is substituted, only *ortho* adducts were produced as observed for *N*-methyl-*N*-(-4-substitutedphenyl) nitrenium ions.[37] For example, reaction of *N*-methyl-*N*-(-4-substitutedphenyl) nitrenium ions with chloride yields only ortho adducts. (Scheme 2.20) Hence, hard nucleophiles, such as chloride, azides, H_2O and alcohol, are observed to add only at the ring carbons and not at the nitrogen center.

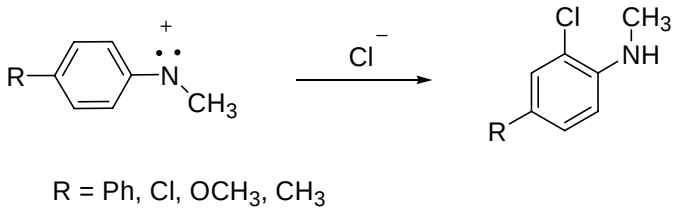

R = Ph, Cl, OCH_3, CH_3

Scheme 2.20 Reaction of *N*-methyl-*N*-(-4-substitutedphenyl) nitrenium ions with chloride

Singlet nitrenium ions react readily with π-nucleophiles such as arenes readily to also to form nucleophilic addition products. For example, *N*,*N*-diphenylnitrenium ion (**49**) reacts with 1,3,5-trimethoxybenzene (TMB) and 1,3-dimethoxybenzene (1,3-DMB) to yield *N*, *ortho* and *para* adducts.[46] (Scheme 2.21) It can be observed that unlike simple nucleophiles, arenes add to the nitrogen as well as to the *ortho* and *para* carbons. The electron rich arenes initially forms a π-complex with the arylnitrenium ion which is eventually converted to a covalent bond.

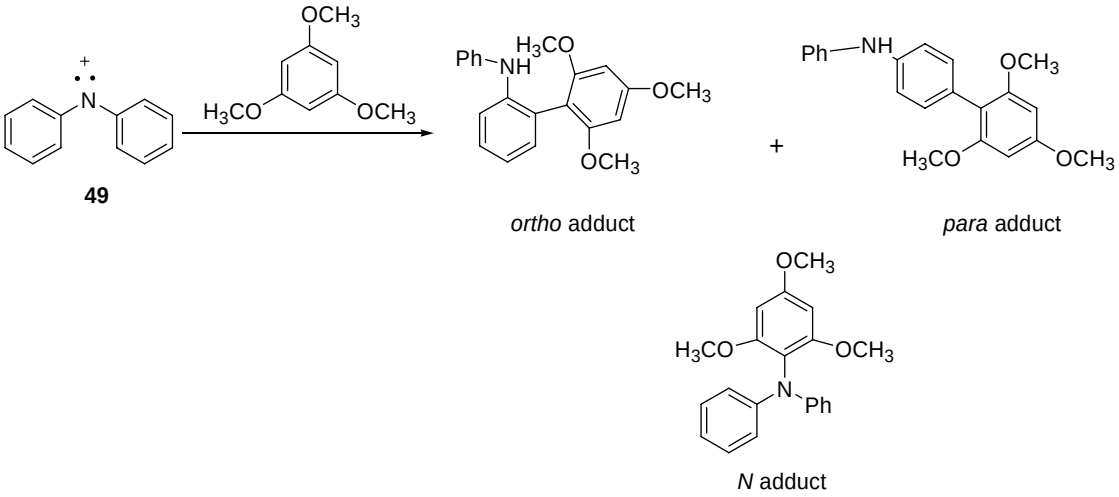

Scheme 2.21 Reactions of *N*,*N*-diphenylnitrenium ions with 1,3,5-TMB

N-methyl-*N*-(-4-biphenylyl) nitrenium ion (**48**) also was shown to yield *N* and *ortho* adducts. Reactions with arenes such as 1,3,5-TMB, 1,4-DMB, mesitylene, durene resulted in σ-adducts with the nitrenium ion.[46] Since the *para* carbon is

substituted with a phenyl group, no substitution of the arenes at this site was observed. Even though, *N* adducts were observed, they were obtained only in small amounts with the most reactive arenes such as such as 1,3,5-TMB and 1,3-DMB. The other arenes give rise to only ortho adduct and the parent amine.

In addition to nucleophilic substitution reactions, arenes also react with arylnitrenium ion via electron abstraction process. Along with the σ-adducts, reduction products such as the addition of two electrons and a proton to the arylnitrenium ion were also observed in the reaction between arenes and arylnitrenium ion. Photolysis of (*N*-4-biphenylyl-*N*-methylamino)pyridinium BF_4^- salts with various arenes generated the parent amine as the major product.[46] The parent amines were explained to have occurred as a result of the electron transfer from the arene to the arylnitrenium ions to yield a radical cation of both species. (Scheme 2.22) It was observed that *N*,*N*-diphenylnitrenium ion (**49**) reacts with *N*,*N*-dimethylaniline (DMA) with a rate constant of 7.3 x 10^9 $M^{-1}s^{-1}$ and yields parent amine (**53**) as the major product.[47] This diffusion limited rate coincides with oxidation potential of DMA (k_{diff} CH_3CN = 1.9 x 10^{10} $M^{-1}s^{-1}$). DMA has an oxidation potential of 0.53 V, therefore is easily oxidized. The diffusion-limited quenching of **49** by DMA along with LFP and product analysis results support that the reaction pathway is electron transfer. Other arenes were also observed to undergo electron transfer reactions with arylnitrenium ions.

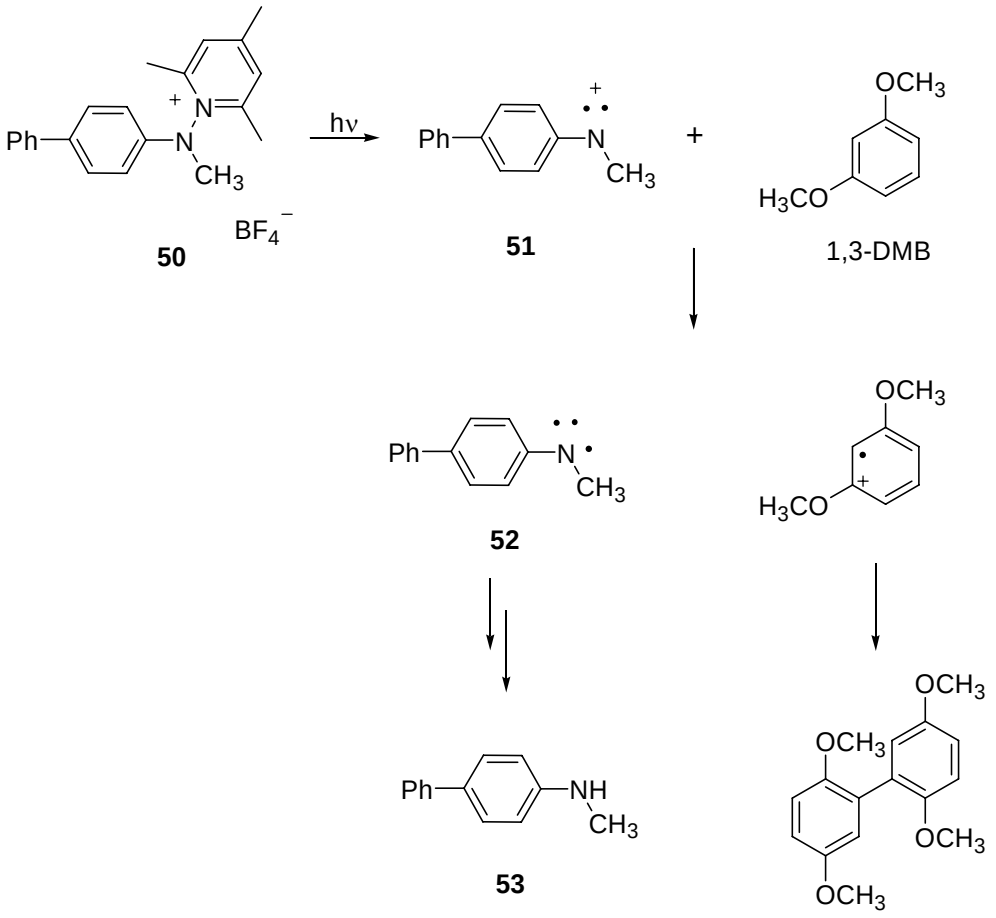

Scheme 2.22 Photolysis of (*N*-4-biphenylyl-*N*-methyl)pyridinium BF_4^- with 1,4-DMB

Being cationic, nitrenium ions are also capable of undergoing rearrangement type reactions. Reactions with *N*-methyl-*N*-phenylnitrenium ion and *N*-tert-Butyl-3-methylanthranilium ions generated photoproducts resulting from methyl or hydride shift to the nitrogen. Aniline was one of the photoproducts obtained from the decay of *N*-methyl-*N*-phenylnitrenium ion; therefore, it was proposed that it was formed as a result of the hydride shift from the methyl to the nitrogen to yield an iminium ion.[44] (Scheme 2.23) The iminium ion was then hydrolyzed to form aniline. In anthranilium salt (**54**), compound **57** was obtained as a result of the methyl shift from the tert-butyl group to the nitrogen.[29,39] (Scheme 2.24) Similar methyl and hydride shifts are

common in carbenium ions. From these examples, it can be concluded that singlet nitrenium ions behave as carbocations.

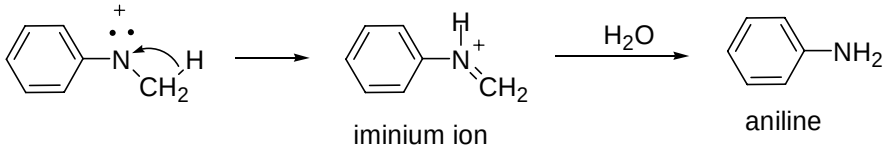

Scheme 2.23 Hydride shift in *N*-methyl-*N*-phenylnitrenium ion

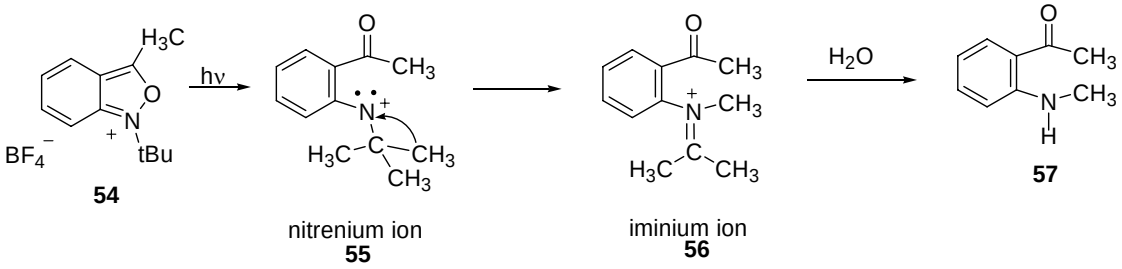

Scheme 2.24 Methyl shift in arylnitrenium ion from anthranilium ion

2.5.2 Reactivity of Triplet Nitrenium Ion

Triplet nitrenium ions generally undergo one electron chemistry such as radical chemistry since the σ and p orbital are partially filled. Therefore, the most common reaction by these ions are hydrogen atom abstractions from other nucleophiles or solvents. The reactivities of triplet nitrenium ion were clearly illustrated by the work of Anderson and Srivastava on anthranilium salts.

Photolysis of anthranilium ion (**54**) in the presence of nucleophiles such as methanol or H_2O yields 4-substituted-*N*-*tert*-butyl-phenylamines (**58**) as the sole products and in the absence of any nucleophiles, iminium ion (**56**) and parent amines (**59**) were produced.[29] (Scheme 2.25) The products, **58** and **56**, were confirmed to have occurred from the singlet nitrenium ion generated from the heterolytic cleavage of the N-O bond. Since the positive charge is delocalized to the ring carbon,

nucleophiles such as methanol or H_2O, adds to the para carbon of the nitrenium ion (**55**) that was formed. Iminium ions (**56**) were formed as a result of 1,2-alkyl shift of the methyl from the butyl to the nitrogen. However, **59** could originate from either one of the pathways: (1) hydride abstraction, a singlet pathway or (2) hydrogen atom abstraction from the solvent, a triplet pathway. Based on competitive trapping studies, it was confirmed that the amine was formed via hydrogen atom abstraction by the triplet nitrenium ion.

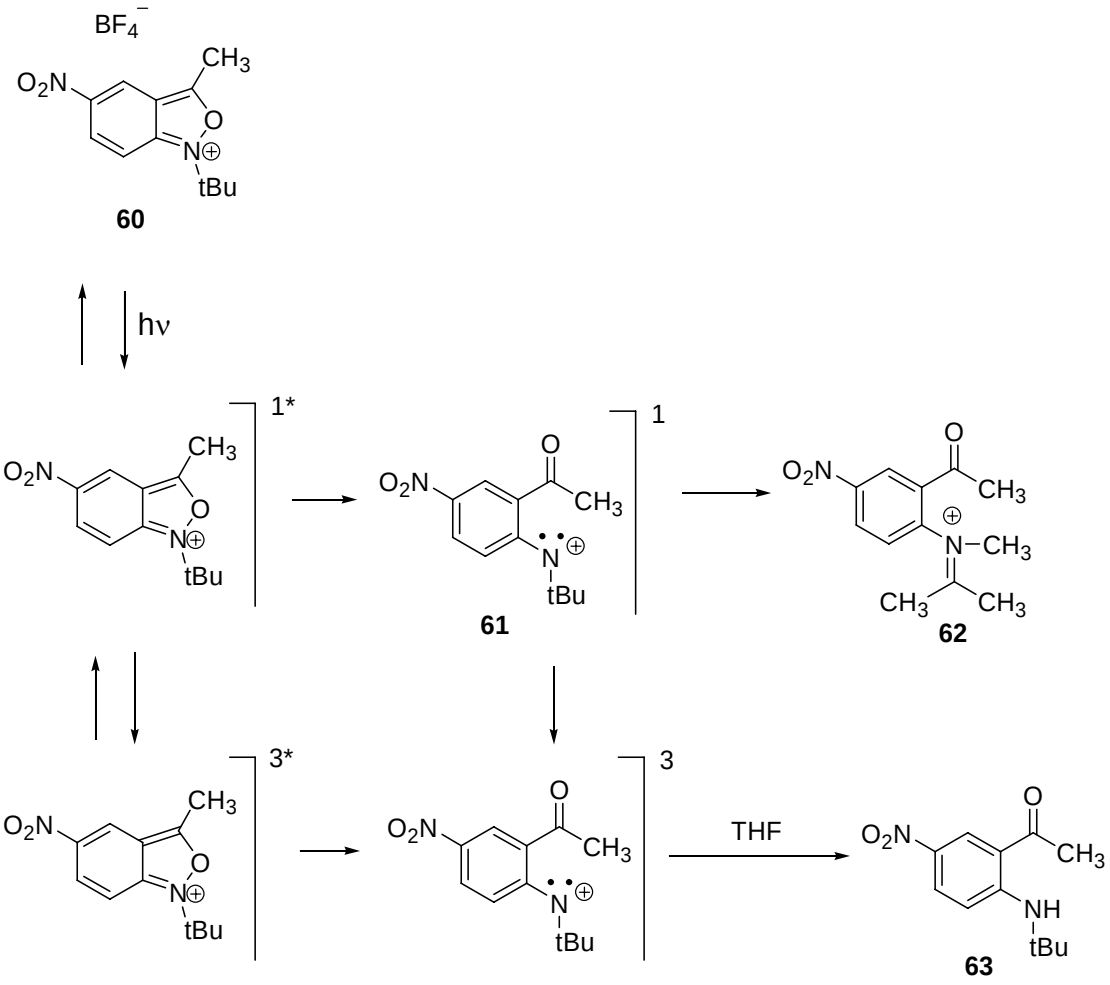

Scheme 2.25 Photolysis of *N*-tert-butyl-3-methylanthranilium ion

The triplet nitrenium ion pathway was validated by triplet sensitization and triplet quenching studies. Triplet sensitizers are compounds that upon excitation,

transfer energy to a photosubstrate thus exciting it directly to its triplet state bypassing the excited singlet state. (Figure 2.9) Triplet sensitized photolysis on **54** in CH_2Cl_2 and THF with no nucleophiles present produces a higher yield of parent amine (**59)** than iminium ion (**56)**; however, in neat THF, no iminium ion (**56)** is formed; only parent amine (**59)** is observed. THF is a good hydrogen atom source; therefore, enhanced yield of **59** indicates that a triplet nitrenium ion is present during the reaction. Triplet nitrenium ions generally undergo radical chemistry, therefore, in the presence of a hydrogen atom source, abstracts hydrogen atom to yield to a radical cation of **59** which eventually abstracts another hydrogen atom followed by deprotonation to yield **59**. Since both singlet and triplet products were obtained in CH_2Cl_2 and THF and only triplet products in THF, it indicates both products originate from different species, but in the presence of a hydrogen atom source, the triplet pathway is preferred. Based on this data, it is concluded that the triplet nitrenium ion forms from the excited triplet state of anthranilium ion, decays by either one of the pathways. It either intersystem crosses to the lower energy singlet nitrenium ion state that was responsible for **56**, or it abstracts a hydrogen atom to form **59**.

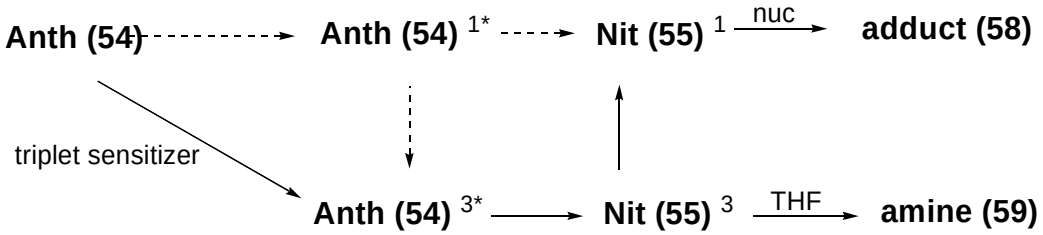

Figure 2.9 Triplet sensitization of *N-tert*-butyl-3-methylanthranilium ion

Competitive trapping studies with triplet quenchers also confirm the presence of the triplet nitrenium ion pathway. Irradiation of **54** in the presence of tetramethyldiazetine dioxide (TMDD) in H_2O and THF reduces the yield of **59**

relative to **58**. (Figure 2.10) TMDD is a triplet quencher that would remove the energy from the excited triplet anthranilium ion reversing it back to the ground state, thus suppressing the triplet pathway. The production of **59** was diminshed even in THF, indicating that the triplet pathway is suppressed and thus confirming that the triplet nitrenium ion is responsible for the formation of **59**. The lower yield of **59** was assumed to have originated from the intersystem crossing of the singlet **55** to the triplet state.

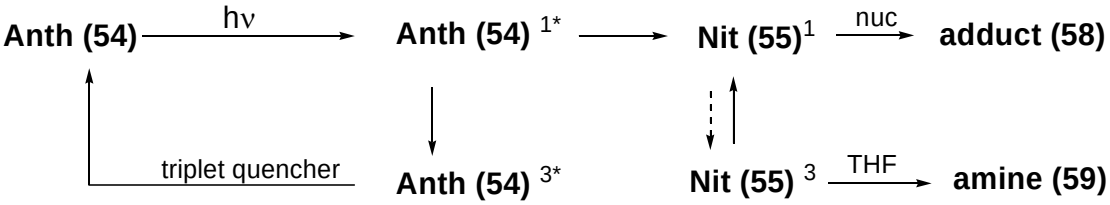

Figure 2.10 Triplet quenching of *N-tert*-butyl-3-methylanthranilium ion

Based on these observations, it was proposed that the direct irradiation of **54** generates the excited singlet **54** which partitions between ring opening and intersystem crossing to the excited triplet **54**. The singlet **55** generated from the excited singlet **54** either reacts with nucleophiles or relaxes back to ground state **54**. The excited triplet **54** undergoes N-O bond heterolysis to form the triplet **55** which either abstracts a hydrogen atom to yield **59** or intersystem crosses back to the low lying singlet state of **54**.

Studies done by Srivastava et. al. on (*N-tert*-butyl-5-nitro)-3-methylanthranilium ion (ClO_4^- or BF_4^- salts) (**60**) showed that the nitrenium ion (**61**) generated from this compound is a ground state triplet due to the electron withdrawing nitro group.[39] Irradiation of **60** in acetonitrile containing H_2O or methanol yields the parent amine (**63)** as the major product and the iminium ion (**62**)

as the minor product. (Scheme 2.26) Since **63** was obtained as the major product, the ion, **61**, was assumed to be ground state triplet. However, the reduced yield of **62** indicates that the singlet state was also present in the reaction mechanism.

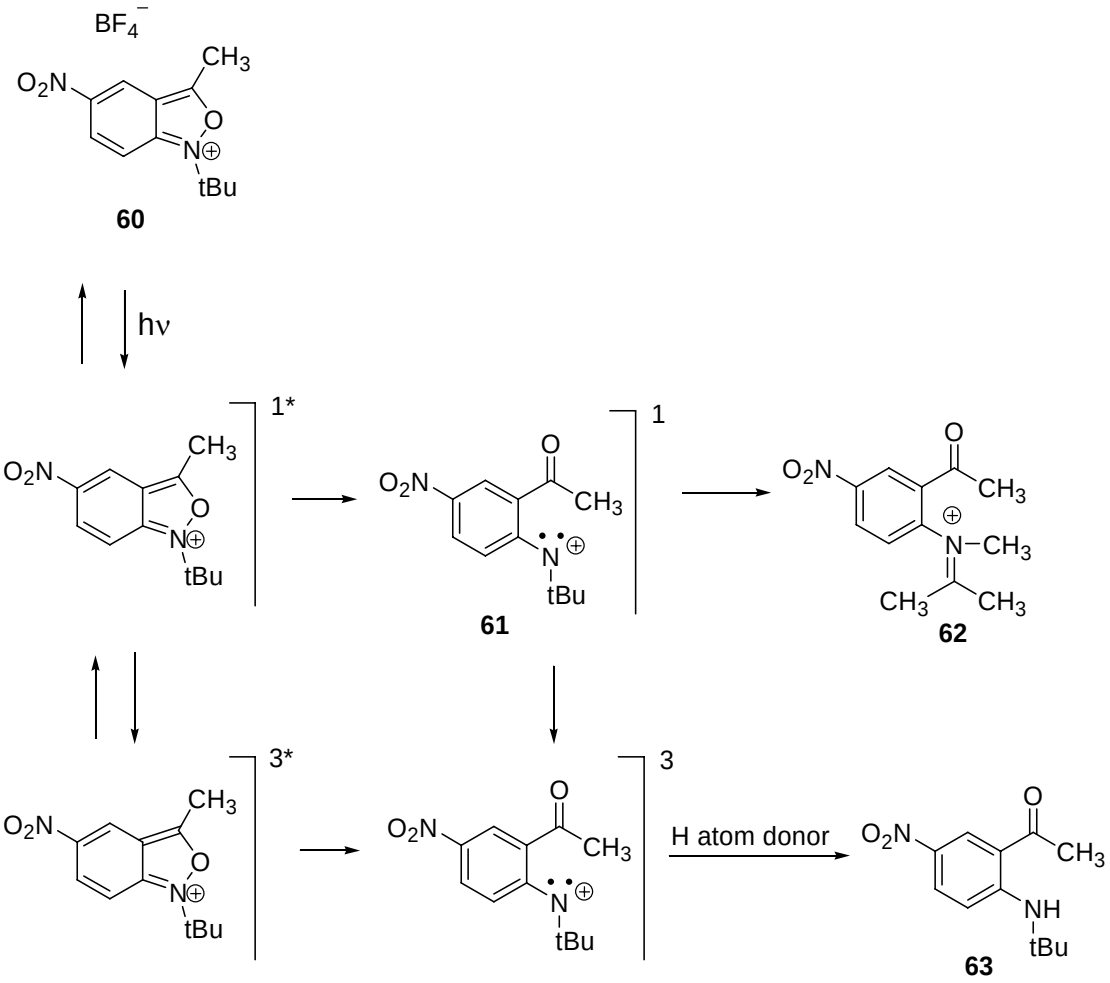

Scheme 2.26 Photolysis of (*N-tert*-butyl-5-nitro-3-methyl)anthranilium ion

The decay pathway of the nitrenium ion was studied extensively by competitive trapping experiments and LFP. Triplet sensitization experiments on **60** in THF, CH_2Cl_2 and $\mathbf{CH_3CN}$ yielded only **63**, supporting the fact that the latter was obtained from the triplet **61**, which was the result of ring opening of the excited triplet **60**. (Figure 2.11) The triplet **61** pathway was again verified by conducting the experiment with triplet quenchers. Molecular oxygen was used as the quencher and

purging the reaction with oxygen reduces the yields of **63**, suggesting that the triplet pathway was blocked. (Figure 2.12) Molecular O_2 generally quenches the triplet state by relaxing it back to the singlet ground state by promoting spin inversion of the electrons. Since **63** was exclusively affected with the absence of **62** when the triplet pathway was promoted or hindered, it was confirmed that the triplet state was the lower in energy than the singlet state.

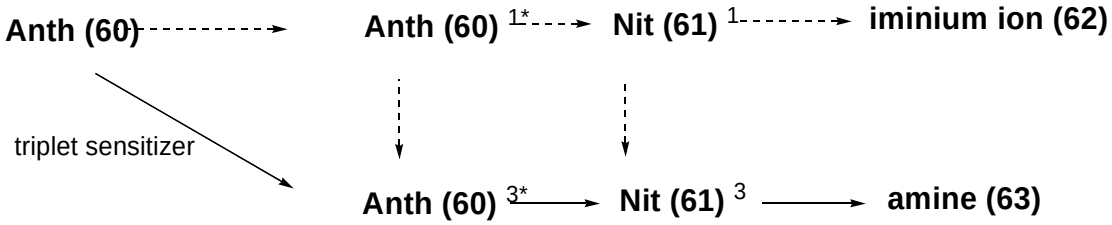

Figure 2.11 Triplet sensitization of *N-tert*-butyl-5-nitro-3-methylanthranilium ion

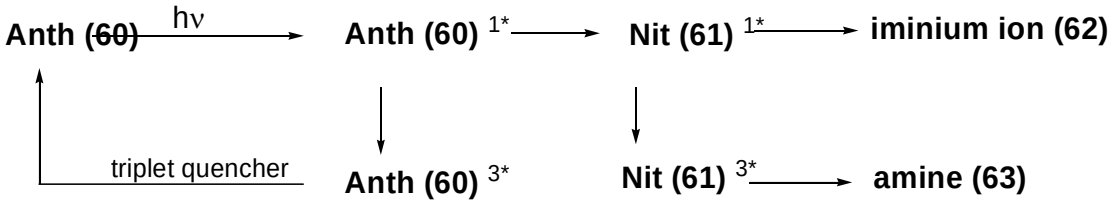

Figure 2.12 Triplet quenching of *N-tert*-butyl-5-nitro-3-methylanthranilium ion

Additional photolysis experiments done in the presence of Ph_3CH supported the notion of a lower energy triplet state. Irradiation of the precursor with Ph_3CH yields **63** and the dimer of Ph_3CH. Ph_3CH is a good hydrogen atom donor; therefore could serve as the hydrogen atom source for the triplet **61**. If the singlet **61** was the ground state, then Ph_3COH should be formed via hydride abstraction. Absence of Ph_3COH suggested that **63** was generated from triplet nitrenium ion.

Based on the evidence, the proposed decay process for **60** was that upon irradiation, the latter was excited to the excited singlet **60** which partitions to ring opening to yield the singlet **61** or intersystem crosses to the excited triplet state of **60**.

The ion, excited triplet **60** then ring opens to yield the triplet **61** which could either react by abstracting a hydrogen atom to produce **63** or relaxed back to the ground state **60**. The singlet **61** either undergoes rearrangement to give **62** or mostly intersystem crosses to the lower energy triplet **61**.

With the aid of LFP, Anderson and Srivastava were able to show that the singlet and triplet nitrenium ion reacted differently with nucleophiles and yielded different products. They demonstrated that LFP could be used to determine the ground state of a nitrenium ion and follow the reaction pathway of the latter with different nucleophiles that occurs at the nanosecond range.

2.6 Biological Relevance of Nitrenium Ions

Nitrenium ions, especially arylnitrenium ions were mainly studied for their role in causing cancer. It was first noticed by a German clinician Ludwig Rehn in 1895 that there were high incidences of bladder cancer among workers of the manufactures of aniline dye.[48] Studies based on that finding showed that aniline was not the cause of the problem, but contaminants such as 2-aminonaphthalene, 4-aminobiphenyl and benzidine were the potential carcinogens. (Figure 2.13)

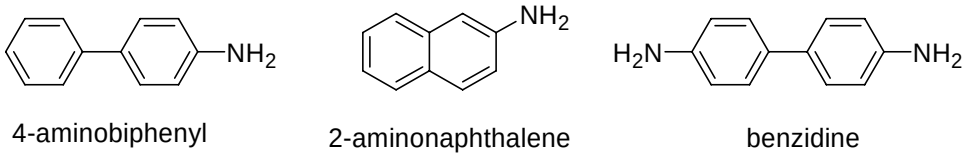

Figure 2.13 Structures of some carcinogens

In vivo studies of several aromatic amines and their derivatives showed that these compounds react with the nucleophilic components of the cell to eventually produce covalently bound protein, DNA or RNA derivatives.[49-51] These macromolecular adducts affected the replication or translation of the nucleic acids or

proteins leading to mutations or transformations leading to cancerous growths. The covalent adduct resulted from the addition of arylamine to an amino acid or nucleic acid base. For example, reactions of *N*-methyl-4-aminoazobenzene (MAB) with methionine yielded 3-methylmercapto-MAB, with part of the alkyl chain of the methionine not present in the final product and reaction of guanosine with 2-acetylaminofluorene (AAF) yielded adduct with the amine covalently bounded to the C8 position of guanosine.[52] (Figure 2.14) Similar covalent adducts were observed for other nucleophilic components such as tryptophan, tyrosine, cysteine, adenosine and histidine with arylamines.[52]

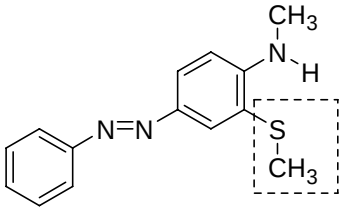

3-methylmercapto-MAB

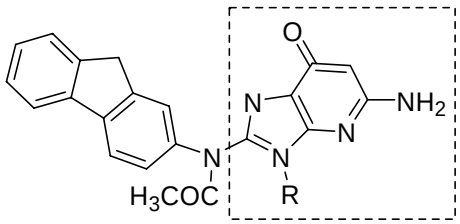

C8 adduct of guanosine

Figure 2.14 Covalent adducts with arylamines

In vivo studies on a wide range of arylamines and their deriviatives show that not all arylamines have carcinogenic properties but become carcinogenic depending on the substituents and the substitution pattern on the ring and the nitrogen. For example, 4-aminobiphenyls with amines, fluoride or nitro groups in the *para* position and nitro, amines or acyl groups on the nitrogen atom of the compound were shown to induce tumor growth in small animals tested. Most importantly, the carcinogenicity was specific to the *N*-substituents. Compounds with *N*-acyl or *N*-hydroxy groups on arylamines were more carcinogenic than the parent amine indicating that having a hydroxyl group or a group that could be easily hydrolyzed on

the nitrogen increases the toxicity of the compound. Application of *N*-hydroxy-*N*-acetyl-2-aminofluorene and *N*-acetyl-2-acetylaminofluorene (AAF) in mouse and hamster caused tumor growths at the site of application of the *N*-hydroxy AAF; however,for AAF, tumors were not observed at the site of application but away from the site of application.[53] (Figure 2.15) This implied that the *N*-hydroxylated arylamine was more potent than the parent amine and that the parent amine was *N*-hydroxylated inside the cell before becoming carcinogenic.

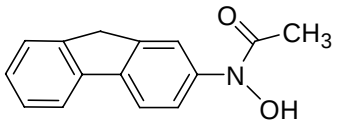

N-hydroxy-*N*-acetyl-2-aminofluorene

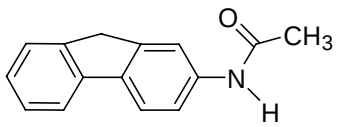

N-acetyl-2-aminofluorene

Figure 2.15 Examples of 2-aminofluorene carcinogens

Additional work done *in vitro* revealed that the ultimate carcinogenic metabolite is the ester of the *N*-hydrolated arylamine. *In vitro* at pH 7, the *N*-hydroxylated arylamines such as *N*-hydroxy-AAF or MAB fail to yield any covalently-bound adducts *in vivo* but displayed reactivity in acidic media.[50] While, the esters of these compounds, *N*-benzoyloxy-MAB or *N*-acetoxy-AAF react with the nucleophilic components in neutral conditions *in vitro* to yield arylamine bound macromolecules. Since the *N*-hydroxlated arylamine didn't react at neutral pH, it was concluded that *in vivo* the metabolite responsible for reacting with the nucleophiles was the esters of the arylamines.

Based on several *in vivo* and *in vitro* studies, it was confirmed that the N-hydroxylated arylamines are esterified via enzymatic activation. *In vivo*, the arylamines are initially oxidized by cytochrome P-450 monooxygenase enzyme to *N*-

hydroxylated amine which is then esterified by N,O-acetyl transferase.[40,48,51] (Scheme 2.27) The esters then react with nucleophiles via S_N1 or S_N2 pathways to yield the covalent adducts. For example, *N*-acetoxy-AAF reacts with methionine to yield 3-methylmercapto-AAF. It was proposed that the reaction could occur by one of two pathways: (1) S_N2, addition of methionine to *N* followed by the elimination of the acetoxy group or (2) S_N1, addition of methionine to the electrophilic intermediate, nitrenium ion, generated upon the elimination of acetoxy group.[48,51] (Scheme 2.28) Since the positive charge can be delocalized between the *ortho* carbon and the nitrogen, methionine adds to either one of the resonance forms. Methionine on the nitrogen rearranges on to the ortho carbon followed by the intramolecular cyclization of the methionine side chain to yield 3-methylmercapto-AAF and homoserine lactone. Methionine, free or linked to a peptide chain, produced similar final products confirming that the mechanism for the reaction was the same in both case. The other nucleophilic components were also assumed to react with esterified arylamines in similar manner.

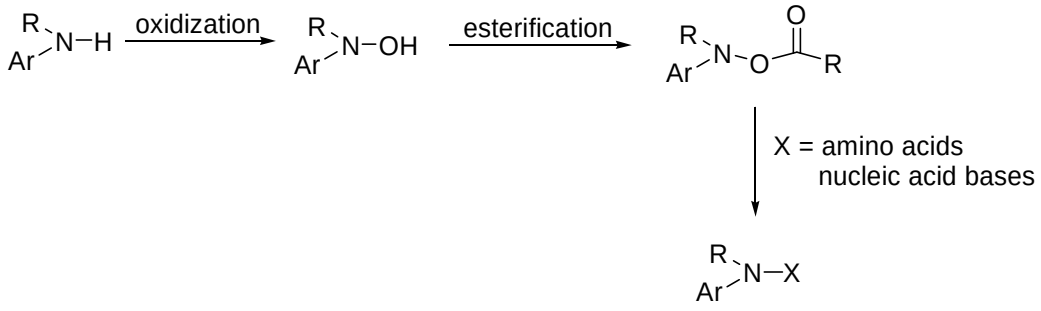

Scheme 2.27 Carcinogenic pathway of arylamines

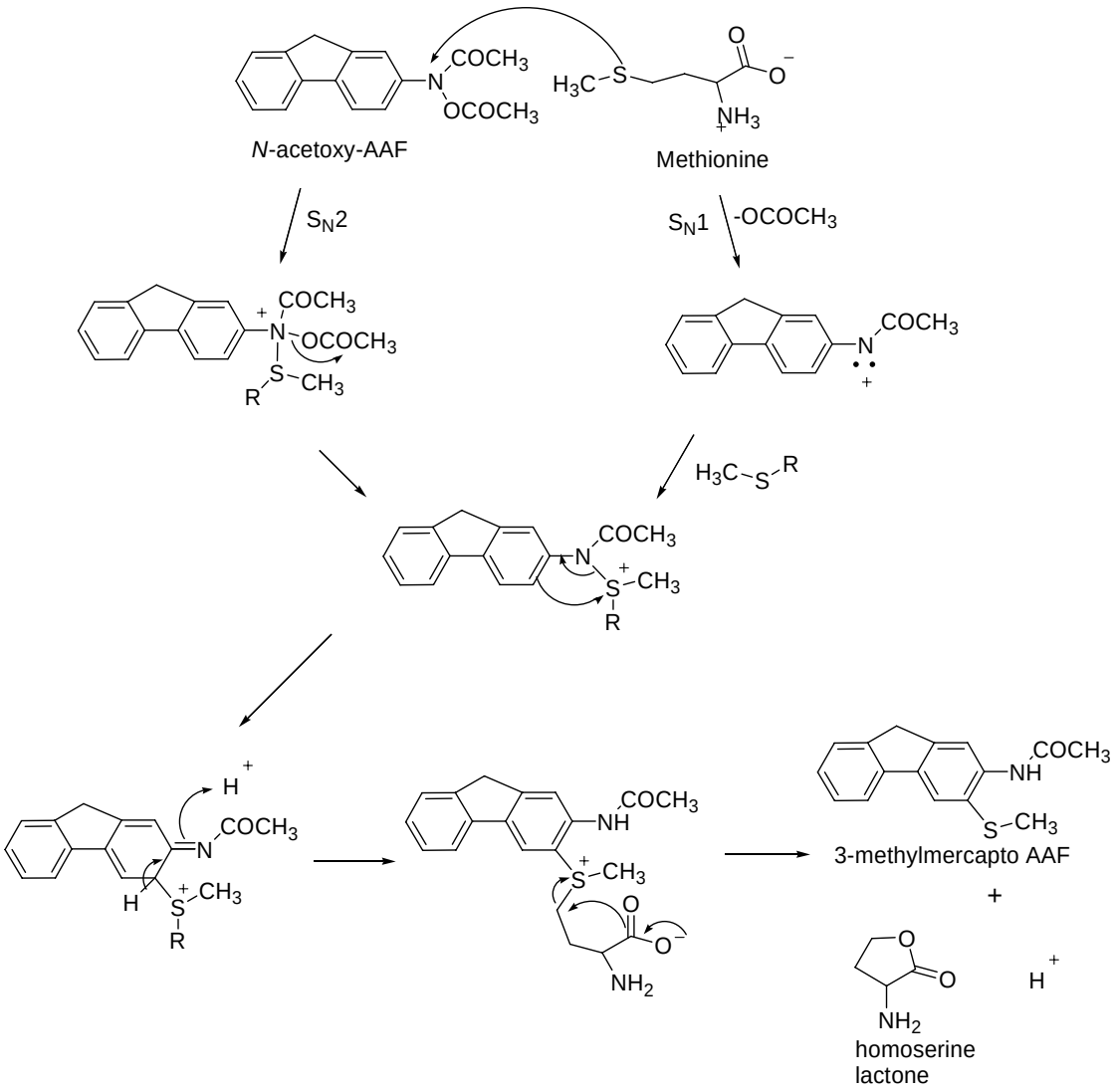

Scheme 2.28 Reaction of *N*-acetoxy-AAF with methionine

In addition to arylamines and amino dyes, several other amines were also observed to be converted to ultimate carcinogens via enzymatic activation. For examples, compounds such as dimethylnitrosoamine (**64**), *N*-phenyl-*N*-nitrosourea (**65**), 4-nitroquinoline *N*-oxide (**66**) are converted to electrophilic reagents that result in covalently bound proteins or nucleic acids.[51] (Scheme 2.29) These data suggest that the ultimate carcinogen is a strong electrophilic compound that is generated at the site of the tumor and was extremely reactive in neutral conditions. Even though it

was not obvious if the ester reacts directly with methionine or was initially converted to nitrenium ion before reaction. Since it was not possible to isolate the intermediate and the fact that it reacts with weak nucleophiles such as guanosine, it was concluded that final carcinogenic species was most likely nitrenium ion.

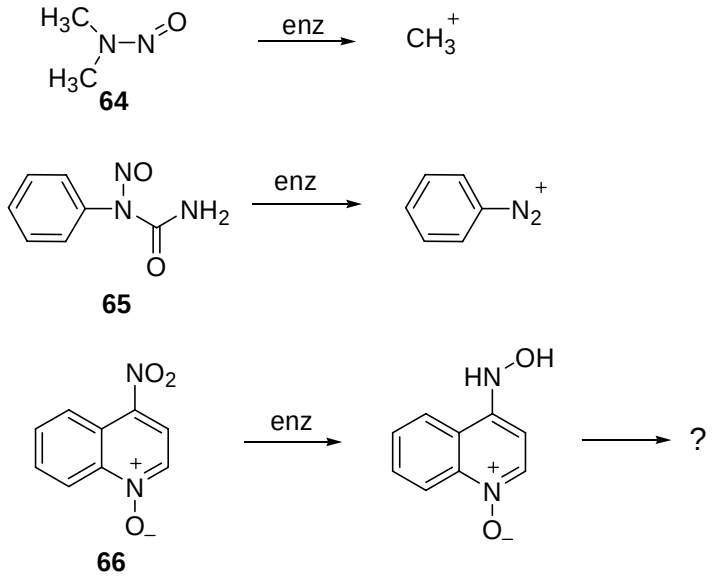

64 65 66

Scheme 2.29 Decomposition of potential carcinogens in biological systems

2.7 Nitrenium ions as carcinogens

Extensive studies conducted on a wide range of arylnitrenium ions confirmed that the latter are the final carcinogenic metabolites responsible for reacting with nucleophilic cell components in nucleic acids and proteins. The general chemical and physical characteristics required to exhibit carcinogenic properties were determined by competitive trapping and LFP methods. It was found that the remarkable stability of these ions in aqueous solution combined with their selectivity for nucleophiles contributes to the carcinogenicity.

The enhanced selectivity of these arylnitrenium ions for nucleophiles was one of the reasons that allow these ions to be carcinogenic. Most arylnitrenium ions react

with azides at the diffusion limit with a rate constant of ~10^9 $M^{-1}s^{-1}$. For 4-biphenylyl (**33**) and 2-fluorenyl nitrenium ions, these rate constants are 3-5 orders of magnitude faster than the reaction with H_2O.[20,21,26] Similar reactivities were observed with halides. Chloride and bromide react with 2,6-dimethylphenylnitrenium ion (**38**) with rate constants of (1.5-1.8) x 10^9 $M^{-1}s^{-1}$ and (4.1-4.3) x 10^9 $M^{-1}s^{-1}$ respectively.[24] These reaction rate constants show that the selectivity of the arylnitrenium ions for azide is greater than that for halides. For example, the selectivity ratio of *N*-acetyl-*N*-(4-biphenylyl)nitrenium ion for chloride and azide were measured to be the following: k_{cl}/k_s of 15.7 $\pm$ 0.8 M^{-1} and k_{az}/k_s of (2.9 $\pm$ 0.2) x 10^3 M^{-1} where k_{cl} and k_{az} were reaction rate constant of chloride and azide with the arylnitrenium ion and k_s was the decay constant of arylnitrenium in H_2O.[23,24,28] These values indicate that the both nucleophiles compete with the solvent for the arylnitrenium; however, the selectivity for azide is much greater than that for chloride.

Since DNA damage was of major concern, reactivities with several nucleic acids bases were studied. Guanosine and its derivatives react with various arylnitrenium ions at a rate constant of ~10^8-$10^9$$M^{-1}s^{-1}$. Deoxyguanosine (dG) is found to quench *N*-acetyl-*N*-(2-fluorenyl) nitrenium at a rate constant of 6.2 x 10^8 $M^{-1}s^{-1}$.[21,27,54,55] The reduced selectively for guanosine than for azide might be due to the cation-neutral vs cation-anion interaction. However, these rates showed that guanosine reacts efficiently with the nitrenium ion.

The major characteristics that allow arylnitrenium ions to be carcinogenic are their relative stability in aqueous solution. Compared to their arylcarbenium analogs, arylnitrenium ion live longer in aqueous media.[19,21,26] For example, the lifetimes of

67 and **68** in H_2O were measured to be 150 ns and 300 ns respectively.[19,56] (Figure 2.16) Also, the carbon analog (**69**) of *N*-acetyl-*N*-(2-fluorenyl) nitrenium ion (**70**) decays in H_2O with a rate constant of ~10^9 s^{-1}, whereas, the nitrenium ion decays only at a rate constant of 3.4 x 10^4 s^{-1}.[26,27] This showed that the nitrogen analog was much more stable in aqueous solution than the carbon analog. In **69**, the positive charge resides on the outside carbon; hence H_2O adds to that site readily. (Scheme 2.30) However, in **70**, the positively charge is delocalized into the ring causing the ring to lose its aromaticity. Hence, H_2O has a larger activation barrier to overcome in order to add to the carbon, thus reducing its reactivity with arylnitrenium ions. As a result, arylnitrenium ion are able to survive in aqueous solution long enough to react with other nucleophiles which is the case in biological systems.

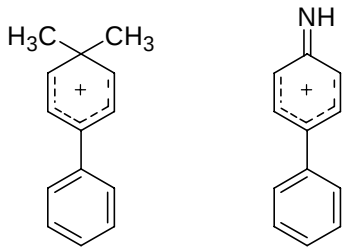

67 **68**

Figure 2.16 Structures of cyclohexadienyl cation from carbon and nitrogen analogs

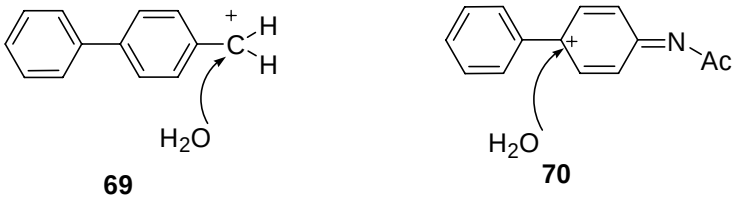

69 **70**

Scheme 2.30 Addition of H_2O to *N*-acetyl-*N*-(2-fluoreny)l nitrenium ion and its carbon analog

More attention has been focused in understanding the reaction mechanisms of the arylnitrenium ions with nucleic acid bases because DNA is responsible for the

genetic information. Since guanosine showed a greater affinity for arylnitrenium, its reaction pathway was studied extensively. Even though it has been established that the guanosine reaction with arylnitrenium results in the formation of the ion covalently binding to the C8 site in the guanosine to yield C8 adduct its actual reaction pathway is yet to be confirmed.

Novak and Humphreys proposed that the arylnitrenium ion initially adds to the N7 of guanosine and then rearranges to C8. According to Humphreys, N7 is the most basic site and C8 is the least basic site on guanosine, hence the most logical mechanism would be the attack of N7 on arylnitrenium ion.[57] He proposed that upon addition of the arylnitrenium on N7, the resultant positively charged species causes the C8 proton to become acidic. Therefore, deprotonation of the C8 carbon facilitates the shift of arylnitrenium ion from N7 to C8. (Scheme 2.31) In order to prove that the C8 proton become acidic, he conducted experiments using C^8, N^9-dimethylguanine and *N*-acetoxy-AAF. (Scheme 2.32) Following the reaction by ^{1}H-NMR, he reported observing a doublet and a quartet corresponding to the CH_3 group and the H which he claimed were on C8 of the intermediate **72**. However, upon waiting, these signals were replaced by a singlet. He suggested that the doublet and quartet belonged to the intermediate **72** that resulted from the addition of hydride to the carbocation formed by arylnitrenium ion attack. Since this C8 proton is now acidic, it can be deprotonated to facilitate the shift of the arylnitrenium ion.

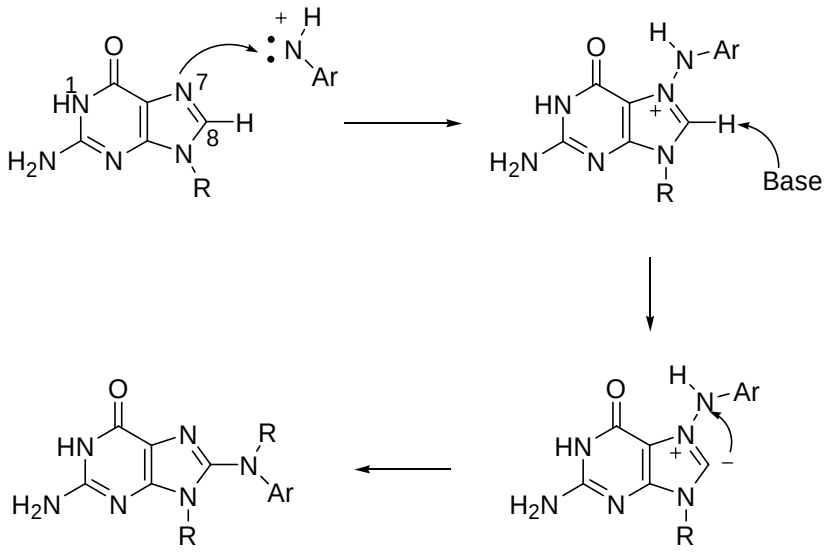

Scheme 2.31 Proposed mechanism for C8 adduct by Humphreys

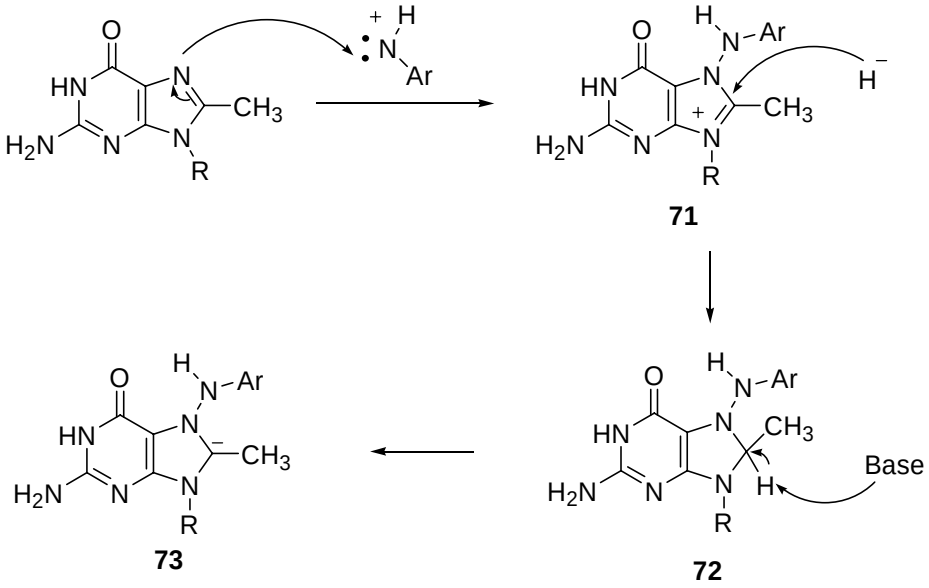

Scheme 2.32 Reaction of C^8, N^9-dimethylguanine with an arylnitrenium ion

Novak supported Humphreys' argument by conducting kinetic studies on various guanosine derivatives. Kinetic analysis of guanosine derivatives with varying N7-H^+ pKa showed that as the basicity of N7 of the derivatives decreases, the trapping rate constant by the nucleophiles also decreased.[58] At pKa $\leq$ 2.3, which is

the pKa for the protonated N7 of guanosine, rate of quenching by guanosine approached the diffusion limit. This was supported by the rates measured for the guanosine quenching of arylnitrenium ions such as 4-biphenylyl and 2-fluorenylnitrenium ions. The rates measured for 4-biphenylyl and 2-fluorenylnitrenium ions were 1.7×10^9 and 6.8×10^8 $M^{-1}s^{-1}$ respectively.[27,55] Novak argued that since guanosine is able to quench the arylnitrenium ion at the diffusion limit at the pKa that could protonate N7, it shows that the arylnitrenium ions has to add to the N7. Hence he was convinced that the arylnitrenium ion initially added to N7 before rearranging to C8.

McClelland argued against Novak and Humphreys' conclusions, claiming that the arylnitrenium ion adds directly to the C8 position of guanosine. He supported his theory by providing kinetic and LFP evidence for the formation of a C8 adduct.[21,59] McClelland followed the reaction between *N*-acetyl-2-aminofluorene with guanosine using LFP. Upon photolysis, the absorbance band corresponding to 2-fluorenylnitrenium ion was observed immediately after the laser; however, this signal was quenched rapidly to yield a weak absorption band below ~380 nm. He attributed this weak absorption to the positively charged C8 adduct, (**74**) formed as a result of the addition of arylnitrenium ion to C8 as shown in Scheme 2.33. He claimed that positively charge C8 adduct then undergoes deprotonation at C8 to yield the final compound (**75**). He verified this by conducting kinetic isotope studies. C8 deuterium isotope effects (k_H:k_D) of 7.4 and 6.1 at pH 7.6 and 4.6 respectively were observed for the decay of C8 adduct, indicating that the C-H bond at C8 was broken in RDS. Since it was confirmed that the C-H bond was broken, it supported the fact that a

positively charged C8 intermediate was formed, which suggesting that the arylnitrenium ion adds directly to C8.

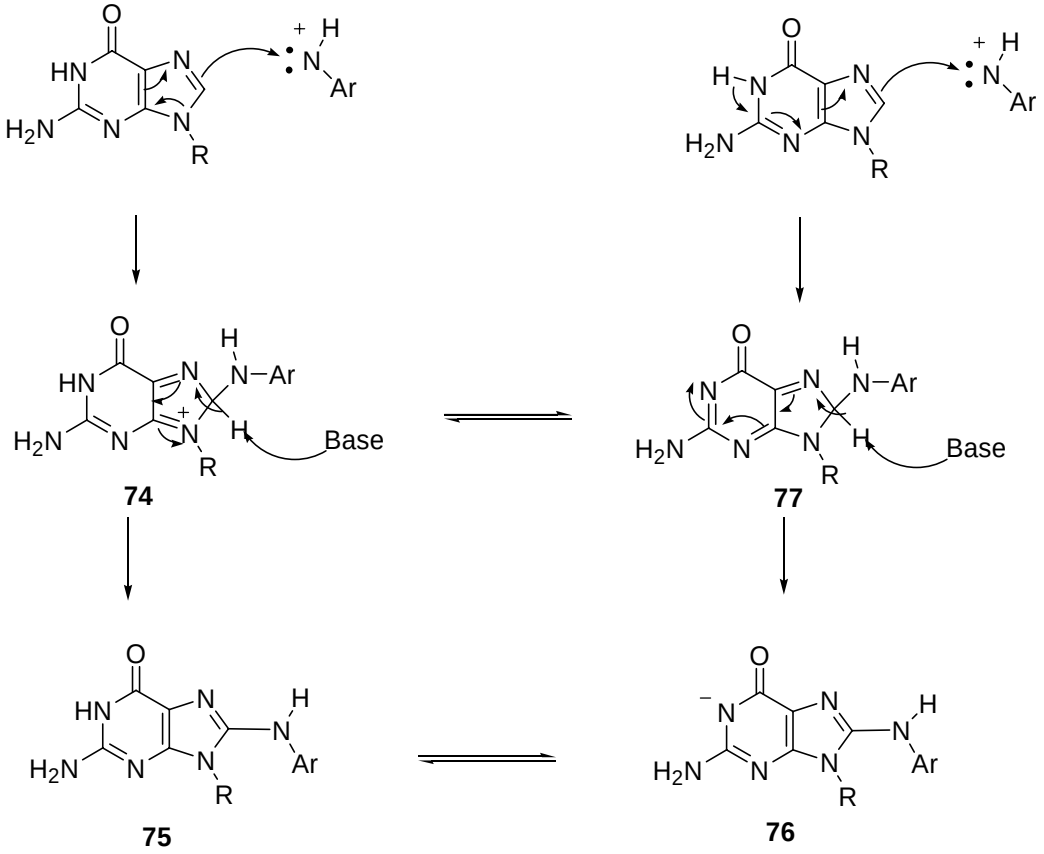

Scheme 2.33 Proposed mechanism for the formation of C8 adduct

Additionally, the pKa of 3.9 measured for the reaction supports the reaction scheme proposed by McClelland. This pKa was attributed to the acid/base capabilities of the C8 adduct mainly due to the N1 proton. Therefore, at this pKa, the N1 proton can be easily deprotonated or protonated during the reaction. He argued that if the attack occurred at N7, then the pKa of the reaction should be much higher. The pKa for the N7 methylated guanosine was measured to be 6.4. He felt that having arylnitrenium ion at N7 would not lower the pKa to 3.9. Hence the structure

present during the reaction was the C8 adduct and not N7 adduct. According to McClelland, the proposed mechanism showed more agreement with the process involving DNA. In DNA, N1 protons are involved in the H-bonding in DNA, therefore, they are easily protonated and deprotonated. Based on these results, McClelland proposed that the arylnitreniumion added directly to the C8 site of the guanosine because this pathway allowed for easier protonation and deprotonations of the nitrogen centers.

In addition to guanosine, adenosine and amino acids were shown to form covalently bound macromolecules with arylnitrenium. Adenosine was found to quench *N*-acetyl-4-biphenylyl and 4-biphenylyl nitrenium ion at a rate constant of 1.4 x 10^8 $M^{-1}s^{-1}$ and 3.1 x $10^7 M^{-1}s^{-1}$ respectively.[58] Only the purine nucleosides were observed to show reactivity towards arylnitrenium ions. Additionally, kinetic analysis performed on single and double stranded DNA reveals only the single stranded DNA was susceptible to arylnitrenium ion. A DNA oligomer d-ATGCAT reacts with *N*-acetyl-*N*-(2-fluorenyl) nitrenium ion with a rate constant of 9.62 x 10^7 $M^{-1}s^{-1}$ whereas the double stranded DNA shows very little reactivity.[54] This indicates that double stranded DNA is not affected by the arylnitrenium ion; however, the concern is during replication. During replication, the DNA is single stranded; hence it has a greater chance of being exposed to arylnitrenium ions in cells.

Even though, much importance has being given to DNA damage by arylnitrenium ions, these ions have also been shown to react with proteins. These ions react with the amino acids that are free or bound to the proteins. Vivo studies have isolated hepatic protein bound amino dyes which showed that proteins are also

susceptible to arylnitrenium ions.[49] Since DNA was involved in transferring genetic informations, more study was focused on its effects.

References

(1) Bamberger, E.; Lagutt, J. *Chem. Ber.* **1898**, *31*, 1500.

(2) Heller, H. E.; Hughes, E. D.; Ingold, C. K. *Nature* **1951**, *168*, 909-910.

(3) Abramovitch, R. A.; Davis, B. A. *Chem. Rev.* **1964**, *64*, 149-185.

(4) Stieglitz, J. L., P.N. *J. Am. Chem. Soc.* **1914**, *36*, 272-301.

(5) Gassman, P. G. *Acc. Chem. Res.* **1970**, *3*, 26-33.

(6) Gassman, P. G.; Campbell, G. A. *J. Am. Chem. Soc.* **1972**, *94*, 3891 - 3896.

(7) Gassman, P. G.; Cryberg, R. L. *J. Am. Chem. Soc.* **1969**, *91*, 5176-5177.

(8) Hoffman, R. V.; Christopher, N. B. *J. Org. Chem.* **1988**, *53*, 4769-4773.

(9) Hoffman, R. V.; Kumar, A.; Buntain, G. A. *J. Am. Chem. Soc.* **1985**, *107*, 4731-4736.

(10) Claus, P.; Doppler, T.; Gakis, N.; Georgarakis, M.; Giezendanner, H.; Gilgen, P.; Heimgartner, H.; Jackson, B.; Marky, M.; Narasimhan, N. S.; Rosenkranz, H. J.; Wunderli, A.; Hansen, H. J.; Schmid, H. *Pure Appl. Chem.* **1973**, *33*, 339-361.

(11) Haley, N. F. *J. Org. Chem.* **1977**, *42*, 3929-3933.

(12) Georgarakis, E.; Schmid, H.; Hensen, H.-J. *Helv. Chim. Acta.* **1979**, *62*, 234-269.

(13) Giovanni, E.; deSousa, B. F. S. E. *Helv. Chim. Acta.* **1979**, *62*, 185-197.

(14) Giovanni, E.; deSousa, B. F. S. E. *Helv. Chim. Acta.* **1979**, *62*, 198-204.

(15) Doppler, T.; Schmid, H.; Hensen, H.-J. *Helv. Chim. Acta.* **1979**, *62*, 271-303.

(16) Doppler, T.; Schmid, H.; Hensen, H.-J. *Helv. Chim. Acta.* **1979**, *62*, 304-313.

(17) Abramovitch, R. A. J., R. *Azides and Nitrenes*: *Reactivity and Utility;* Academic: New York, 1984.

(18) Takeuchi, H. H., S; Tanahashi, T; Kobayashi,A; Adachi, T; Higuchi, D. *J. Chem. Soc., Perkin. Trans. 2* **1991**, 847-855.

(19) McClelland, R. A. *Tetrahedron* **1996**, *52*, 6823 - 6858.

(20) McClelland, R. A.; Davidse, P. A.; Hadzialic, G. *J. Am. Chem. Soc.* **1995**, *117*, 4173-4174.

(21) McClelland, R. A.; Gadosy, T. A.; Ren, D. *Can. J. Chem.* **1998**, *76*, 1327-1337.

(22) Ramlall, P.; Li, Y.; McClelland, R. A. *J. Chem. Soc., Perkin Trans. 2* **1999**, 1601-1607.

(23) McClelland, R. A.; Kahley, M. J.; Davidse, P. A.; Hadzialic, G. *J. Am. Chem. Soc.* **1996**, *118*, 4794-4803.

(24) Fishbein, J. C.; McClelland, R. A. *Can. J. Chem.* **1996**, *74*, 1321-1328.

(25) Fishbein, J. C.; McClelland, R. A. *J. Am. Chem. Soc.* **1987**, *109*, 2824-2825.

(26) Davidse, P. A.; Kahley, M. J.; McClelland, R. A.; Novak, M. *J. Am. Chem. Soc.* **1994**, *116*, 4513-4514.

(27) McClelland, R. A.; Kahley, M. J.; Davidse, P. A. *J. Phys. Org. Chem.* **1996**, *9*, 355-360.

(28) Novak, M.; Kahley, M. J.; Eigen, E.; Helmick, J. S.; Peters, H. E. *J. Am. Chem. Soc.* **1993**, *115*, 9453-9460.

(29) Anderson, G. B.; Yang, L. L.-N.; Falvey, D. E. *J. Am. Chem. Soc.* **1993**, *115*, 7254-7262.

(30) Baetzold, R. C.; Tong, L. K. J. *J. Am. Chem. Soc* **1971**, *93*, 1347.

(31) Falvey, D. E. *Organic, Physical, and Materials Photochemistry*; Ramamurthy, V. S., K.S;, Ed.; Marcel Dekker: New York, 2000; Vol. 6, pp 249-284.

(32) Falvey, D. E. *Reactive Intermediate Chemistry*; Moss, R. A., Platz, M. S., Maitland Jones, J., Eds.; Wiley-Interscience: Hoboken, 2004; Vol. 1, pp 593 - 650.

(33) Falvey, D. E. *J. Phys. Org. Chem.* **1999**, *12*, 589 - 596.

(34) Falvey, D. E.; Cramer, C. J. *Tetrahedron Lett.* **1992**, *33*, 1705-1708.

(35) Chiapperino, D.; Anderson, G. B.; Robbins, R. J.; Falvey, D. E. *J. Org. Chem.* **1996**, *61*, 3195-3199.

(36) Sullivan, M. B.; Brown, K.; Cramer, C. J.; Truhlar, D. G. *J. Am. Chem. Soc.* **1998**, *120*, 11778-11783.

(37) Srivastava, S.; Ruane, P. H.; Toscano, J. P.; Sullivan, M. B.; Cramer, C. J.; Chiapperino, D.; Reed, E. C.; Falvey, D. E. *J. Am. Chem. Soc.* **2000**, *122*, 8271-8278.

(38) Srivastava, S.; Toscano, J. P. *J. Am. Chem. Soc.* **1997**, *119*, 11552-11553.

(39) Srivastava, S.; Falvey, D. E. *J. Am. Chem. Soc.* **1995**, *117*, 10186 - 10193.

(40) Gonzalez, C.; Restrepo-Cossio, A.; Marquez, M.; Wilberg, K.; Rosa, M. D. *J. Phys. Chem. A.* **1998**, *102*, 2732-2738.

(41) Cramer, C. J.; Falvey, D. *Tetrahedron Lett.* **1997**, *38*, 1515-1518.

(42) Srivastava, S.; Kercher, M.; Falvey, D. E. *J. Org. Chem.* **1999**, *64*, 5853-5857.

(43) Robbins, R. J.; Yang, L. L.-N.; Anderson, G. B.; Falvey, D. E. *J. Am. Chem. Soc.* **1995**, *117*, 6544 - 6552.

(44) Chiapperino, D.; Falvey, D. E. *J. Phys. Org. Chem.* **1997**, *10*, 917-924.

(45) Robbins, R. J.; Yang, L. L.-N.; Anderson, G. B.; Falvey, D. E. *J. Am. Chem. Soc* **1995**, *117*, 6544-6552.

(46) Chiapperino, D.; McIlroy, S.; Falvey, D. E. *J. Am. Chem. Soc.* **2002**, *124*, 3567-3577.

(47) Kung, A. C.; McIlroy, S.; Falvey, D. E. *J. Org. Chem.* **2005**, *70*, 5283-5290.

(48) Kriek, E. *Biochim. Biophys. Acta* **1974**, *355*, 177-203.

(49) Miller, E. C.; Miller, J. A. *Pharmacol. Rev.* **1966**, *18*, 805-838.

(50) Miller, E. C.; Lotlikar, P. D.; Miller, J. A.; Butler, B. W.; Irving, C. C.; Hill, J. T. *Mol. Pharmacol.* **1968**, *4*, 147-154.

(51) Miller, J. A.; Miller, E. C. *Physico-Chemical Mechanisms of Carcinogenesis, Jerusalem Symposia on Quantum Chemistry and Biochemistry. The Israel Academy of Sciences and Humanities,*; Bergmann, E. D., Pullman, B., Eds.: Jerusalem, 1969; Vol. 1, pp 237-261.

(52) Poirier, L. A. M., J. A.; Miller, E.C.; Sato, K *Cancer Res.* **1967**, *27*, 1600-1613.

(53) Cramer, J. W.; Miller, J. A.; Miller, E. C. *J. Biol. Chem.* **1960**, *235*, 885-888.

(54) Novak, M.; Kennedy, S. A. *J. Phys. Org. Chem.* **1998**, *11*, 71-76.

(55) Novak, M.; Kennedy, S. A. *J. Am. Chem. Soc.* **1995**, *117*, 574-575.

(56) McClelland, R. A.; Ren, D.; Ghobrial, D.; Gadosy, T. A. *J. Chem. Soc., Perkin Trans. 2* **1997**, 451-.

(57) Humphreys, G. W.; Kadlubar, F. F.; Guengerich, F. P. *Proc. Natl. Acad. Sci. USA.* **1992**, *89*, 8278-8282.

(58) Kennedy, S. A.; Novak, M.; Kolb, B. A. *J. Am. Chem. Soc.* **1997**, *119*, 7654-7664.

(59) McClelland, R. A.; Ahmad, A.; Dicks, A. P.; Licence, V. E. *J. Am. Chem. Soc.* **1999**, *121*, 3303-3310.

Chapter 3. Photolytic Studies of *N*-(4,4'-Dichlorodiphenyl) Nitrenium Ion and *N*-(4,4'-Dibromodiphenyl) Nitrenium Ion

Diphenylnitrenium ion (**78a**) is an example of a simple diarylnitrenium ion that has been studied extensively. Experimental and theoretical calculations show that these ions are ground state singlets. The π donating characteristics of the phenyl ring destabilizes the empty p orbital of the nitrogen, thus stabilizing the singlet state. Hence for the most part the highest charge density of **78a** is on the *ortho* and *para* phenyl carbons giving the ion an 'iminocyclohexadienyl cation-like' structure.[1,2] (Scheme 3.1)

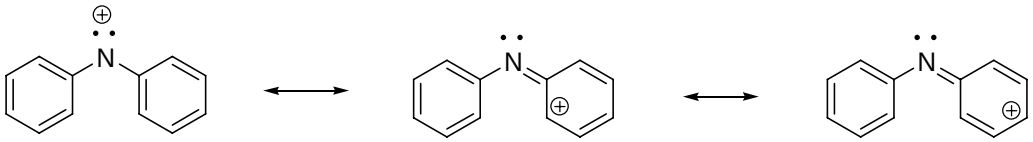

78a iminocyclohexadienyl cation

Scheme 3.1 Resonance structures for diarylnitrenium ion

Taking this into consideration, the goal of the research described in this chapter was to understand the effects of halogen substituents on **78a**. Halogens are generally considered to be electron-withdrawing through sigma bonds. However, due to the vast electron density around these atoms, halogens can also be electron-donors via π donation. Since **78a** is a known ground state singlet due to the electron-donating characteristics of the phenyl rings, our objective was to observe how substituting halogens in the phenyl would alter the chemical and kinetic properties of the **78a**.

3. 1 General Characteristics of Precursors (77b & 77c)

N-(4,4'-dichlorodiphenyl) nitrenium ion (**78b**) and *N*-(4,4'-dibromodiphenyl) nitrenium ion (**78c**) are the two halogenated nitrenium ions chosen for our study. These ions are photochemically generated from *N*-(4,4'-dichlorodiphenylamino)-2,4,6-trimethylpyridinium (**77b)** and *N*-(4,4'-dibromodiphenylamino)-2,4,6-trimethypyridinium (**77c**) tetrafluoroborate salts. (Scheme 3.2) These *N*-aminopyridinium salts were chosen for our study because they have proven to be ideal useful precursor for generating nitrenium ions photochemically.[3] Upon photolysis, the N-N bond is cleaved heterolytically to yield the desired nitrenium ion and 2,4,6-trimethylpyridine (collidine). Collidine is a mild base and is usually protonated. The tetrafluoroborate ion is very weakly nucleophilic and rarely reacts with electrophiles.

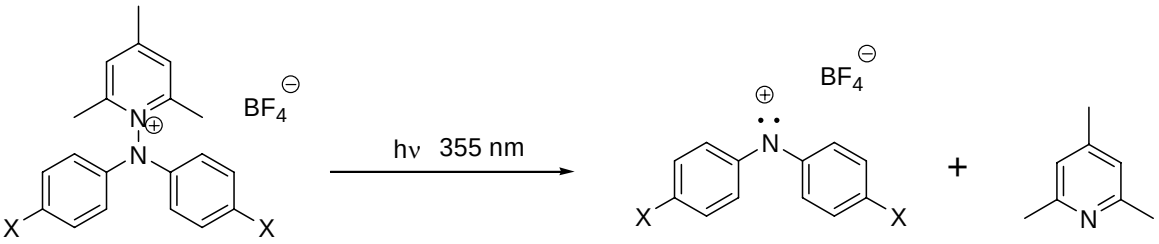

77a X = H
b X = Cl
c X = Br

78a X = H
b X = Cl
c X = Br

Scheme 3.2 General scheme for the photolysis of **77**

In addition, with *N*-aminopyridinium precursors one has the freedom to substitute any functional groups on nitrogen, thus allowing the study of nitrenium ions of a wide range of compounds. Before the introduction of *N*-aminopyridinium precursors, nitrenium ions were generated photochemically from anthranilium salts or azides. These methods are less flexible because nitrenium ions from anthranilium salts generate nitrenium ions with an *ortho* acetyl group and nitrenium ions from

azides require aqueous or acidic media. With pyridinium salts, nitrenium ions of any size and functional group can be generated with no restrictions to the solvent systems.

Precursor **77b** and **77c** were synthesized by coupling the corresponding hydrazines with 2,4,6-trimethylpyrylium tetrafluoroborate salts. (Scheme 3.3) The halogenated hydrazines were not available commercially, therefore, they were synthesized using procedures employed to synthesize similar pyridinium compounds such as **77a** and *N*-methyl-*N*-biphenylyl pyridinium salts. Dichlorodiphenyl amine (**79b**) is synthesized using the Goldberg procedure by refluxing 4-chloroacetanilide with 4-bromochlorobenzene in the presence of K_2CO_3 and CuI.[4] Compound **77c** was synthesized following the procedure developed in our lab.[5] Bromination of diphenylamine was accomplished by refluxing *N*-benzoyl-diphenylamine in bromine/CH_2Cl_2 followed by deprotection in NaOH and ethanol. The amines (**79b** and **79c**) were nitrosated using HCl and $NaNO_2$, followed by reduction using Zinc to yield the respective hydrazines (**81**). (Scheme 3.3) The hydrazines were then refluxed for an hour in substoichiometric amounts of pyrylium salt to produce the corresponding **77c** and **77b** in around 75 % yield.

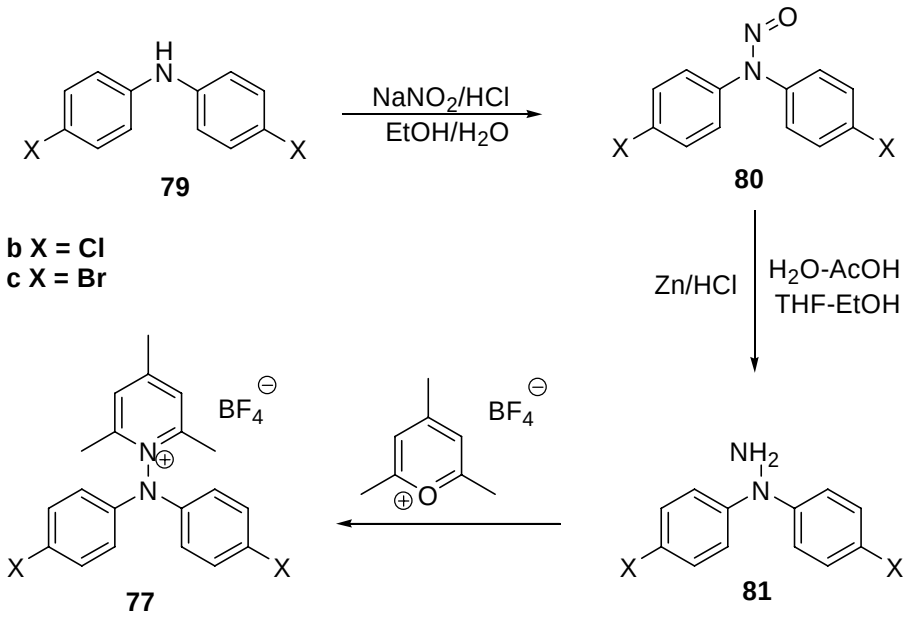

Scheme 3.3 General synthesis scheme of **77**

The chemical properties of these pyridinium precursors make them ideal for LFP studies. Compounds **77b** and **77c** are soluble in relatively polar solvents and have a weak UV absorption band between 300 – 400 nm. This property allows one to employ a 355 nm laser pulse to selectively excite **77b** and **77c** and thus avoid any possible secondary photolysis.

3.2 Characteristics of 78b and 78c

The species **78b** and **78c** were generated photochemically from **77b** and **77c** using laser flash photolysis (LFP, 355 nm, 20 ns, 50 mJ/pulse). Upon irradiation of **77b** or **77c** in CH_3CN, two strong UV absorbance bands with λ_{max} at 440 and 680 nm for **78b** and 450 and 690 nm for **78c** are observed immediately after the laser pulse. (Figure 3.1) These transient signals are attributed to the nitrenium ion generated upon the heterolytic cleavage of the N-N bond of the precursors as shown in scheme 3.2. The transient species are long-lived and decay in a first-order fashion. The photochemistry of these transient species studied by LFP, NMR, UV-Vis, product

analyses and density functional theory (DFT) calculations indicate that these transient species are indeed **78b** and **78c**.

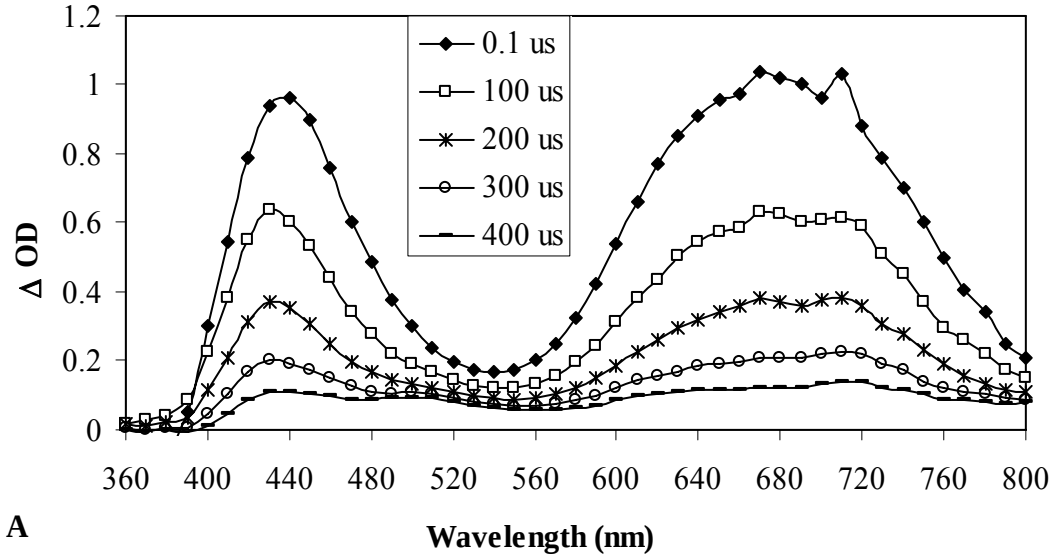

A

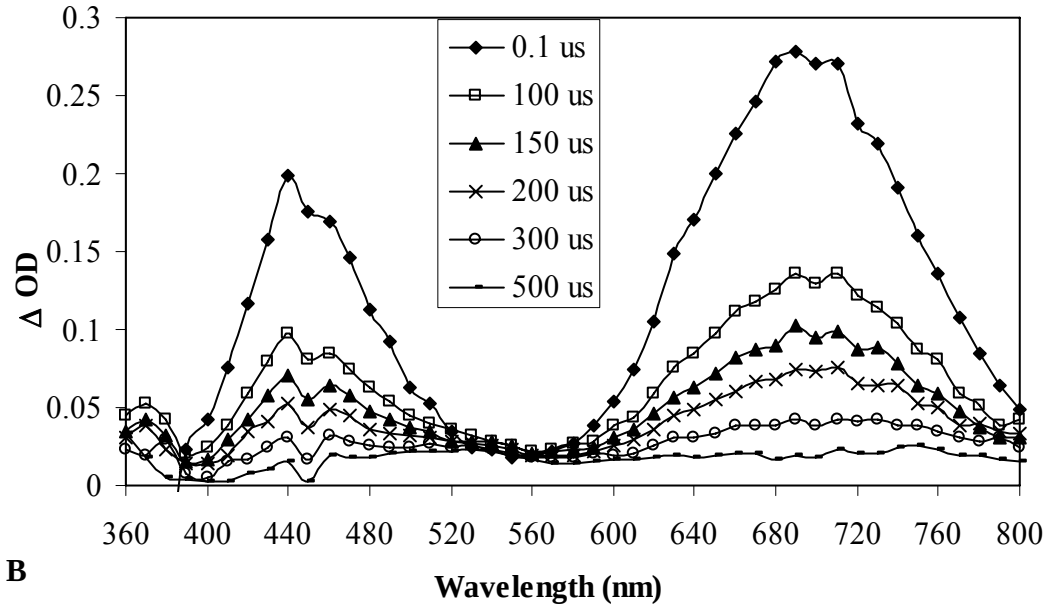

B

Figure 3.1 Transient spectra obtained upon photolysis of (A) **77b** and (B) **77c** in CH_3CN at longer time

These halogenated nitrenium ion are significantly more stable than any other arylnitrenium ions studied so far. They exist in CH_3CN or CH_2Cl_2 for few

microseconds with a lifetime of 240 μs for **78b** and 124 μs for **78c** in CH_3CN. Most arylnitrenium ions live only for several microseconds such as **78a** and *N*-4-biphenyly-*N*-methylnitrenium ion with lifetime of 1.5 and 24 μs respectively in CH_3CN.[2,6] Other arylnitrenium ions have similar lifespan which makes it difficult to detect and study these species.

Irrespective of the solvent, these ions are long-lived in almost all conditions. The transient spectra obtained in CH_3CN are indistinguishable to those obtained in CH_2Cl_2 and aqueous media. The only difference is that these transients decay much faster in aqueous media with a rate constant of 1.2×10^5 s^{-1} for **78b** (8.5 μs) and 1.5×10^5 s^{-1} for **78c** (6.5 μs) which is still slower than most arylnitrenium ions. Identical transient spectra were obtained both in N_2 or O_2 purged system. Especially in the presence of oxygen, the lifetime or the behavior of the transients are unaffected confirming that the transients obtained do not belong to any radical species as oxygen is a known radical quencher.

Calculations preformed by Density Functional Theory (DFT) predicted that these ions are ground state singlets. According to the calculations, the singlet states of **78b** and **78c** are 10.1 and 8.6 kcal/mol lower in energy than the triplet states (Table 3.1). These values are similar to the calculated ΔE_{ST} of most ground state singlet arylnitrenium ion that are in the range of -11.6 - -18.8 kcal/mol.[7] The ΔE_{ST} for diphenylnitrenium ion, the unsubstituted counterpart of **78b** and **78c** was calculated to be -11.2 kcal/mol.

Table 3.1 DFT Calculated ΔE_{ST} and singlet and triplet absorption and experimentally obtained absorbance and lifetimes

Nitrenium ions	ΔE_{ST} (kcal/mol)	Calculated singlet absorption (nm)	Calculated triplet absorption (nm)	Experimentally measured absorbance (nm)	τ (μs)
78a	-11.2[a]	645[b]	-	425, 680[c]	1.5 (CH_3CN)[c]
78b	-10.1	465, 637	589 (weak)	440, 680	240 (CH_3CN) 8.47 (H_2O) 291.5 (CH_2Cl_2)
78c	-8.6	465, 647	580 (weak)	450, 690	124 (CH_3CN) 6.57 (H_2O) 135.1 (CH_2Cl_2)

[a]Ref 8.[b]Ref 9.[c]Ref 6,10

Furthermore, UV-Vis absorption signals observed experimentally for these ions match the UV-Vis absorption signals predicted for the singlet state by time dependent-density functional theory (TD-DFT). The calculations predicted the singlet nitrenium ions to have absorbance maxima at 465 and 637 nm for **78b** and 465 and 647 nm for **78c**. (Table 3.1) As observed in Figure 3.1, the absorbances observed experimentally agree with the theoretical values within a few nanometers. DFT calculations also predict a weak band for triplet absorbance around 589 nm and 580 nm for **78b** and **78c** respectively. Careful examinations of the transient spectra do not show any such absorbance in that range. Based on these evidence, we conclude that **78b** and **78c** are ground state singlets.

3.3 Reaction with Simple Nucleophiles

Arylnitrenium ions generally react with simple nucleophiles (water, alcohols, azide, and chlorides) via nucleophilic substitution pathway. These nucleophiles

usually add to the *para* or *ortho* position of the phenyl ring of the arylnitrenium ion to yield σ-adducts. For example, **78a** reacts with chloride or methanol to give *para* and *ortho* addition products.[6,10] Hence **78b** and **78c** were also exposed to these nucleophiles to see if they follow the general trend observed for other arylnitrenium ions.

3.3.1 Product Analysis with Chloride

The salts **77b** or **77c** were photolyzed in the presence of NaCl to yield three stable photoproducts: *ortho* adduct (**82**), parent amine (**79**) and a carbazole-like product (**83**) with 100 % conversion. (Figure 3.2) 0.002 M of **77b** or **77c** with 0.015 M NaCl in 9:1 H_2O and CH_3CN was photolyzed under room light for a week. The final photoproducts obtained were isolated and characterized by NMR and MS. Compound **82** and **79** were obtained in a 1:1 mol ratio with trace amounts of compound **83**.

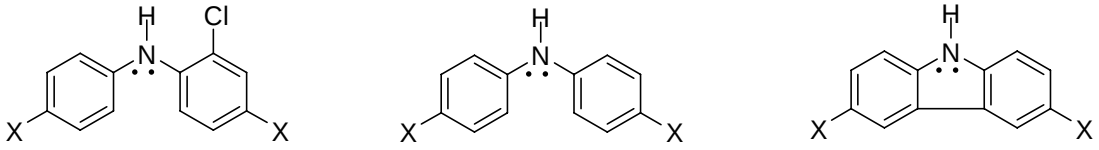

82 b X = Cl
c X = Br

79 b X = Cl
c X = Br

83 b X = Cl
c X = Br

Figure 3.2 Photoproducts obtained upon photolysis of precursor in the presence of chloride

Compound **82** was formed as a result of the nucleophilic addition of chloride to the *ortho* position of one of the phenyl ring of the nitrenium ion. (Scheme 3.4) Since the positive charge of the nitrenium ion is delocalized between the nitrogen and the *ortho* or *para* carbon of the phenyl ring, chloride can add to either one of the positive sites. However, due to substitution at the *para* position, only the *ortho*

adduct was isolated. It is possible that the *para* adduct was also formed but is not observed because the chloride adds reversibly to the *para* position but was eliminated to give back **78b** or **78c**. This has been observed before with other *para* substituted *N*-methyl-*N*-arylnitrenium ions.[2,11] In the case of **78b** and **78c**, both *para* and *ortho* adducts are obtained because the *para* position is unsubstituted.

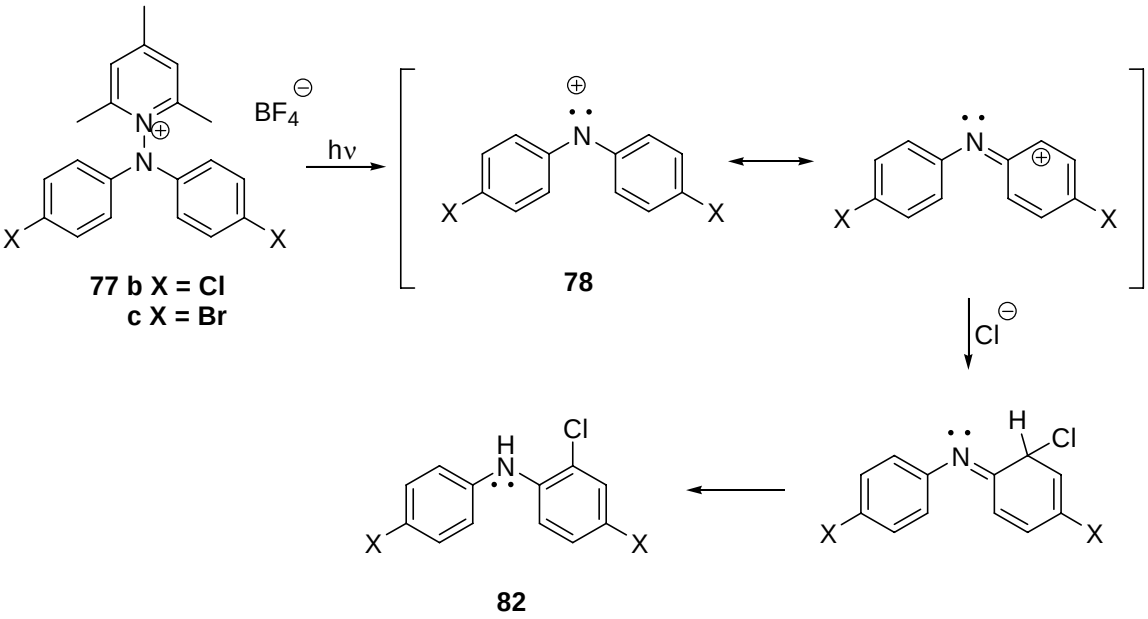

Scheme 3.4 Mechanism for the formation of **82**

In addition to the **82**, non-nucleophilic addition products such as **79** and **83** are also obtained. In order to obtain **79** from **78b** or **78c**, two electrons and subsequent protonation was required. This is thought to occur via oxidative elimination of chlorine from the *N*-adduct obtained as a result of the nucleophilic addition of chloride to the nitrogen center. (Scheme 3.5) However, more experiments are needed to verify this pathway.

In addition to **79**, trace amounts of **83** are observed. It is not unusual to observe **83** for diphenyl systems; yet it is generally observed only in the absence of

traps as a result of the intramolecular cyclization of **78a**.[12] Therefore, it is quite unusual to obtain **83** in the presence of a trap, especially chloride. Chloride reacts with **78b** and **78c** at an order of 10^{10} $M^{-1}s^{-1}$, at the diffusion limit. Hence, at this diffusion limited step, no carbazole should be formed due to the fact that chloride quenches the nitrenium ion before it could cyclize. We believe that **83** is formed as a result of the secondary photolysis of **79**. Since only trace amounts of **83** was obtained, further study of this matter was not pursued.

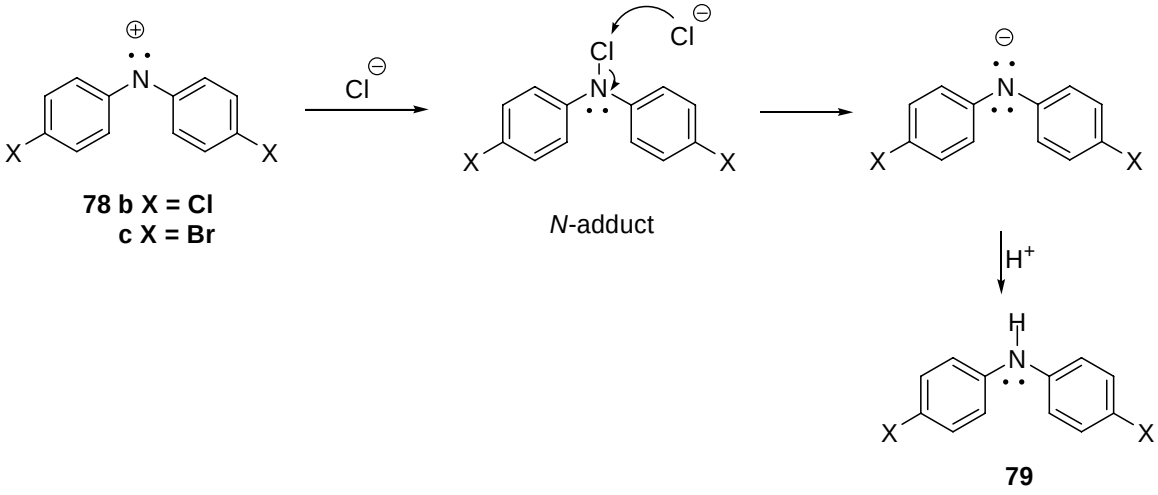

Scheme 3.5 Proposed mechanism for the oxidative elimination of chloride to yield **79**

3.3.2 Competitive Trapping Studies with Simple Nucleophiles

Quenching studies were performed to determine the relative reactivities of nitrenium ions with simple nucleophiles. Shown in Table 3.2 are the bimolecular reaction rate constants of the quenching of **78b** and **78c** by some nucleophiles measured by LFP. The rates depend on the nucleophilicity of the traps. Chloride reacts with **78b** and **78c** at the diffusion limit as expected based on similar results with **78a**.[6] This diffusion limited rate confirms that **78b** and **78c** are ground state

singlet because chlorides usually undergo two electron chemistry and react rapidly with electron deficient site.

Table 3.2 Second order reaction rate constant of **78b** and **78c** in the presence of nucleophile

Traps	k_{nuc} ($M^{-1}s^{-1}$)		
	78a	**78b**	**78c**
chloride[a]	1.0×10^{10} [b]	$(1.06 \pm .03) \times 10^{10}$	$(9.83 \pm .60) \times 10^{9}$
water	6.1×10^{5} [b]	$(1.51 \pm .16) \times 10^{4}$	$(1.12 \pm .01) \times 10^{4}$
methanol	5.2×10^{6} [b]	$(1.07 \pm .12) \times 10^{5}$	$(7.74 \pm .48) \times 10^{4}$
ethanol	4.9×10^{6} [b]	$(1.05 \pm .08) \times 10^{5}$	$(8.18 \pm .59) \times 10^{4}$
2-propanol		$(4.28 \pm .38) \times 10^{4}$	$(2.30 \pm .61) \times 10^{4}$
dGMP[c]		$(5.56 \pm .41) \times 10^{8}$	$(7.65 \pm .20) \times 10^{8}$

[a] nBu_4NCl is the source of chloride. [b] Ref 6.
[c] deoxyguanosine 5'-monophosphate disodium salt in 9:1 buffer (phosphate buffer, 25 mM, pH 7.5) / CH_3CN.

However, **78b** and **78c** react with water and alcohols at a much slower rate than **78a**. The reduced reactivity of **78b** and **78c** with water and alcohol might be due to the inhibition of substitution at the *para* position and the stability of the nitrenium ion. Water and alcohols generally add to the *para* position of the phenyl ring of any arylnitrenium ion. Reactions between **78a** and methanol yielded products with $-OCH_3$ on the *para* position.[6] Additionally, the positive charge on the nitrogen is stabilized by the halogens via π-donation reducing the electrophilicity of the ion, thus causing it to be less reactive to traps that are less nucleophilic.

The reduced reactivities of **78b** and **78c** with water compared to other nucleophiles become relevant in biological environments. Trapping studies with dGMP (deoxyguanosine 5'-monophosphate disodium salt) showed that the nucleic base quenches **78b** and **78c** at a rate constant of 10^8 $M^{-1}s^{-1}$, 4 orders of magnitude faster than water (10^4 $M^{-1}s^{-1}$). (Table 3.2) As a result of this, nitrenium ion can exist

long enough in aqueous medium to react with guanosine. This stability would pose a threat to the biological systems, since these systems are comprised mostly of water. Most arylnitrenium ions are carcinogens because they exist long enough in the aqueous media of the cells to be able to react with other electron rich nucleophiles such as amino acids and nucleic bases in the cells. Hence **78b** and **78c** can be a potential carcinogen if exposed to living cells.

3.4 Reaction with π-Nucleophiles

Most arylnitrenium ions react rapidly with arenes via the electron transfer pathway or the nucleophilic substitution pathway.[11,13] The nitrenium ions, **78b** and **78c,** were also exposed to nine arenes shown in Figure 3.3 to determine their reaction mechanism. These arenes have a wide range of oxidation potential and some were chosen for the orientation of the substituents on the phenyl ring. The reactivity of the arenes with the nitrenium ion and the reaction process between the arenes and the nitrenium ions were followed by LFP.

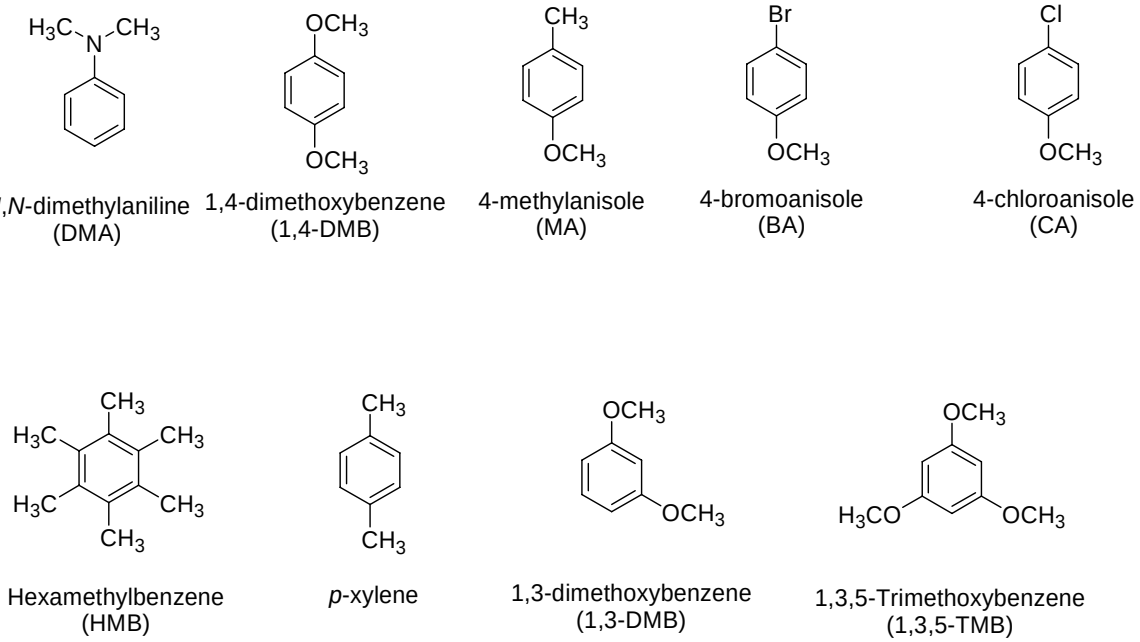

Figure 3.3 Arenes used for the study

3.4.1 Electron Transfer from Arenes

Transient spectra recorded following LFP show that arenes such as *N*,*N*-dimethylaniline (DMA), 1,4-dimethoxybenzene (DMB), hexamethylbenzene (HMB) and 4-methylanisole (MA) react with **78b** and **78c** via an electron transfer pathway. Shown in Figure 3.4 is the transient spectrum of **78b** and **78c** in the presence of DMA. Upon photolysis of **77b** or **77c** in the presence of 0.5-1 mM DMA, signals corresponding to **78b** or **78c** were observed immediately after the laser pulse. As these signals decays and a new long-lived broad absorbance band with λ_{max} at 760 nm was observed. The signal at 760 nm was assigned to the aminyl radical (**84**) resulting from electron transfer from DMA to the nitrenium ion **78b** or **78c** to yield **84** and $DMA^{\bullet+}$. (Scheme 3.6) The signal corresponding to $DMA^{\bullet+}$ was observed at 480 nm.[14] In order to verify that the signal at 760 nm does indeed belong to **84**, the latter was generated via an alternate pathway. Lustzyk el. al have shown that irradiation of *N*-nitrosoamine cleaves the N-N bond homolytically to produce the aminyl radical of the parent amine and NO radical.[15] (Scheme 3.7) Therefore, 1,1-di(4-chlorophenyl) nitrosoamine (**80b**) and 1,1-di(4-bromophenyl) nitrosoamine (**80c**) were photolyzed in CH_3CN. (Scheme 3.7) A broad signal at 760 nm resembling that seen in Figure 3.5 was observed, confirming that the signal at 760 nm was due to the formation of **84** from the nitrenium ion and DMA.

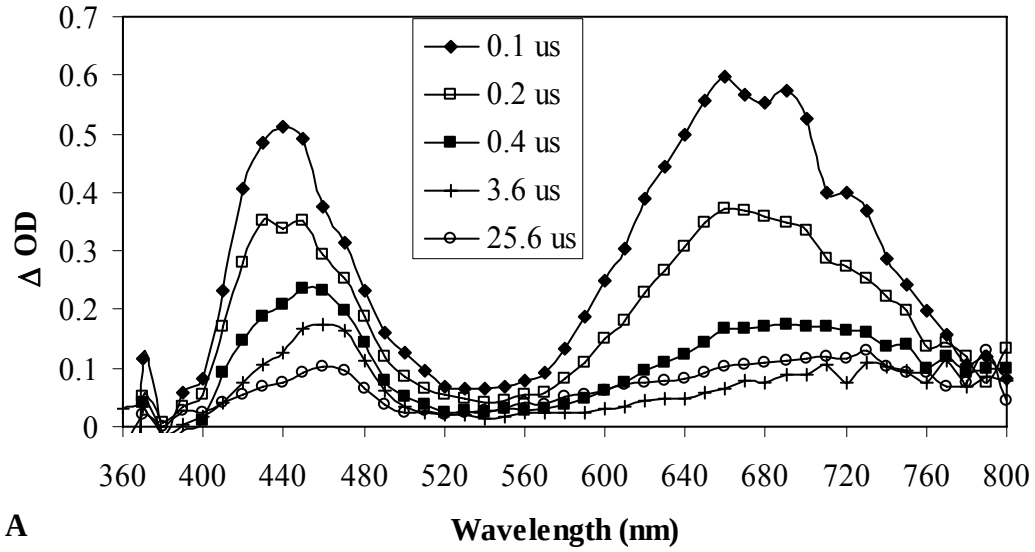

A

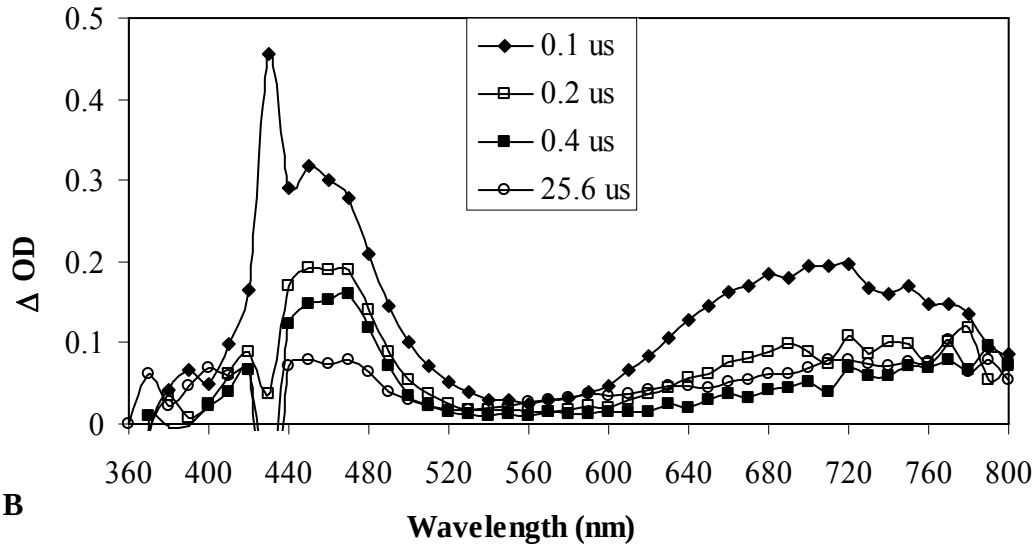

B

Figure 3.4 Transient spectra of the photolysis of (A) **77b** and (B) **77b** in the presence of 0.001 and 0.005 M *N*,*N*-DMA respectively in CH_3CN

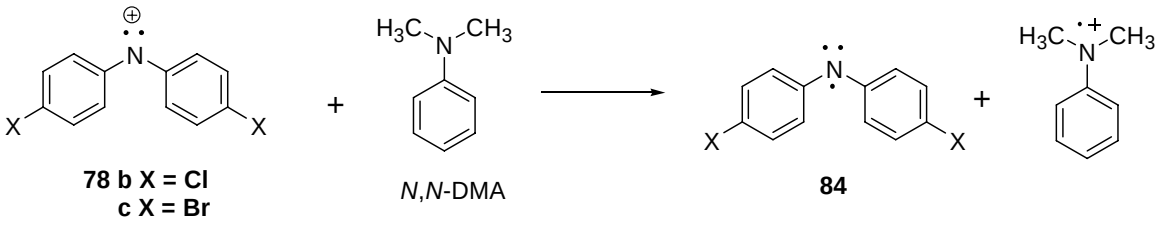

Scheme 3.6 Mechanism of electron transfer from *N*,*N*-DMA to **78**

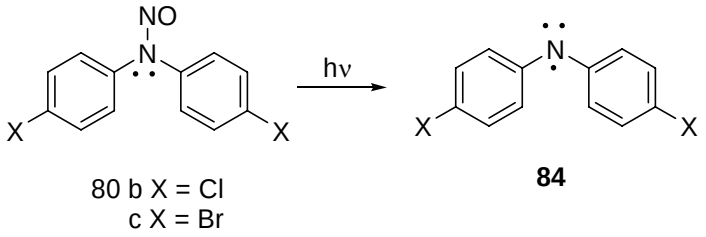

Scheme 3.7 Photolysis of **80**

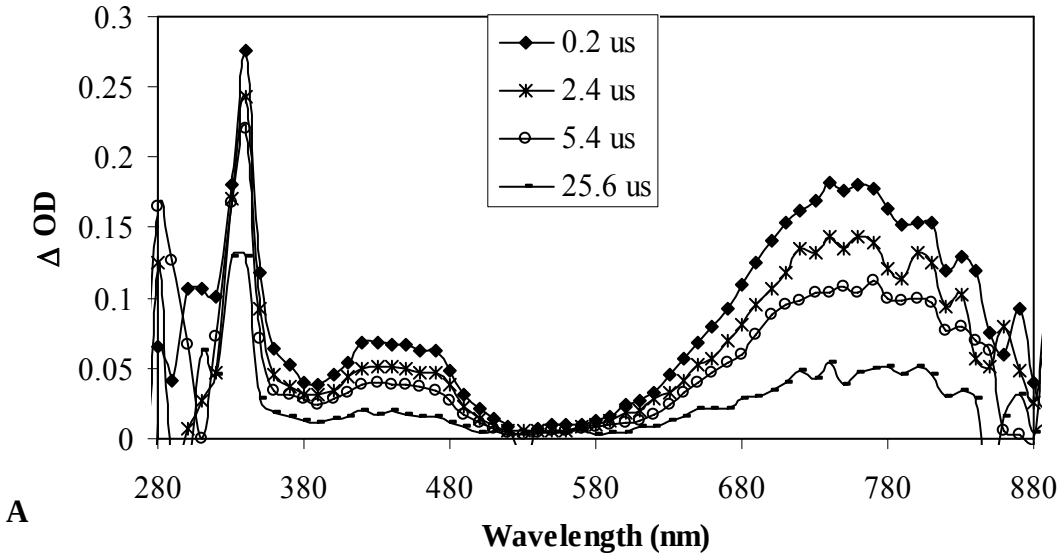

A

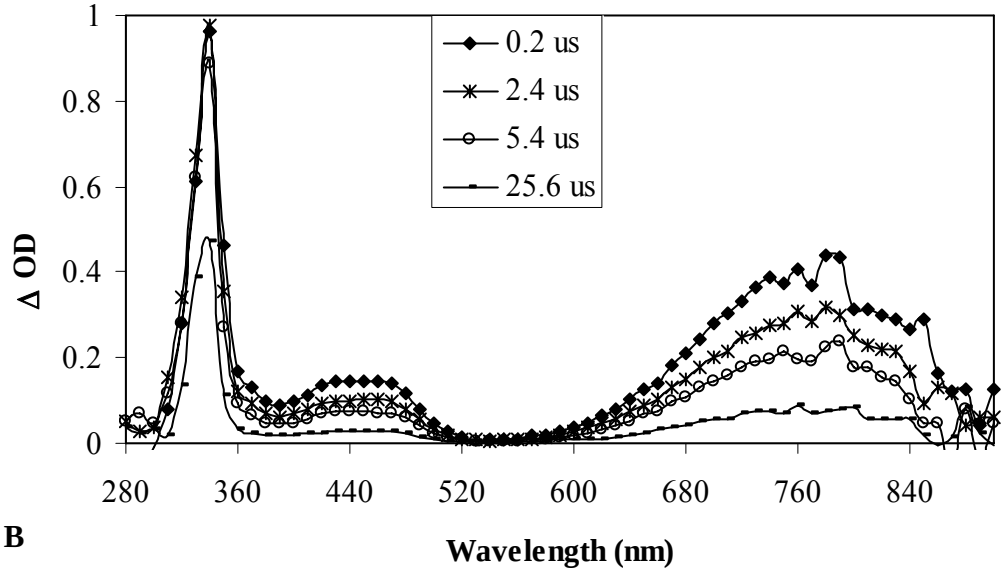

B

Figure 3.5 Transient spectra of the photolysis of (A) **80b** and (B) **80c** in CH_3CN

Likewise, shown in Figure 3.6 are the transient spectra from the photolysis of **77b** and **77c** with 0.05 M 1,4-DMB. Formation of the nitrenium ion was observed immediately following the laser pulse along with a new signal at 720 nm or 730 nm. (Figure 3.6) This new species was attributed to be the radical cation (**85**) of **79** formed via electron abstraction followed by protonation of the nitrenium ion. The

nitrenium ions, **78b** or **78c** abstracts an electron from the arene to generate **84** which is protonated immediately to yield **85**. (Scheme 3.8) Since **84** are basic, they are easily protonated in protic solvents, which was not observed in the presence of *N*,*N*-DMA.[16]

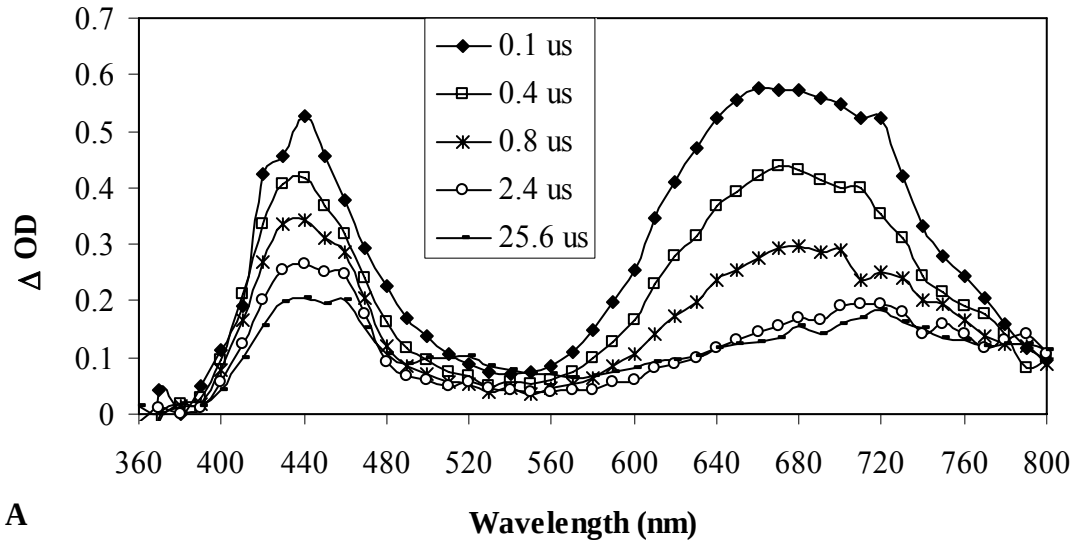

A

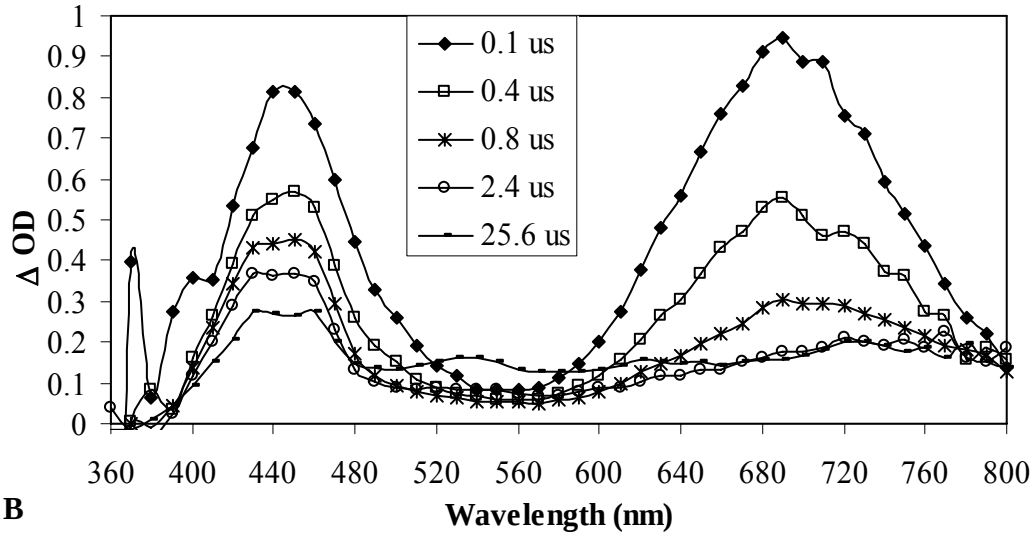

B

Figure 3.6 Transient spectra of the photolysis of (A) **77b** and (B) **77c** in the presence of 1,4-DMB (0.05 M) in CH_3CN

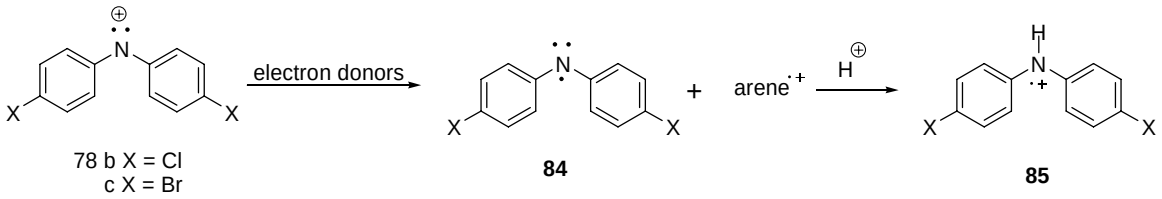

Scheme 3.8 Mechanism for the formation of **85** from **78b** and **78c**

The species **85** was generated by a different route in order to confirm the identity of the signal at 720/730 nm. The corresponding parent amines **79** were irradiated in the presence of 1,4-dicyanobenzene (DCB) causing the transfer of an electron from the excited state of **79** to DCB resulting in the formation of **85** and $DCB^{\bullet -}$. (Scheme 3.9) Radical cation obtained by this route also generates a sharp peak around 720/730 nm (Figure 3.7), confirming that the new transient observed in Figure 3.6 is indeed **85**. Even though both DMA and 1,4-DMB initially donated an electron to **78b** and **78c** to generate **84**, the latter generated in the presence of DMB is protonated immediately to **85**.

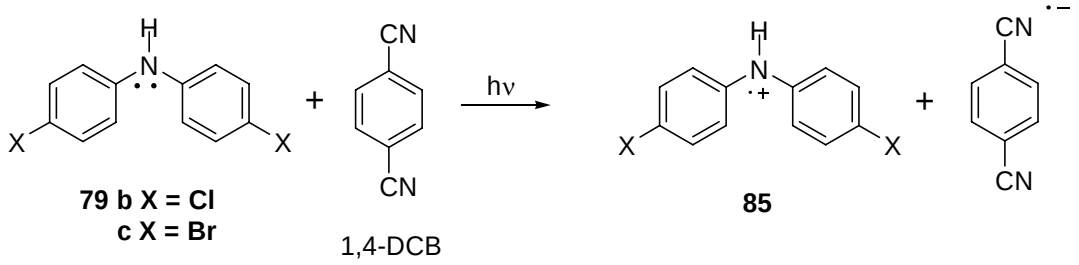

Scheme 3.9 Mechanism of electron transfer from **79** to DCB

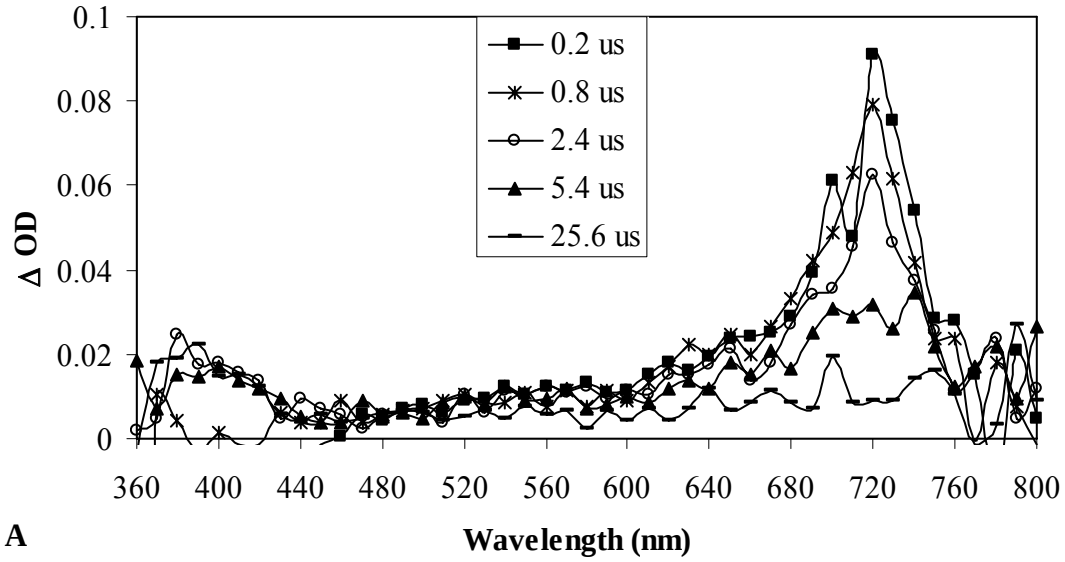

A

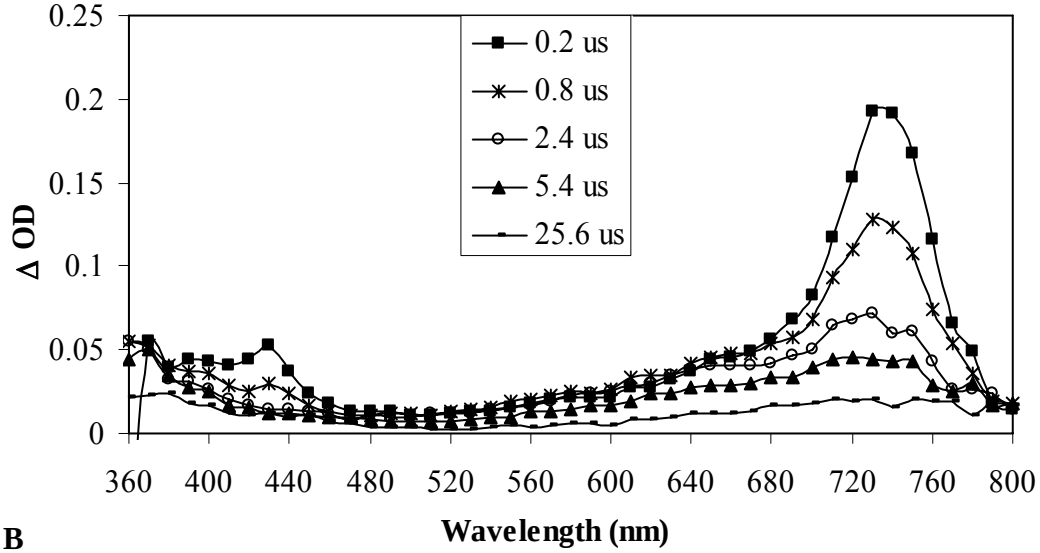

B

Figure 3.7 Transient spectra of the photolysis of (A) **77b** and (B) **77c** in the presence of 1,4-DCB (0.05 M) in CH_3CN

The species **85** was also observed in the presence of other arenes such as HMB and MA indicating electron transfer mechanism. (Figure 3.8 & 3.9) However, arenes such as 4-bromoanisole, 4-chloroanisole and *p*-xylene had no significant effect on the lifetime of **78b** and **78c**. This might be due to the fact that the oxidation

potential of these arenes is too high to donate electrons to the nitrenium ions. This will be discussed in detail later in the chapter.

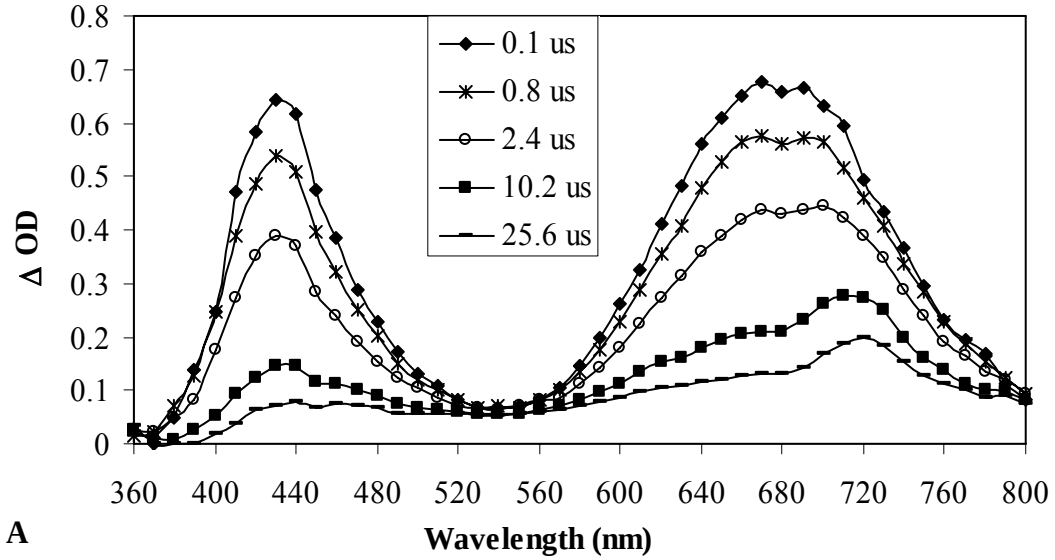

A

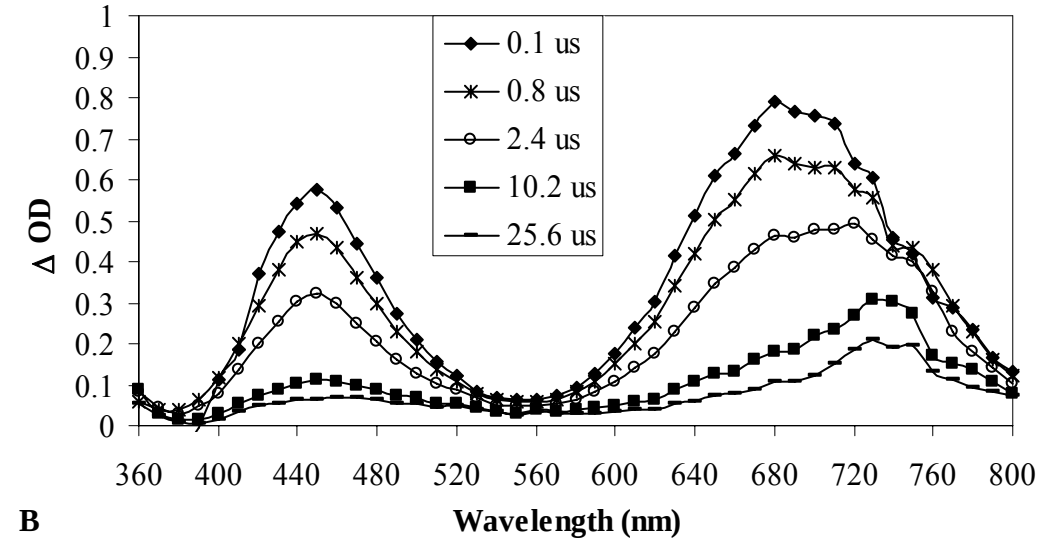

B

Figure 3.8 Transient spectra of the photolysis of (A) **77b** and (B) **77c** in the presence of 0.02 M HMB in CH_3CN

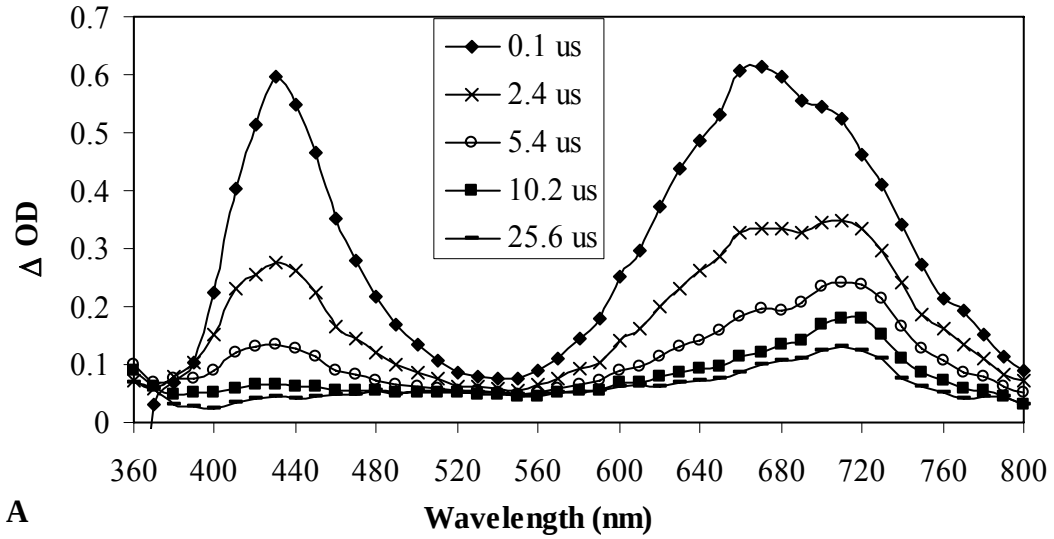

A

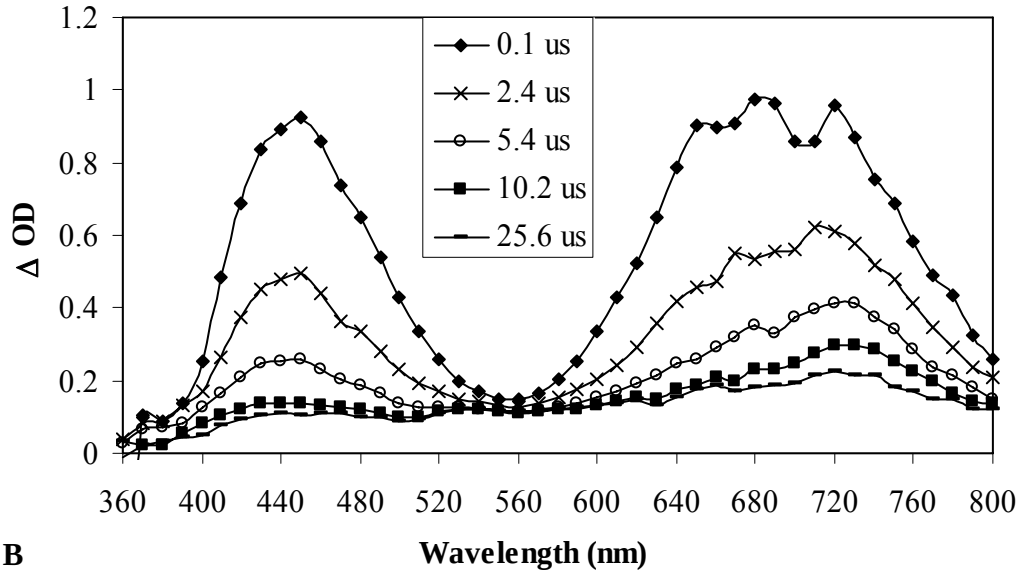

B

Figure 3.9 Transient spectra of the photolysis of (A) **77b** and (B) **77c** in the presence of 0.8 M 4-MA in CH_3CN

3.4.2 Competitive Trapping studies with Arenes

The bimolecular reaction rate constants of the arenes with **78b** and **78c** measured in CH_3CN are shown in table 3.3. From table 3.3 (excluding 1,3-DMB and 1,3,5-TMB), it can be seen that there is some correlation between the rate constants

and the oxidation potentials (E_{ox}) of the arenes. 1,3-DMB and 1,3-5-TMB react with **78b** and **78c** via a nucleophilic addition pathway which will be discussed later in the chapter.

Table 3.3 Second order rate constant for the quenching of **78b** and **78c** by the arenes

Traps	E_{ox} (V vs. SCE)	k_{nuc} ($M^{-1}s^{-1}$)		
		78a	**78b**	**78c**
N,*N*-DMA	0.53[a]	7.3×10^{9}[e]	$(5.06 \pm .20) \times 10^{9}$	$(6.01 \pm .40) \times 10^{9}$
1,4-DMB	1.34[b]	2.0×10^{9}[e]	$(2.45 \pm .14) \times 10^{7}$	$(4.03 \pm .23) \times 10^{7}$
Hexamethylbenzene	1.62[c]		$(7.49 \pm .12) \times 10^{6}$	$(8.08 \pm .40) \times 10^{6}$
4-methylanisole	1.67[d]	3.9×10^{5} [f]	$(2.45 \pm .10) \times 10^{5}$	$(3.85 \pm .03) \times 10^{5}$
4-bromoanisole	1.78[d]		-	-
4-chloroanisole	2.00[d]		-	-
p-xylene	2.01[c]		-	-
1,3-DMB	1.49[b]	3.3×10^{8} [f]	$(2.45 \pm .08) \times 10^{8}$	$(4.21 \pm .75) \times 10^{8}$
1,3,5-TMB	1.49[b]	2.4×10^{9} [f]	$(1.34 \pm .09) \times 10^{9}$	$(5.17 \pm .24) \times 10^{9}$

[a]Ref 17. [b]Ref 18. [c]Ref 19. [d]Ref 20. [e]Ref 12. [f]Ref 21

Of the arenes that react via electron transfer, we observed that only DMA quenches **78b** and **78c** at the maximum allowed rate or the diffusion limit. DMA has an E_{ox} of 0.53 V, therefore is easily oxidized. However, as the E_{ox} of the arenes increases, the reaction rate decreases. 1,4-DMB quenches **78b** and **78c** at a rate constant of 10^{7} $M^{-1}s^{-1}$, where as 4-MA with an E_{ox} of 1.67 V quenches the species at a rate constant of 10^{5} $M^{-1}s^{-1}$. Similar correlation between the reaction rate and the E_{ox} was observed for **78a**. However, for **78a**, arenes with E_{ox} of 1.34 V and below reacted at the diffusion limit.[21] Even though we do not have enough data to estimate this limit for **78b** and **78c**, we believe that this limit is much lower than 1.3 V, somewhere closer to 0.53 V.

In addition, we observe that only arenes with E_{ox} below 1.78 V are capable of reducing **78b** or **78c**. LFP experiments on **77b** and **77c** in the presence of *p*-xylene

and 4-chloroanisole show that these nucleophiles have little or no effect on the lifetime of **78b** and **78c**. (Figure 3.10 & 3.11) Furthermore, no measurable quenching of **78b** or **78c** was observed with 4-bromoanisole. (Figure 3.12) All three arenes have E_{ox} above 1.78 V. Since these arenes are unable to donate electrons to **78b** or **78c**, no reactivity was observed. Even though we do not have enough data to exactly predict the E_{ox} required to do electron transfer, it is reasonable to assume that this threshold level is somewhere between 1.67 V and 1.78 V.

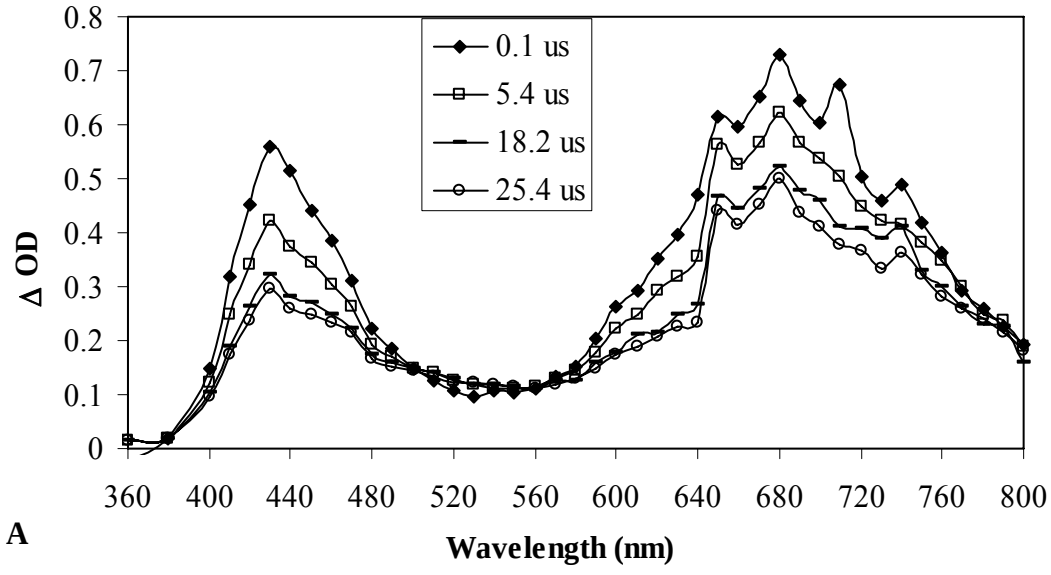

A

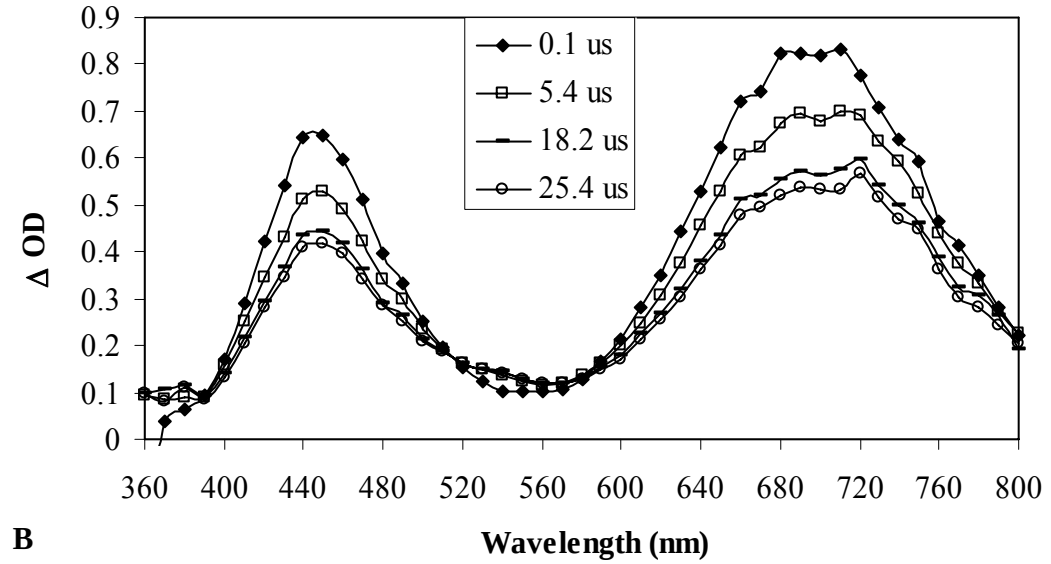

B

Figure 3.10 Transient spectra of the photolysis of (A) **77b** and (B) **77c** in the presence of 1 M *p*-xylene in CH_3CN

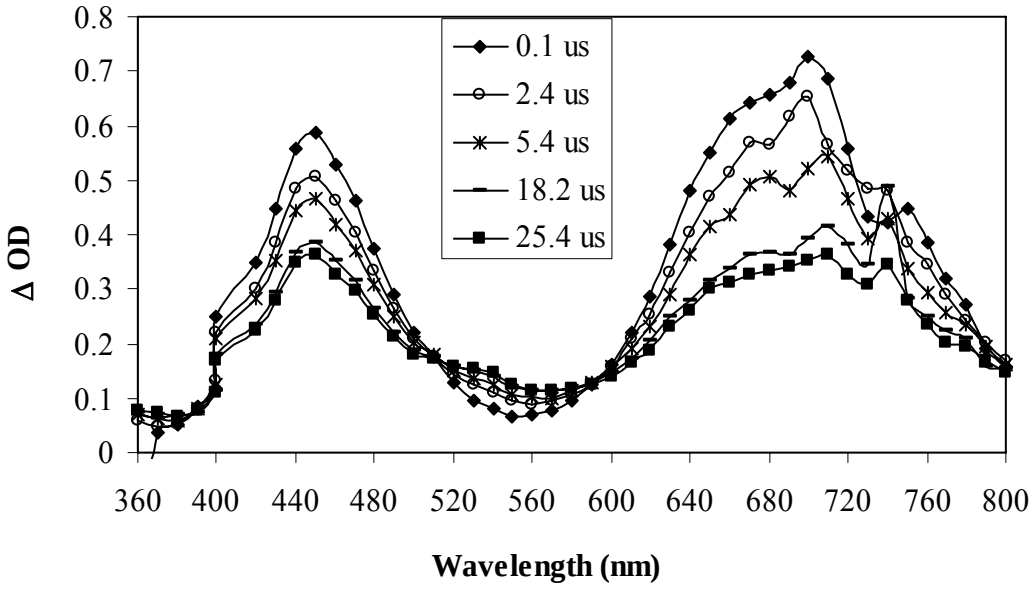

Figure 3.11 Transient spectra of the photolysis of **77c** in the presence of 1 M 4-chloroanisole in CH_3CN

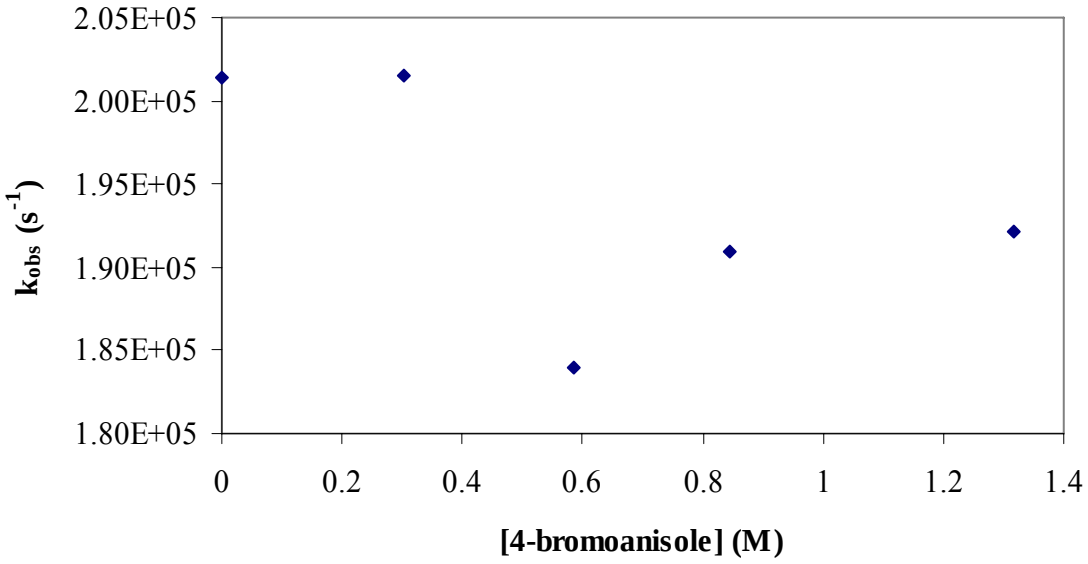

Figure 3.12 Plot of decay rate constant of **77c** at different concentration of 4-bromoanisole

3.4.3 Nucleophilic Substitution Reaction with Arenes

Some arenes react with arylnitrenium ion to form covalent adducts. For example, photolysis of **77a** in the presence of 1,3,5-TMB and 1,3-DMB yielded σ-adducts by forming covalent bonds with the *ortho* or *para* carbons of the phenyl ring of the arylnitrenium ions.[22] Likewise, **78b** and **78c** were exposed to 1,3,5-TMB and 1,3-DMB to determine if similar results would be obtained.

In the presence of 1,3,5-TMB and 1,3-DMB, **78b** and **78c** decay via electrophilic substitution pathway. This process was confirmed both by LFP and product analysis. Upon photolysis of **77b** or **77c** in the presence of 1,3,5-TMB or 1,3-DMB, signals corresponding to **78b** or **78c** was observed. (Figure 3.13 & 3.14) However, the signal decays rapidly and a new absorbance signal forms at 410 nm. Based on previous results with **78a**, this new signal at 410 nm was assigned to a positively charged σ-complex (**86**). (Scheme 3.10) These intermediates are formed upon the addition of the arene to the *ortho* carbon of **78b** or **78c** before deprotonation to yield the σ-adducts (**87**). (Scheme 3.10) Similar σ-complexes that resulted from the protonation of the 1,3,5-TMB and 1,3-DMB ring yielding cyclohexadienyl cation have been previously characterized.[23,24] These complexes absorb in the range of 315 – 345 nm. Also similar σ-complexes between **78a** and TMB or 1,3-DMB with absorbances around 350 and 360 nm are observed.[22] However, unlike other σ-complexes, the complexes of with **78b** or **78c** absorb at a higher wavelength. Additional experiments were done to confirm this assignment.

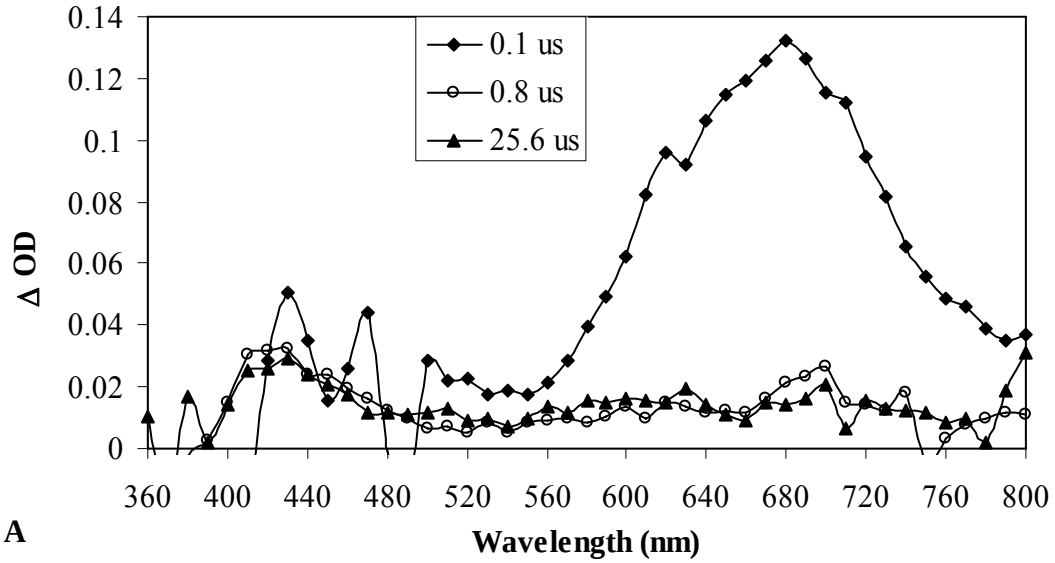

A

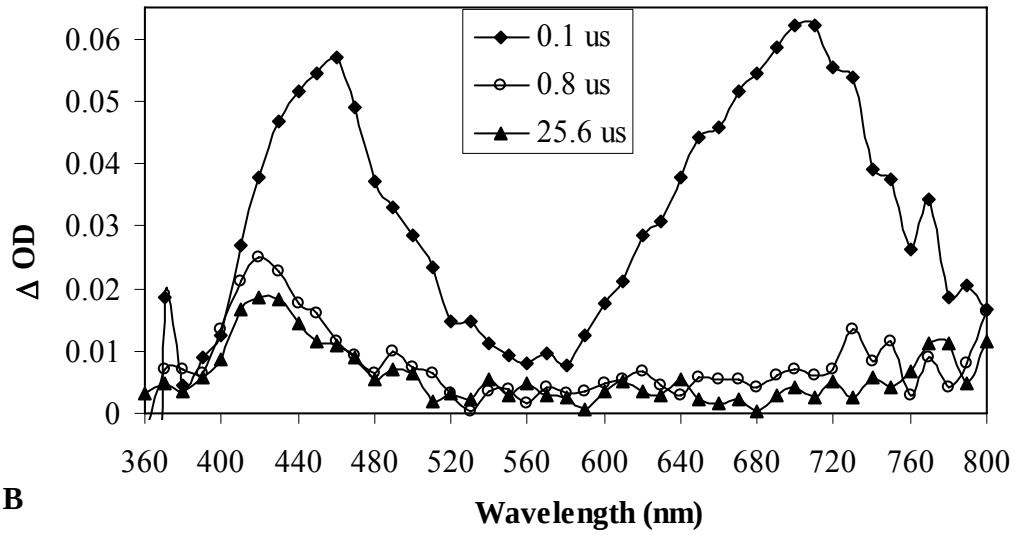

B

Figure 3.13 Transient spectra of the photolysis of (A) **77b** and (B) **77c** in the presence of 1,3,5-TMB (0.01 M) in CH_3CN

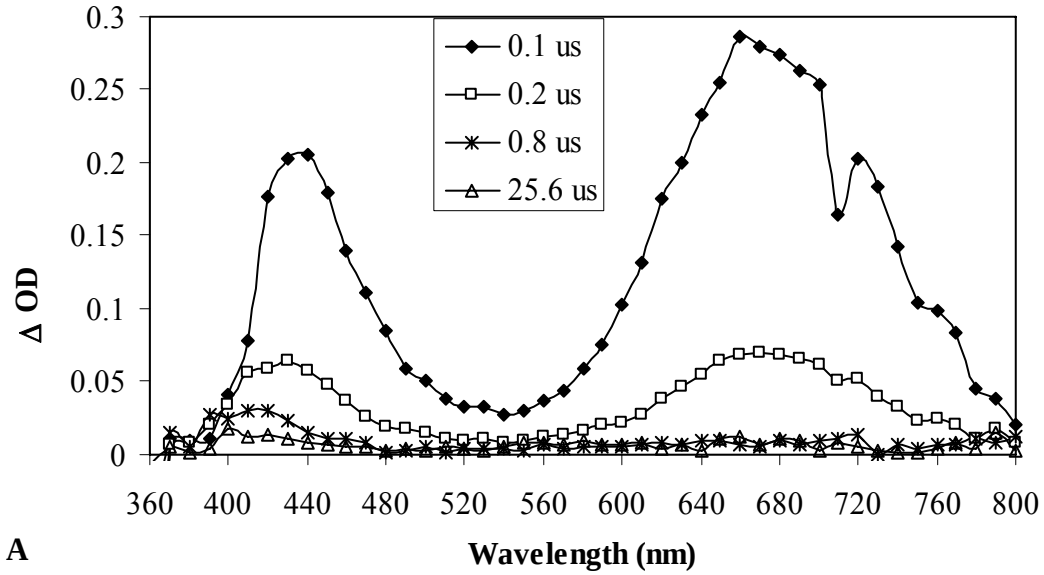

A

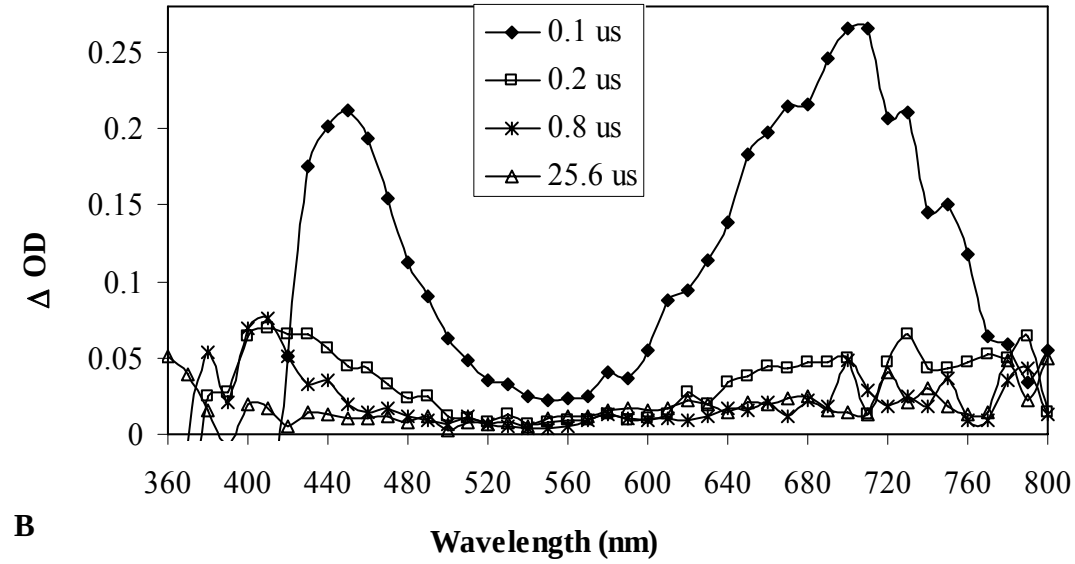

B

Figure 3.14 Transient spectra of the photolysis of (A) **77b** and (B) **77c** in the presence of 1,3-DMB (0.05 M) in CH_3CN

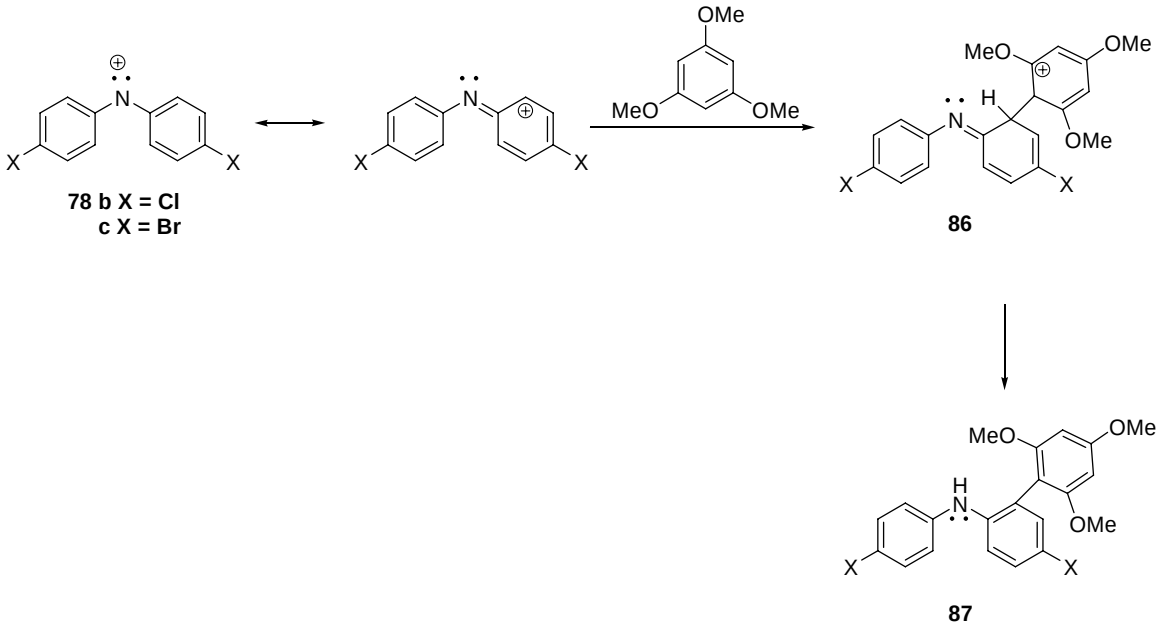

Scheme 3.10 Proposed mechanism for the formation of the **86** to yield the **87**

The 410 nm signal was investigated by carrying out the photolysis of the precursor in the presence of an arene and a base. The hypothesis tested was that if **86** was formed, then the presence of the base would accelerate the deprotonation step and the signal at 410 nm would decay rapidly. According to the transient spectra shown in Figure 3.15, the 410 nm signal decays rapidly when **78c** is generated in the presence of 11.8 mM 1,3,5-TMB and 0.4 mM pyridine in CH_3CN. From the waveforms shown in Figure 3.16, it can be observed that the species absorbing at 410 nm decays rapidly in the presence of pyridine. This indicated that the signal at 410 nm was influenced by the presence of the base, which in turn supports our assignment about the σ-complexation.

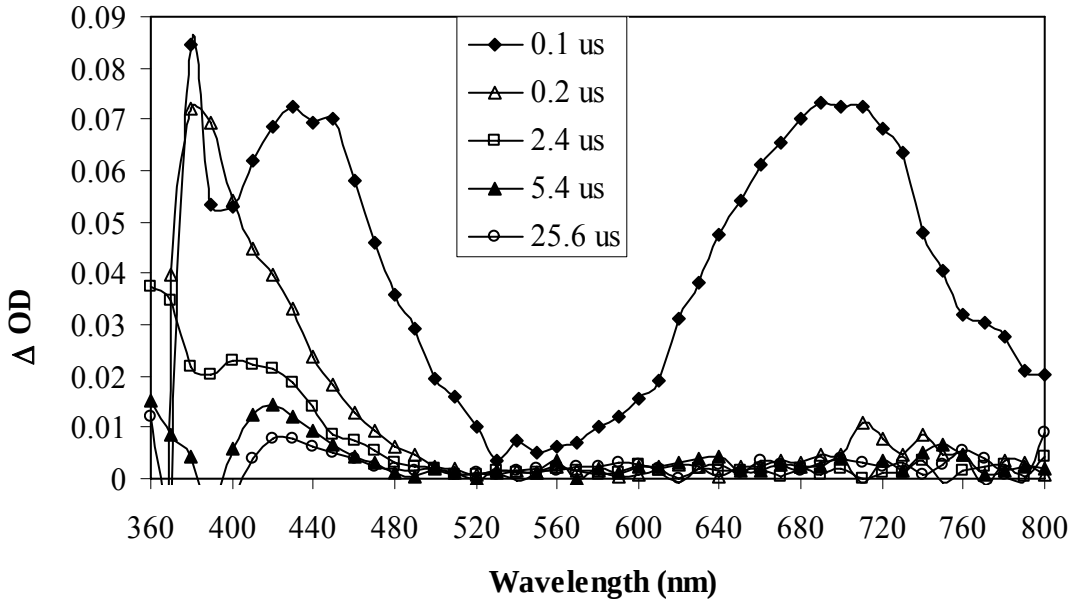

Figure 3.15 Transient spectra of the photolysis of **77c** in the presence of 11.8 mM 1,3,5-TMB and 0.41 mM pyridine in CH_3CN

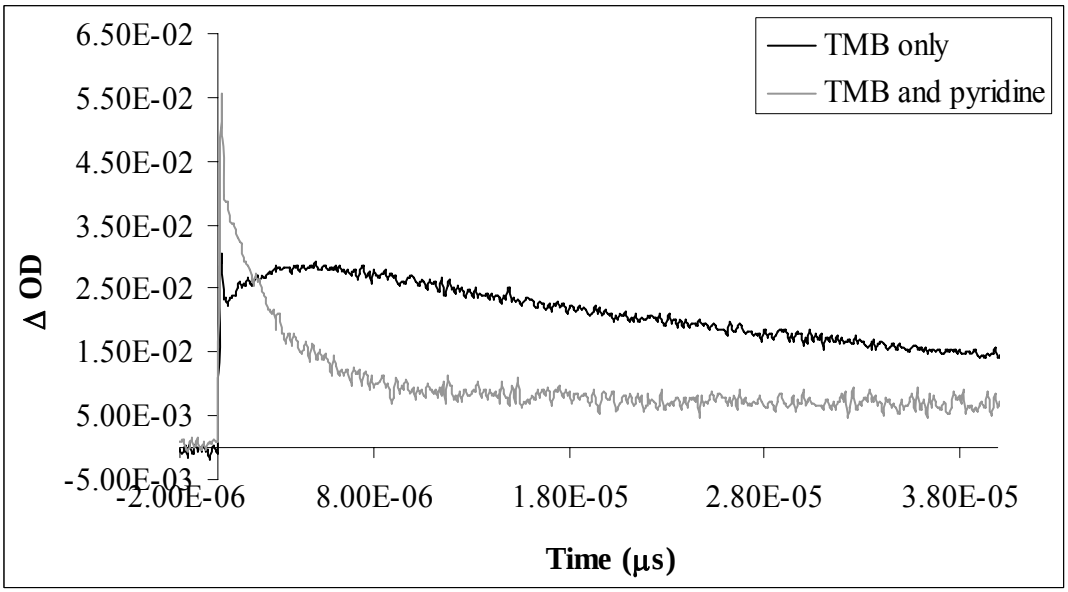

Figure 3.16 Waveform at 410 nm of the photolysis of 77c in the presence of 1,3,5-TMB with and without pyridine

Formation of **86** was further verified via product studies with 1,3,5-TMB. Photolysis of 0.002 M **77b** or **77c** in the presence of 0.02 M 1,3,5-TMB in CH_3CN yields three stable photoproducts: *ortho* adduct (**87**), *N*-adduct (**88**) and the parent amine (**79**) in 2.5:2.0:1.0 mol ratio. (Figure 3.17) Formation of **87** and **88** occurred via the nucleophilic addition of the arene to the two resonance forms of the nitrenium ion. (Scheme 3.11) Similar products are isolated when **78a** was generated in the presence of 1,3,5-TMB. However, in the case of **78a**, the *para* adduct was also obtained along with the three other photoproducts.[22]

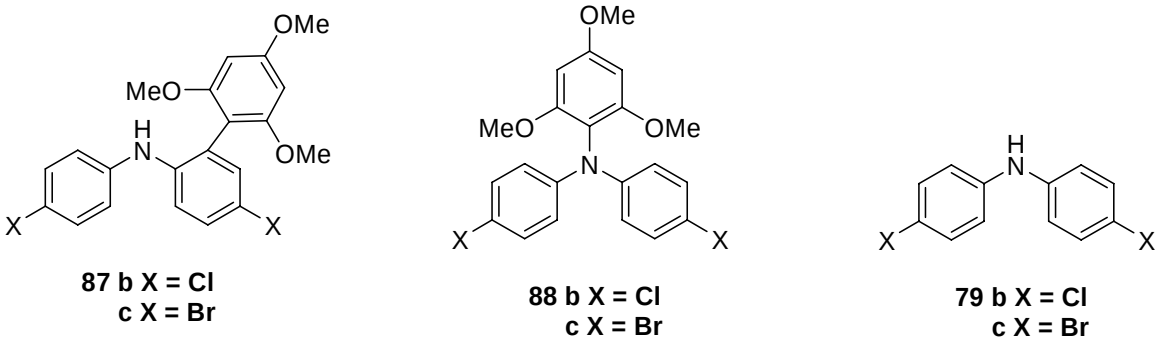

Figure 3.17 Photoproducts isolated upon reacting **77b** and **77c** with 1,3,5-TMB

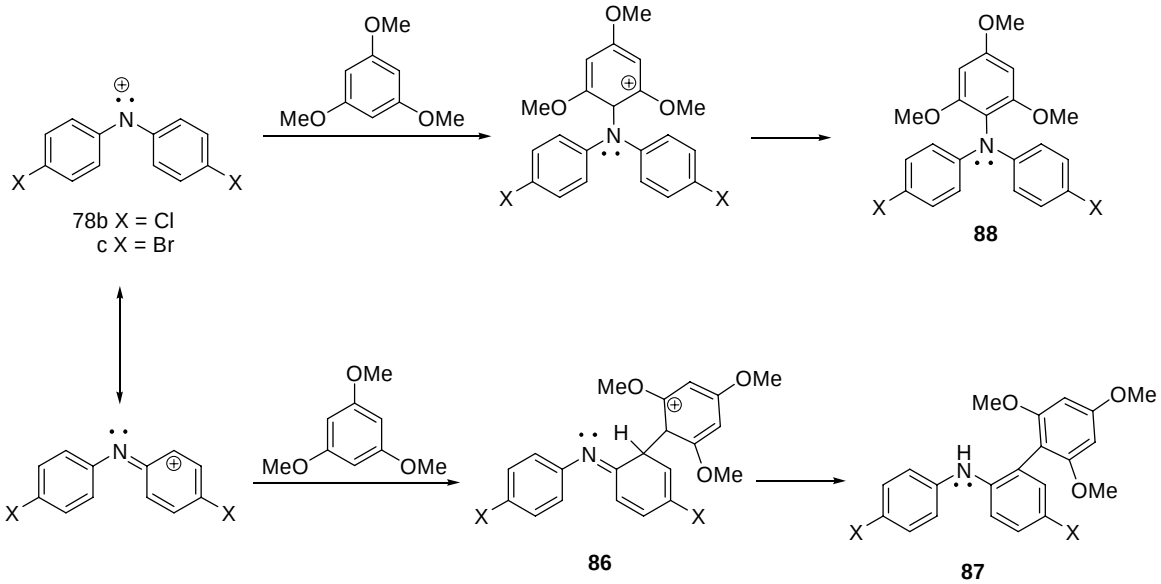

Scheme 3.11 Proposed mechanism for the formation of **87** and **88**

Even though no product analysis was conducted with 1,3-DMB as the trap, based on LFP results, it was assumed that 1,3-DMB also underwent nucleophilic substitution. Similar to 1,3,5-TMB, 1,3-DMB quenches **78b** and **78c** rapidly at a rate constant of 10^8 $M^{-1}s^{-1}$ and the transient signal at 410 nm indicating the formation **86** is also observed by LFP. In addition, previous work with **78a** has shown that 1,3-DMB reacts with the latter to give only *ortho* and *para* adducts; no *N*-adducts are obtained.[22] Since no para adduct can be obtained as photoproducts upon reacting **78b** and **78c** with 1,3-DMB, it is reasonable to assume that only ortho adducts would be obtained.

Although 1,3,5-TMB, 1,3-DMB and 1,4-DMB are all methoxy based arenes, they react differently with **78b** and **78c**. 1,3,5-TMB and 1,3-DMB do nucleophilic addition, while 1,4-DMB react via electron transfer. This difference in behavior could be due to the stability of the intermediate (σ-complex) that is formed during the reaction. When 1,3,5-TMB and 1,3-DMB formed **86**, the positive charge that results on the methoxybenzene ring can be delocalized to the carbons bearing the methoxy group. (Scheme 3.12) Hence, the intermediate formed is more stable than the one formed with 1,4-DMB. When 1,4-DMB forms the same σ-complex, the positive charge resonates between the carbon with and without the methoxy group. (Scheme 3.13) Thus the intermediate is less stable. In addition, 1,4-DMB has a lower E_{ox} than the other two arenes making it a better electron donor. Even though the E_{ox} of 1,3,5-TMB and 1,3-DMB (1.49 V) are lower than HMB (1.62 V), these traps react via nucleophilic addition. If electron transfer processes were present, then we would observe signals corresponding to the radical cations of the arenes (TMB: 613 nm and

645 nm; 1,3-DMB: 477 nm and 505 nm). No peaks were observed in this region, excluding the possibility of electron transfer by these traps.

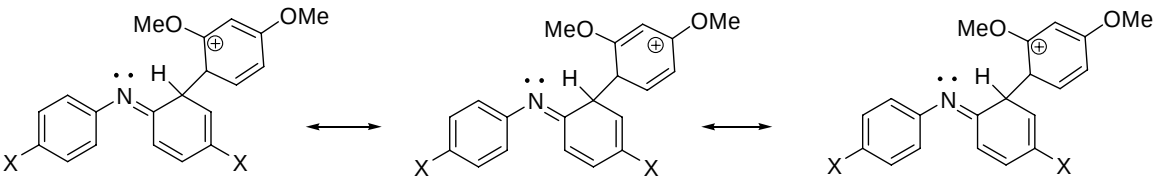

89 b X = Cl
c X = Br

Scheme 3.12 Delocalization of the positive charge in the σ-complex between **78b** or **78c** and 1,3-DMB

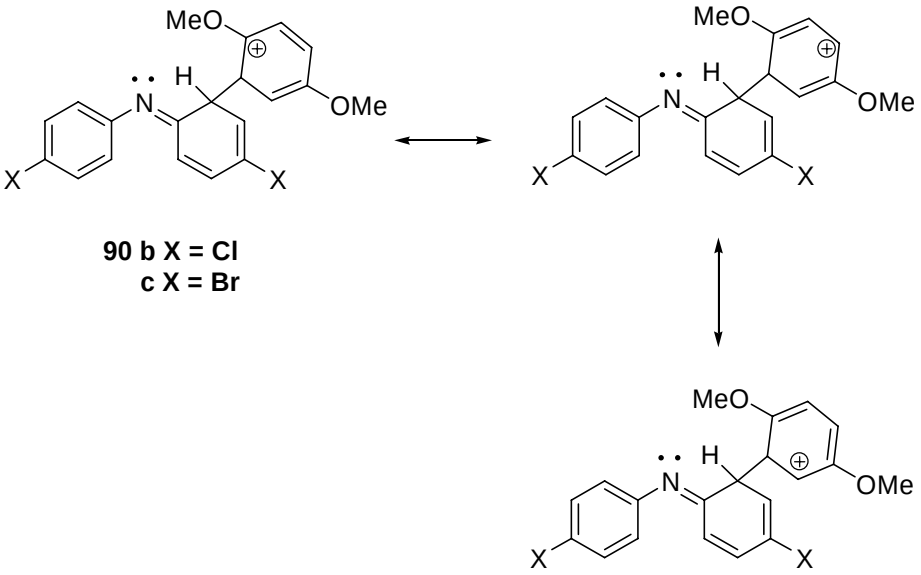

90 b X = Cl
c X = Br

Scheme 3.13 Delocalization of the positive charge in the σ-complex between **78b** or **78c** and 1,4-DMB

3.5 Reaction with Hydrogen Atom Donors

In addition to simple and π-nucleophiles, **78b** and **78c** were also reacted with hydrogen atom donors. It is generally accepted that triplet nitrenium ions undergo radical-like chemistry and hence abstract hydrogen atoms from available sources. Therefore, in order to understand the reactivity of **78b** and **78c** with hydrogen atom donors, they were generated in the presence of five potential hydrogen atom donors: 1,4-cyclohexadiene (CHD), cycloheptatriene, phenol, 4-bromophenol and 4-cyanophenol. (Figure 3.18) The reaction mechanism with these traps was followed by LFP and ^{1}H-NMR.

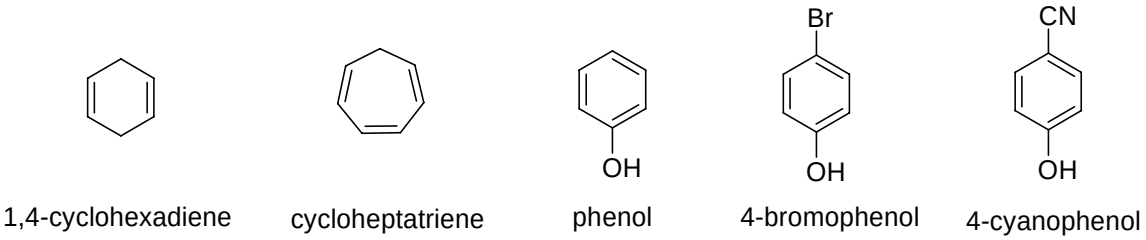

Figure 3.18 Hydrogen atom donors used for the study

LFP results showed that **78b** and **78c** react with hydrogen atom donors to yield **85**. Shown in Figure 3.19 are the transient spectra obtained upon photolyzing **77b** and **77c** in the presence of 1,4-CHD in CH_3CN. Upon excitation, signals corresponding to **78b** or **78c** are observed. The latter is replaced within 2.4 μs by a new signal at 720 nm or 730 nm. As described before, these new long-lived species is assigned to **85**. Since 1,4-CHD is a hydrogen atom donor, the likely mechanism to form **85** would be hydrogen atom transfer from 1,4-CHD to **78b** or **78c**. However, this type of reaction is a radical chemistry which is generally observed for triplet

nitrenium ions. Therefore for this to occur, **78b** and **78c** will have to exist in the triplet state.

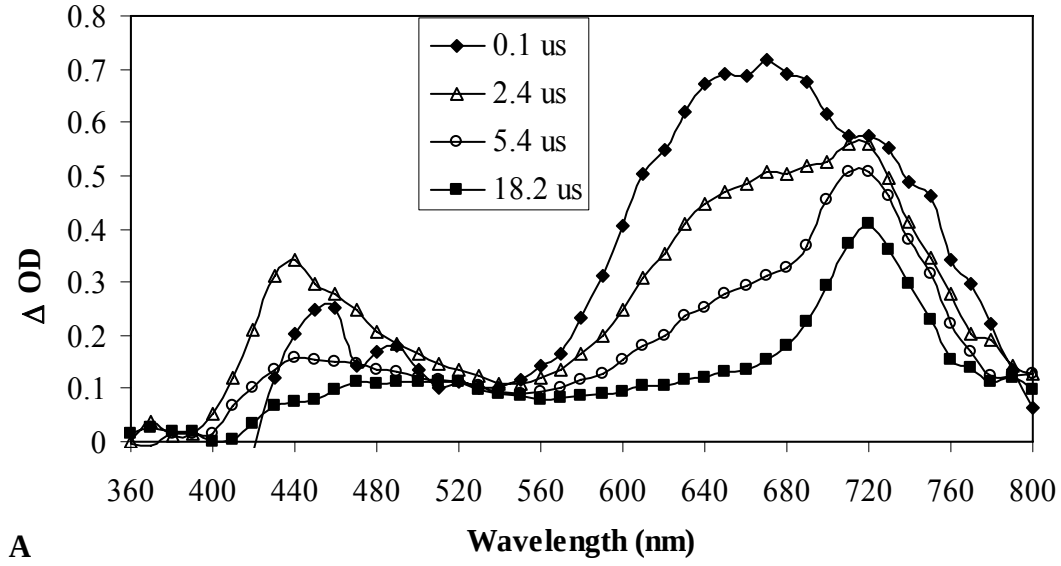

A

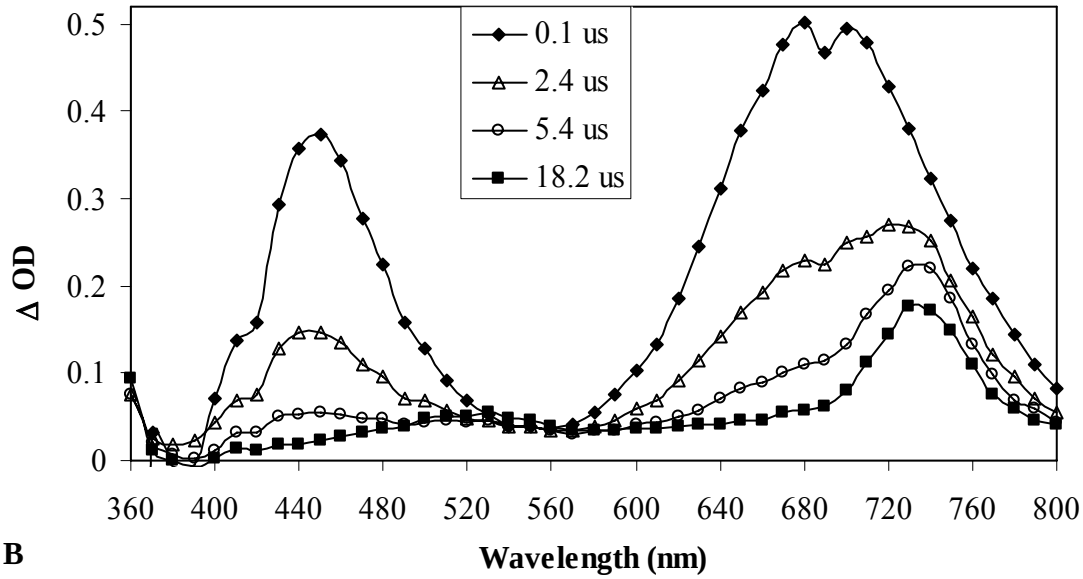

B

Figure 3.19 Transient spectra of the photolysis of (A) **77b** and (B) **77c** with 0.05 M 1,4-CHD in CH_3CN

However evidence obtained by LFP and product analysis showed that **78b** and **78c** behaves as singlets which are also supported by the DFT calculations.

Experimental evidence such as the addition of chloride and 1,3,5-TMB to the nitrenium ion, and formation of **84** and **85** due to electron transfer from DMB, all are characteristics of a singlet nitrenium ion. These observations are supported by the predictions made by the DFT calculations. The calculations show that the singlet state of **78b** and **78c** is lower in energy than the triplet state. In addition, the UV-Vis absorption bands observed for **78b** and **78c** agree with those values predicted by the DFT calculations for the singlet nitrenium ions. Moreover, other arylnitrenium ions with similar experimental data and theoretical calculations are ground state singlets. Hence the possibility of **78b** and **78c** existing in a triplet state is unlikely but the triplet behavior that was observed with 1,4-CHD could not be ignored.

There are two possible pathways to **85** from **78b** and **78c**: (1) electron abstraction and protonation, as observed with 1,4-DMB or (2) abstraction of a hydrogen atom from a donor. (Scheme 3.14) 1,4-CHD is a good hydrogen atom donors due to its low C-H bond dissociation energy (76 kcal/mol).[25] Therefore, the most likely mechanism to form the radical cation would be hydrogen abstraction. But this would mean that at some point of the chemical decay process, **78b** or **78c** would have to exist in their triplet states. The other possibility that would be satisfactory for a singlet state behavior would be for 1,4-CHD to donate an electron to **78b** and **78c** to form **84**, which is then protonated. Alabugin et. al. reported similar electron transfer mechanism involving 1,4-CHD.[26] In their work with bis-tetrafluoropyridinyl (TFP) enediynes, they proposed that the excited singlet enediynes abstracts an electron from 1,4-CHD to form a radical anion which yields the final stable product via cyclization, protonation and hydrogen atom abstraction. Even though this mechanism was

plausible for **78b** and **78c**, more experiments were conducted to determine the decay pathway.

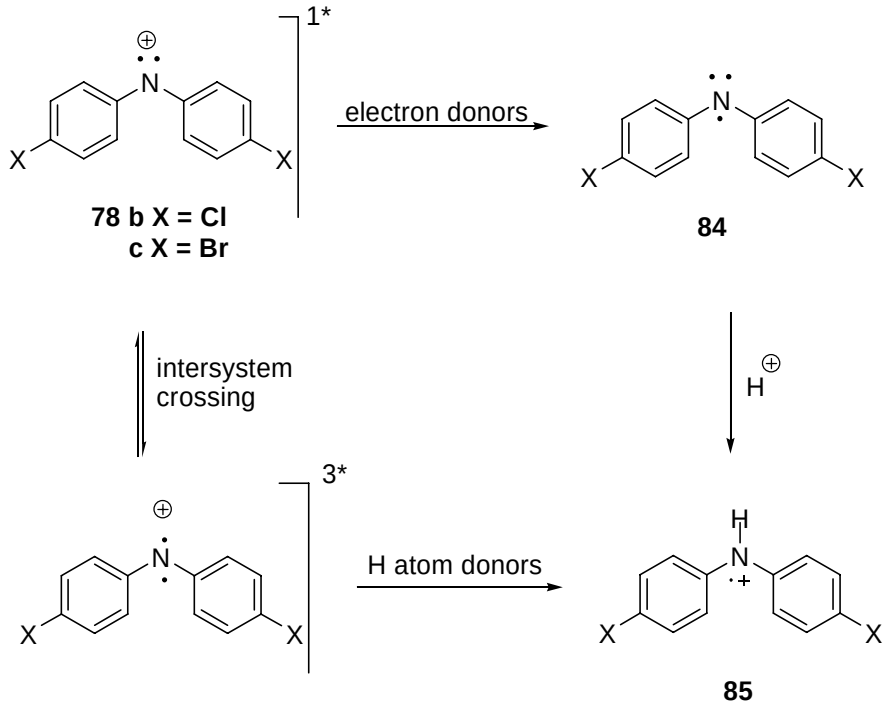

Scheme 3.14 Possible pathways to the formation of **85**

The triplet behavior of **78b** and **78c** was investigated further by carrying out LFP experiments using other potential hydrogen atom donors such as cycloheptatriene, phenol, 4-bromophenol and 4-cyanophenol. (Figure 3. 20, 21, 22 and 23) Radical cation **85** was observed in the presence of these traps too. Similar to 1,4-CHD, cycloheptatriene is a good hydrogen atom donor with a low C-H BDE (76 kcal/mol).[25] These two traps also have reasonably low oxidation potentials (CHD: 1.74 V and cycloheptatriene: 1.43 V) which could allow these traps to donate electrons to **78b** or **78c**. Above we showed that arenes with these potentials donate single electrons to **78b** or **78c**. Hence, it might be possible that **85** was formed due to electron donation from 1,4-CHD and cycloheptatriene.

However, the formation of **85** in the presence of phenol and its derivatives disproved the assumption of electron transfer suggested for 1,4-CHD and cycloheptatriene. As shown in Table 3.4, the E_{ox} of phenol and its derivatives is above 2.00 V, therefore based on our work with arenes, we know that these traps are incapable of single electron transfer. Arenes with E_{ox} above 1.78 V showed no reactivity towards **78b** and **78c**. Also we see discrepancies in the rates of quenching by various traps. 4-MA with an E_{ox} of 1.64 V reacts with **78b** and **78c** at a rate constant of 10^5 $M^{-1}s^{-1}$ (Table 3.3), whereas 1,4-CHD with an E_{ox} of 1.74 V quenches these ions at a rate constant of 10^6 $M^{-1}s^{-1}$ (Table 3.4). 1,4-CHD with a higher E_{ox} trapped the ions at a faster rate. If the decay mechanism in the presence of 1,4-CHD was electron transfer, then we should observe a much slower quenching rate. Also phenol and its derivatives reacts with the ions at a rate constant of 10^5 $M^{-1}s^{-1}$, almost at the same rate as 4-MA. Based on our conclusions on E_{ox}, these traps were not supposed to quench **78b** or **78c**. Therefore, it is likely that these nucleophiles could be reating with **78b** and **78c** by some other mechanisms other than electron transfer.

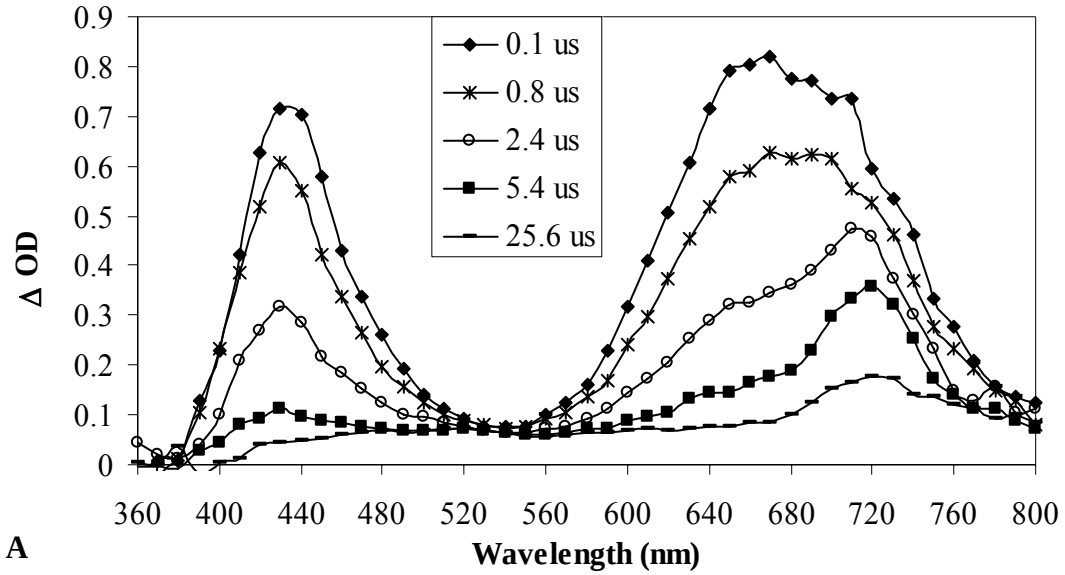

A

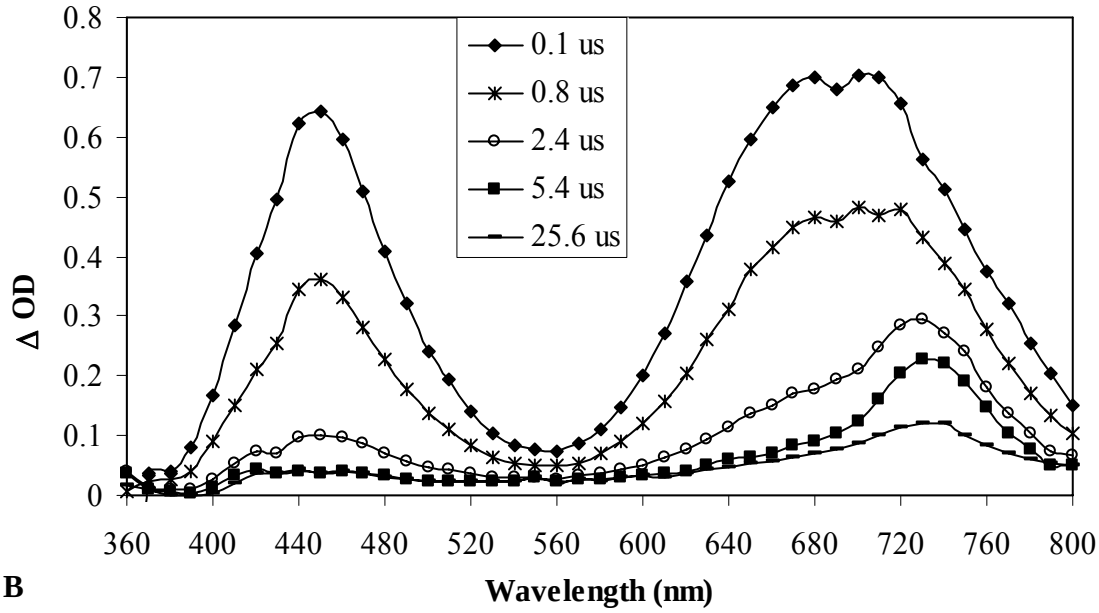

B

Figure 3.20 Transient spectra of photolysis of (A) **77b** and (B) **77c** in the presence of 0.01 M cycloheptatriene in CH_3CN

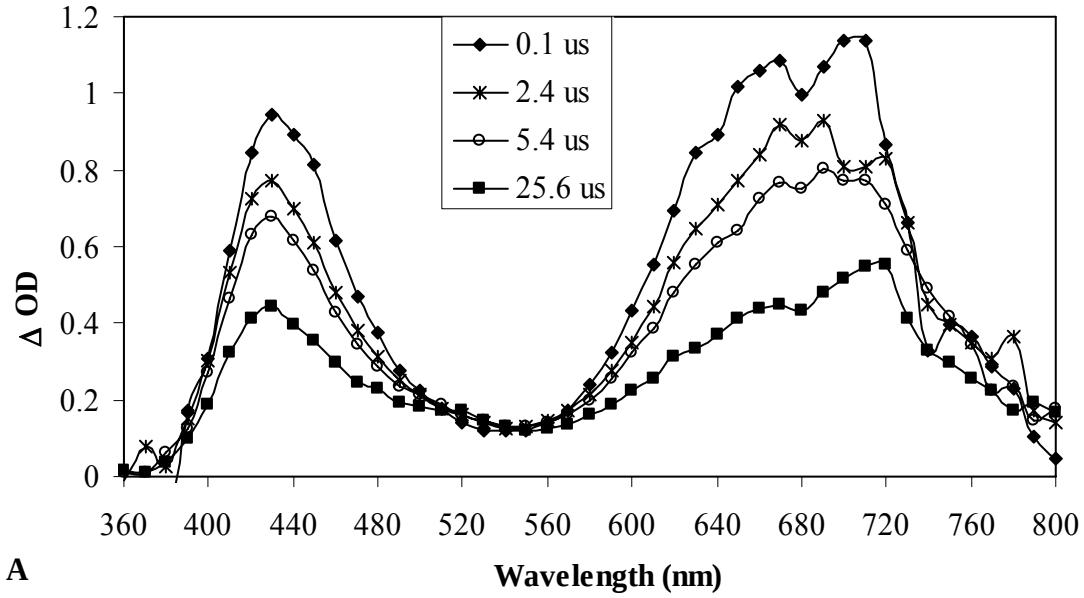

A

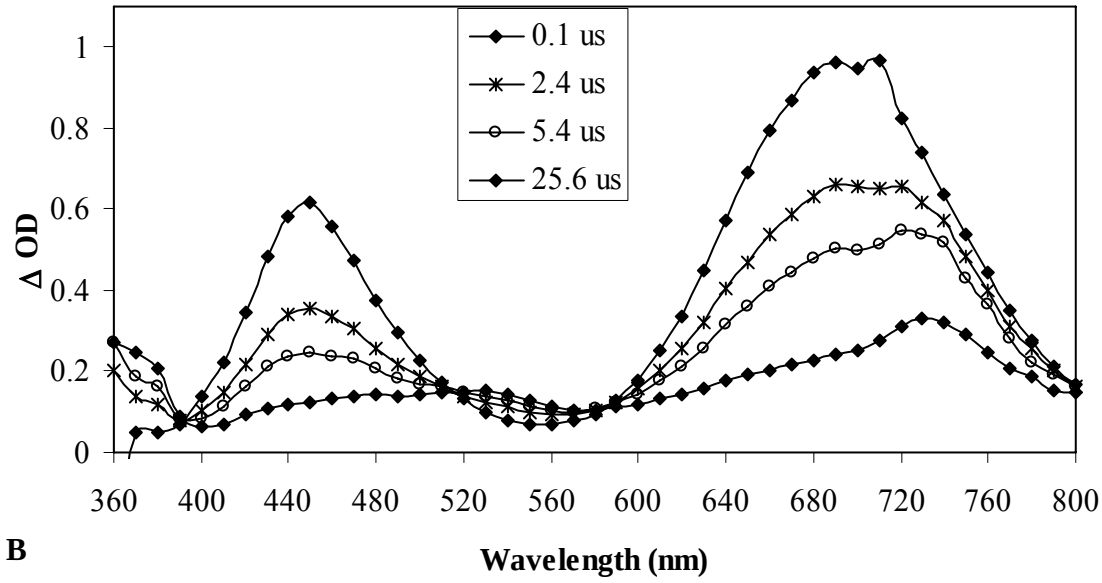

B

Figure3.21 Transient spectra of the photolysis of (A) **77b** and (B) **77c** in the presence of 0.011 M phenol in CH_3CN

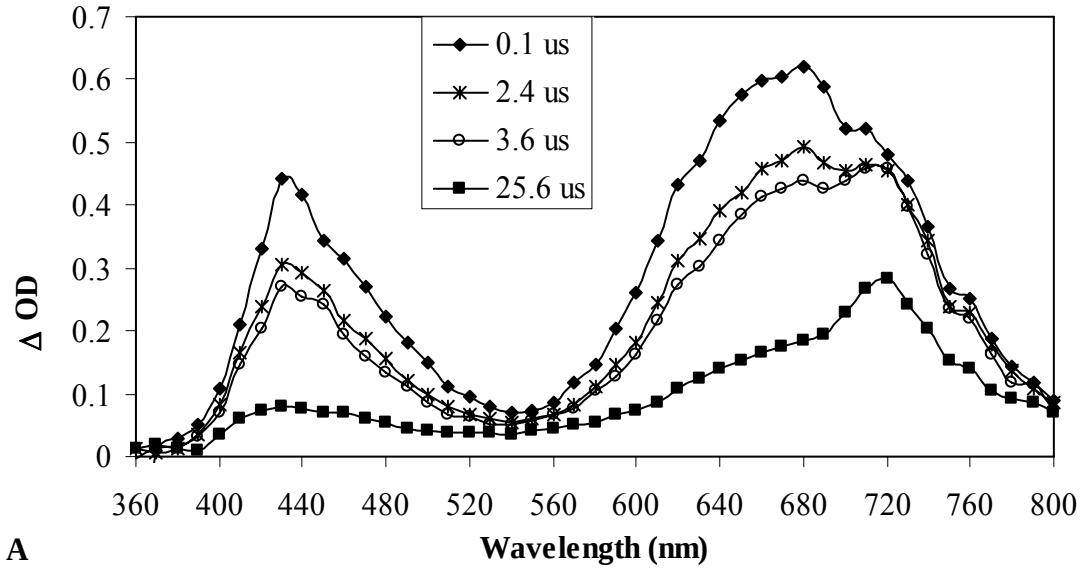

A

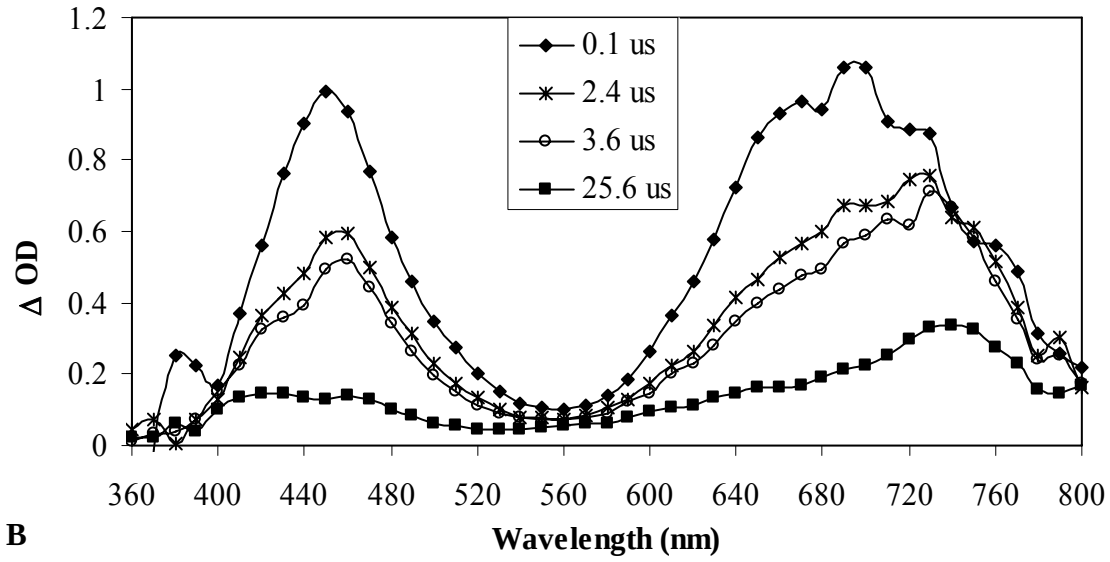

B

Figure3.22 Transient spectra of the photolysis of (A) **77b** and (B) **77c** in the presence of 0.01 M 4-Bromophenol in CH_3CN

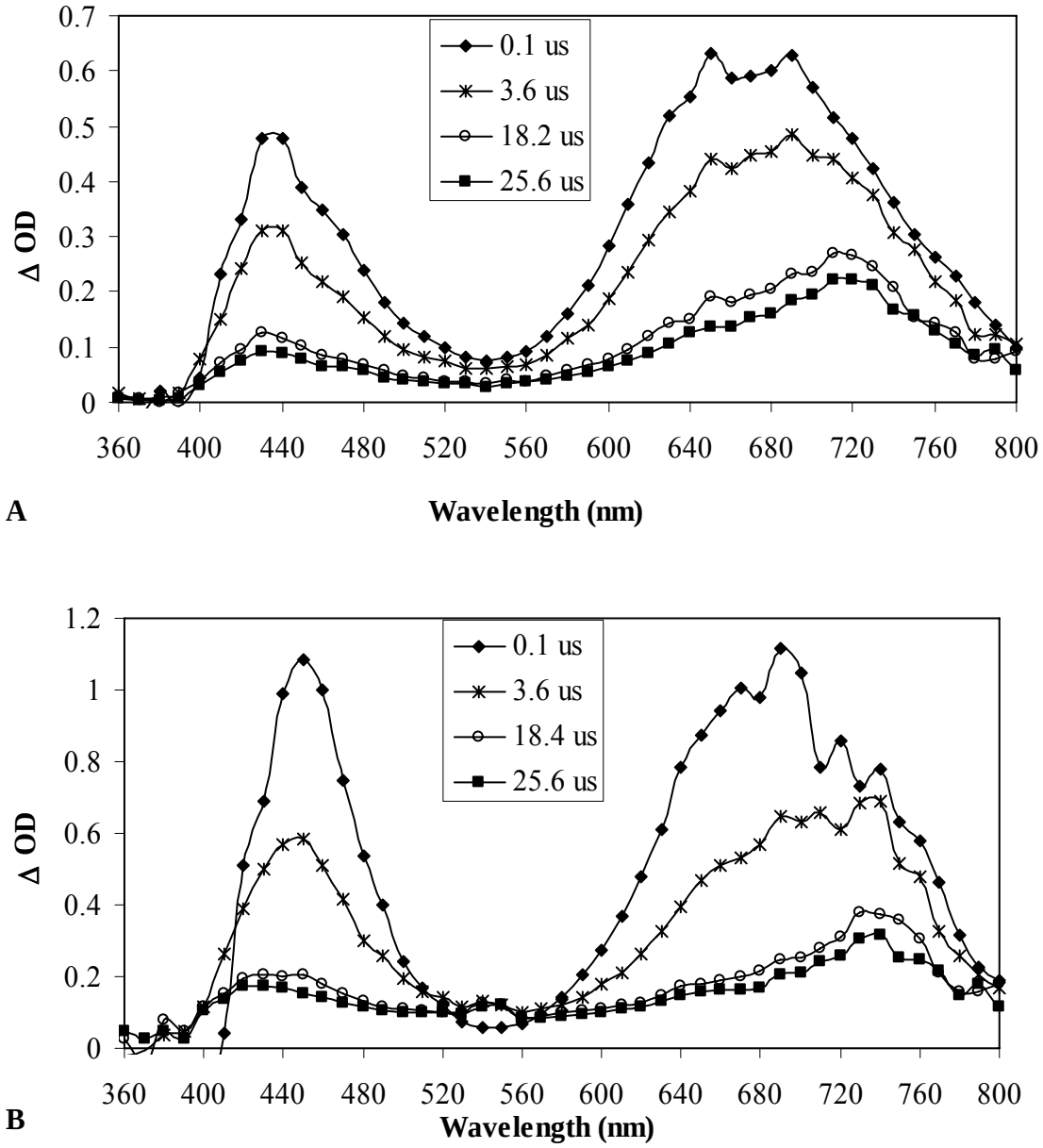

Figure 3.23 Transient spectra of the photolysis (A) **77b** and (B) **77c** in the presence of 0.1 M 4-Cyanophenol in CH_3CN

Table 3.4 Second order reaction rate constant of the quenching of **78b** and **78c** by hydrogen atom donors

Traps	E_{ox} (V vs. SCE)	BDE (kcal/mol)	k_{nuc} ($M^{-1}s^{-1}$)		
			78a	**78b**	**78c**
1,4-cyclohexadiene	1.74[a]	76.6 ± 1.2[b]	(6.5 ± .2) x 10^{6}[c]	(5.86 ± .31) x 10^{6}	(5.13 ± .15) x 10^{6}
Cycloheptatriene	1.43[d]	76.6 ± 3[b]	(1.4 ± .1) x 10^{7}[c]	(5.65 ± .14) x 10^{6}	(5.99 ± .67) x 10^{6}
Phenol	2.10[e]	90.4 ± 1[b]		(6.81 ± .22) x 10^{5}	(6.46 ± .95) x 10^{5}
4-bromophenol	2.18[e]	90.7[b]		(3.76 ± .33) x 10^{5}	(4.73 ± .37) x 10^{5}
4-cyanophenol	2.57[e]	94.2[b]		(3.31 ± .89) x 10^{5}	(4.89 ± .87) x 10^{5}

[a]Ref 27. [b]Ref 25. [c]Ref 10. [d]Ref 28. [e]Ref 29

An alternative pathway by which phenol and its derivatives could react with **78b** and **78c** to yield radical cation (**85**) is via a hydrogen atom transfer. Kinetic isotope experiments were conducted to further confirm hydrogen atom transfer mechanism. Reacting **78b** and **78c** with deuteriated and undeuteriated phenol gave a kinetic isotope effect of 1.32 (k_H = 3.49 x 10^6 $M^{-1}s^{-1}$ and k_D = 2.64 x 10^6 $M^{-1}s^{-1}$). A value of 1.32 is consistent for a hydrogen atom transfer from the nucleophile to the transient species. The value closer to 1 implies that the transistion state is less symmetrical and reactant-like. Therefore, based on these reasonings, the likely mechanism in the presence of 1,4-CHD and other potential hydrogen atom donors could be hydrogen atom transfer which is typically a triplet behavior.

The triplet behavior that was exhibited by **78b** and **78c** can be due to either one of the following reasons: (1) singlet **78b** and **78c** undergoing radical-like chemistry or (2) rapid equilibrium of **78b** and **78c** between the singlet and triplet states. There are three possible electronic states for singlet nitrenium ions where the two non-bonding electrons occupy either one of the non-bonding orbital (σ or p) with antiparallel spins or the two non-bonding electrons occupy the two non-bonding orbitals separately with parallel spins.[7] (Figure 2.6) When these electrons occupy the orbitals separately, they could behave as triplets and undergo radical-like chemistry. Even though this is possible, it is rare due to the fact that this is a higher energy excited singlet state.[7,8] The **78b** and **78c** generated has to be in that higher energy state before it could abstract a hydrogen atom. This cannot be true because most nitrenium ions prefer to reside in the lower energy state unless it's excited to that higher level.

Therefore, an alternative explanation to the triplet behavior would be a triplet state of **78b** and **78c** resulting from the rapid equilibrium between the singlet and triplet state. The hypothesis was that even though the singlet state of **78b** and **78c** is lower in energy than the triplet state, the ions could be capable of intersystem crossing to the triplet state due to smaller ΔE_{ST}. Since **78b** and **78c** are relatively stable, it is possible that they can exist long enough to intersystem cross to the triplet state under the right conditions. Based on the DFT calculations, we assumed that this could not happen because the calculations predicted that the triplet state was around 8-10 kcal/mol higher in energy than the singlet state, an ΔE_{ST} too high for intersystem crossing. However, it is possible for the calculation to have some uncertainties and that the actual ΔE_{ST} may be much smaller than that predicted.

There might be two reasons for the disagreement between the calculated values and the experimental observations. If the ΔE_{ST} predicted by DFT calculations were in fact accurate, then the rate constant for the diffusion limited hydrogen abstraction by the triplet should match with the experimentally obtained rate constant of hydrogen atom transfer. The rate constant for the diffusion limited hydrogen abstraction can be estimated from the free-energy and the equilibrium constant assuming rapid equilibrium between singlet and triplet states.

Assuming $S \underset{}{\overset{K_{ST}}{\rightleftharpoons}} T$

DFT Calculated ΔG for **78b** = $-RT \ln K_{ST}$

$= -10.1$ kcal/mol $= 4.23 \times 10^4$ J/mol

$K_{ST} = \exp(-\Delta G/RT) = \exp((-4.23 \times 10^4 \text{ J/mol})/((8.31 \text{ J/K.mol})(298.15 \text{ K})) = 3.72 \times 10^{-8}$

$k_H = K_{ST} \times k_{diff}$ k_H = diffusion limited hydrogen atom transfer

k_{diff} = diffusion limit in $CH_3CN = 2 \times 10^{10}$ $M^{-1}s^{-1}$

$k_H = K_{ST} \times k_{diff} = (3.72 \times 10^{-8}) (2 \times 10^{10}\ M^{-1}s^{-1}) =$ **$7.45 \times 10^3\ M^{-1}s^{-1}$**

DFT Calculated ΔG for **78c** = $-RT \ln K_{ST}$

$= -8.63$ kcal/mol $= 3.61 \times 10^4$ J/mol

$K_{ST} = \exp((-3.61 \times 10^4 \text{ J/mol})/((8.31 \text{ J/K.mol})(298.15 \text{ K}) = 4.68 \times 10^{-7}$

$k_H = K_{ST} \times k_{diff}$ k_H = diffusion limited hydrogen atom transfer

k_{diff} = diffusion limit in $CH_3CN = 2 \times 10^{10}$ $M^{-1}s^{-1}$

$k_H = K_{ST} \times k_{diff} = (4.68 \times 10^{-7}) (2 \times 10^{10}\ M^{-1}s^{-1}) =$ **$9.37 \times 10^3\ M^{-1}s^{-1}$**

According to the calculations, the diffusion limited hydrogen atom abstraction by the triplet nitrenium ion should be around 7-9 x 10^3 $M^{-1}s^{-1}$. However, the rate constant obtained experimentally for the quenching of **78b** and **78c** by these hydrogen atom donors are in the range of $(3 \times 10^5) - (5 \times 10^6)$ $M^{-1}s^{-1}$, that is 2-3 orders of magnitude faster than that predicted for diffusion limited hydrogen atom transfer. But if we assume that the rates of hydrogen atom abstraction observed experimentally were in fact accurate and the ΔE_{ST} predicted for **78b** and **78c** had some error associated with it, then the actual ΔE_{ST} based on the experimental rates

should be around 5-6.5 kcal/mol (calculations shown below). This value is 2-3 kcal/mol lower than that predicted by the DFT calculations. Hence, at this estimated ΔE_{ST}, **78b** and **78c** should be able to undergo intersystem crossing to the triplet state. Therefore, in the presence of hydrogen atom donors, the singlet **78b** and **78c** cannot react with the trap; hence it undergoes intersystem crossing to the triplet state, then abstracts a hydrogen atom to generate **85**.

Assuming $S \overset{K_{ST}}{\rightleftharpoons} T$

$\Delta G = -RT \ln K_{ST}$

$K_{ST} = \exp(-\Delta G/RT)$

Upper limit of the experimentally obtained $k_H = K_{ST} \times k_{diff} = 5 \times 10^6\ M^{-1}s^{-1}$

$K_{ST} = k_H/k_{diff} = (5 \times 10^6\ M^{-1}s^{-1})/(2 \times 10^{10}\ M^{-1}s^{-1}) = 2.5 \times 10^{-4}$

ΔG for highest rate observed = -(8.31 J/K.mol) (298.15 K) ln (2.5×10^{-4})

$= 2.05 \times 10^4$ J/mol = 4.91 kcal/mol

Lower limit of the experimentally obtained $k_H = K_{ST} \times k_{diff} = 3 \times 10^5\ M^{-1}s^{-1}$

$K_{ST} = k_H/k_{diff} = (3 \times 10^5\ M^{-1}s^{-1})/(2 \times 10^{10}\ M^{-1}s^{-1}) = 1.5 \times 10^{-5}$

ΔG for lowest rate observed = -(8.31 J/K.mol) (298.15 K) ln (1.5×10^{-5})

$= 2.75 \times 10^4$ J/mol = 6.57 kcal/mol

The radical cation **85** obtained via a hydrogen atom abstraction was eventually converted to **79**. This is confirmed by ^{1}H-NMR studies. 1.3 mM of **77c** with 12.8 mM 1,4-CHD in 5.0 mL of CD_3CN was photolyzed using 200 W Hg lamp. The photolysis was followed by ^{1}H-NMR taken every 30 minute interval. As the

photolysis progressed, the depletion of the precursor was observed, along with the growth of **79** and collidine. The products **79** and collidine grew at the same rate. Other than excess 1,4-CHD and small amount of benzene, no other impurities were observed in the sample. Compound **79** is a triplet product; therefore, it might be possible that **78b** and **78c** does exist in their triplet state at some stage of the decay process.

3.6 Chemical Decay in the Absence of any Trap

We have seen that **78b** and **78c** react with various traps to yield photoproducts specific to each energy states. They reacted with singlet traps to yield singlet products and with triplet traps to yield products specific to a triplet states. The next objective was to determine the chemical decay pathway of **78b** and **78c** in the absence of any traps. Previous work on **78a** has shown that in the absence of traps, the latter decays to yield carbazole and a polyaniline polymeric compound.[12] The polymer that is obtained resulted from the head-to-tail dimerization of **78a** and **79a**. Therefore, the decay pathway of **78b** and **78c** in the absence of trap was followed by LFP, ^{1}H-NMR and product analysis.

Photolysis of **77b** or **77c** in CH_3CN in the absence of traps leads to the formation of hydrazine (**92**), a head-to-head dimerization product. The chemical decay process of **78b** and **78c** is followed by ^{1}H-NMR and product studies. The precursor, **77b** or **77c**, (~2-5 mg) dissolved in 1 mL of CD_3CN was photolyzed under room light. The photolysis was followed by ^{1}H-NMR taken every 10-30 minute interval. As the photolysis progressed, the gradual depletion of the precursor was

observed, along with the growth of **92** and collidine. After an hour of photolysis, only peaks corresponding to the precursor and collidine were observed. The hydrazine (**92)** peaks were either diminished or not observed in the ^{1}H-NMR spectrum. However, continued photolysis of the reaction mixture resulted in the complete consumption of the precursor (**77b** or **77c**) and the reappearance of **92** along with collidine and trace amounts of **79**. The final photoproducts were isolated and characterized by ^{1}H-NMR, ^{13}C-NMR and MS.

As shown in Scheme 3.15, there were two possible mechanisms for the formation of **92**. The latter could be formed via pathway **A**, where **78b** or **78c** generated could couple with **79** to form the protonated dimer (**91**) which is then deprotonated. Amines are good electron sources. LFP experiments of the photolysis of **77c** in the presence of **79c** generates **85c** resulting from the abstraction of electron by **78b** or **78c** from the amine. (Figure 3.24) Hence in order to decay by pathway **A**, the presence of **79** along with the formation of **78b** or **78c** was required. However, ^{1}H-NMR data taken during the photolysis showed that no **79** was present in the reaction mixture until the end of the experiment. If this was indeed the decay mechanism, then **79** should be generated along with **78b** or **78c** and the peaks corresponding to **79** should be observed by ^{1}H-NMR before or along with the peaks of **92** and collidine. Since no **79** peaks were observed, it is possible that **78b** or **78c** did not decay by this pathway.

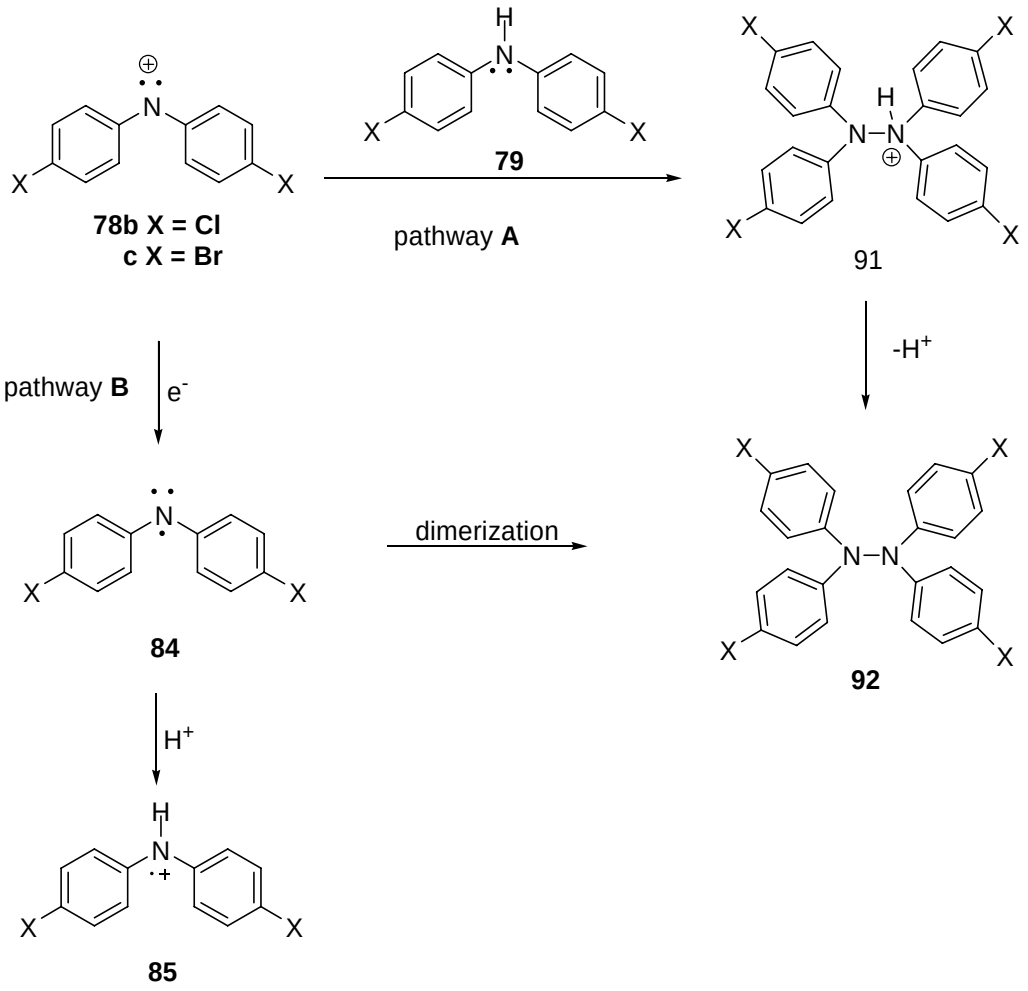

Scheme 3.15 Possible mechanism for the formation of **92**

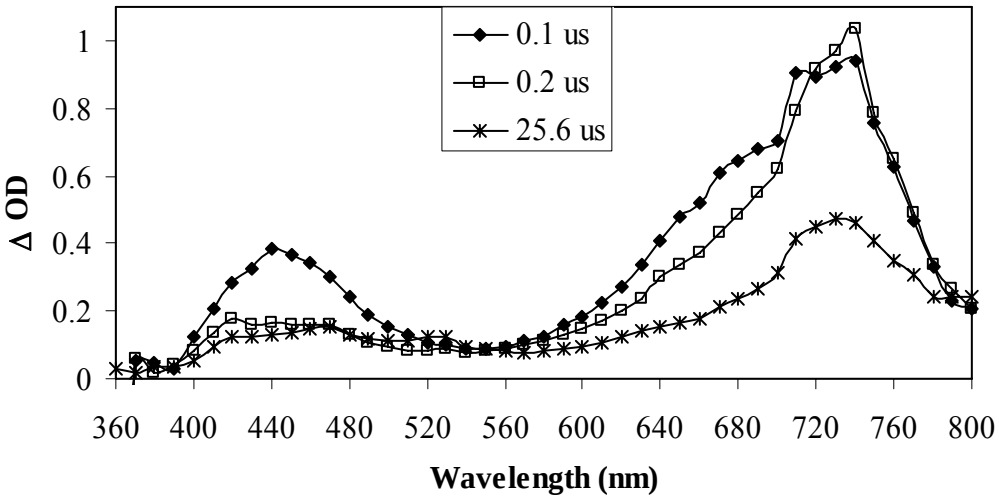

Figure 3.24 Transient spectra of the photolysis of **77c** with **79c** in CH_3CN

Based on the information obtained by NMR studies, pathway **B** seemed more appropriate for the formation of **92**; abstraction of an electron by **78b** or **78c** to form **84** which then dimerizes to yield **92**. This pathway agreed with the data obtained by ^{1}H-NMR because the growth of peaks corresponding to **92** was observed as the peaks corresponding to **77b** or **77c** diminished. This implied that **78b** and **78c** abstracted an electron from the solvent (or some impurity) before dimerization.

UV-Vis spectroscopy experiments were conducted to confirm pathway **B**. The reasoning was that if **78b** or **78c** did in fact abstract an electron before dimerization, then it should be possible to trap the intermediate **84** before it undergoes dimerization. This can be done by, protonating the aminyl radical as soon as it was generated. In addition, since **78b** and **78c** exist in solution for a long time and then dimerized in the absence of a trap, it should be possible to stabilize **78b** and **78c** long enough if the dimerization could be prevented to a certain extent and may be observed it by steady state UV-Vis.

In order to stabilize **78b** and **78c** and prevent electron abstraction, the latter was generated in solvents incapable of donating electrons and followed by UV-Vis spectroscopy. The photolysis of **77b** and **77c** was carried out in different aprotic solvents and an acid (H_2SO_4 or Trifluoroacetic acid (TFA)). The solvents chosen for the study were those that usually do not donate hydrogen atom or electrons (CH_2Cl_2, chlorobenzene and nitrobenzene). The precursor (**77b** or **77c**) (~2-5 mg) was dissolved in 3 mL of the solvent with 1-2 drops of acid and allowed to photolyze under room light. Figure 3.24 is the time resolved UV-Vis spectra taken during the course of the experiment in CH_2Cl_2 with TFA. Before photolysis, only an absorbance

band with the maximum around 390 nm corresponding to **77b** or **77c** was observed. As the photolysis progressed, two new absorbance bands with maxima around 350 and 730 nm or 740 nm grew in. Based on previous results with arenes and hydrogen atom donors, these peaks are assigned to **85**. Even though, **78b** or **78c** itself was not observed, **85** was stable enough to be observed by steady state UV-Vis. Similar steady state UV-Vis analyses were preformed in chlorobenzene and nitrobenzene with TFA with similar results. (Figures shown in experimental section) In the absence of TFA, no intermediates were observed by UV-Vis, however, the hydrazine **92** was formed because the latter was detected by product analysis.

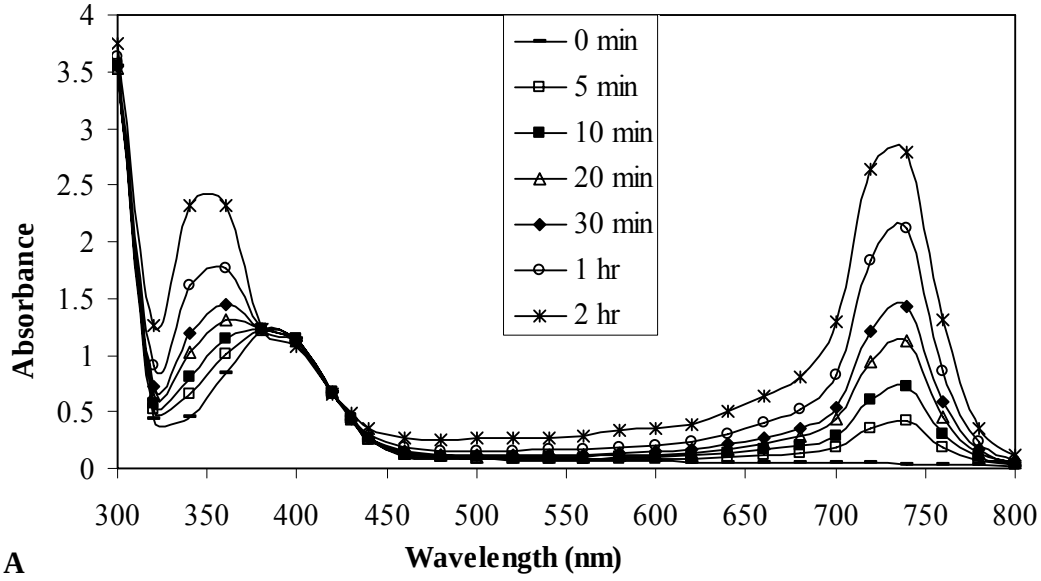

A

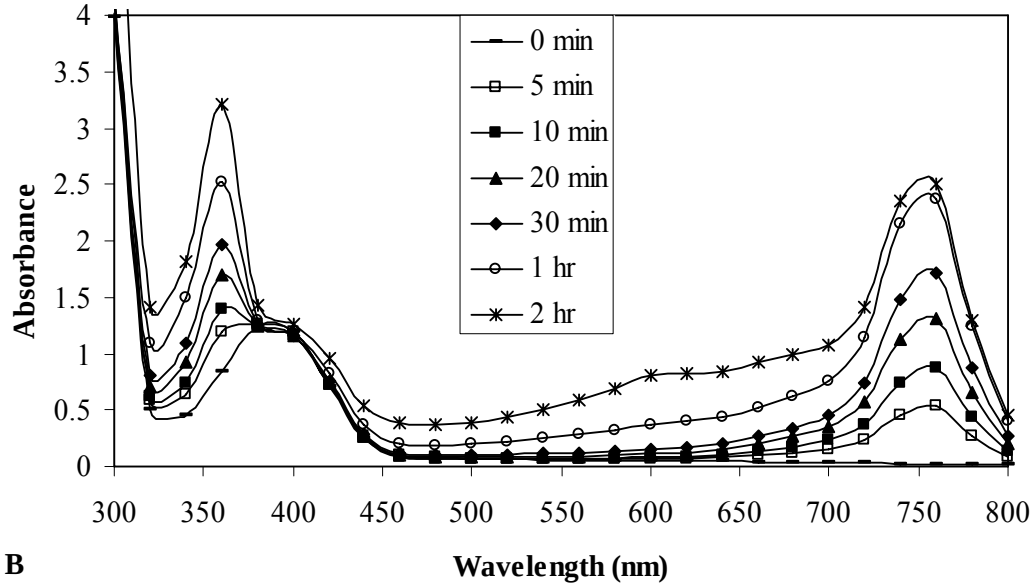

B

Figure 3.25 UV spectra of the photolysis of (A) **77b** and (B) **77c** in CH_2Cl_2 with TFA

The experiment is repeated by LFP to verify the results obtained by steady state UV. The precursor **77b** was photolyzed in CH_3CN with 10% H_2SO_4. (Figure 3.26) On excitation, the signal corresponding to **78b** was initially observed which decays rapidly to be replaced by a new sharp long-lived signal at 720 nm. The long-

lived species is the same species **85** observed by steady state UV analysis. In steady state UV spectra, these signals are red shifted due to acidic media.

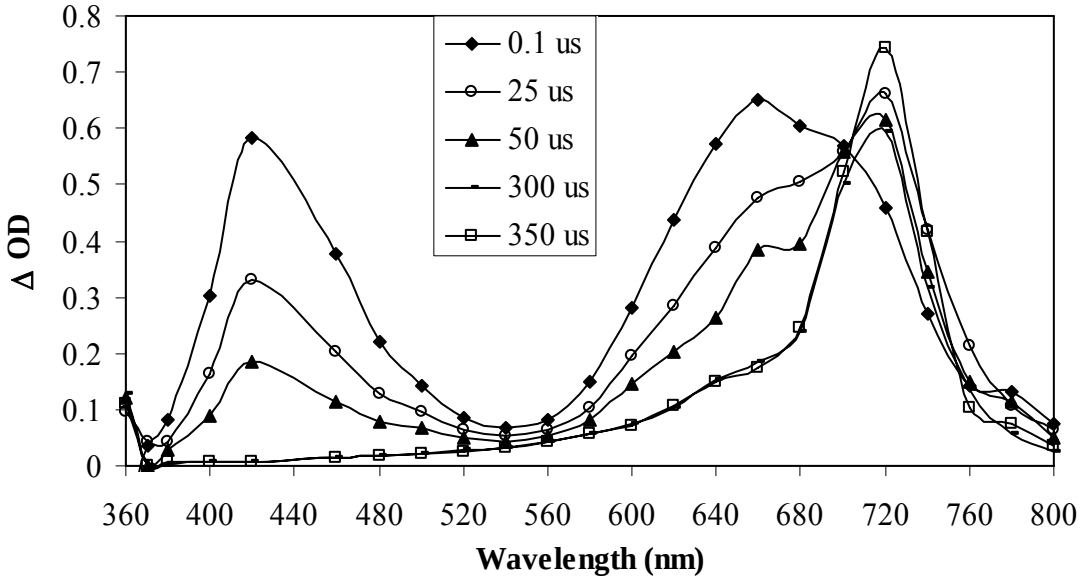

Figure 3.26 Transient spectrum of the photolysis of **77b** in CH_3CN with 10 % H_2SO_4.

Therefore, the nitrenium ions (**78b** or **78c**) generated undergoes one of the following processes: electron abstraction and then protonation or hydrogen atom abstraction to yield **85**. (Scheme 3.16) Hydrogen atom abstraction can be discounted as a possible mechanism because nitrobenzene and chlorobenzene are not good hydrogen atom sources. The C-H bond dissociation energy for benzene is 112.9 kcal/mol[25]; therefore, the C-H BDE of nitrobenzene and chlorobenzene should be higher than that making it harder to donate a hydrogen atom. Hence the other option would be electron abstraction followed by protonation.

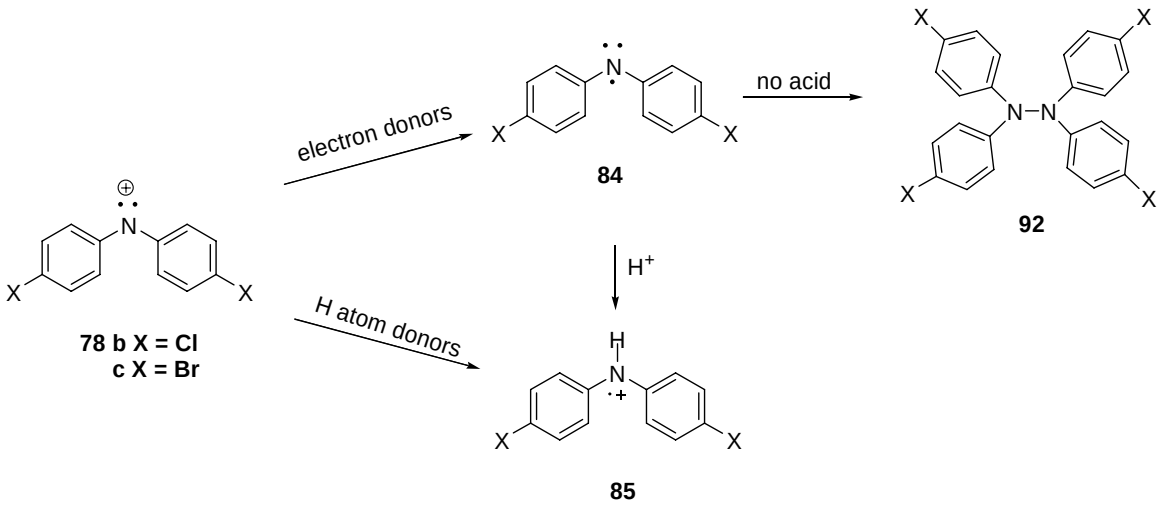

Scheme 3.16 Proposed chemical decay mechanism in acidic and non-acidic media

From the LFP results, it is evident that **78b** or **78c** is generated upon photolysis which is then converted to **84** and later protonated by the acid present in the solution. Even though **85** is formed in solvents such as chlorobenzene and nitrobenzene, it would seem unlikely for these solvents to donate electrons. It would seem that these solvent would have a higher E_{ox}, probably higher than benzene (E_{ox} 2.62 V)[19]; hence unable to contribute any electrons. An alternative source for the electrons would be some impurities present in the solvents. No matter what source produces the electrons, **78b** or **78c** abstracts it to form **84**. In the presence of an acid, **84** is protonated to form **85**. In the absence of the acid, it undergoes dimerization to yield **92**.

3.7 Reaction with Anions

An interesting observation was made during the course of our study of the **78b** and **78c** systems. Photolysis of **77b** or **77c** in the presence of certain anions (such as chloride, bromide, iodide and azide) resulted in the formation of a long-lived species with an absorption maximum at 420 nm. This long-lived species is attributed

to the π-complex formed between the nitrenium ion and the anion, since similar complexes are usually observed between aromatic systems and cation or anions. However, there are other possibilities for this 420 nm species. It could be the result of a σ-complex as observed with 1,3,5-TMB or some sort of a charge-transfer (CT) complex. These various possibilities were investigated. Even though a definite conclusion was not reached, a number of observations suggest that the species with absorption at 420 nm was a π-complex species.

LFP experiments conducted with various nucleophiles show that the 420 nm signal is specific to smaller anions. Shown in Figure 3.27 is the transient spectra obtained upon excitation of **77b** or **77c** in the presence of ~1 mM nBu_4NCl. The signals corresponding to **78b** or **78c** formed immediately after the laser pulse is quenched rapidly and the signal at 420 nm appears instantaneously. The photolysis was repeated by varying the nucleophiles and the conditions of the photolysis. Transient spectra are taken using tetrabutylammonium salts of bromide, iodide and azide. All these nucleophiles quenched the nitrenium ion rapidly and produced a signal at 420 nm. Iodide behaved slightly differently from that of the other anions and will be explained later. However, in the presence of acetate ion or perchlorate ion, the 420 nm signal was not produced, suggesting that the anions have to be smaller in size. Carrying out the photolysis in CH_2Cl_2 or oxygen purged systems did not alter the kinetic behavior of the transient signal. Varying the counter ion of the salts from tetrabutylammonium ion to tetraethylammonium ion still produced the 420 nm signal. This was tested by photolyzing **77c** in CH_3CN with Et_4NBr. Therefore,

these evidence suggested that this 420 nm species is specific to the nitrenium ion and smaller anions.

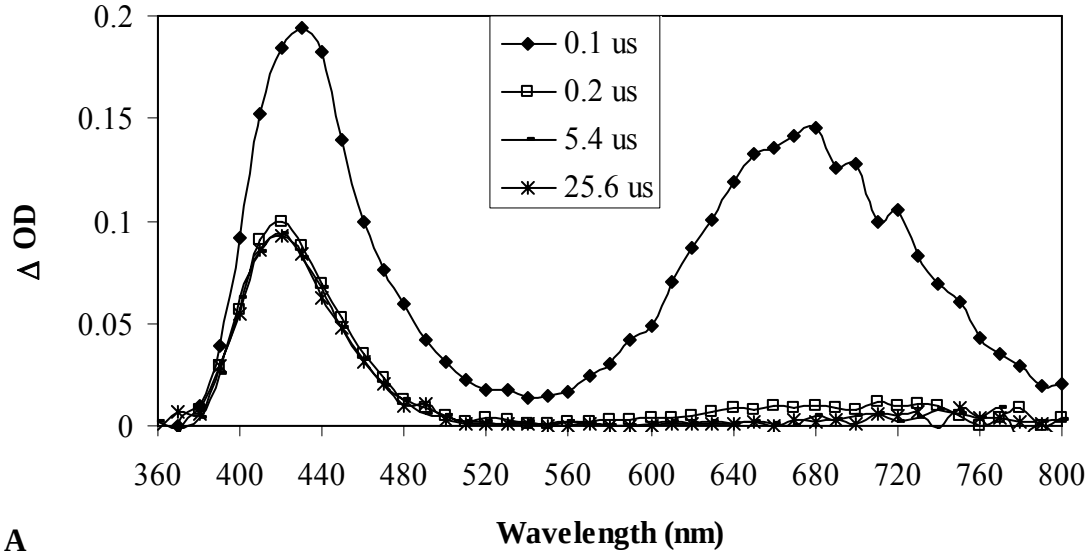

A

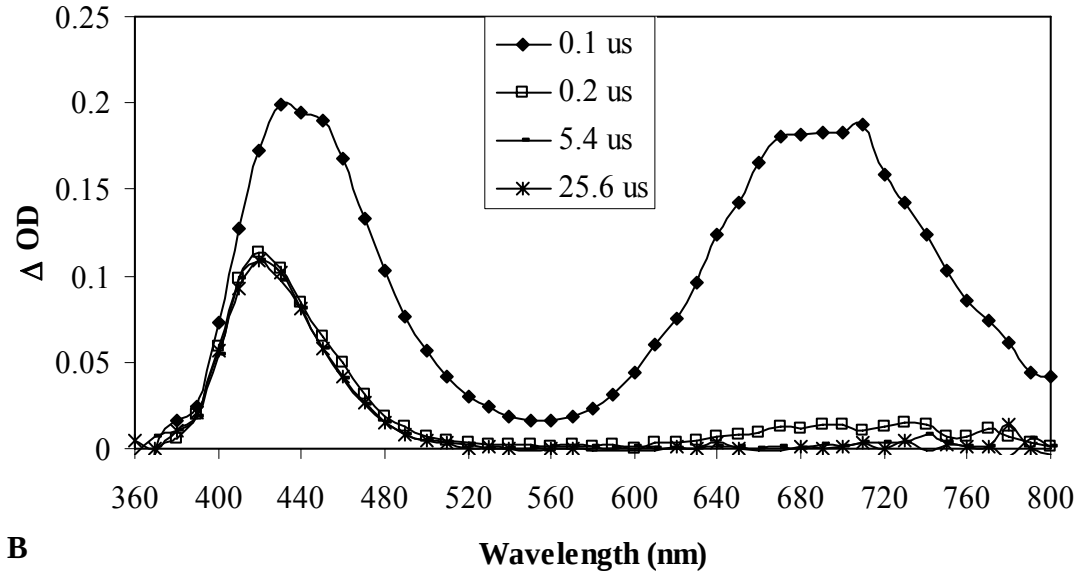

B

Figure 3.27 Transient spectra of the photolysis of (A) **77b** and (B) **77c** in the presence of 1 mM nBu_4NCl in CH_3CN

The possibility of the species being a σ-complex between **78b** or **78c** and the nucleophile was investigated. The protonated σ-complex between 1,3,5-TMB and

78b or **78c** was observed to absorb at 410 nm that eventually led to the covalent adduct **87**. Similarly chlorides also added to the nitrenium ion to yield an *ortho* adduct **82**; hence it was possible for the new species to be the intermediate (**93**) formed before **82**. (Scheme 3.17) This assumption was tested by photolyzing **77b** or **77c** with nBu_4NCl and pyridine assuming that if the species was in fact **93**, then the base should accelerate the deprotonation to yield the stable product causing the 420 nm signal to decay faster. However, the lifetime of the 420 nm signal was not affected by pyridine, suggesting that the species might not be a σ-complex.

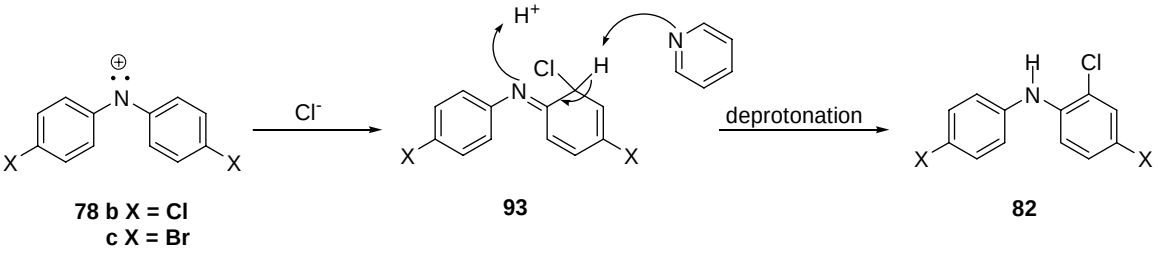

Scheme 3.17 Sigma complexation by chloride

The second assignment for the 420 nm signal was a charge-transfer (CT) complex between **77b** or **77c** and the nucleophile or between **78b** or **78c** and the nucleophile. Charge-transfer complexes are common between aromatic rings and electron-deficient or electron-rich systems and can be observed by steady state UV. Similar complex could be formed between the anion and **77b** or **77c**. The anion could donate an electron to the precursor, thus form a complex. (Scheme 3.18) To test this pathway, the photolysis of **77b** or **77c** with halides as the trap was followed by steady state UV. Except for the depletion of the precursor, no CT bands were observed. There are two reasons for this observation: either the complex was not formed or it was formed but not long-lived enough to be observed by steady state UV.

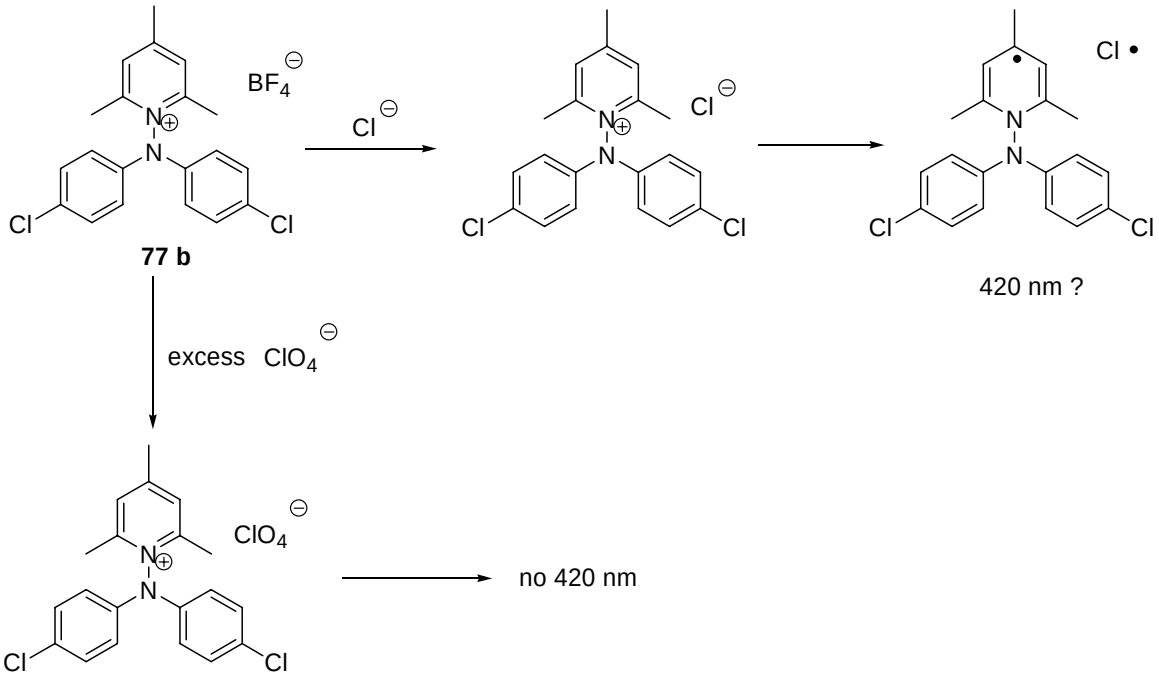

Scheme 3.18 Proposed mechanism for charge transfer

The second experiment conducted to test for CT complex formation was to add a different counter ion to the photolysis mixture along with the halide. The assumption was that the chloride ion displaces the BF_4^- ion of **77b** or **77c** to form an ionic complex with the positively charge precursor and upon photolysis undergoes electron transfer to give rise to the CT complex. Therefore, if excess perchlorate ion was present in the solution, it should compete with the chloride in displacing the BF_4^- ion either preventing or decreasing the formation of the ionic complex. The photolysis was carried out in the presence of 0.002 M nBu_4NCl and 0.19 M nBu_4NClO_4. Shown in Figure 3.28 is the transient spectrum of the photolysis. No significant change to 420 nm signal was observed, disproving this hypothesis. These results were inconclusive but at the same time did not provide enough evidence to support the CT complex between the precursor and the anion.

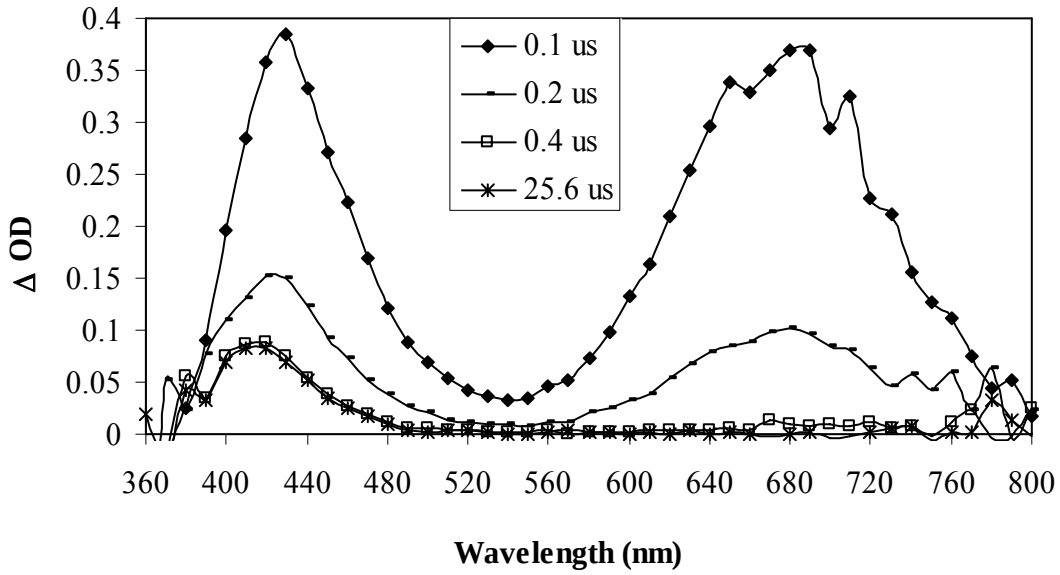

Figure 3.28 Transient spectra of the photolysis of **77b** in the presence of 0.002 M nBu_4NCl and 0.19 M nBu_4NClO_4 in CH_3CN

Since the signal corresponding to **78b** and **78c** was initially observed in all cases, it is possible that the new species resulted from some modification to **78b** and **78c** in the presence of these traps. Besides, the possibility that the long-lived species pre-existed in the solution and was hidden underneath the nitrenium signal can be discounted. Transient spectra taken over a longer time scale range (0-500 μs) with no traps showed no new signals other than those belonging to **78b** and **78c**. (Figure 3.1)

The final option that was investigated is the formation of a π-complex between **78b** or **78c** and the anion. π-complexes are usually observed for aromatic systems but mostly with metal cations. Some work associated with the π-complexation between electron deficient aromatic rings and anions were found in the literature and were referred to as anionic-π interactions.[30-33] Rosokha et. al. reported

observing a UV absorption band at 400 nm for the complex formed between tetracyanopyrazine (TCP) and chloride and bromide. Therefore, it is possible that the species that we observed at 420 nm is the anion-π complex formed between **78b** or **78c** and the halide.

Based on these similaries, the anion-π complex observed at 420 nm was believed to be the non-covalent interaction between **78b** or **78c** and the anion. In order to form a covalent bond with the *ortho* carbon of one of the phenyl rings, the negatively charged nucleophile initially formed a non-covalent interaction with the π electrons of one of the phenyl rings or both phenyl rings by being sandwiched between the two rings. (Scheme 3.19) This non-covalent interaction is eventually converted to a covalent bond between the anion and the phenyl ring which is immediately deprotonated to give the final stable product. The π-complexation seemed to be the rate determining step; hence once a non-covalent interaction was established between the two opposite charged species, the rest of the mechanism can occur immediately.

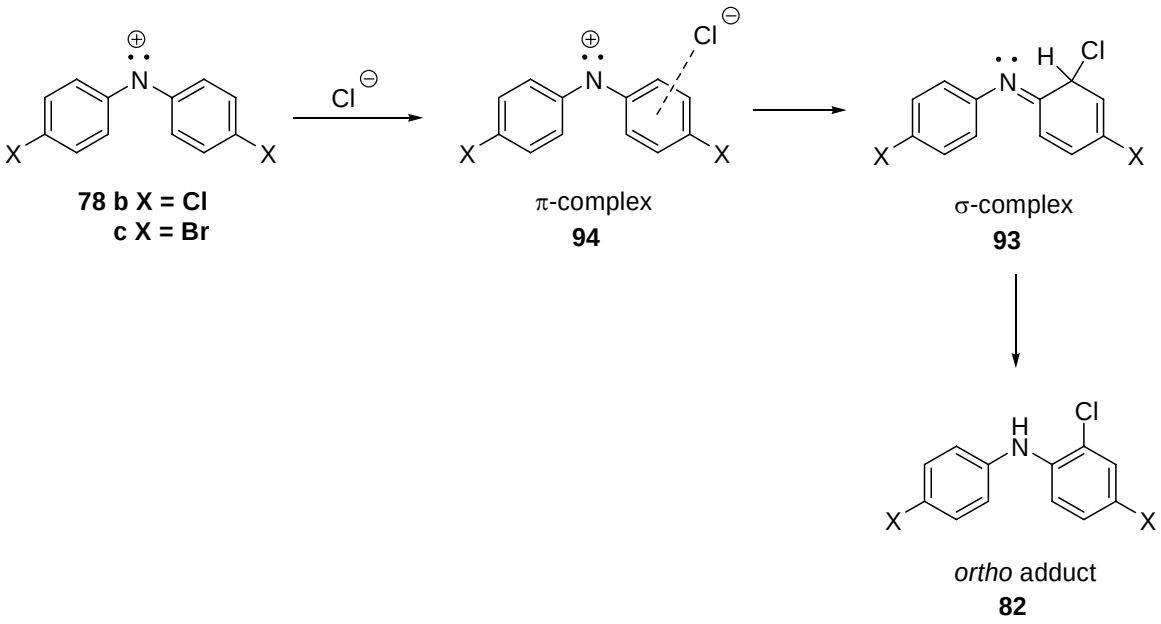

Scheme 3.19 Proposed mechanism for **82** involving the π-complex

The anionic-π complexation theory was supported by several experiments. The 420 nm species seemed to be solvent dependent. This species was persistent in solvents such as CH_3CN and CH_2Cl_2 but addition of H_2O decreased the production of the 420 nm signal. The precursor **77b** or **77c** was photolyzed in the presence of nBu_4NCl in H_2O/CH_3CN by keeping the chloride concentration constant but varying the H_2O concentration (0 – 11 M). (Figure 3.29) As the concentration of H_2O is increased, less and less of the 420 nm species is generated; the production of 420 nm species is hindered by H_2O. Since H_2O is capable of hydrogen bonding with the anions, it could prevent these ions from getting closer to the electron deficient phenyl ring. But in solvents such as CH_3CN and CH_2Cl_2, the anions are not enclosed by the solvent, therefore free to form π-complexes. If this species was a σ-complex, then the presence of H_2O should not affect the signal. Since the σ-complexation is an

event that happens after the ions come together, we should still be able to see the 420 nm signal, maybe with a delayed response.

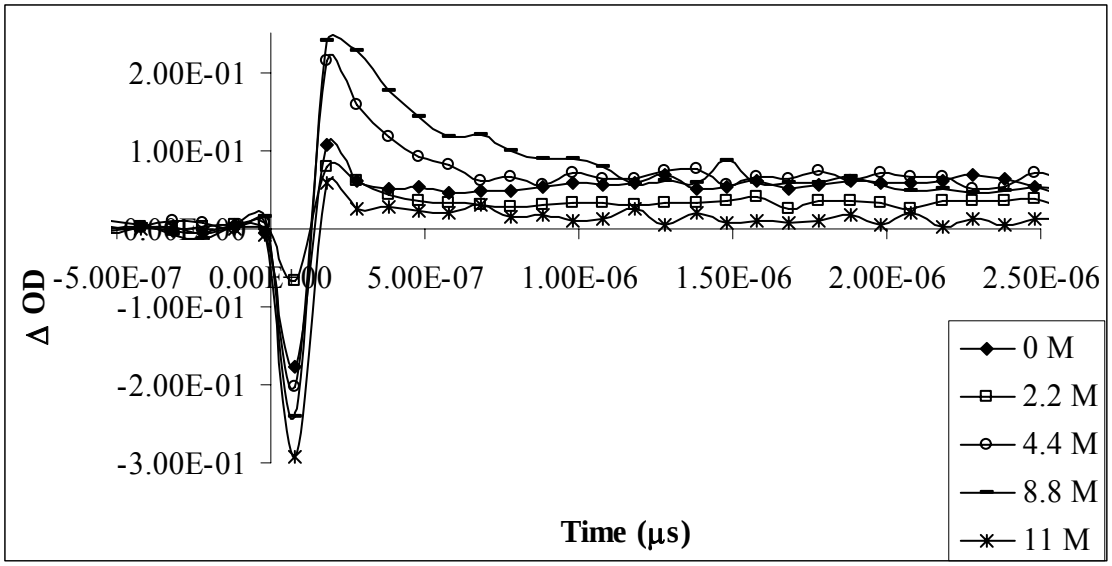

Figure 3.29 Waveform for the quenching of 420 nm peak from the photolysis of **77b** in the presence of nBu_4NCl by H_2O

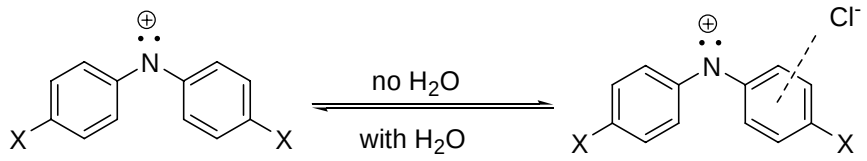

78 b X = Cl
c X = Br

94

Scheme 3.20 π-complexation in the presence of H_2O

In addition CT band was observed in the presence of iodide as the trap. Being easily oxidizable, in photochemical reactions, iodide is known to undergo charge transfer reactions that are observable by steady state UV. Transient spectra measured for the photolysis of **77b** in the presence of nBu_4NI displayed two new absorbance bands: a sharp long-lived band at 420 nm and a broad band around 760 nm. (Figure 3.30) The 420 nm band appears immediately after the laser pulse; however, the 760

nm band grew in around 2.4 μs and then decays. Based on our observations, we know that **84** absorbed at 760 nm. The fact that the 760 nm band grew in after the formation of the 420 nm signal indicates that **84** results from the 420 nm species. Therefore, if iodide is in fact donating an electron to **78b** or **78c**, then initially it has to form a non-covalent interaction with the latter initially. Hence, this non-covalent interaction between **78b** or **78c** and the anion absorbs at 420 nm. (Scheme 3.21) Since the nitrenium ion is relatively stable, these complexes live long enough to be detected by LFP.

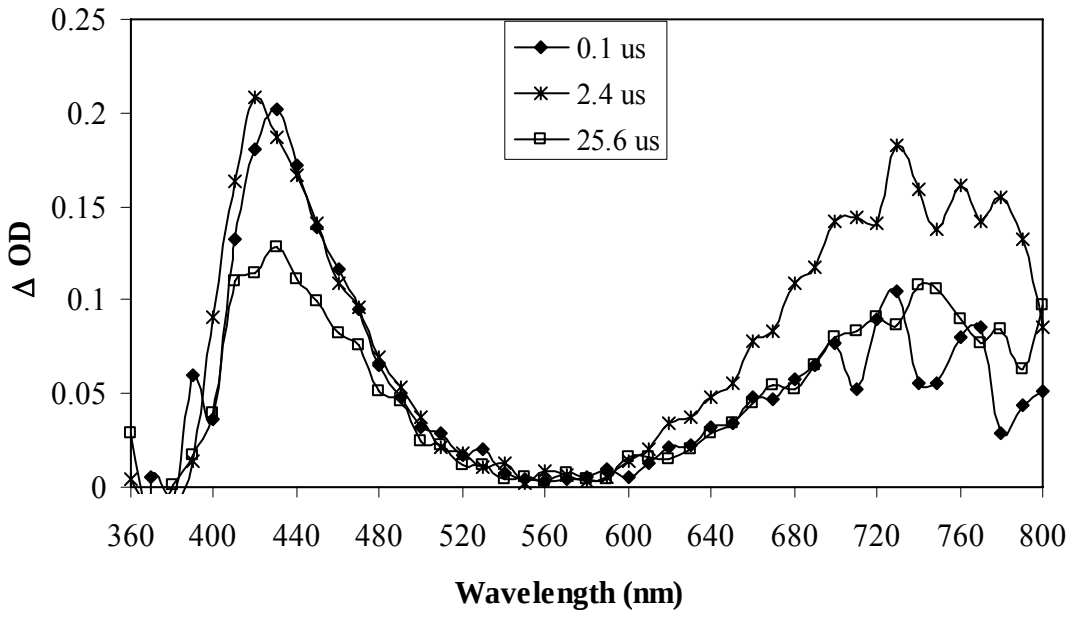

Figure 3.30 Transient spectra of the photolysis of **77b** in the presence of nBu_4NI (0.002 M) in CH_3CN

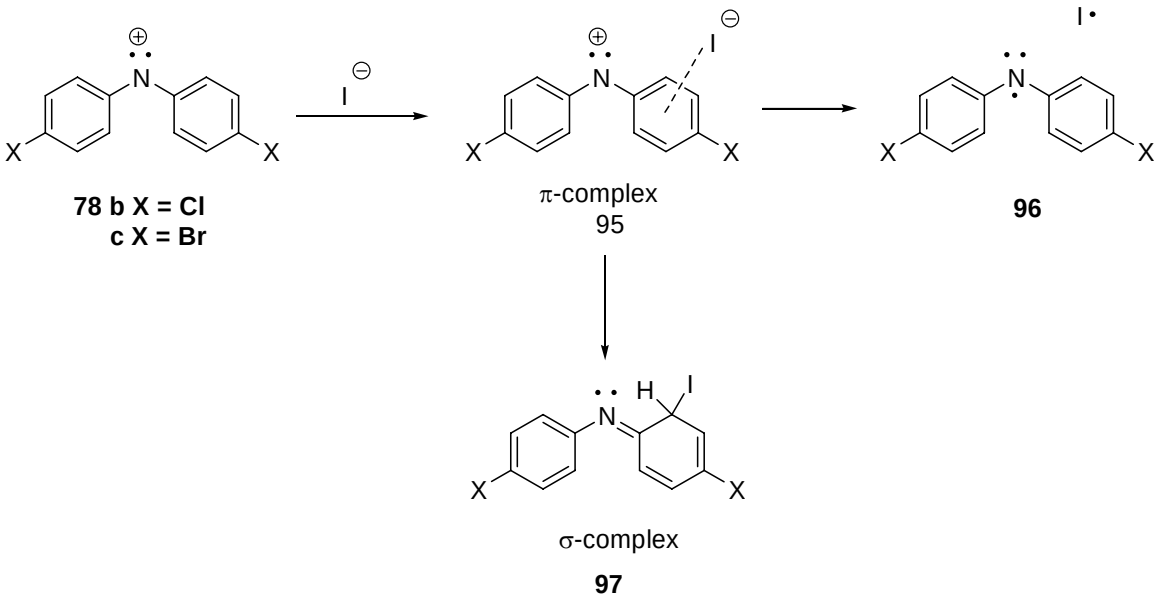

Scheme 3.21 Proposed mechanism for charge transfer by iodide

3.8 Conclusion

Based on the theoretical and experimental evidence discussed in this chapter, the halogenated diarylnitrenium ions (**78b** and **78c**) are concluded to be ground state singlets. These ions, generated photochemically, have absorbance maxima at 440 nm and 680 nm for **78b** and 450 nm and 690 nm for **78c**, respectively. They are relatively stable in most solvents with lifetime over 100 μs in CH_3CN.

The ions, **78b** and **78c** react with nucleophiles such as H_2O, alcohols and anions over a wide range of rate constants depending on the size and nucleophilicity of the traps. They react with chlorides and dGMP at the diffusion limit but much more slowly with H_2O (10^4 $M^{-1}s^{-1}$) to yield covalent adducts. Therefore, the reduced reactivity with H_2O than other nucleophiles increases the chances of these arylnitrenium ions being carcinogenic.

In the presence of arenes, **78b** and **78c** react via electron transfer or nucleophilic addition pathway. The reactivity of the ions depends on the E_{ox} of the arenes and the orientation of the substituents on the phenyl ring. 1,3,5-TMB and 1,3-DMB react with **78b** and **78c** via the nucleophilic addition pathway to yield *N* and *ortho* adducts. Reactions with electron donating arenes have shown that it is much harder to reduce **78b** and **78c** than the unsubstituted counterpart. As the E_{ox} of arenes increases, the quenching rate constants decrease ranging from 10^7 $M^{-1}s^{-1}$ to 10^5 $M^{-1}s^{-1}$. 4-bromoanisole with an E_{ox} of 1.78 V does not react with **78b** and **78c**, showing that arenes with oxidation potential above 1.78 V do not quench the ions.

In the absence of any nucleophiles, **78b** and **78c** decay to form **92**, a head-to-head dimer. Since the para position of the nitrenium ion is blocked, a head-to-tail dimerization as observed with **78a** is not observed.

Unlike the unsubstituted system, **78b** and **78c** are long-lived and exhibit triplet characteristics. These ions, **78b** and **78c**, display triplet behavior by undergoing hydrogen atom transfer in the presence of hydrogen atom donors. We assume that the triplet behavior results from the singlet-triplet equilibrium due to the smaller ΔE_{ST}. We assume that the ΔE_{ST} of **78b** and **78c** are slightly smaller than those predicted by the DFT calculations, allowing the nitrenium ion to undergo intersystem crossing to the triplet state. We believe that this is possible because the singlet arylnitrenium ions of **78b** and **78c** are stable that they exist long enough in solution to be able to intersystem cross to the triplet state. Since the singlet 78b and 78c do not react with the hydrogen atom donors, they intersystem cross to the triplet state which then reacts with the nucleophiles. Therefore, the stability of the nitrenium ion does seem to play

a role in the triplet behavior exhibited by **78b** and **78c**, which is possible due to the presence of halogens. Our evidence is supported by Gonzalez et. al. where by using *ab initio* molecular orbital calculations and DFT calculations, they showed that nitrenium ions containing halogens or nitrile groups have smaller values for ΔE_{ST}.[34] They attributed the smaller ΔE_{ST} to π-donation-π-acceptor effect of the species.

Moreover, **78b** and **78c** are more stable than **78a**. The longer lifetime of **78b** and **78c** are considered to be the consequence of π donation of the non-bonding electrons of halogens. Similar stability has been observed for 2,3,5,6-tetrafluorophenylnitrenium ion.[7,35] This ion lives for more than 1 ms in CH_3CN and is believed to be stable due to the π-donation from fluorines. Hence substituting halogens in **78a** lowers the ΔE_{ST} and increases the lifetime of the ion.

References

(1) Srivastava, S.; Toscano, J. P. *J. Am. Chem. Soc.* **1997**, *119*, 11552-11553.

(2) Srivastava, S.; Ruane, P. H.; Toscano, J. P.; Sullivan, M. B.; Cramer, C. J.; Chiapperino, D.; Reed, E. C.; Falvey, D. E. *J. Am. Chem. Soc.* **2000**, *122*, 8271-8278.

(3) Abramovitch, R. A.; Evertz, K.; Huttner, G.; Gibson, H. H., Jr.; Weems, H. G. *J. Chem. Soc. Chem. Commun.* **1988**, *4*, 325-327.

(4) Freeman, H. S.; Butler, J. R.; Freedman, L. D. *J. Org. Chem.* **1978**, *443*, 4975-4978.

(5) Moran, R. J. Ph. D Dissertation, University of Maryland, College Park, MD, 1997.

(6) Moran, R. J.; Falvey, D. E. *J. Am. Chem. Soc.* **1996**, *118*, 8965-8966.

(7) Falvey, D. E. In *Organic, Physical, and Materials Photochemistry*; Ramamurthy, V. S., K.S;, Ed.; Marcel Dekker, Inc: New York, 2000; Vol. 6, pp 249-284.

(8) Cramer, C. J.; Falvey, D. *Tet. Lett.* **1997**, *38*, 1515-1518.

(9) Winter, A. H.; Thomas, S. I.; Kung, A. C.; Falvey, D. E. *Org. Lett.* **2004**, *6*, 4671-4674.

(10) McIlroy, S.; Moran, R. J.; Falvey, D. E. *J. Phys. Chem.* **2000**, *104*, 11154-11158.

(11) Chiapperino, D.; Falvey, D. E. *J. Phys. Org. Chem.* **1997**, *10*, 917-924.

(12) Kung, A. C.; McIlroy, S.; Falvey, D. E. *J. Org. Chem.* **2005**, *70*, 5283-5290.

(13) Chiapperino, D.; McIlroy, S.; Falvey, D. E. *J. Am. Chem. Soc.* **2002**, *124*, 3567-3577.

(14) Shida, T. *Electronic Absorption Spectra of Radical Ions*; Elsevier: Netherlands, 1988; Vol. 34.

(15) Wagner, B. D.; Ruel, G.; Lusztyk, J. *J. Am. Chem. Soc.* **1996**, *118*, 13-19.

(16) Jonsson, M.; Wayner, D. D.; Lusztyk, J. *J. Phys. Chem.* **1996**, *100*, 17539-17543.

(17) Murov, S. L.; Charmichael, I.; Hug, G. L. *Handbook of Photochemistry*; 2 ed.; Marcel Dekker: New York, 1993.

(18) Zweig, A.; Hodgson, W. G.; Jura, W. H. *J. Am. Chem. Soc.* **1964**, *86*, 4124-4129.

(19) Rathore, R.; Kochi, J. K. *Adv. Phys. Org. Chem.* **2000**, *35*, 193-318.

(20) Sankararaman, S.; Haney, W. A.; Kochi, J. K. *J. Am. Chem. Soc.* **1987**, *109*, 7824-7838.

(21) McIlroy, S. Ph. D Dissertation, University of Maryland, College Park, MD, 2002.

(22) McIlroy, S.; Falvey, D. E. *J. Am. Chem. Soc.* **2001**, *123*, 11329-11330.

(23) Mathivanan, N.; Cozens, F.; McClelland, R. A.; Steenken, S. *J. Am. Chem. Soc.* **1992**, *114*, 2198-2203.

(24) Steenken, S.; McClelland, R. A. *J. Am. Chem. Soc.* **1990**, *112*, 9648-9649.

(25) Luo, Y.-R. *Handbook of Bond Dissociation Energies in Organic Compounds*; CRC Press: Washington, D. C, 2003.

(26) Alabugin, I. V.; Kovalenko, S. V. *J. Am. Chem. Soc.* **2002**, *124*, 9052-9053.

(27) Shono, T.; Ikeda, A.; Hayashi, J.; Hakozaki, S. *J. Am. Chem. Soc.* **1975**, *97*, 4261-4264.

(28) Grubert, L.; Jacobi, D.; Abraham, W. *J. Prakt. Chem.* **1999**, *341*, 620-630.

(29) Bordwell, F. G.; Cheng, J.-P. *J. Am. Chem. Soc.* **1991**, *113*, 1736-1743.

(30) Rosokha, Y. S.; Lindeman, S. V.; Rosokha, S. V.; Kochi, J. K. *Angew. Chem. Int. Ed. Engl.* **2004**, *43*, 4650-4652.

(31) Lenoir, D. *Angew. Chem. Int. Ed. Engl.* **2003**, *42*, 854-857.

(32) Quinonero, D.; Garau, C.; Rotger, C.; Frontera, A.; Ballester, P.; Costa, A.; Deya, P. M. *Angew. Chem. Int. Ed. Engl.* **2002**, *21*, 3389-3392.

(33) Mascal, M.; Armstrong, A.; Bartberger, M. D. *J. Am. Chem. Soc.* **2002**, *124*, 6274-6276.

(34) Gonzalez, C.; Restrepo-Cossio, A.; Marquez, M.; Wilberg, K.; Rosa, M. D. *J. Phys. Chem. A* **1998**, *102*, 2732-2738.

(35) Michalak, J.; Zhai, H. B.; Platz, M. S. *J. Phys. Chem.* **1996**, *100*, 14028-14036.

Chapter 4. Photochemically Generated Nitrenium Ions from Protonated Hydrazines

Nitrenium ions are intermediate species that exist for few microseconds; therefore there has been a general interest in learning more about these transient intermediates. However, due to the shorter lifespan, the study of these intermediates was limited until recently. The development of photochemical methods made the detection and study of these intermediates much easier.[1,2] But only limited photochemical methods are available for the generation of the nitrenium ions.

Nitrenium ions are usually generated photochemically from precursors such as anthranilium salts (**98**), azides (**99**) and *N*-aminopyridinium salts (**100**).[3-7] (Scheme 4.1) These precursors are excited by light to cause heterolytic cleavage to yield nitrenium ions. However, these precursors have some advantages and disadvantages associated with them. Photolysis of **98** generates *N*-alkyl-*N*-arylnitrenium ions with an acetyl group *ortho* to the nitrogen atom. Azides (**99**) are easier to synthesize and they generate nitrenium ions in protic media, but these ions can only be monosubstituted. *N*-aminopyridinium salts (**100**) have so far proven to be a better source for generating nitrenium ions photochemically. These salts allow the substitution of any functional groups on the nitrogen of the nitrenium ion and are relatively soluble in most solvents. The drawback for this precursor is that it requires a multi-step synthesis. Hence, it is always of great interest to find new methods to the generation of nitrenium ions.

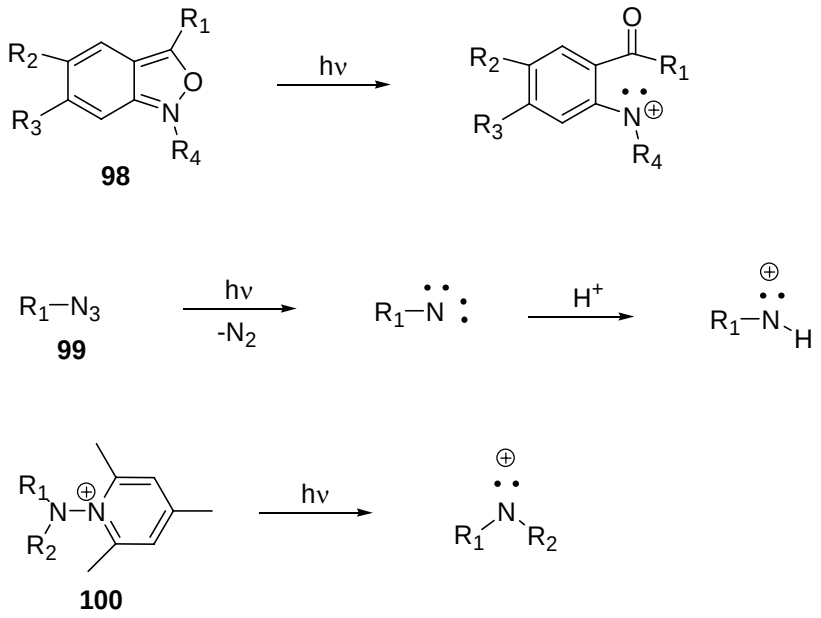

Scheme 4.1 General photochemical generation of nitrenium ions

4.1 General Characteristics of the Precursor

This chapter discusses an alternative pathway for photochemically generating dihalogenated diarylnitrenium ions, (**78b** and **78c**) from the protonated form of their respective hydrazines. 1,1-di(4-chlorophenyl) hydrazine (**81b**) and 1,1-di(4-bromophenyl) hydrazine (**81c**) were the two hydrazines used for our study. The photochemistry of the nitrenium ions generated upon photolysis of the free bases in protic media were studied using LFP techniques, product analysis and time-dependent density functional theory (TD-DFT) (Table 3.1 in chapter 3) and were found to agree with the results obtained for the same nitrenium ion generated from pyridinium precursors (**77b** and **77c**) discussed in chapter 3.

The hydrazine precursors (**81b** and **81c**) were synthesized employing the procedures used for the pyridinium salts. (See chapter 3) Since hydrazines were not commercially available, they were synthesized from the diphenylamine via a series of step. The free bases of **81b** and **81c** are soluble in slightly polar solvents with an

absorption maximum at 305 nm. The free bases were protonated with HBF_4 to generate the hydrazinium ions, **101b** and **101c**. The precursors, **101b** and **101c**, have a weak absorption tail below 250 nm with an extinction coefficient of 3.8 x 10^3 $M^{-1}cm^{-1}$ and 3.6 x 10^3 $M^{-1}cm^{-1}$ at 266 nm respectively. HBF_4 is chosen for the study because it is a mild acid.

4.2 Generation of the Nitrenium Ions

Photolysis of **101b** or **101c** in CH_3CN/HBF_4 using a Nd:YAG (266 nm, 4 ns, 10-25 mJ/pulse) generates three signals with absorption maxima around 440 nm, 680 nm and 720/730 nm. (Figure 4.1) The signals with absorption maxima at 440 nm and 680 nm appear immediately after the laser pulse and are attributed to the corresponding nitrenium ions, **78b** or **78c**, which result from the heterolytic cleavage of **101** into **78** and neutral ammonia. (Scheme 4.2) However, unlike those generated from pyridinium salts, these ions decay rapidly and a new signal at 720/730 nm grows within 5-7 μs. The new long-lived species was identified as the radical cation **85** of the corresponding parent amine **79**.

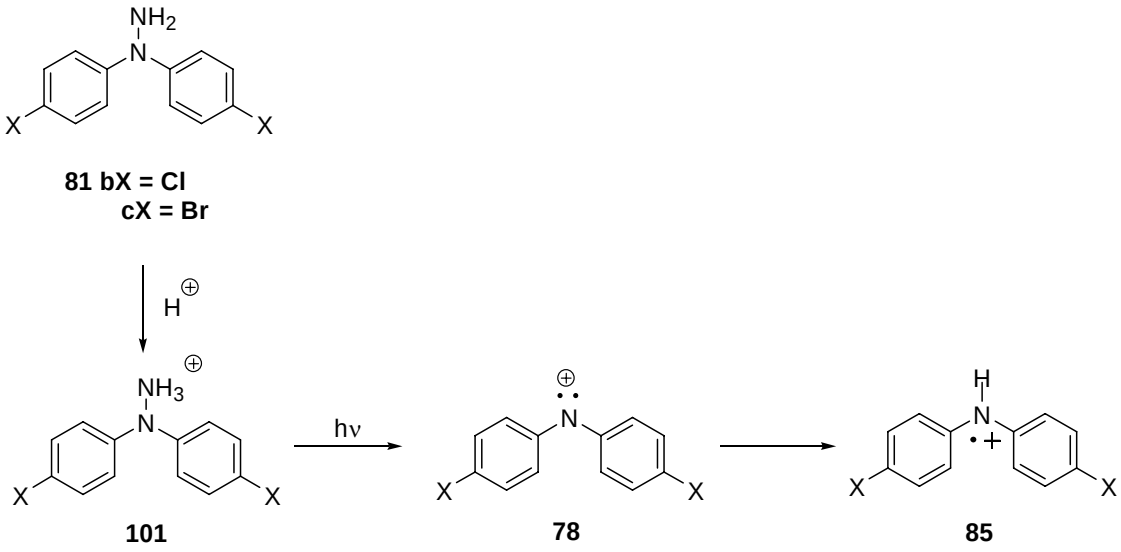

Scheme 4.2 Photolysis of **101**

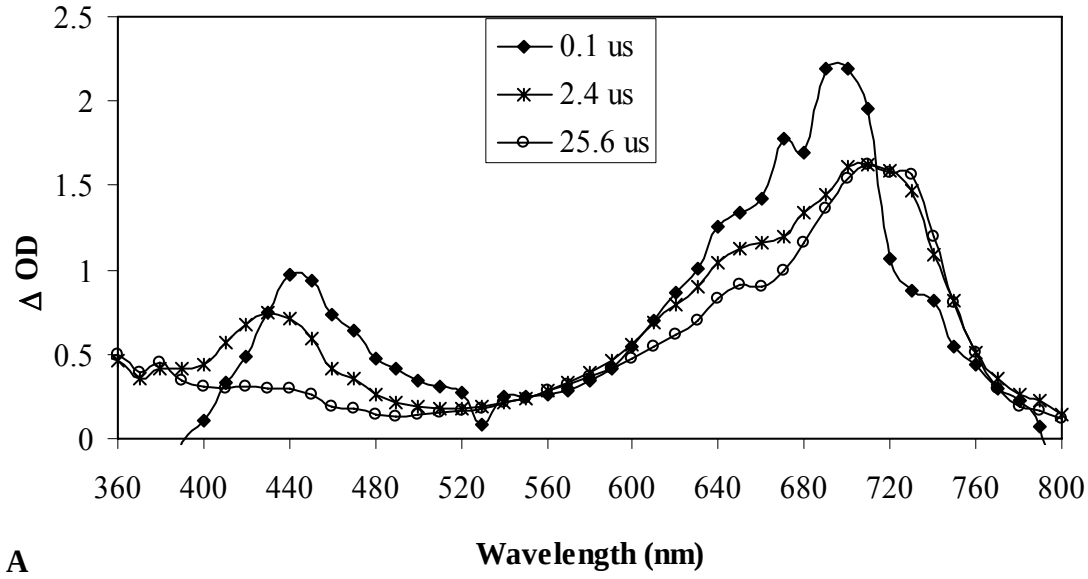

A

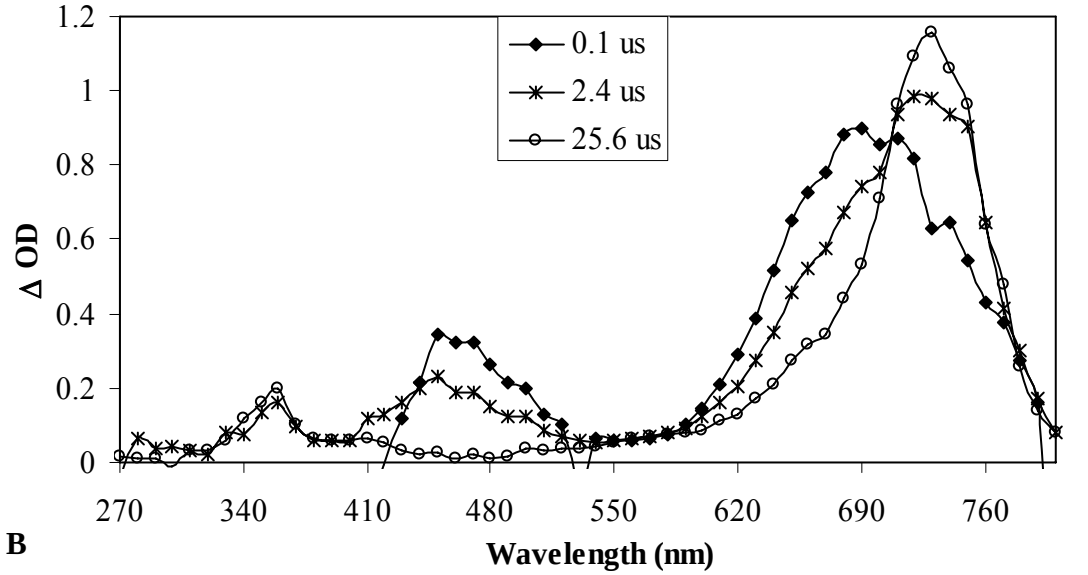

B

Figure 4.1 Transient spectra of the photolysis of (A) **101b** and (B) **101c** in CH_3CN.

The hydrazinium generated **78** was established to be the same transient intermediate generated from the pyridinium precursors (**77b** and **77c**). The signals observed for **78** generated from hydrazinium ion and the pyridinium salt show excellent agreement with each other, having strong absorbance bands around 440 and 680 nm. As shown in Table 3.1 in chapter 3, these signals closely match the UV-Vis

signals predicted by TD-DFT calculations for singlet **78**. However, the lifetimes of these hydrazinium generated **78** vary. The pyridinium generated **78** are very stable and lived for more than 100 μs in CH_3CN. In addition, no intermediate was detected upon the decay of **78**. On the other hand, the life span of the hydrazinium generated **78** in CH_3CN was only 5-6 μs. They were not that stable and decayed rapidly to a long-lived **85**.

4.3 Reaction of 78 with Chloride

The identity of the hydrazinium generated **78** was verified by conducting kinetic trapping studies with chloride. The hydrazinium generated **78** is quenched using chloride because the latter is known to react with nitrenium ions at or close to the diffusion limit (k_{diff} CH_3CN = 1.9 x 10^{10} $M^{-1}s^{-1}$).[8] Shown in Table 4.1 is the second order reaction rate obtained from the pseudo-first order decay rate of the nitrenium ions at varying concentration of chloride. The chlorides reacts with the hydrazinium generated **78** at a rate constant of 10^9 $M^{-1}s^{-1}$, whereas the pyridinium generated **78** reacts at an order of 10^{10} $M^{-1}s^{-1}$. This reduced reactivity of the hydrazinium generated **78** could be due to the protonation of the chloride ion by the acid required to generate hydrazinium ion **101**. However, these rates were high enough to establish that the species being trapped was the nitrenium ion.

Table 4.1 Second order rate constant from the reaction of chloride with **78** generated by different methods

Nitrenium ions	k_{nuc} ($M^{-1}s^{-1}$)	
	Hydrazinium generated	Pyridinium generated
78b	(4.67 ± .48) x 10^9	(1.06 ± .03) x 10^{10}
78c	(5.47 ± .07) x 10^9	(9.83 ± .60) x 10^9

In addition to competitive trapping studies, product analysis confirmed that these hydrazinium generated **78** react with chlorides to yield nucleophilic addition products similar to pyridinium generated **78**. Photolysis of **101** in the presence of chloride to yields two photoproducts: parent amine **79** and the chloride addition product **82**. (Figure 4.2) Isolation of **82** supported the fact that the intermediates generated from both precursors were the same. HCl was used as the source for chloride ion and the photolysis was done with excess amount of HBF_4 to ensure that the chloride stayed deprotonated. The photoproducts obtained were analyzed by GC against the authentic samples obtained from the photolysis of **77**.

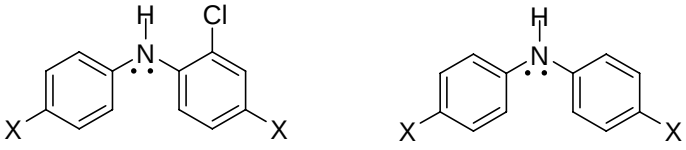

82 b X = Cl
c X = Br

79 b X = Cl
c X = Br

Figure 4.2 Photoproducts isolated from the reaction of **101** with chlorides.

4.4 Mechanism for the Formation of the Radical Cation

Even though both precursors generated the same nitrenium ion **78**, unlike the pyridinium generated **78**, the hydrazinium generated **78** decays quite rapidly to form **85**. The same species **85** was observed for the pyridinium generated **78**. In the case of pyridinium generated **78**, **85** was formed as a result of single electron transfer or hydrogen atom abstraction. In this situation, additional nucleophiles were not present except for HBF_4 and the precursor which could possibly be the source for electrons or hydrogen atom.

One possible route for electron abstraction would be that the hydrazinium generated **78** could abstract an electron from the unreacted **101** to form the aminyl

radical (**84)** that is protonated immediately. (Scheme 4.3) This pathway was investigated by generating **78** from pyridinium precursors (**77b** or **77c**) in the presence of the **101**. Since **101** did not absorb above 300 nm, **77** could be selectively irradiated to generate **78**. Shown in Figure 4.3 is the transient spectra obtained upon the excitation of **77b** or **77c** with the respective **101b** or **101c**. Generally, in the absence of any trap, pyridinium generated **78** decays slowly with the formation of no intermediates. However, in the presence of **101**, the pyridinium generated **78** decays rapidly and the growth of **85** is observed around 2.4 μs. In order to form **85**, the pyridinium generated **78** had to abstract electrons from some sources which in this instance are **101**. The species **84** that resulted from the electron transfer is protonated by HBF_4 to yield **85**.

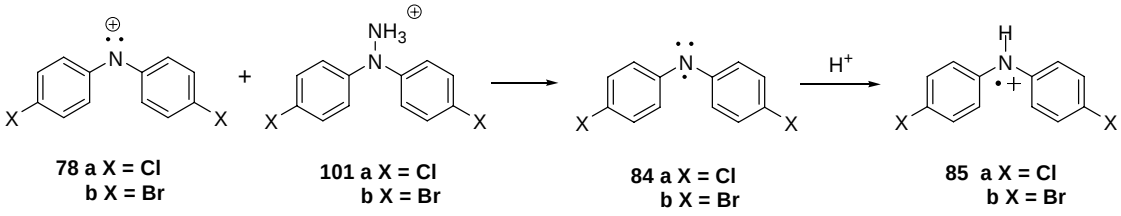

Scheme 4.3 Proposed mechanism for the decay of pyridinium generated **78** in the presence of **101**

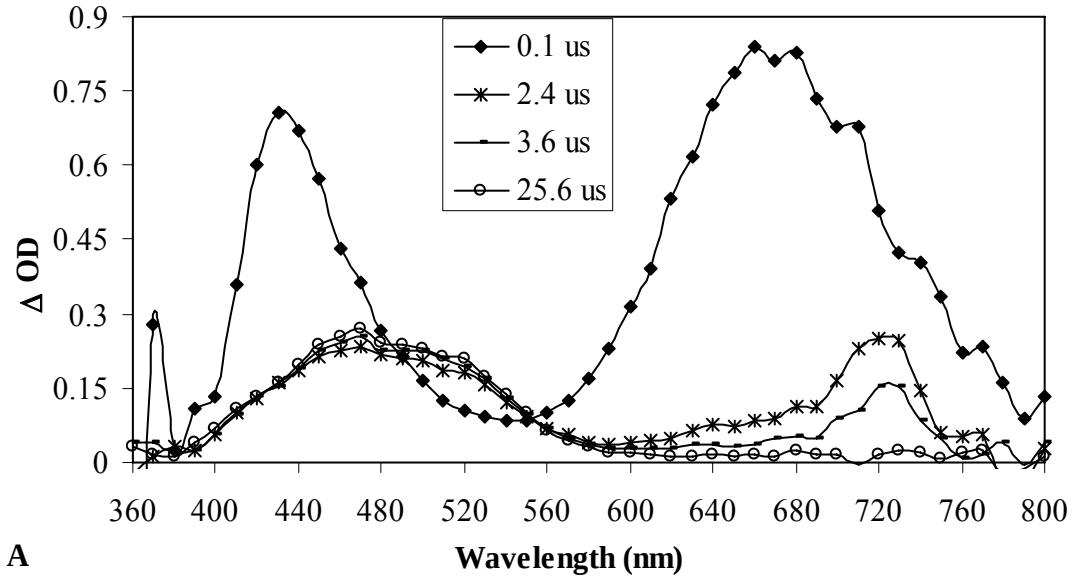

A

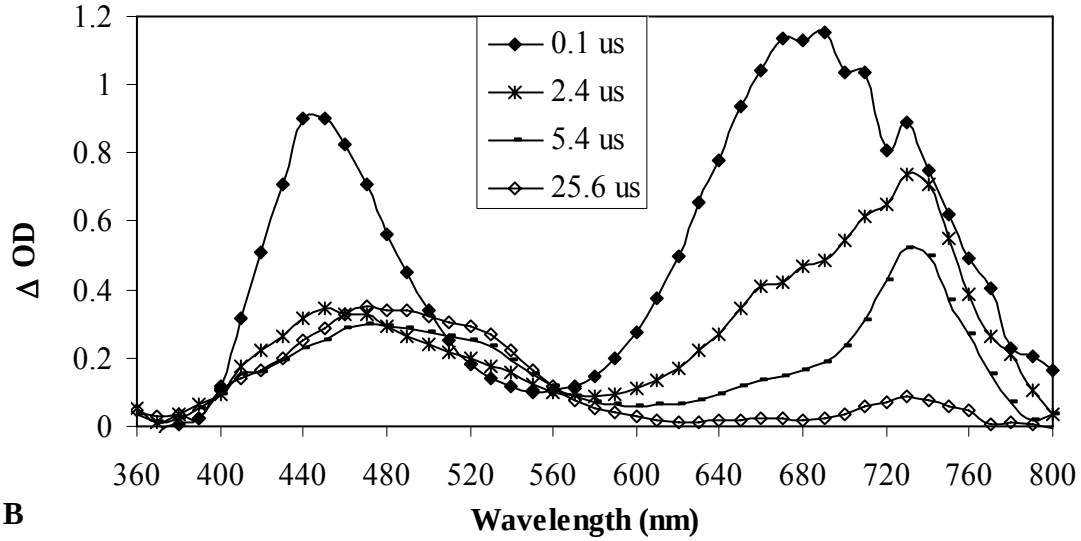

B

Figure 4.3 Transient spectra of the photolysis of (A) **77b** and (B) **77c** with corresponding **101**.

The second experiment to confirm the electron transfer mechanism was conducted by photolyzing **77b** or **77c** in the presence of the corresponding **81**. In the presence of **81**, the pyridinium generated **78** reacts to yield **84** observed in the transient spectrum by a broad absorbance band around 760 nm. (Figure 4.4) The

species **84** stayed unprotonated due to the absence of acid. These observations support that **81** and **101** are capable of donating electrons contributing to the rapid decay of the hydrazinium generated **78**.

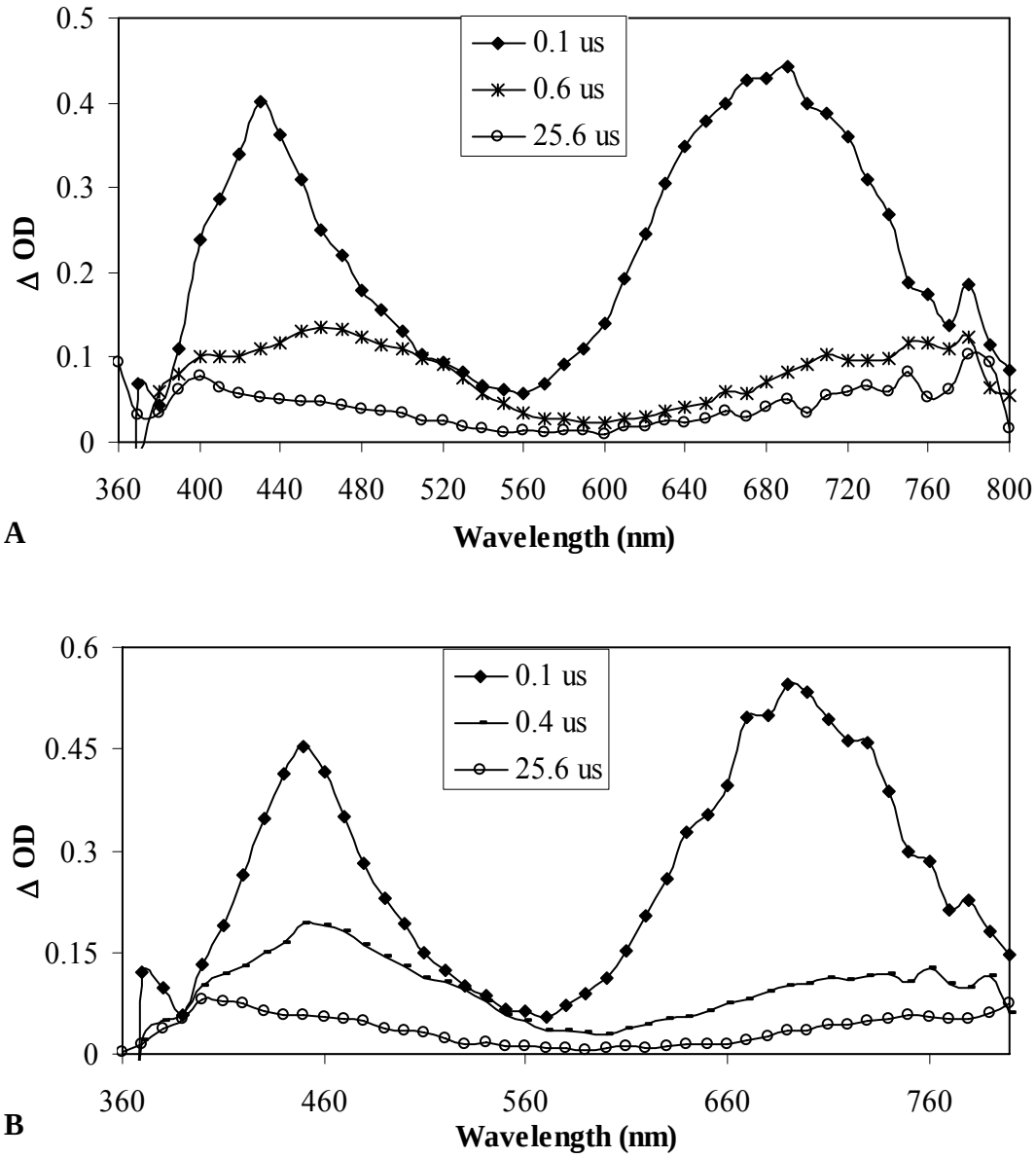

Figure 4.4 Transient spectra of the photolysis of (A) **77b** and (B) **77c** with the corresponding **81**.

Alternatively, **85** could also be formed via hydrogen atom abstraction pathway. For this pathway, the likely source for the hydrogen atom would be the unreacted **101** but this pathway was rejected based on the following reasonings. Hydrogen atom abstraction is generally a triplet pathway, therefore, in order to decay via this pathway, the hydrazinium generated **78** will have to exist in its triplet state to accept a hydrogen atom. Experimental evidence for the pyridinium generated **78** suggest that these species are ground state singlets except in rare instances. Additionally **81** are electron rich; therefore, it would most likely donate electrons rather than hydrogen atoms. Also the formation of **84** upon photolysis of **77b** or **77c** in the presence of **81** confirms that these ions decay via a electron abstraction. Based on these reasonings, hydrogen atom abstraction pathway would seem unlikely.

4.5 Conclusion

Photolysis of **101b and 101c** yields respective **78** in high yield with strong UV absorbances around 440 and 680 nm. These intermediate species are identical to those ions generated from **77b** and **77c** in all aspects except for their stability. They decay within 5-7 μs to **85** by abstracting an electron from the unconverted **101** to form the **84** that is protonated immediately. Similar to the pyridinium generated **78**, hydrazinium generated **78** reacts rapidly with chloride to yield chloro adducts along with the parent amine. This is a typical photoproduct of a singlet nitrenium ion.

The data presented in this chapter have shown that nitrenium ions can be generated photochemically from protonated hydrazines. Similar to the azide methods, these ions were generated in protic media but unlike the azide, the nitrenium ions generated can be disubstituted. *N*-aminopyridinium salt precursors are ideal

methods for the generation of nitrenium ions, but it is sometimes difficult to couple the hydrazine with the pyrylium salts to give the final pyridinium salt. With hydrazine as precursor the need for the final coupling step required for the pyridinium salt synthesis can be eliminated.

Despite the advantages, there are some disadvantages associated with the hydrazinium method that could affect the experimental results. These precursors are excited using laser pulse of a lower wavelength (266 nm). Many organic compounds absorb at this wavelength. Therefore it will be difficult to selectively excite the hydrazinium precursor when conducting competitive trapping studies. In addition, even though **78** lives longer than any other arylnitrenium ions, the latter decayed rather rapidly due to the presence of a good electron source present in the solution. Hence it would be difficult to observe the nitrenium ions that have shorter lifetime than **78**. The acidic media would also pose a problem for competitive trapping studies. Since the acidic media could protonate the nucleophiles, it could introduce uncertainties in the results. Therefore, this method is probably best for conducting pilot studies on nitrenium ions but not designed for obtaining elaborate and extensive knowledge on the transient intermediates.

References

(1) Novak, M.; Rajagopal, S. *Adv. Phys. Org. Chem.* **2001**, *36*, 167-254.

(2) Falvey, D. E. In *Reactive Intermediate Chemistry*; Moss, R. A., Platz, M. S., Maitland Jones, J., Eds.; Wiley-Interscience: Hoboken, 2004; Vol. 1, pp 593 - 650.

(3) Anderson, G. B.; Yang, L. L.-N.; Falvey, D. E. *J. Am. Chem. Soc.* **1993**, *115*, 7254-7262.

(4) McClelland, R. A.; Kahley, M. J.; Davidse, P. A.; Hadzialic, G. *J. Am. Chem. Soc.* **1996**, *118*, 4794-4803.

(5) Srivastava, S.; Toscano, J. P. *J. Am. Chem. Soc.* **1997**, *119*, 11552-11553.

(6) Abramovitch, R. A.; Shi, Q. *Heterocycles.* **1994**, *37*, 1463-1466.

(7) Chiapperino, D.; Anderson, G. B.; Robbins, R. J.; Falvey, D. E. *J. Org. Chem.* **1996**, *61*, 3195-3199.

(8) Falvey, D. E. In *Organic, Physical, and Materials Photochemistry*; Ramamurthy, V. S., K.S;, Ed.; Marcel Dekker, Inc: New York, 2000; Vol. 6, pp 249-284.

Chapter 5. Laser Flash Photolysis Studies of *N*-(4-Biphenylyl-*N*-Methyl) Nitrenium Ion with Amino Acids and Proteins

The work reported in this chapter is the final segment of an ongoing project on (*N*-4-biphenylyl-*N*-methyl) nitrenium ion (**103**). This arylnitrenium ion is considered to be the electrophilic intermediate of 4-aminobiphenyl that is responsible for cancer in living cells.[1-4] Earlier work done in our lab showed that this ion reacts readily with any nucleophilic agents such as chlorides, azides, arenes even purine nucleosides especially guanosine to form covalent adducts.[5-7] Since guanosine mutation leads to DNA damage that is responsible for cancer, a lot of research has been devoted to the study of nitrenium ions and DNA.[8,9]

Work published in the late 1960s and early 1970s showed that aromatic amines or amides *in vivo* and *in vitro* react with amino acids similarly to DNA.[1,10-16] These reactions with aromatic amino compounds resulted in covalent adducts between the amino acids and the amines which was suspected to occur via nitrenium ion then referred to as "aminonium ion".[17] Except for *in vitro* and *in vivo* studies done on these systems, no work has been done to understand the reactivity of any nitrenium ion with amino acids since the development of laser flash techniques. Hence, the goal of this research was understand the reactivity of amino acids and proteins with the arylnitrenium ions and understand their decay pathway by directly monitoring their reaction.

5.1 General Characteristics of (*N*-4-Biphenylyl-*N*-Methyl) Nitrenium Ion

The nitrenium ion, **103**, was photochemically generated from 1-(*N*-4-biphenylyl-*N*-methyl)-2,4,6-trimethylpyridinium tetrafluoroborate salt (**102**). The

photochemical properties and synthesis of the precursor is reported elsewhere.[5] Upon irradiation using a Nd:YAG laser (355 nm, 20 mJ/pulse, 4 ns), the N-N bond of the precursor undergoes heterolysis to produce **103** in considerable yields. (Scheme 5.1) The latter has an absorption maximum at 480 nm, was confirmed through experimental studies conducted by several groups to be a singlet nitrenium ion with a lifetime of 24 $\pm$ 4 μs in CH_3CN.[5,18 7]

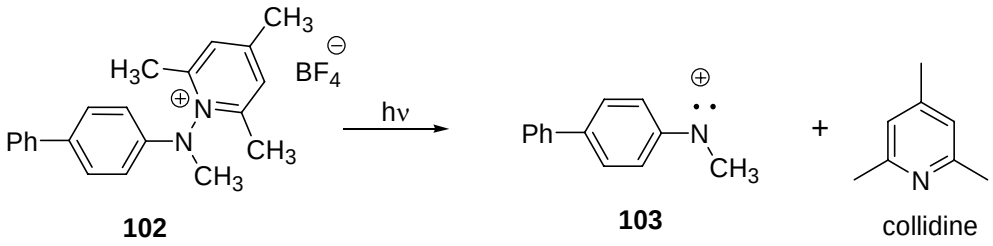

Scheme 5.1 Photolysis of **102**

Similar to other singlet arylnitrenium ions, **103** reacts with most simple nucleophiles and electron-rich arenes. The reactivity of the ion with these nucleophiles depends on their nucleophilicity and chemical reaction pathway between the ion and the nucleophile. Chloride, a strong nucleophile, adds to the *ortho* carbon of **103** with a rate constant of 8 x 10^9 $M^{-1}s^{-1}$ while methanol a poor nucleophile reacts only at 3.7 x 10^5 $M^{-1}s^{-1}$.[5] Likewise, reactions with arenes showed no definite correlation with respect to sterics or oxidation potential of the arenes. Arenes such as 1,3,5-TMB with an E_{ox} of 1.49 V quenches this ion at 1.7 x 10^9 $M^{-1}s^{-1}$, however 1,4-DMB which has an E_{ox} of 1.34 V reacts only at 8.9 x 10^6 $M^{-1}s^{-1}$.[7] These differences in rate constants observed were attributed to the different chemical reaction mechanism between the nitrenium ion and the arenes. Arenes such as 1,3,5-TMB forms covalent adducts with **103** while 1,4-DMB reacted with **103** through single electron transfer.[7] Based on the work done in our lab, it was proposed that **103**

initially forms a π complex with the arene which decays by either one of the pathway: σ-complexation to form σ-adducts or homolytic cleavage to yield radicals. (Scheme 5.2) The parent amines, *ortho* or *N*-adducts are the major photoproducts obtained from these reactions depending on the arenes.

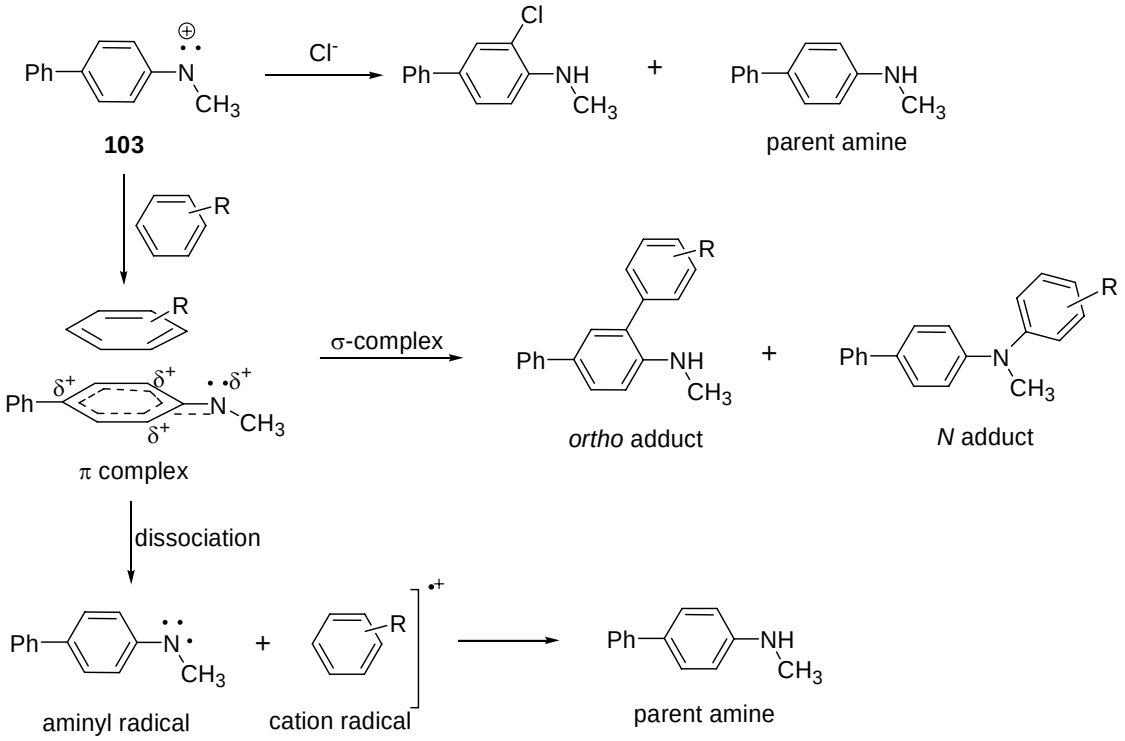

Scheme 5.2 Overall chemical decay pathway of 103 in the presence of nucleophiles

Since **103** shows greater affinity towards electron-rich nucleophiles such as amines and arenes, we assumed that similar reactivity should be observed for amino acids. Amino acids have side chains containing nucleophilic functional groups such as hydroxyl or amine; hence the compounds should be able to react with **103**. Therefore, competitive trapping studies were conducted to measure the relative reactivity of amino acids toward **103**.

5.2 Competitive Trapping Studies with Amino Acids

Of the 20 amino acids studied by competitive trapping experiments, only 8 of them show measurable reactivity towards **103**. (Figure 5.1) The experiments were performed in phosphate buffer solution (25 mM, pH 7.5) with 10% acetonitrile. Since biological systems are mostly comprised of H_2O, all experiments described in this chapter were done in aqueous media to mimic the biological systems. Acetonitrile was added to aid the solubility of the precursor in the buffer. The reaction rate constant of amino acid was calculated from the pseudo-first order decay rate of **103** at 480 nm at different concentrations of the amino acids.

According to the values shown in Table 5.1, only 8 amino acids react with **103**, the rest showed little or no reactivity excluding glycine. These amino acids react with the ion at a rate constant of $10^6 – 10^9$ $M^{-1}s^{-1}$, which is significant compared to the reaction rates by H_2O and guanosine. H_2O and deoxyguanosine react with the ion at 9.30×10^4 $M^{-1}s^{-1}$ and 1.9×10^9 $M^{-1}s^{-1}$ respectively[7,19,20] and are considered to be the lower and upper limit of the reactivities of **103** with any nucleophiles. Therefore, these amino acids quenches **103** about 10^2 times faster than H_2O and some even roughly the rate as guanosine.

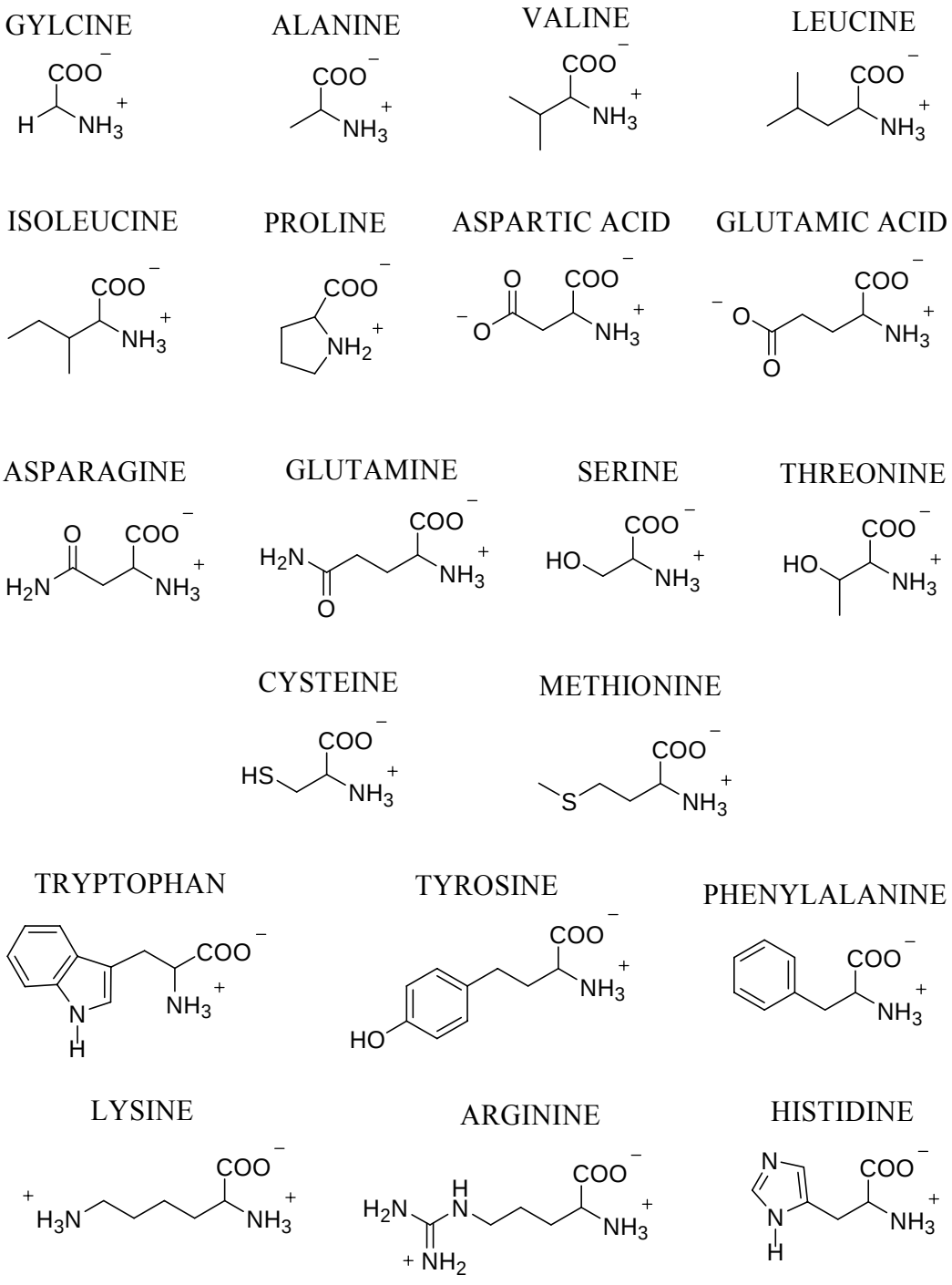

Figure 5.1 Amino acids used in the study

Table 5.1 Second order reaction rate constant of the quenching of **103** by amino acids

Amino acids	Functional groups in the side chain	knuc (M-1s-1)
L-Serine	hydroxyl	$(7.93 \pm .72) \times 10^6$
L-Cysteine	thiony	$(2.79 \pm .23) \times 10^8$
L-Methionine		$(1.29 \pm .07) \times 10^9$
L-Tyrosine	aromatic	$(2.95 \pm .69) \times 10^8$
L-Tryptophan		$(2.91 \pm .14) \times 10^9$
L-Lysine	amine	$(8.04 \pm 1.6) \times 10^7$
L-Arginine		$(3.04 \pm .46) \times 10^7$
L-Histidine		$(5.39 \pm .51) \times 10^7$
L-Glycine	alkyl	8×10^7*

Rest of the amino acids showed no measurable quenching.
* Non-linear quenching observed.

5.2.1 Reactions with Amino Acids with Non-Nucleophilic Side Chains

The reaction rate constant measured for each amino acid appeared to have some correlation with the nucleophilicity of the side chain. Amino acids with side chains containing hydroxyl groups, sulfur, aromatic rings and amines showed reactivity except for threonine and phenylalanine. The rest of the amino acids with side chains containing carboxylate, amide and alkyl groups (except glycine) did not react with **103**. This trend in the reactivity suggested that the route of reaction with **103** was via a nucleophilic attack by the amino acid. In addition, other than the depletion of **103**, no new intermediates are observed in the transient spectra determined following LFP of **102** in the presence of the amino acids. If electron abstraction or hydrogen atom transfer processes were present, then intermediates corresponding to radicals or radical cations of the parent amine should be observed in the transient spectrum. However, it is also possible that the new intermediates were formed but too unstable to be detected by LFP.

The absence of reactivity by amino acids with non-nucleophilic side chains confirmed that the ion reacts exclusively with the side chains. Alanine, valine, leucine, isoleucine and glycine are amino acids with alkyl side chains. Kinetic analysis conducted with these acids give no measurable quenching of **103** confirming that the reacting moiety of the acid was the side chains. Since alkyl groups are generally unreactive, no interaction with **103** was expected. Proline, a cyclic alkyl amino acid also showed no interaction with **103**. These observations also confirmed that the terminal carboxylate and amino groups do not react with the nitrenium ion. With glycine, we observed a non-linear relationship between the decay rate of **103** at the different glycine concentration. (Figure 5.2) This plot indicates a non-bimolecular quenching of the nitrenium ion that involved two or more glycine molecules. Further study on this matter was not pursued.

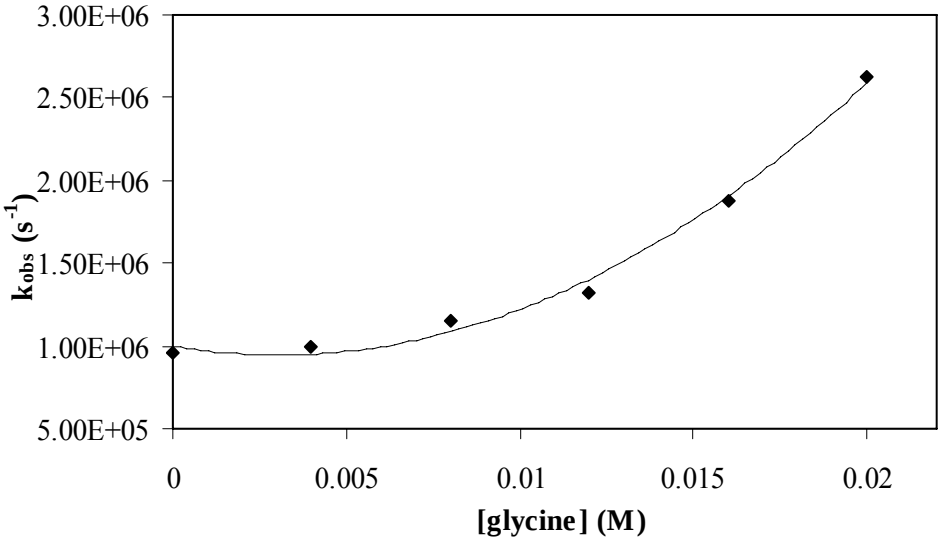

Figure 5.2 Non-linear trapping **103** by glycine

Aspartic acid, glutamic acid, asparagines and glutamine are the rest of the amino acids with carboxylate and amide side chains that failed to react with **103**. Carboxylate and amides are resonance stabilized; hence they are unavailable for nucleophilic attacks. These findings further confirmed that the reaction is between the side chain of the amino acid and **103**.

5.5.2 Reaction with Amino Acids with Nucleophilic Side Chains

5.5.2.1 Hydroxyl Groups

Reaction with serine and threonine, amino acids that have hydroxyl group in their side chain showed that only serine reacts with **103**. Threonine, a secondary alcohol showed no measurable quenching of **103**, while serine reacts at a rate constant of 7.93×10^6 $M^{-1}s^{-1}$. Previous work have shown that **103** reacts with alcohols at an order of 10^5 $M^{-1}s^{-1}$ with slight variations depending on the steric bulk of the alcohols..[7] (Table 5.2) Therefore, sterics could also be the factor that prevents threonine from reacting with **103**. The hydroxyl group of threonine is not that easily accessible, it is embedded in the core of the molecule. Whereas, the hydroxyl group in serine is on the peripheral of the molecule; hence it are free to interact with other molecules.

Table 5.2 Trapping rate constants of **103** by some nucleophiles.[7]

Nucleophiles	k_{nuc} ($M^{-1}s^{-1}$)
H_2O	9.30×10^4
methanol	3.70×10^5
ethanol	3.30×10^5
isopropyl alcohol	1.90×10^5
toluene	$<10^3$
$nBuNH_2$	5.80×10^9
$tBuNH_2$	3.80×10^9

Serine was observed to react with **103** slightly faster than the standard alcohol. Shown in figure 5.3 is the trapping of biphenylylnitrenium ion by serine. A linear relationship is observed between the pseudo-first order decay rate of the latter and the concentration of the quencher confirming a bimolecular reaction. Since the quenching rate is only slightly higher than other alcohols and the goal was just to measure the reactivity rate of these amino acids, this matter was not further pursued.

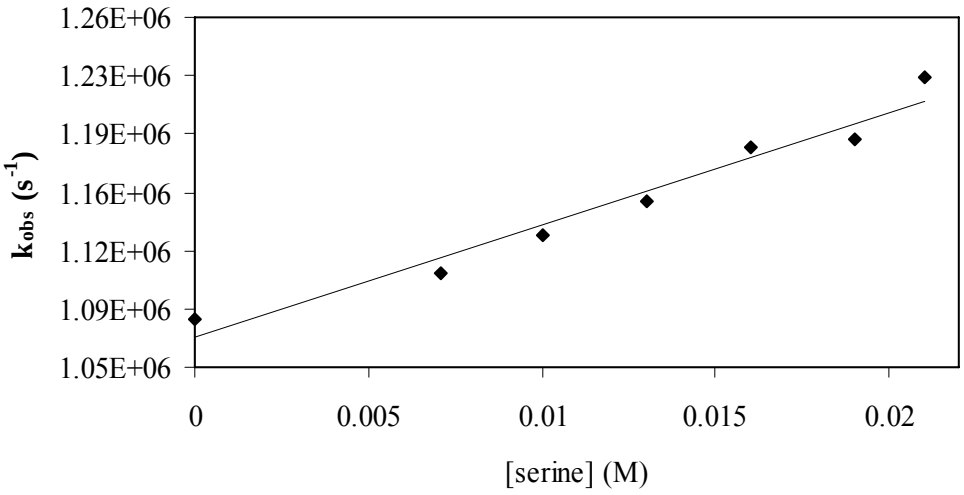

Figure 5.3 Trapping of **103** by serine

5.2.2.2 Thiol Groups

Cysteine and methionine are sulfur based amino acids that react with **103** at the diffusion limit at a rate constant of 2.79 x 10^8 and 1.29 x $10^9 M^{-1}s^{-1}$ respectively (k_{diff} H_2O = 5 x 10^9 $M^{-1}s^{-1}$ and k_{diff} CH_3CN = 1.9 x 10^{10} $M^{-1}s^{-1}$).[18] Similar reactivity was observed for glutathione, a thiol based non-protein where the latter reacts with 4-biphenylylnitrenium ion at 1.8 x 10^9 $M^{-1}s^{-1}$ to yield *N* or *ortho* adducts. [21] Therefore, cysteine and methionine were expected to react with **103** rapidly. Methionine being a methyl sulphide reacts faster than cysteine.

5.2.2.3 Aromatic Groups

Tryptophan, tyrosine and phenylalanine are amino acids with aromatic side chains. Except for phenylalanine, tryptophan and tyrosine react with **103** at the diffusion limit. We believe that the reacting moiety of tryptophan and tyrosine is the aromatic side chain based on observations from previous studies with arenes. Arenes such as 1,3,5-TMB, 1,3-DMB and mesitylene were known to add to **103** to yield *N* or *ortho* adducts.[7] In addition, the reactivity of the side chain in tryptophan was verified by conducting control experiments by reacting indole with **103**. The rate constant for this reaction was 6.29 x 10^9 $M^{-1}s^{-1}$ which was similar to tryptophan. Indoles are good nucleophiles, hence are capable of undergoing nucleophilic attack on the electrophilic nitrenium ion. The reduced reactivity of phenylalanine, an aromatic amino acid, was however expected based on previous analysis with toluene where the rate of reactivity was observed to be less than 10^3 $M^{-1}s^{-1}$.

5.2.2.4 Amino Groups

Amine based amino acids such as lysine, arginine and histidine react with **103** at a rate constant of 10^7 $M^{-1}s^{-1}$. However, the rates observed for amino acids such as lysine, arginine and histidine showed that these amino acids react with **103** much slower than standard amines. This was peculiar especially because amines generally react with arylnitrenium ions at the diffusion limit. For example, *n*-butyl amine and *tert*-butyl amine react with **103** at 10^9 $M^{-1}s^{-1}$.[7,22] (Table 5.2) We believe that this difference in reactivities that was observed could be due to the protonation or hydrogen bonding of the nitrogen of the side chain that is responsible for the nucleophilic attack.

Kinetic analysis of lysine performed in buffer solutions of different pH's showed that the rate of reactivity depends on the pH of the solvent. Shown in Table 5.3 is the reaction rate constants of lysine measured at pH 2.0, 4.0, 6.0 and 7.5. As the pH decreased, the rate of reactivity also decreased except for pH 2.0 at which no activity was observed. Since the rates at pH 4.0 and 6.0 were similar but lower than at 7.5, we presume that lysine exists in different forms at different pHs. (Scheme 5.3) At pH below 4.0, all of the functional groups are protonated to give the dicationic form; hence the amine is not available for reaction. However, at pH above 4.0, lysine is in equilibrium between the monocationic form and the free amine. Since the rate observed at pH 4.0 and 6.0 is lower than that at 7.5, the equilibrium should be shifted more to the left, in other words, more of the monocationic form may present than the free amines. But at pH 7.5, more of the free amines are present, hence increased reactivity was observed. Similar arguments may apply to arginine and histidine. In addition to protonation, the terminal amino group of the side chain in arginine is not that nucleophilic due to the adjacent iminium ion. In histidine, N-3 of the imidazole ring that is responsible for the nucleophilic attack is also the most basic; therefore is readily protonated.

Table 5.3 Second order reaction rate constant of the quenching of **103** by lysine at different pHs

pH	k_{nuc} ($M^{-1}s^{-1}$)
7.5	$(8.04 \pm 1.6) \times 10^7$
6.0	$(3.39 \pm .35) \times 10^7$
4.0	$(3.56 \pm 1.2) \times 10^7$
2.0	no reaction

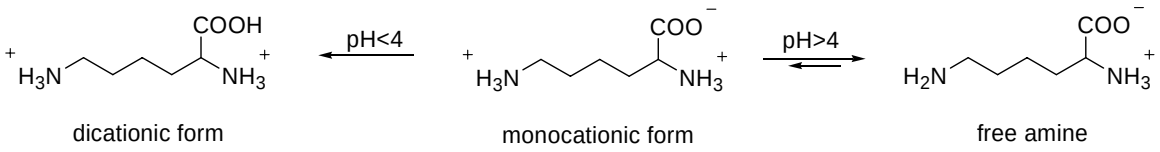

Scheme 5.3 Protonation of lysine

Based on the data explained in this chapter, it is clear that **103** reacts readily with nucleophilic amino acids. Therefore, similar to nucleic acid bases, amino acids are also susceptible to react with carcinogenic arylnitrenium ions. The property that makes this ion carcinogenic is its affinity for electron-rich nucleophiles along with their relative stability in aqueous solutions. The ion, **103** has a lifetime of 590 ns in aqueous solution and reacts with H_2O at a rate constant of 9.30 x 10^4 $M^{-1}s^{-1}$.[7,18] Comparing the data in Table 5.1, we see that **103** shows a greater affinity for amino acids than for H_2O. Due to this slow reaction with H_2O, the ion can exist long enough in aqueous solution to react with other nucleophiles present in the media. As a result of this, when generated *in vivo*, **103** can form covalent bonds with the nucleophilic components of nucleic acids or proteins.

5.3 Product Analysis with TFA-Methionine

The reaction mechanism between the amino acids and **103** was investigated by conducting product studies with methionine. Methionine was chosen for the study because along with tyrosine and tryptophan, it shows the highest reactivity towards **103**. The product analysis was performed using the protected analog of methionine: *N*-trifluoroacetic methionine methyl ester (**104**), in order to eliminate possible side reactions by the terminal carboxylate and amino group and to ensure complete

solubility in acetonitrile. Comparable to the unprotected analog, this compound react with **103** at a rate constant of 1.6×10^9 $M^{-1}s^{-1}$.

Photolysis of **104** with **102** yields the dimeric hydrazine (**108**), parent amine (**109**) and some other dimeric product resulting from oxidative coupling of the intermediates and photoproducts. (Scheme 5.4) Even though, these were not nucleophilic addition products, they were assumed to have originated from a nucleophilic addition pathway. The proposed mechanism for the reaction holds that **103** initially adds to **104** to form a N-S bond, yielding an amino-sulphonium ion (**105**). This intermediate **105** then undergoes homolytic cleavage to yield aminyl radicals (**106**).

The formation of **105** had been suggested previously in the earlier work involving carcinogenic arylamines and methionine. Vivo studies done in late 1960s with methionine and amino dyes or *N*-acylated arylamines have isolated products resulting from the formation of covalent bonds between methionine and the amino dyes. [1,10,14,17] For example, the Miller's group showed that compounds such as *N*-acetoxy-2-acetylaminofluorene or *N*-benzolyoxy-4-monomethylaminoazobenzene (MAB) react with methionine to yield 3-methyl-mercapto derivatives.[14,23] The reaction scheme proposed by the Miller's group is shown in Scheme 5.5. They proposed that the methionine adds to the arylamine via S_N1 or S_N2 to yield a amino-sulphonium ion. Following the addition, methionine undergoes intramolecular nucleophilic attack on the methylene group adjacent to the sulfur to yield 3-methylmercapto-MAB and lactone. (Scheme 5.5) It is possible that the initial process involved in the reaction between **103** and **104** is a nucleophilic addition step because

the reactivities of the amino acids depend on the nucleophilicity of the side chain. The intermediate **105**, being unstable, decomposes rapidly.

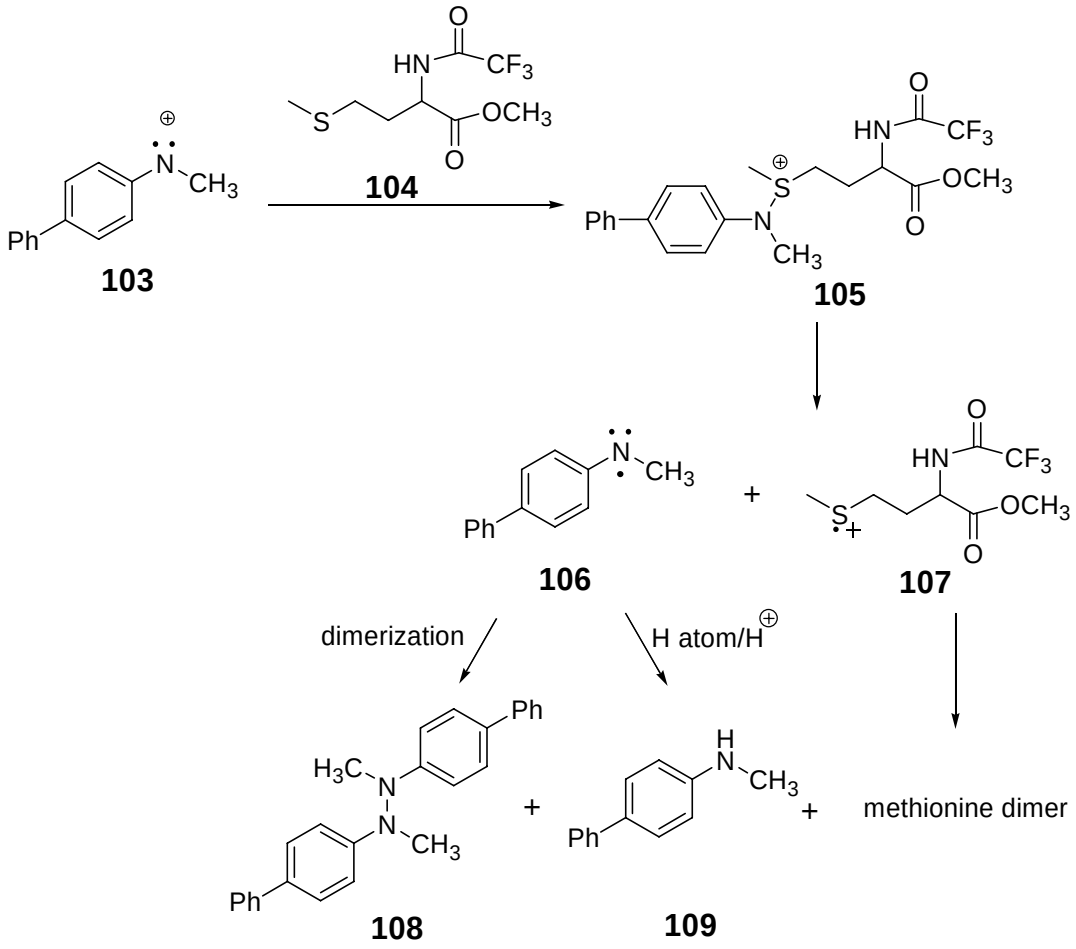

Scheme 5.4 Proposed mechanism for the formation of the photoproducts in the presence of **104**

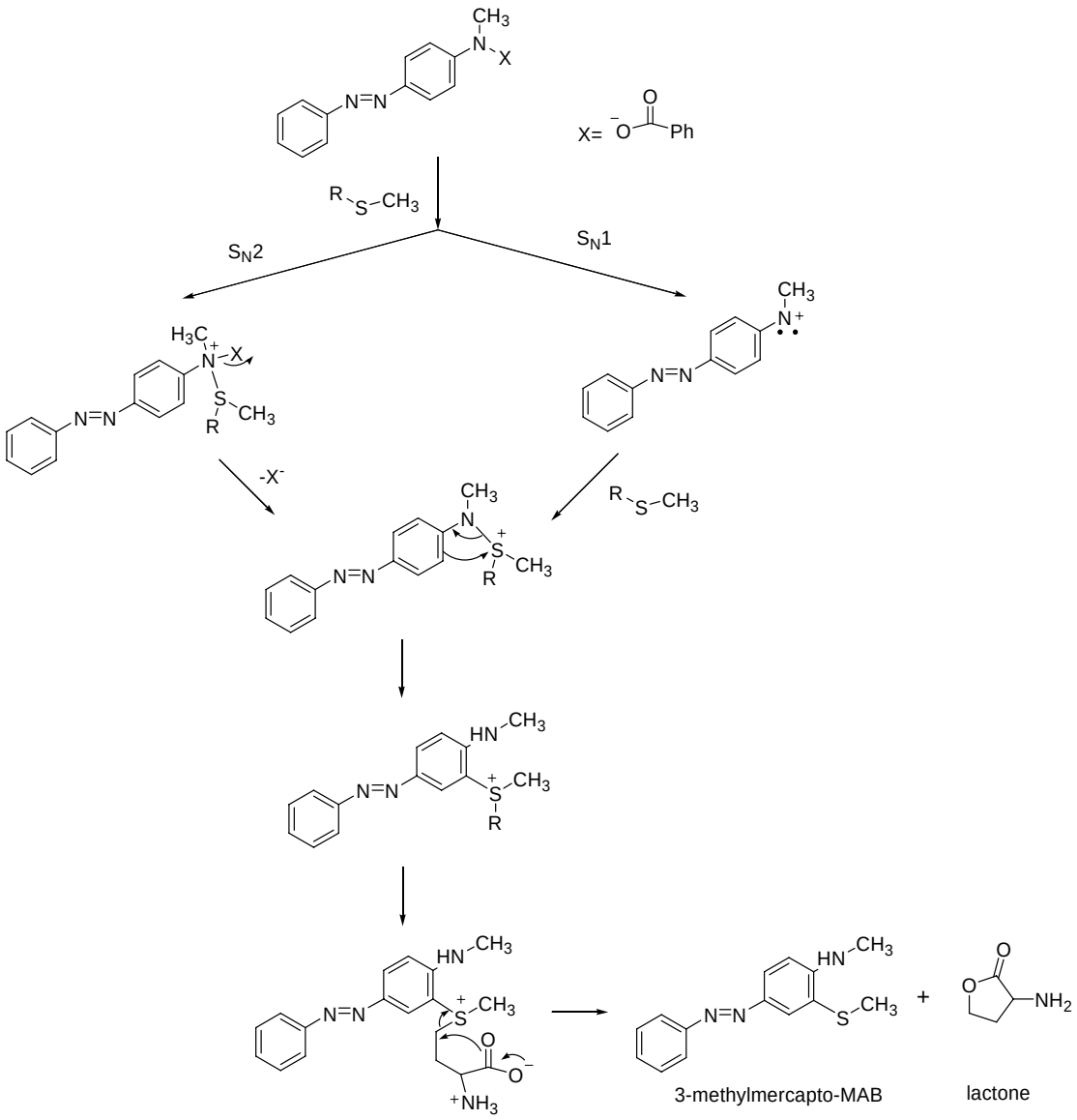

Scheme 5.5 Mechanism for the methionine reaction with *N*-benzolyoxy-4-monomethylaminoazobenzene.[14,23]

One of the major photoproduct isolated is **108**. The most likely pathway for the formation of **108** would be dimerization of **106**. However, since this compound was not observed previously for any of the reactions involving **103**, it was assumed to form through a different pathway. We believe that the dimer forms as a result of the nucleophilic attack on **105** by **109**, with the concomitant elimination of methionine.

Sulfenamide bonds are generally unstable and subject to rearrangement or homolysis under thermal or photolytic conditions.[24,25] Since the reaction mixture was under continuous irradiation, the unstable **105** dissociates or is attacked almost immediately once it forms.

The parent amine **109** obtained as one of the major photoproducts was assumed to have occurred from **106** via either by electron abstraction and then protonation or hydrogen atom abstraction from the unreacted **104** or the solvent. Parent amines have been observed previously in the presence of other nucleophiles and are formed by hydride or hydrogen atom abstraction from the solvent.

In addition to these products, a higher mass corresponding to the formation of the oxidative dimeric products of **104** was detected by MS. The dimeric **104** can arise from the radical coupling of the radical cations of methionine resulting from the electron or hydrogen atom abstraction from methionine. Since only trace amount of are detected, its reaction pathway was not further pursued.

5.4 Reactions with Proteins

Since **103** showed greater affinity for several amino acids, the latter was reacted with proteins to determine its reactivity. Bovine serum albumin (BSA), bovine pancreatic ribonuclease (BPR), lysozyme, insulin and chymotrypsin were the five proteins chosen for the study because they are inexpensive and readily available in sufficient quantities for LFP experiments. The kinetic studies were done in similar conditions as the amino acids, in 9:1 phosphate buffer (pH 7.5, 25 mM) with acetonitrile.

The proteins react with **103** with bimolecular rate constant of 10^8 $M^{-1}s^{-1}$ which is significant compared to water. (Table 5.4) The rates showed no definite correlation to the size of the protein or with the number of reactive amino acids present in the protein. Chymotrypsin with the least number of reactive amino acids shows the highest reactivity, while BPR with the most number of reactive amino acids had the lowest reactivity.

The solubility of chymotrypsin and insulin in the aqueous media was aided with the addition of a few microliters of NH_4OH.[26] About 0.012 M NH_4OH was introduced to the reaction sample containing the pyridinium precursor. Control experiments conducted with just NH_4OH and **102**, but with no protein show that at the concentrations (0-0.012 M) used, NH_4OH had negligible effect on the lifetime of **103**. Over the range of 0–0.012 M NH_4OH, the pH of the buffer changed from 7.65–8.21, which should be safe for the protein without denaturating it. Hence the reactivity observed by chymotrypsin and insulin was not due to the combined effect from the protein and NH_4OH, but solely from the proteins.

Table 5.4 Bimolecular trapping rate constants of **103** measured for each proteins, the molecular weights and the percentage of reactive amino acids for each proteins (based on k_q of amino acids $\geq 10^7$ $M^{-1}s^{-1}$)

Proteins	k_q ($M^{-1}s^{-1}$)	Molecular weight of protein (Da)	% of reactive amino acids
BSA	$(8.22 \pm 0.9) \times 10^8$	66465.8[b]	32[b]
BPR	$(4.59 \pm 0.4) \times 10^8$	13686[c]	41[d]
Lysozyme	$(5.79 \pm 0.6) \times 10^8$	14388[e]	36[e]
Insulin[a]	$(8.96 \pm 0.8) \times 10^8$	5800[f]	33[f]
Chymotrypsin[a]	$(7.71 \pm 0.8) \times 10^9$	25000[g]	29[g]

[a]NH_4OH was added to aid the solubility of the proteins in buffer
[b]Ref 27. [c]Ref 28. [d]Ref 29. [e]Ref 30. [f]Ref 31. [g]Ref 32.

These results suggest that similar to nucleic acids, proteins could also be potential targets for arylnitrenium ions. Even though, it is not clear if the site of the amino acids within the protein is important for the reactivity, we can be sure that the amino acids in the tertiary structure of the proteins can react with the ion. However, this is not the case with DNA. Previous investigations done with 2-aminofluorenyl nitrenium ion show that only single stranded DNA reacts with the ion, double stranded DNA is unaffected.[9] Similar result is obtained upon photolyzing **102** in the presence of calf thymus DNA. No reactivity was observed between the ds-DNA and **103**. The concern over DNA however is that since arylnitrenium ions can react with the nucleic bases of single stranded DNA; it's more vulnerable during replication. Even though we are not sure of the biological consequences of the nitrenium ion reaction with protein, our data proves that proteins are also equally affected by arylnitrenium ions as nucleic acids.

5.5 Conclusions

Based on the evidence presented in this chapter, we conclude that amino acids with nucleophilic side chains react readily with **103**. Among twenty amino acids, only eight of them reacted, with methionine and tryptophan undergoing diffusion limited reactivity. Amino acids that react are those that contain hydroxyl, sulfur and amino group in their side chains. The reactivity of these amino acids depend on the nucleophilicity of the side chains suggesting that the mode of reaction is nucleophilic substitution process, which was further confirmed by product studies. Reaction between **102** and **104** yields mainly **108**, **109** and trace amounts of dimeric methionine, all occurred via an amino-sulphonium ion intermediate. Finally, competitive trapping studies showed that proteins react with **103** efficiently; confirming that in biological systems nitrenium ions is a threat not only to nucleic acids but also to proteins.

References

(1) Kriek, E. *Biochim. Biophys. Acta* **1974**, *355*, 177-203.

(2) Talaska, G.; Dooley, K. L.; Kadlubar, F. F. *Carcinogenesis* **1990**, *11*, 639-646.

(3) Talaska, G.; Aljuburi, A. Z. S. S.; Kadlubar, F. F. *Proc. Natl. Acad. Sci. USA.* **1991**, *88*, 5350-5354.

(4) McClelland, R. A.; Gadosy, T. A.; Ren, D. *Can. J. Chem.* **1998**, *76*, 1327-1337.

(5) Srivastava, S.; Ruane, P. H.; Toscano, J. P.; Sullivan, M. B.; Cramer, C. J.; Chiapperino, D.; Reed, E. C.; Falvey, D. E. *J. Am. Chem. Soc.* **2000**, *122*, 8271-8278.

(6) Chiapperino, D. Ph.D Dissertation, University of Maryland, College Park, MD, 2000.

(7) Chiapperino, D.; McIlroy, S.; Falvey, D. E. *J. Am. Chem. Soc.* **2002**, *124*, 3567-3577.

(8) Kennedy, S. A.; Novak, M.; Kolb, B. A. *J. Am. Chem. Soc.* **1997**, *119*, 7654-7664.

(9) Novak, M.; Kennedy, S. A. *J. Phys. Org. Chem.* **1998**, *11*, 71-76.

(10) Miller, E. C.; Miller, J. A. *Pharmacol. Rev.* **1966**, *18*, 805-838.

(11) Miller, E. C.; Lotlikar, P. D.; Miller, J. A.; Butler, B. W.; Irving, C. C.; Hill, J. T. *Mol. Pharmacol.* **1968**, *4*, 147-154.

(12) Cramer, J. W.; Miller, J. A.; Miller, E. C. *J. Biol. Chem.* **1960**, *235*, 885-888.

(13) Scribner, J. D.; Miller, J. A.; Miller, E. C. *Biochem. Biophys. Res. Commun.* **1965**, *20*, 560-565.

(14) Poirier, L. A. M., J. A.; Miller, E.C.; Sato, K *Cancer Res.* **1967**, *27*, 1600-1613.

(15) Miller, E. C.; Miller, J. A. *Cancer* **1981**, *47*, 2327-2345.

(16) Miller, J. A. *Cancer Res.* **1970**, *30*, 559-576.

(17) Miller, J. A.; Miller, E. C. In *Physico-Chemical Mechanisms of Carcinogenesis, Jerusalem Symposia on Quantum Chemistry and Biochemistry. The Israel Academy of Sciences and Humanities,*; Bergmann, E. D., Pullman, B., Eds.: Jerusalem, 1969; Vol. 1, pp 237-261.

(18) Falvey, D. E. In *Organic, Physical, and Materials Photochemistry*; Ramamurthy, V. S., K.S;, Ed.; Marcel Dekker, Inc: New York, 2000; Vol. 6, pp 249-284.

(19) McClelland, R. A.; Kahley, M. J.; Davidse, P. A. *J. Phys. Org. Chem.* **1996**, *9*, 355-360.

(20) Novak, M.; Kennedy, S. A. *J. Am. Chem. Soc.* **1995**, *117*, 574-575.

(21) Novak, M.; Li, Y. *J. Am. Chem. Soc.* **1996**, *118*, 1302-1308.

(22) Kung, A. C.; Chiapperino, D.; Falvey, D. E. *Photochem. Photobiol. Sci.* **2003**, *2*, 1205-1208.

(23) Arcos, J. C.; Argus, M. F. *Adv. Cancer Res.* **1968**, *11*, 305-471.

(24) Davis, F. A.; Wetzel, R. B.; Devon, T. H.; Stackhouse, J. F. *J. Org. Chem.* **1971**, *36*, 799-803.

(25) Davis, F. A.; Fretz, E. R.; Horner, C. J. *J. Org. Chem.* **1973**, *38*, 690-699.

(26) McPherson, A. *Crystallization of Biological Macromolecules*; Cold Spring Harbor: New York, 1999.

(27) Brown, J. R. *Fed. Proc. Fed. Am. Soc. Exp. Biol.* **1975**, *34*, Abstract 2105.

(28) Raines, R. T. *Chem. Rev.* **1998**, *98*, 1045-1065.

(29) Smyth, D. G.; Stein, W. H.; Moore, S. *J. Biol. Chem.* **1963**, *238*, 227-234.

(30) Canfield, R. E. *J. Biol. Chem.* **1963**, *238*, 2698-2707.

(31) Ryle, A. P.; Sanger, F.; Smith, L. F.; Katai, R. *Biochem. J.* **1955**, *60*, 541.

(32) Hartley, B. S. *Nature* **1964**, *201*, 1284-1287.

Chapter 6. Photochemical Generation of Quinoline *N*-Oxide Nitrenium Ions from Azide and *N*-aminopyridium Precursors

The goal of this project was to determine whether the ultimate carcinogenic metabolite of 4-nitroquinoline *N*-oxide **110** is a heteroaromatic nitrenium ion. Studies *in vivo* and *in vitro* have shown that **110** is reduced to 4-hydroxyquinoline *N*-oxide (**111**) which then covalently adds to the nucleophilic components of DNA and proteins to yield σ-adducts. (Scheme 6.1) Based on the similarities to the carcinogenicity of arylamines and amino dyes, we presume that the reaction of **110** might be occurring through a heteroaromatic nitrenium ion intermediate.

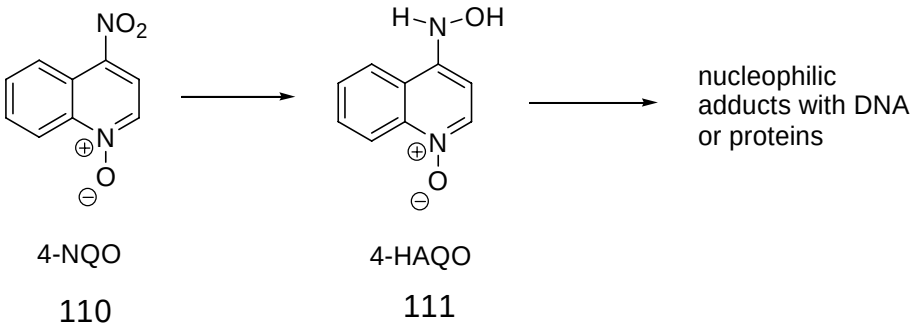

Scheme 6.1 Proposed carcinogenic pathway of **110**

6.1 Biological Implications of 4-Nitroquinoline *N*-Oxide

4-NQO (**110**) is a derivative of quinoline *N*-oxide, which along with aromatic amines and amino dyes, has been known for its carcinogenic properties since 1957.[1,2] This compound was synthesized by Ochiai in 1942 and was widely used for its antifungal and antibacterial properties. In bacteria and phages, these compounds were observed to cause DNA inactivation and gene mutation during transcription and translations. Some of the mutations induced by this compound were shown to be

temporary and were eventually reversed. However, it is this mutagenic property that enabled this compound to be an effective carcinogen.

Studies *in vivo* and *in vitro* have shown that the interaction of **110** with DNA and proteins result in the formation of tumors.[3] Painting **110** on the skin of mice led to the formation of sarcomas. Experiments *in vivo* showed that painiting ^{3}H-4-NQO on the skin of mice resulted in a higher concentration of the carcinogen in the intraepithelial region rich in SH group proteins. This was expected because 110 has been observed to react readily with compounds that contain this group such as cysteine and glutathione. The interaction between DNA and **110** was also observed by thin layer chromagraphy where incubating Euglena DNA with **110** resulted in a quinoline-bound DNA.[4] Additionally, increased incidents of pulmonary tumors and lung cancer were observed in mice that were subjected to subcutaneous injection of **110**. In another study, **110** bound DNA was isolated from cells injected with ^{14}C-4-NQO. Likewise, several studies done *in vitro* and vivo confirmed that **110** interacted with the DNA or protein.

However, more probing into the carcinogenicity of **110** showed that the reduction product, 4-HAQO **111** was more potent than **110**.[5] Higher incidents of tumor were observed in mice subjected to equal doses of **111** than **110**, suggesting **111** is the proximate carcinogen.[3] It was also observed that incubation of **111** with DNA promoted single strand scission while incubation with **110** or 4-aminoquinoline n-oxide did not show any significant reactivity.[6] Further studies confirmed that the carcinogenicity depended on the generation of **111** from **110**, suggesting that, similar

to aromatic amines and amino dyes, **110** was converted enzymatically to **111** before being carcinogenic. (Scheme 6.2)

Even though the actual mode of reaction is not yet confirmed, based on *in vivo* and *in vitro* studies it was concluded that **110** was reduced to **111** which in turn forms covalent adducts with the nucleophilic components of DNA and proteins. Covalently bound adducts of quinoline *N*-oxide with guanosine and adenine were isolated upon treatment of cellular DNA with **110** and **111**.[7-9] Even though covalently bound adducts were obtained, a definite pathway to its formation has not yet been proposed.

There are mainly two different mechanisms that have been proposed by which **110** is believed to be reacting with the nucleophiles. Based on spectroscopic studies, it has been speculated that the quinoline *N*-oxide derivatives react with DNA or proteins via charge transfer interactions.[3] Since the aromatic ring is electron deficient, this compound is a good electron acceptor. Hence based on molecular orbital calculations, it was predicted that the initial interaction between the compound and DNA or protein would be charge transfer. The difference spectra measured of **110** with various amino acids or protein such as bovine serum albumin showed absorption bands corresponding to the charge transfer from the nucleophiles to **110**.[10] Based on this result, it was suggested that the mode of reaction might be electron transfer from nucleophile to **110**.

However, based on the carcinogenity of arylamines and amino dyes, there are speculations that the reaction between the quinoline *N*-oxide derivatives and the nucleophiles might be proceeding via a heteroaromatic nitrenium ion. Kohda et. al. showed that in the presence of **111** and seryl-AMP, 8-hydroguanosine residue (**112**)

along with quinoline-guanosine adducts were obtained.[7] (Scheme 6.2) He argued that the 8-hydroguanosine results from the hydrolysis of the N7-adduct of the quinoline-guanosine which results from the addition of guanosine to the arylnitrenium ion generated from the acetylated form of **111**. It was also observed that the O,O'-diacetylated derivative of **111** exhibit carcinogenic properties, which as observed with arylamines, suggested that the acetyl group might be eliminated before adding to the guanosine.[5] Several studies using *N*-acetylated **111** were also conducted to prove the intermediacy of heteroaromatic nitrenium ion.[11,12] However, definite evidence that proves that the reaction proceeds through a heteroaromatic nitrenium ion has not yet been obtained.

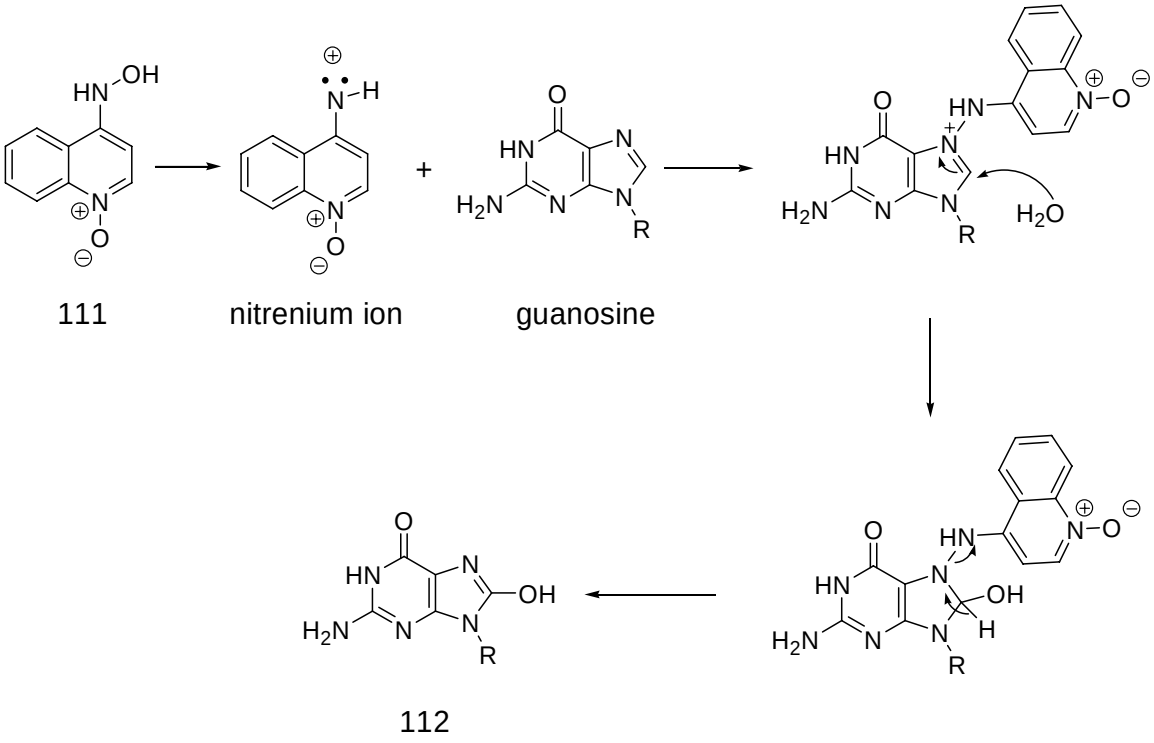

Scheme 6.2 Proposed mechanism for 8-hydroguanosine

6.2 Generation of Nitrenium Ions by LFP

Our hypothesis is that **110** is converted to the nitrenium ion through a series of enzymatic steps, the latter can covalently bind to nucleophiles to yield σ-adducts. This hypothesis is based on the following reasoning: (1) The isolation of the covalently bound quinoline *N*-oxide to guanosine or adenosine, (2) 4-Hydroxyquinoline *N*-oxide **111** (4-HAQO) was observed to be more potent than **110**, suggesting that the latter is converted to a species whose *N*-substituent can be easily hydrolyzed to yield an electrophilic intermediate, and (3) based on previous knowledge on the reaction mechanism of carcinogens such as arylamines and amino dye. Therefore, in order to prove that heteroaromatic nitrenium ions are the ultimate carcinogen, our goal was to generate 4-quinoline *N*-oxide nitrenium ions from conventional photochemical precursors and study their kinetic and chemical properties to understand their carcinogenic behavior.

The work described in this chapter is a preliminary report on the various photochemical approaches taken to generate the nitrenium ions of quinoline derivatives and their general chemical behavior. The quinoline and quinoline *N*-oxide nitrenium ions were generated from azide and *N*-aminopyridinium BF_4^- salts precursors because these precursors had been shown to generate nitrenium ion photochemically. (Scheme 6.3) Photolysis of these precursors generated distinctive LFP transient spectra which could be due to the differences in the chemical structures of the precursors and the transient species generated photochemically from them.

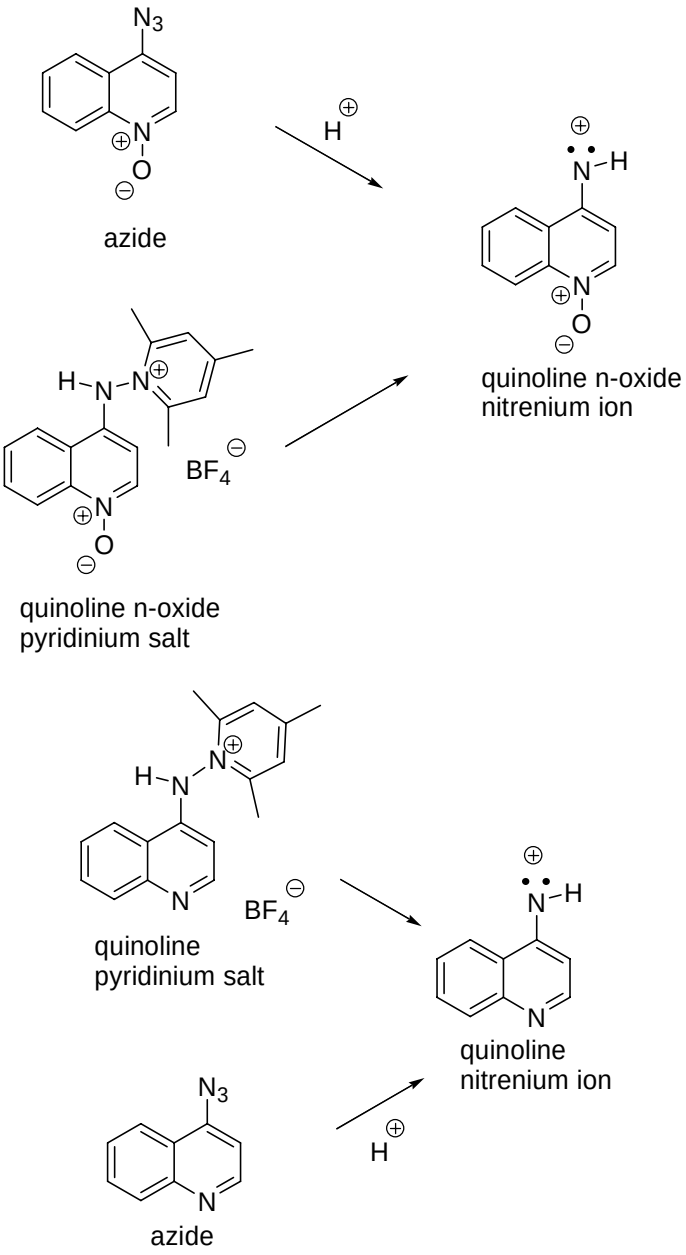

Scheme 6.3 Proposed quinoline *N*-oxide and quinoline nitrenium ions from azide and pyridinium precursors

6.2.1 Quinoline *N*-oxide Nitrenium Ion

6.2.1.1 Quinoline *N*-oxide Nitrenium Ion from 4-Azidoquinoline *N*-Oxide

4-Azidoquinoline *N*-oxide **113** was initially chosen to generate quinoline *N*-oxide nitrenium ion photochemically. Azides were chosen as precursors because as

explained in chapter 2, they are known to generate nitrenium ions upon photolysis in acidic solvents and are easy to synthesize.[13,14] Precursor **113** was synthesized by refluxing **110** with NaN_3 in 60 % ethanol to yield the product as a reddish needle-like solid.[15] This compound is soluble in relatively polar solvents and has a UV absorption band with a maximum at 370 nm. In acidic media, the UV absorption band of **113** is blue-shifted about 30 nm due to the protonation of the *N*-oxide. This was confirmed by steady state UV spectroscopy which is shown in Figure 6.1. As the concentration of HBF_4 increases, the absorption band with maximum at 370 nm corresponding to the free base of **113** decreases while absorbance band with maximum at 340 nm of the protonated **113** increased. If the blue shift was due to the increasing polarity of the solution, then the UV absorption band should shift to lower wavelengths as the concentration of the acid was increased without the formation of an isobestic point. Since the isobestic point was observed, we conclude that the *N*-oxide was protonated under these conditions.

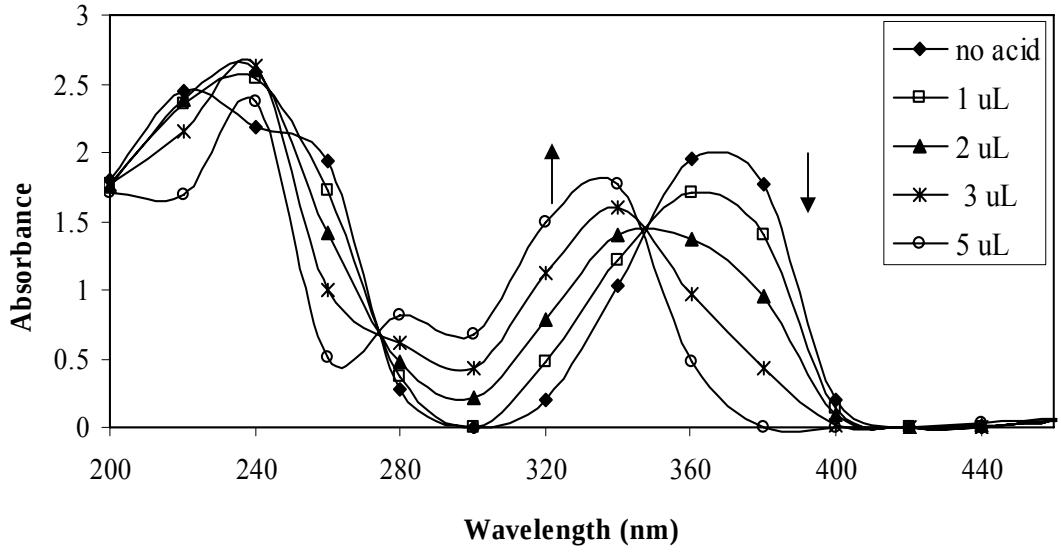

Figure 6.1UV absorption spectrum of **113** in CH_3CN with varying amounts of HBF_4

6.2.1.1.1 LFP Studies

Photolysis of **113** in CH_3CN with 10% H_2SO_4 using a Nd:YAG laser (355 nm, N_2 purged flow cell) generates a broad transient absorption band with maximum at 550 nm which forms immediately after the laser pulse. (Figure 6.2) This transient signal has a lifetime of 5.6 μs and decays in a first order fashion. Based on the assumption that irradiation of **113** would generate nitrene **114**, which would then be protonated to form nitrenium ion **115a**, this 550 nm signal is attributed to the nitrenium ion **115a**. (Scheme 6.4) However, species **115a** could also exist in its tautomeric form **115b** by the transfer of the proton from the exocyclic nitrogen to the oxygen. Similar tautomers were observed in the hydrolysis of 1-acetoxy-4-(acetoxyimino)-1,4-dihydroquinoline *N*-oxide and quinoline *n*-oxide derivatives with SH group in the 4-position.[11,12,16] In addition, **115a** could also exist in the dicationic form due to the protonation of the *N*-oxide and the nitrogen at the 4-position. The latter possibility seems unlikely because quinolines *N*-oxides are electron deficient; hence, placing additional positive charges would make the intermediate even more unstable. Yet due to the possibility of different tautomeric forms, the structure of species giving the transient signal was uncertain. However, based on further LFP studies, competitive trapping studies and product analysis, the transient species generated at 550 nm was assigned to be **115**.

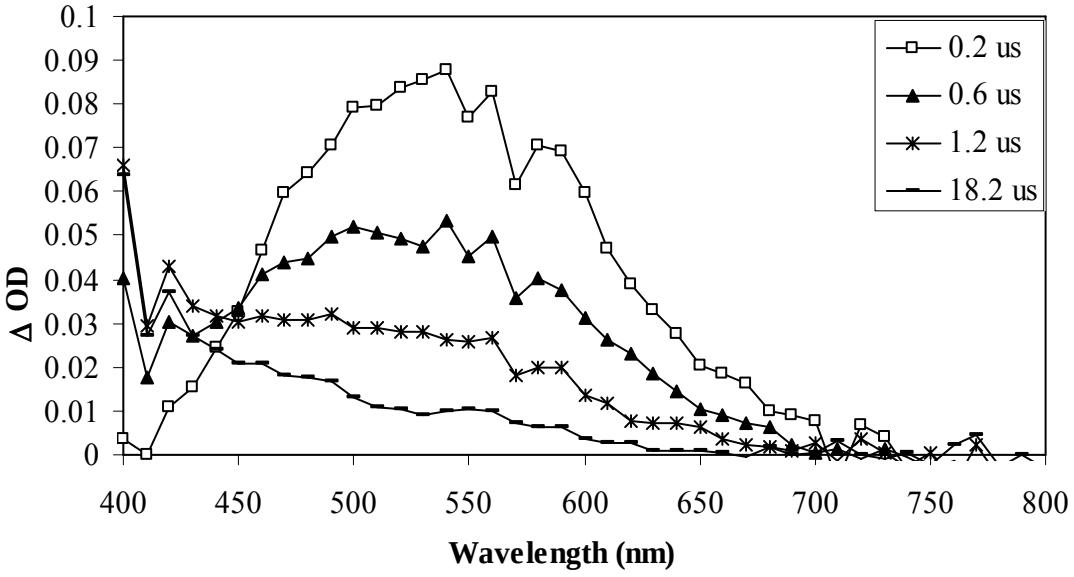

Figure 6.2 Transient spectra of the photolysis of **3** in CH_3CN with 10 % H_2SO_4

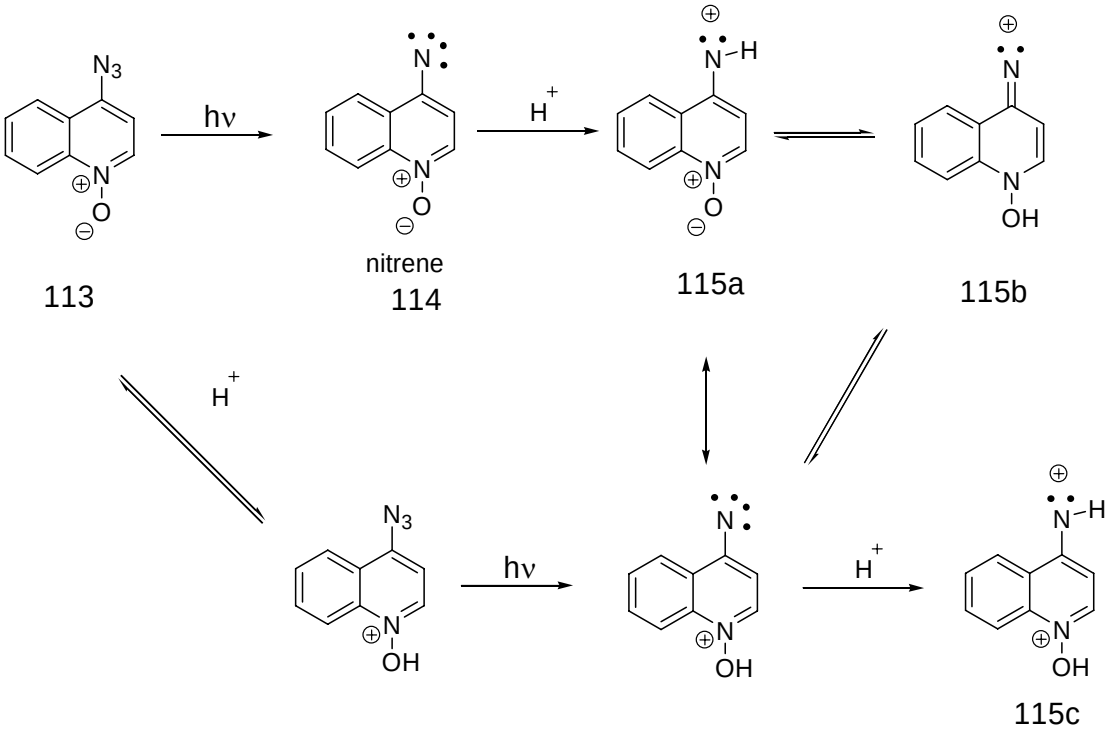

Scheme 6.4 Photolysis of **115** in CH_3CN with 10% H_2SO_4

The formation of **114** was verified by LFP in order to confirm that the transient species observed in Figure 6.2 was in fact the nitrenium ion. Irradiation of **113** in CH_3CN generates a sharp absorbance signal with maximum at 590 nm. (Figure 6.3) This signal with a half life of approximately 10μs decays rapidly and the growth of a new, broader absorbance band with maximum at 490 nm was observed. (Figure 6.6) The signal at 590 nm was assigned to **114** and the long-lived species absorbing at 490 nm was confirmed by product analysis to be the azo compound (**116**) resulting from nitrene dimerization. (Scheme 6.5) Nitrenes typically yield ring expansion and azo compounds.[17] The formation of the azo compound confirms that the photolysis of **113** generates **114**. Hence it is reasonable to assume that the latter was protonated in the acidic media to yield **115** which could be the transient species observed in Figure 6.2.

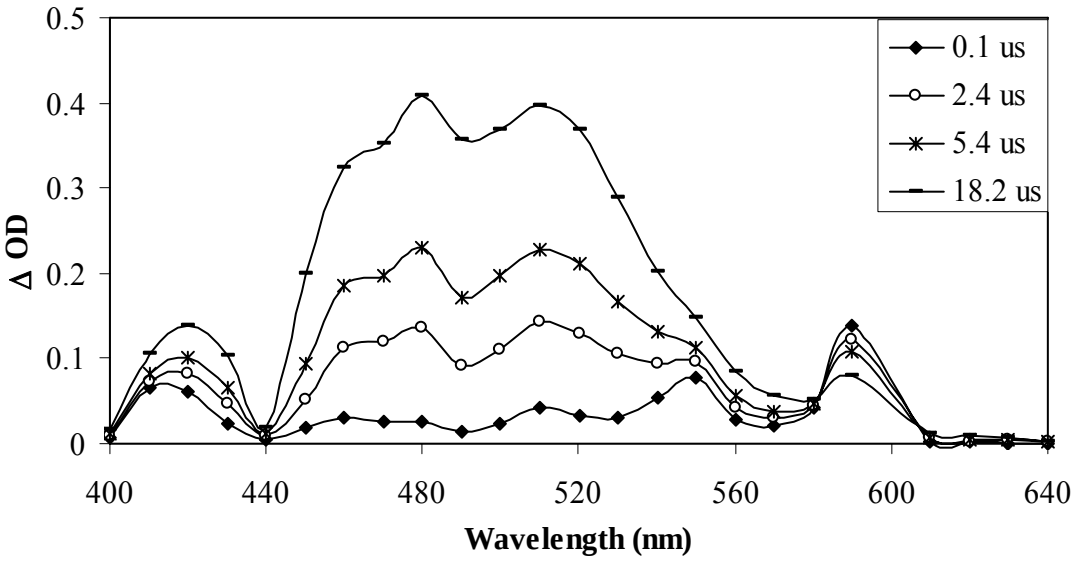

Figure 6.3 Transient spectra of the photolysis of **113** in CH_3CN

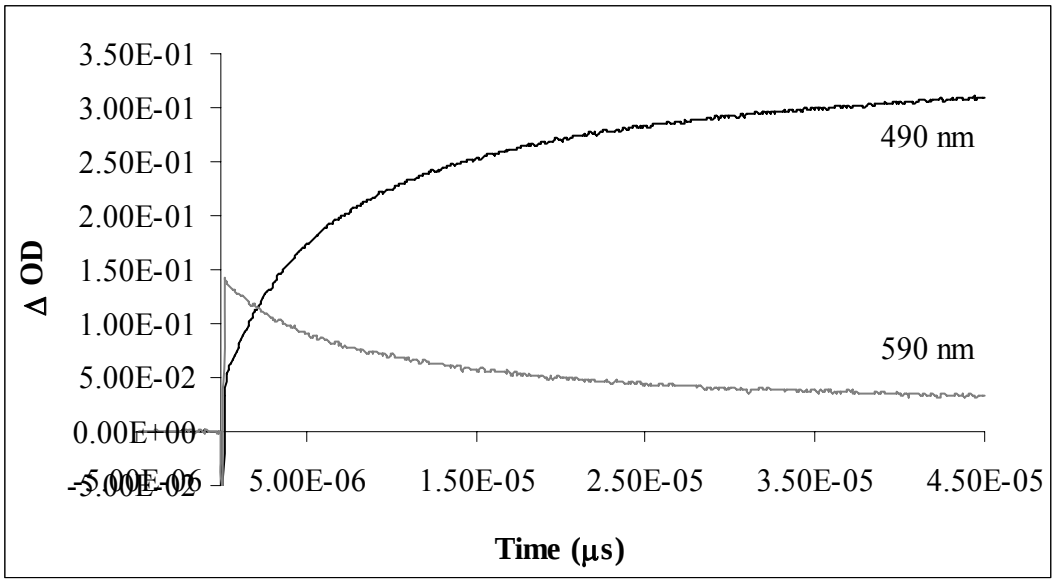

Figure 6.4 Waveform of the photolysis of **113** in CH_3CN at 490 and 590 nm

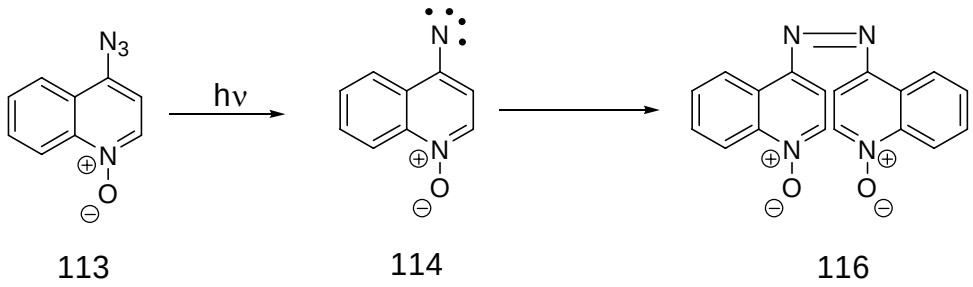

113 114 116

Scheme 6.5 Formation of **116** from **113** in CH_3CN

Further evidence that showed that **115** was generated from **114** was observed by photolyzing **113** in H_2O and CH_3CN with acid. Photolysis of **113** in H_2O with acid showed that the nitrene **114** decays to yield azo compounds as well as the nitrenium ions. The transient spectrum from the photolysis of **3** in 9:1 H_2O and CH_3CN with 10% H_2SO_4 is shown in Figure 6.5. A sharp absorbance peak corresponding to **113** at 590 nm along with a signal at 550 nm was observed. The 550 nm signal was distinct from that observed in Figure 6.2 in that the absorbance band was broad immediately following the laser pulse but narrowed down to few

nanometers at later times due to the growth of **116** around 410 nm. The absorbance of **116** was shifted to the lower wavelength due to the increased polarity of the solvent. Therefore, the growth of **16** along with the signal of **114** and **115** indicates that **114** decays via two competing pathways. We presume that the azo compound is the result of singlet-triplet equilibrium of **114**, of which **115** results from the singlet nitrene. Competition between nitrene pathway and nitrenium ion formation was observed for the photolysis of other azide precursors such as 4-biphenylylazide and 2-fluorenylazide.[13,14] This coupling vs. protonation of the nitrene supported that the nitrenium ion was generated from nitrene during the photolysis.

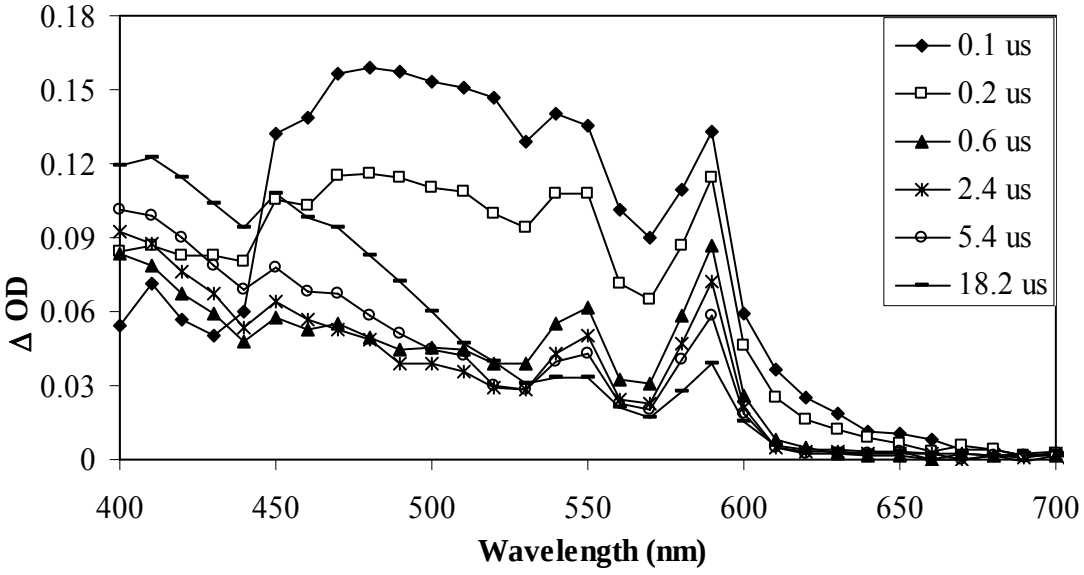

Figure 6.5 Transient spectrum of the photolysis of **113** in 9:1 H_2O/CH_3CN with 10% H_2SO_4

6.2.1.1.2 Product Analysis

Irradiation of **113** in CH_3CN in the absence of traps yields **116** as the sole photoproduct which was verified by ^{1}H-NMR and MS. Compound **116** resulted from

the dimerization of the triplet nitrene. Photolysis of azide precursors generally yields singlet nitrenes which then intersystem cross to the low lying triplet state. The formation of **116** confirms that nitrene was generated when the photolysis was done in the absence of any acids.

Also, irradiation of **113** in the presence of CH_3CN and 10% H_2SO_4 yields **116** as well as trace amounts of the parent amine (**119)**. Parent amines are typically nitrenium ion products and could be formed by either one of the pathways as shown in Scheme 6.6: (1) hydrogen atom transfer, where species **115** could abstract a hydrogen atom from the solvent to yield a radical cation (**118)** of **119** or (2) species **115** could abstract an electron from the solvent to yield an aminyl radical (**117)** of **119** which is then protonated to form **118**. Species **118** is then converted to **119** through electron abstraction or hydrogen atom abstraction and then deprotonation.

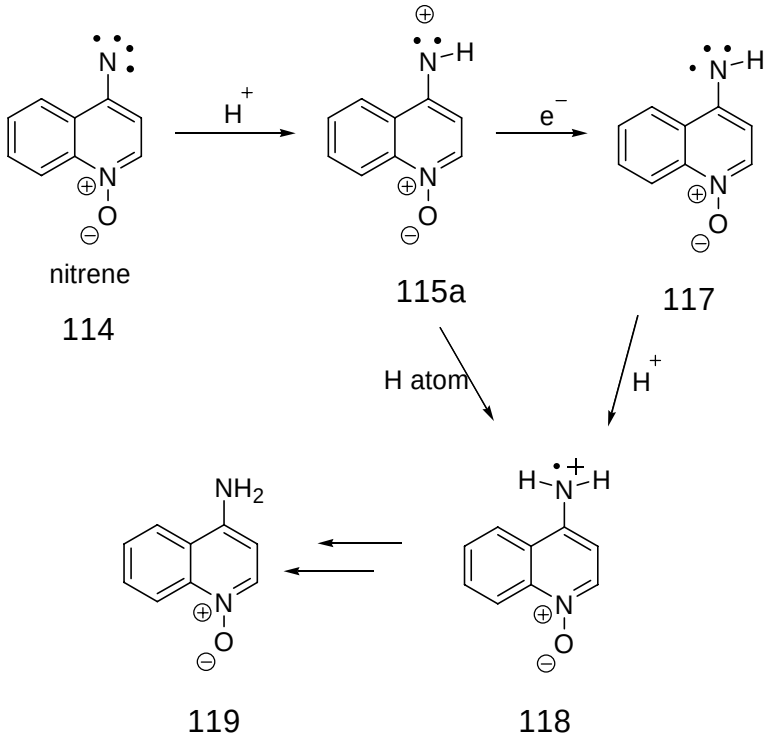

Scheme 6.6 Possible mechanisms for the formation of **119**

6.2.1.1.3 Trapping Studies

Quenching studies with arenes such as 1,3-dimethoxybenzene (1,3-DMB) and naphthalene show that the transient species at 550 nm abstracts electrons from arenes. Shown in Figure 6.6 and 6.7 are the transient spectra obtained in the presence of 1,3-DMB and naphthalene respectively. In the presence of 1,3-DMB, the absorbance signal corresponding to **115** decays to yield a new signal with a maximum at 470 nm. The signal at 470 nm is assigned to 1,3-DMB$^{\bullet+}$ indicating electron transfer from 1,3-DMB to the 550 nm transient species.[18] Similar electron transfer mechanisms have been observed for arylnitrenium ions.[19] Even though **115** is a heteroaromatic nitrenium ion, it is expected to undergo similar electron abstraction reactions with arenes. In addition, quinoline *N*-oxides are known to be good electron acceptors due to the electron deficient aromatic ring. For example, **110** was observed to abstract electrons from arenes such as aniline and *N*,*N*-dimethylaniline.[20] Therefore, **115** reacts with 1,4-DMB by abstracting an electron to yield **117** which is protonated immediately to **118**. (Scheme 6.6) Absorbances corresponding to **117** or **118** were not observed and could be due to the fact that they are short-lived to be detected by LFP.

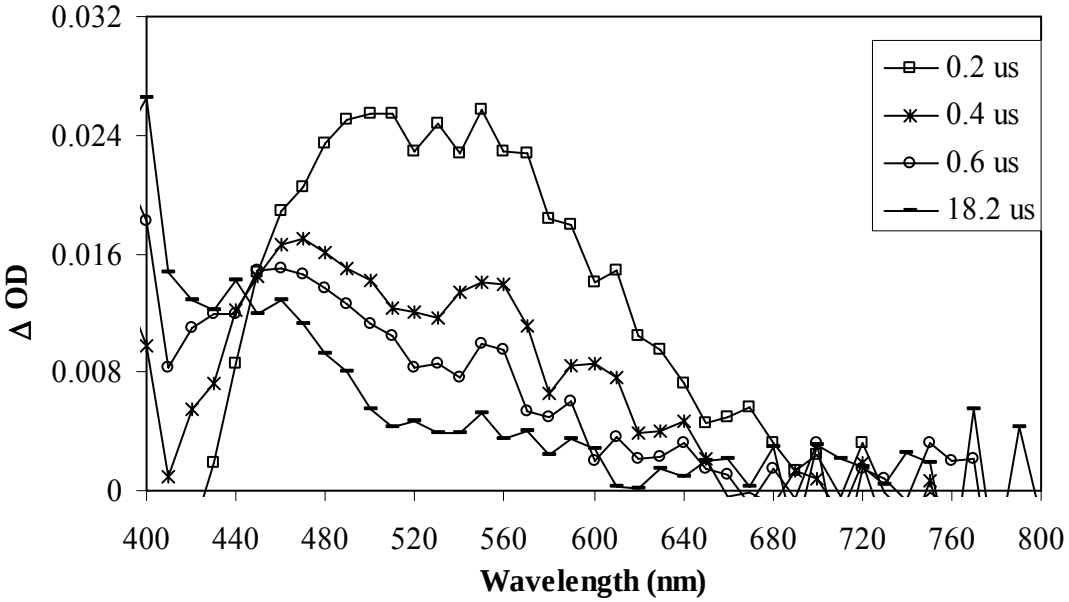

Figure 6.6 Transient spectra of the photolysis of **113** with 1,3-DMB (0.001M) in CH_3CN with 10% H_2SO_4.

Evidence of electron transfer from naphthalene was also observed. Photolysis of **113** with naphthalene in CH_3CN and 10% H_2SO_4 generates the transient signal at 550 nm, which decays rapidly along with two other absorbances with maxima at 400 nm and 690 nm. (Figure 6.7) Naphthalene radical cations generally have absorbance maximums around 390 and 690 nm;[18] therefore, the absorbances observed in the transient spectra were assigned to the naphthalene radical cations. The formation of the naphthalene radical cations accompanied by the quenching of the 550 nm absorbance indicated that electron transfer occurrs from naphthalene to the transient species generated. These electron transfer mechanisms also support the assignment of the transient species at 550 nm to **115**.

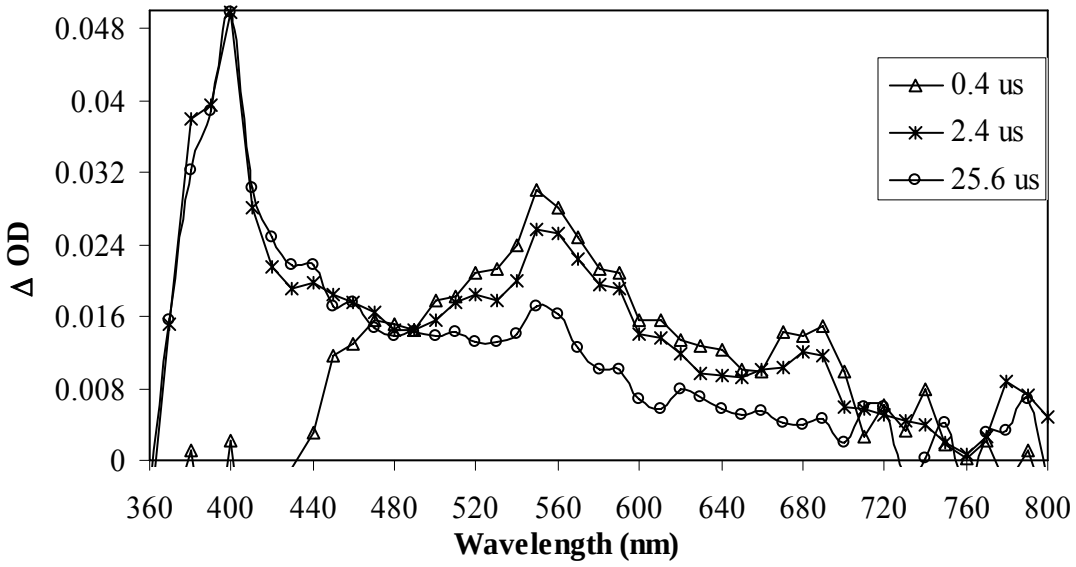

Figure 6.7 Transient spectra of the photolysis of **113** with naphthalene (0.01 M) in CH_3CN and 10% H_2SO_4

However, the choice of the nucleophiles that could be used for the competitive trapping studies was limited due to the presence of the acid. Since there was a possibility that the nucleophiles were protonated by the acid, it was difficult to obtain accurate results from the kinetic studies with these nucleophiles. Therefore, in order to circumvent this problem, the same nitrenium ion was generated from the pyridinium salt precursor.

6.2.1.2 Quinoline *N*-Oxide Nitrenium Ion from 1-(*N*-Aminoquinoline *N*-Oxide)-2,4,6-Trimethylpyridinium BF_4 Salt

1-(*N*-Aminoquinoline *N*-oxide)-2,4,6-trimethylpyridinium tetrafluoroborate salt **120** was synthesized by stirring 4-hydrazino quinoline *N*-oxide with equimolar amounts of 2,4,6-trimethylpyrilium salt in methanol at room temperature. The final product was isolated by flash chromatography to yield a yellow crystalline solid.

Compound **120** is soluble in polar solvents and has a strong UV absorption band in the range of 300 – 400 nm.

However, based on the characterization by ^{1}H and ^{13}C-NMR, it appears as the tautomer **120b** of the intended precursor **120a** was obtained. (Scheme 6.7) Shown in Table 6.1 and 6.2 are the chemical shifts predicted for some of the protons and carbons for the two tautomers. Close examination of the chemical shifts indicate that the observed chemical shift for the compound closely match with that predicted for **120b**. For example, a chemical shift of 5.0 ppm is observed which is close to the predicted shift for the proton-3 in **120b** at 4.3 ppm. More evidence for tautomer **120b** can be observed from the ^{13}C-NMR shifts. The ^{13}C-NMR chemical shifts for some of the carbons in tautomer **120b** are more deshielded than those observed for tautomer **120a**. Similar deshielding of carbon signals to higher ppm such as 159 and 154 are observed for the synthesized compound. In addition, a signal at 92.4 is observed which matches closely with the signal predicted for carbon 3 at 93.0. Due to the similarities with the chemical shifts predicted for tautomer **120b**, it is reasonable to assume that the compound synthesized is tautomer **120b**. However, photolytic studies were conducted on tautomer **120b** presuming that this would be the preferred structure of **111** *in vivo*.

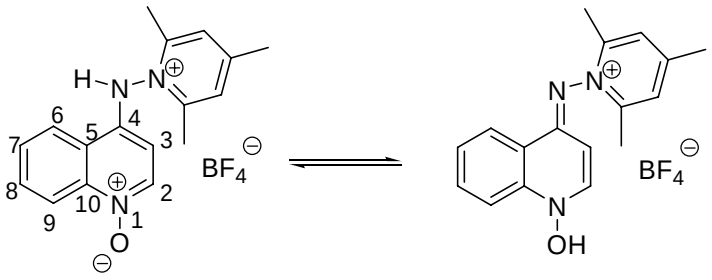

120a 120b

Scheme 6.7 Tautomerisation of **120**

Table 6.1 Predicted and observed proton chemical shifts for **120**

Predicted chemical shifts (ppm)		
	120a	**120b**
proton 2	7.95	6.4
proton 3	6.54	4.3
Observed proton shifts (ppm)		
5.00, 7.67		

Table 6.2 Predicted and observed carbon chemical shifts for **120**

Predicted chemical shifts (ppm)		
	120a	**120b**
carbon 2	142.5	140
carbon 3	129	93
carbon 4	148.4	164
carbon 5	129	118
carbon 6	128.5	126
carbon 7	128.5	123
carbon 8	128.5	128
carbon 9	128.5	115
carbon 10	142	150
Observed carbon shifts (ppm)		
159.2, 154, 152.5,140.4, 138.7, 132.8, 128.1, 125.5, 124.7, 119.4, 115.4, **92.4**, 20.8, 18.4		

Collidine peaks are predicted to appear at ppm: 148, 142, 129, 21, and 12

Photolysis of **120b** in CH_3CN generates two absorbance bands: a medium band with maximum around 440 nm and a broad absorbance band between 490 – 790

nm. (Figure 6.8) The broad signal was assigned to **121b**, formed upon the heterolytic cleavage of the N-N, bond based on the following observations. (Scheme 6.8) Similar to the transient **115**, the signal between 490-790 nm in Figure 6.8 was broad and appeared around the same range as **115**, except for the fact that it was red shifted. The bathochromic shift of absorbance is common in quinoline *N*-oxide due to tautomerism.[16] Therefore, this suggested that the broad transient signal could belong to **121b**. In addition, the broad signal decays in a biphasic manner indicating the presence to two absorbing transient species. (Figure 6.9) This indicated that the both tautomers might be present in the reaction mixture.

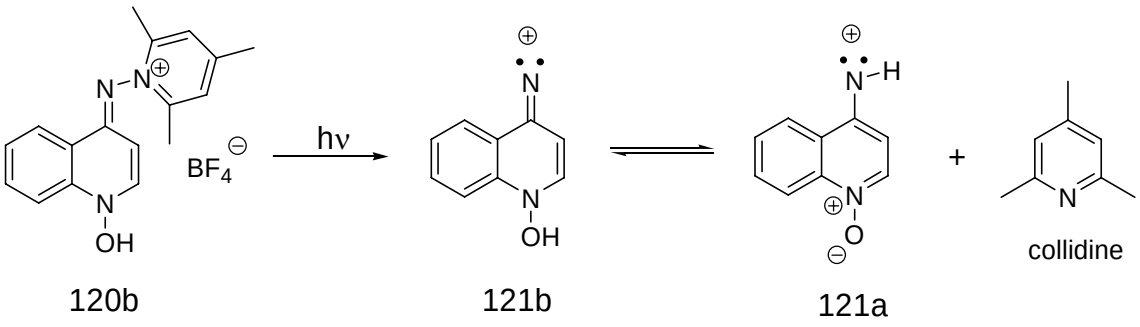

Scheme 6.8 Photolysis of **120b** in CH_3CN

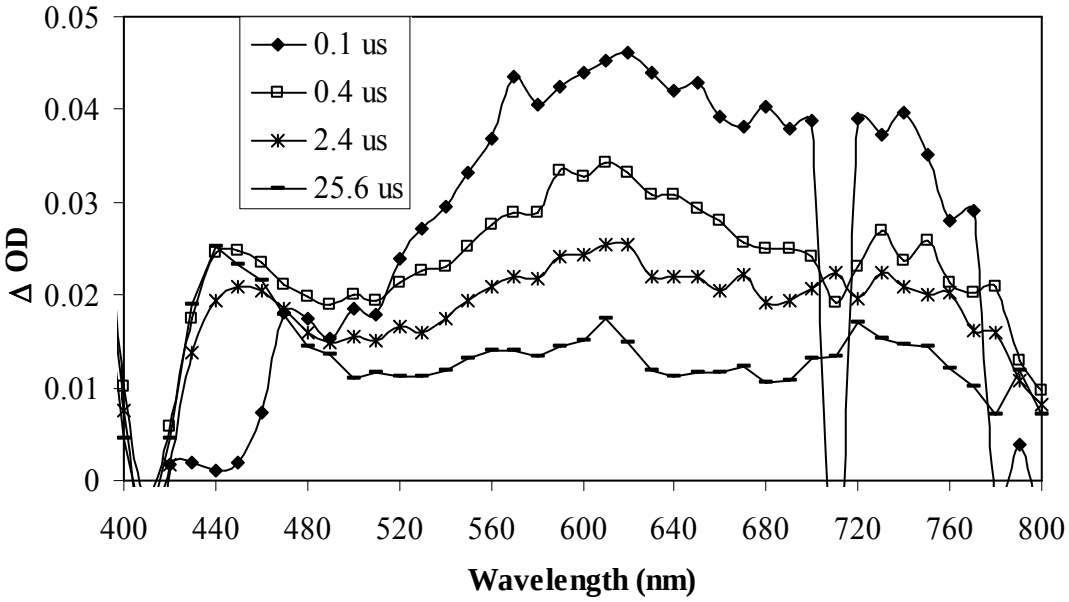

Figure 6.8 Transient spectrum of the photolysis of **120b** in CH_3CN

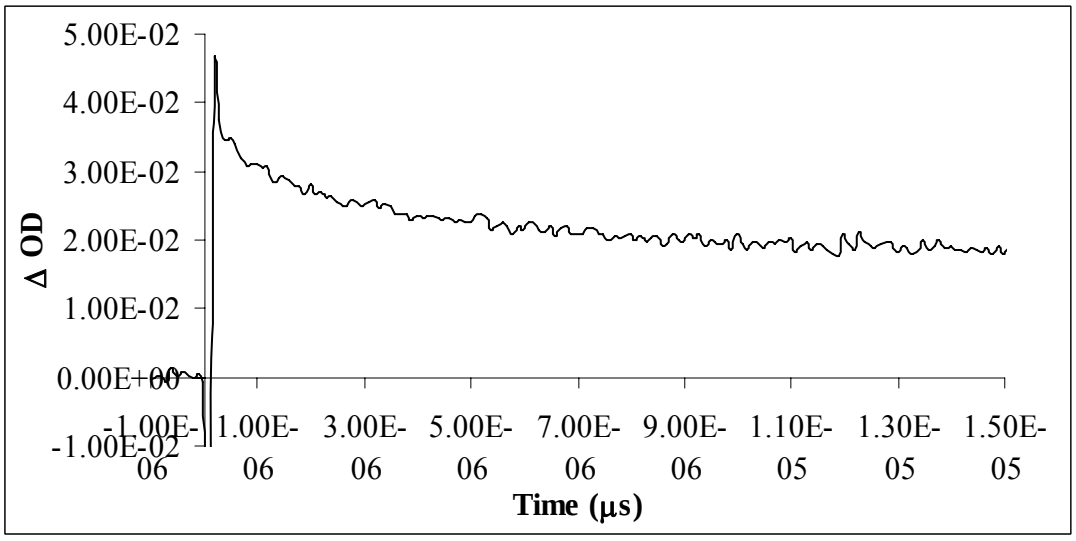

Figure 6.9 Waveform at 610 nm of the photolysis of **120b** in CH_3CN

The N-N bond heterolysis was also confirmed by the detection of collidine. ^{1}H-NMR taken during the photolysis of **120b** showed the growth of the peaks corresponding to collidine and the disappearance of the **120b** peaks. This confirmed that the N-N bond was cleaved during the photolysis to generate one of the tautomers

of **121** and collidine. Based on the biphasic decay of the transient, it is possible that both **121a** and **121b** are in equilibrium. Competitive trapping studies with various nucleophiles were inconclusive and did not provide any qualitative information on the transient species. Since the major problem associated with this precursor was tautomerism due to the protonation of the *N*-oxide, nitrenium ions generated from quinolines were studied.

6.2.2 Quinoline Nitrenium Ions

In order to minimize the effects of tautomerisation, nitrenium ions were generated from quinoline derivatives. The assumption was that the nitrogen in the ring would not be that basic (pKa ~ 4.92)[21] compared to the oxygen in quinoline *N*-oxide; hence would not be protonated, thus eliminating the possibility of tautomerism. The transient spectra obtained from the photolysis of azide and pyridinium precursors yielded conflicting results.

6.2.2.1 Quinoline Nitrenium Ion from 1-(*N*-Aminoquinoline)-2,4,6-Trimethylpyridinium BF_4 Salt

The pyridinium precursor 1-(*N*-aminoquinoline)-2,4,6-trimethylpyridinium tetrafluoroborate salt **122** was synthesized from 4-hydrazinoquinoline[22] and 2,4,6-trimethylpyrilium to yield a pale greenish yellow powder. The final product has a weak UV absoption tail below 350 nm and is soluble in slightly polar solvents. Similar to **120**, the tautomeric form of the intended precursor was obtained. (Scheme 6.9) Shown in Table 6.3 and 6.4 are the predicted chemical shifts for proton and carbon for both tautomers. The predicted proton-3 shift for **122a** and **122b** are 6.54 and 4.3 respectively. A proton signal at 5.23 is observed for the synthesized

compound. Additionally, the chemical shifts for carbon-3 and carbon-6 predicted for 122b are 93 ppm and 164 ppm respectively. Signals around 95.3 ppm and 161.8 ppm are observed, indicating that we might have tautomer **122b**. However, photolytic studies were performed using **122b**.

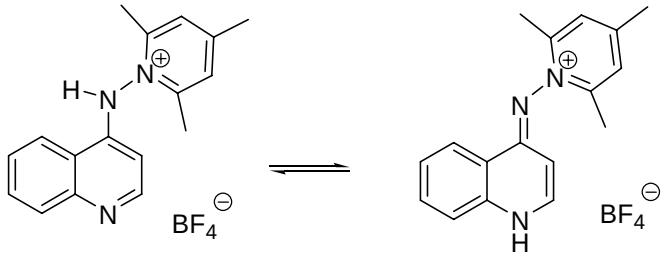

122a 122b

Scheme 6.9 Tautomers of **122**

Table 6.3 Predicted and observed proton chemical shifts for **122**

Predicted proton shifts (ppm)		
	122a	**122b**
proton 2	8.64	6.4
proton 3	6.54	4.3
Observed proton shifts (ppm)		
5.23, 7.58		

Table 6.4 Predicted and observed carbon chemical shifts for **122**

Predicted carbon shifts (ppm)		
	122a	**122b**
carbon 2	150.3	140
carbon 3	104.3	93
carbon 4	149.7	164.6
carbon 5	117.8	117.8
carbon 6	128.3	128.8
carbon 7	125	118.6
carbon 8	128.9	131.6
carbon 9	129.5	115.2
carbon 10	148.7	147.2
Observed carbon shifts (ppm)		
161.8, 154.8, 152.8, 140.1, 138.8, 133.5, 127.7, 126.0, 125.5, 119.6, 95.3, 21.3, 19.0		

Photolysis of **122b** in CH_3CN generates a medium and a strong broad transient absorption signals with maxima around 410 and 610 nm respectively. (Figure 6.10) The broad transient signal decays in a biphasic manner and is unaffected by the presence of O_2. This signal had some similaries to the absorption signal observed in Figure 6.8 suggesting that transient species responsible for the broad signal in both cases could be similar species. Therefore, it was assumed that the transient species observed in Figure 6.10 could be **123a** or its tautomeric form **123b** or both in equilibrium. (Scheme 6.10)

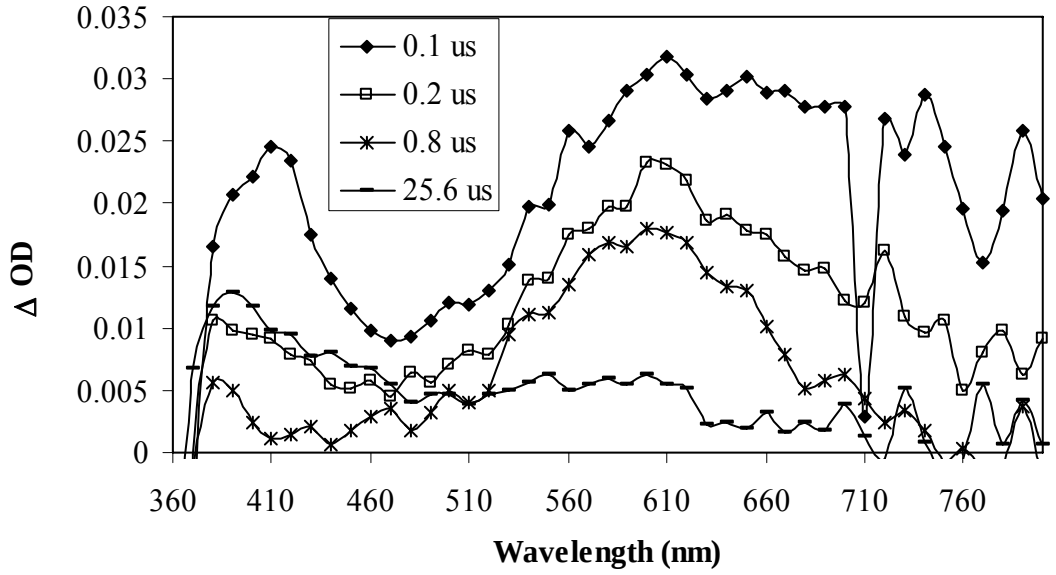

Figure 6.10 Transient spectrum of the photolysis of **122b** in CH_3CN

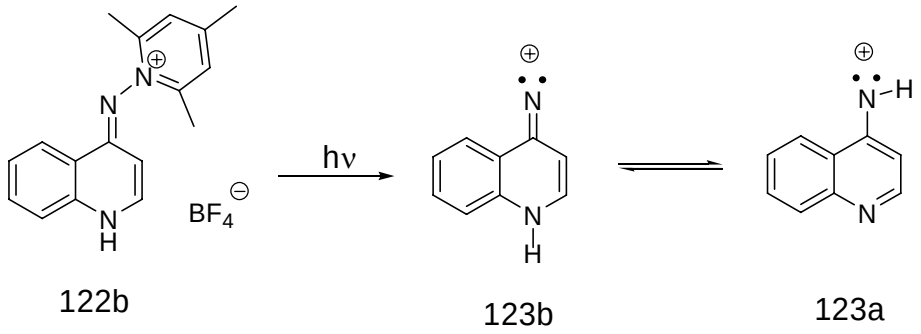

Scheme 6.10 Photolysis of **122b** in CH_3CN

LFP studies in the presence of various nucleophiles did not provide any qualitative information on the kinetic properties of the transient species. The precursor **122b** was photolyzed in the presence of arenes such as 1,3,5-TMB, 1,3-DMB, 1,4-DMB and hydrogen atom donor 1,4-CHD. No significant change in the transient spectra was observed indicating no reactivity between the transient species and the nucleophiles. More experiments and product studies are required to determine the identity of the transient species.

6.2.2.2 Quinoline Nitrenium Ion from 4-Azidoquinoline

Shown in Figure 6.11 is the transient spectra of the photolysis of 4-azidoquinoline **124** in CH_3CN and 10% HBF_4. Precursor **124** was synthesized following the procedure reported in the literature.[22] Upon irradiation of **124**, a strong broad absorbance band with maximum at 560 nm was observed immediately after the laser pulse. The transient signal was long lived and didn't resemble to any of the absorption spectra observed for other precursors. It was presumed that upon photolysis, **125** that is generated is protonated to yield **126a** or its tautomeric form **126b**. (Scheme 6.11) However, it is not certain if this transient signal belonged to nitrenium ion.

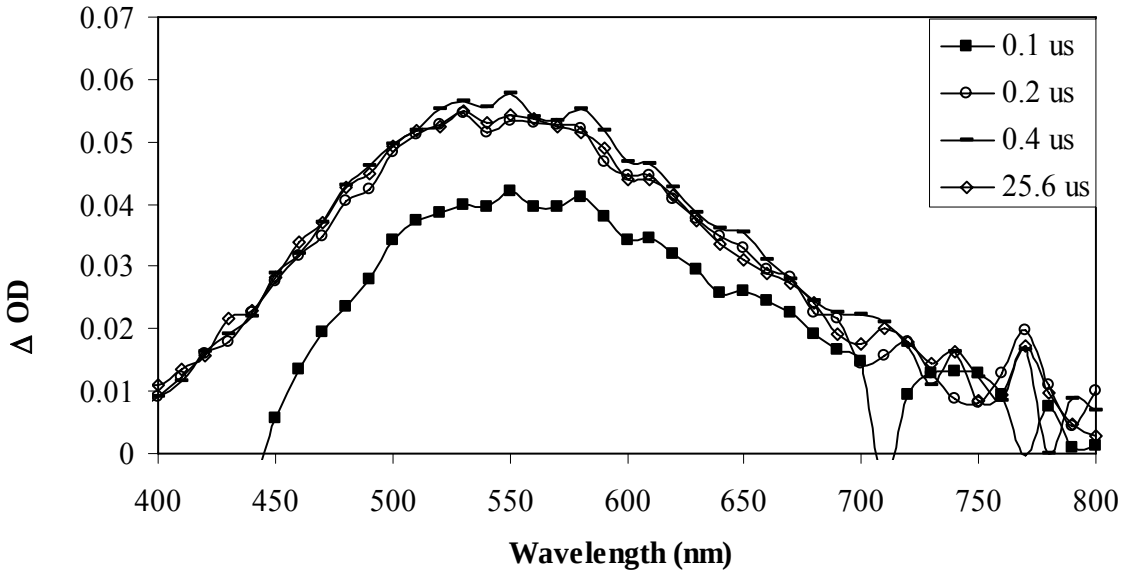

Figure 6.11 Transient spectrum of the photolysis of **124** in CH_3CN/HBF_4.

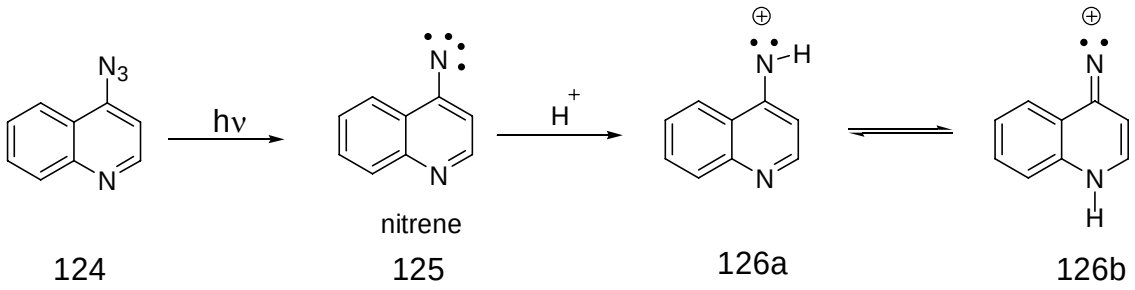

Scheme 6.11 Photolysis of **124** in CH_3CN with 10% HBF_4

6.3 Conclusion

The transient intermediates generated from all four precursors were distinct with strong absorbances in the UV-Vis. As a result, it was difficult to accurately determine if the nitrenium ion was generated during the photolysis of any precursors. However, based on the different experimental evidence, it appears that the transient species from **113** is in fact the quinoline *N*-oxide nitrenium ion. Results from the other precursors were inconclusive.

Due to problems associated with tautomerisation and acidic solvents, it was difficult to accurately interpret the results obtained from the different precursors. Since the photolysis was done in acidic and non-acidic solvents, it was difficult to accurately predict the tautomer generated in each solvent system. From the LFP studies it seemed that the species generated from the pyridinium salts, **120** and **122** was different from the transient species (**115**) generated from **113**. In addition, it was also difficult to determine the tautomer responsible for the transient absorption. However, according to a rough estimation from AM1 calculations for quinoline *N*-oxide, it seems that the tautomer with the deprotonated oxygen is more stable than the tautomer with the protonated oxygen.

The major problems encountered in the work were due to the presence of acid in the solution. Generating quinoline *N*-oxide nitrenium ion from azide precursors proved to be a better method; however, there were limitations to the nucleophiles that could be used for the kinetic studies. Since azide photolysis requires acidic media, it was difficult to obtained accurate kinetic data due to the protonation of the nucleophiles.

Therefore, the problems associated with tautomerism and protonation of nucleophiles can be eliminated by using a precursor with a methyl group and a group leaving group such as acetoxy group on nitrogen that would undergo heterolytic scission to generate a positively charged nitrogen species. Attempts to synthesize *N*-methyl-*N*-quinoline *N*-oxide pyridinium salt were unsuccessful because reaction between the quinoline *N*-oxide derivative and the pyrylium salt is an electrophilic reaction. Quinoline *N*-oxides are extremely electron deficient; therefore do not undergo electrophilic reactions. Hence, some other precursor is required for generating the quinoline *N*-oxide nitrenium ion by LFP method.

References

(1) Miller, J. A.; Miller, E. C. In *Physico-Chemical Mechanisms of Carcinogenesis, Jerusalem Symposia on Quantum Chemistry and Biochemistry. The Israel Academy of Sciences and Humanities,*; Bergmann, E. D., Pullman, B., Eds.: Jerusalem, 1969; Vol. 1, pp 237-261.

(2) Arcos, J. C.; Argus, M. F. *Adv. Cancer Res.* **1968**, *11*, 305-471.

(3) Endo, H. In *Chemistry and Biological Actions of 4-Nitroquinoline 1-Oxide*; Endo, H., Ono, T., Sugimura, T., Eds.; Springer-Verlag: Berlin, 1971, pp 32-52.

(4) Malkin, M. F.; Zahalsky, A. C. *Science* **1966**, *154*, 1665-1667.

(5) Kawazoe, Y.; Araki, M.; Nakahara, W. *Chem. Pharm. Bull.* **1969**, *17*, 544-549.

(6) Sugimutra, T.; Otake, H.; Matsushima, T. *Nature* **1968**, *218*, 392.

(7) Kohda, K.; Tada, M.; Kasai, H.; Nishimura, S.; Kawazoe, Y. *Biochem. Biophys. Res. Commun.* **1986**, *139*, 626 - 632.

(8) Bailleul, B.; Galiegue, S.; Loucheux-Lefebvre, M. H. *Cancer Res.* **1981**, *41*, 4559-4565.

(9) Kawazoe, Y.; Araki, M.; Huang, G. F.; Okamoto, T.; Tada, M.; Tada, M. *Chem. Pharm. Bull.* **1975**, *23*.

(10) Okano, T.; Takenaka, S.; Sato, Y. *Chem. Pharm. Bull.* **1968**, *16*, 556.

(11) Demeunynck, M.; Lhomme, M.-F.; Mellor, J. M.; Lhomme, J. *J. Org. Chem.* **1989**, *54*, 399-405.

(12) Demeunynck, M.; Lhomme, M.-F.; Lhomme, J. *J. Org. Chem.* **1988**, *48*, 1171-1175.

(13) McClelland, R. A.; Kahley, M. J.; Davidse, P. A.; Hadzialic, G. *J. Am. Chem. Soc.* **1996**, *118*, 4794-4803.

(14) McClelland, R. A.; Davidse, P. A.; Hadzialic, G. *J. Am. Chem. Soc.* **1995**, *117*, 4173-4174.

(15) Kamiya, S.; Sueyoshi, S.; Miyahara, M.; Yanagimachi, K.; Nakashima, T. *Chem. Pharm. Bull.* **1980**, *28*, 1485-1490.

(16) Andreev, V. P.; Ryzhakov, A. V. *Chemistry of Heterocyclic Compounds* **1993**, *29*, 1435-1440.

(17) Ramlall, P.; Li, Y.; McClelland, R. A. *J. Chem. Soc., Perkin Trans. 2* **1999**, 1601-1607.

(18) Shida, T. *Electronic Absorption Spectra of Radical Ions*; Elsevier: Netherlands, 1988; Vol. 34.

(19) Chiapperino, D.; Falvey, D. E. *J. Phys. Org. Chem.* **1997**, *10*, 917-924.

(20) Shukla, R.; Mani, R. P. *Asian J. Chem.* **1999**, *11*, 584-590.

(21) Perrin, D. D.; Dempsey, B.; Serjeant, E. P. *pKa Prediction for Organic Acids and Bases*; Chapman and Hall: New York, 1981.

(22) Itai, T.; Kamiya, S. *Chem. Pharm. Bull.* **1961**, *9*, 87-91.

Chapter 7. Conclusion

The work described in this thesis investigated the chemical and kinetic properties of three different nitrenium ions using photolytic methods. Each nitrenium ion was studied with a particular objective; however, the knowledge obtained from these studies can be inferred to understanding other arylnitrenium ions.

The chemical and kinetic studies done on *N*-(4,4'-dichlorodiphenyl) nitrenium ion (**78b**) and *N*-(4,4'-dibromodiphenyl) nitrenium ion (**78c**) showed that substituting halogens in diphenylnitrenium ion (**78a**) does not affect the ground state of the arylnitrenium ion; however this substitution lowers the singlet-triplet energy gap and increases the lifetime of the ions. Similar to other arylnitrenium ions, these species were concluded to be ground state singlets through LFP studies, trapping studies and product analysis. They react with nucleophiles either by forming covalent adducts or by electron transfer. In addition, DFT calculations predict that the singlet state is lower in energy than the triplet state. As further evidence, the UV signals of **78b** and **78c** observed experimentally closely match with the signals predicted from TD-DFT calculations for the singlet state.

Despite the singlet behavior observed for **78b** and **78c**, the latter also exhibit triplet behavior by undergoing hydrogen atom transfer processes in the presence of hydrogen atom donors. Since **78b** and **78c** are established to be ground state singlets, this triplet behavior is attributed to the result of intersystem crossing of the singlet diarylnitrenium ion to the triplet state. This behavior is not observed for the unsubstituted system **78a**. Therefore, these results suggest that the halogens lower the singlet-triplet energy gap enough by stabilizing the triplet state either through

inductive electron-withdrawing characteristics or increase in the R-N-R' bond angle to allow intersystem crossing. Furthermore, these ions are long-lived than other arylnitrenium ions, living for more than 120 μs in CH_3CN which is attributed to electron donation of the non-bonding electrons from the halogens. As a result, halogens increase the stability of the diarylnitrenium ion through π-donation and also lower the ΔE_{ST} by stabilizing the triplet state.

LFP studies *N*-methyl-*N*-biphenylylnitrenium ion (**103**) with amino acid and protein traps showed that these biological molecules react rapidly with the nitrenium ion **103**. Competitive trapping studies showed that eight of the twenty amino acids react with four of them reacting at a rate constant of $10^8 - 10^9$ $M^{-1}s^{-1}$. These results show that the selectivity of **103** for both amino acids and nucleic acid bases is similar. Previous work on nucleic acid bases showed that only purine bases, guanosine and adenosine, react efficiently with arylnitrenium ions with guanosine reacting with **103** with a rate constant of 1.9×10^9 $M^{-1}s^{-1}$.

Moreover, kinetic analysis with proteins show that **103** reacts with the latter at a rate constant of 10^8 $M^{-1}s^{-1}$. The larger rate constants support the in vivo and in vitro studies confirming that proteins may contribute to the carcinogenicity of the arylamines. However, due to their abundance in the cell and greater affinity toward arylnitrenium ions, proteins have a greater chance of adding to arylnitrenium ions than DNA. Novak's work on single and double stranded DNA showed that only the ss-DNA reacts with arylnitrenium ions. Double stranded DNA showed no reactivity with arylnitrenium ion, which was further confirmed by the work done in our lab. Therefore, in order for the arylnitrenium ions to be able to react with the DNA bases,

the latter must be in single stranded form; whereas, proteins are reactive towards arylnitrenium ion in their tertiary structure.

The objective of the work done on quinoline compounds was to generate quinoline *N*-oxide nitrenium ion photochemically from a suitable precursor. Attempts to generate the heteroaromatic nitrenium ion from azide and *N*-aminopyridinium salt precursors photolytically showed that the former method was more successful than the latter method. Based on experimental observations, the transient species from the azide precursor showed more characteristics of being a nitrenium ion than the transient species from the pyridinium salt. However, since the photolysis of azide requires acid to generate nitrenium ion, the choice of nucleophiles that could be used for the kinetic study is limited. Most nucleophiles are protonated by the acid, thus preventing the acquisition of accurate kinetic data. LFP results from the photolysis of the pyridinium salt were inconclusive and provided no qualitative information. Therefore, in order to study the characteristics of quinoline *N*-oxide nitrenium ion, synthesis of a better precursor is required.

These studies with the various arylnitrenium ions show that substituting halogens in diarylnitrenium ion stabilizes the ion considerably. As a result of the stabilization, the halogenated diarylnitrenium ions live long enough to be able to intersystem cross to the higher energy triplet state and thus exhibit triplet characteristics which were not observed previously for any other arylnitrenium ions. Work with *N*-4-biphenylyl-*N*-methyl nitrenium ion showed that arylnitrenium ions are potent not only to nucleic acid bases and DNA but also to amino acids and proteins. Hence, if arylnitrenium ions are generated *in vivo*, due to the abundance of

proteins in cells, the proteins would seem to be affected more by the ions. Even though the long term consequence of this affinity of arylnitrenium ions toward proteins is not known, it is possible that the long term effects would not be as drastic as seen with DNA. Finally, the transient species generated from 4-azidoquinoline *N*-oxide is the first quinoline *N*-oxide nitrenium ion that has been observed and generated photochemically. Therefore, in order to determine if quinoline *N*-oxide nitrenium ions is the ultimate carcinogen in the carcinogenicity of 4-nitroquinoline *N*-oxide, future studies can be done using the azide precursor through product analysis.

Chapter 8. Experimental Methods

8.1 LFP Experiments

Laser Flash Photolysis (LFP) experiments are carried out at 298 K using Nd:YAG laser (Continuum Surelite II-10) that uses second, third and fourth harmonic generator crystals to create output wavelengths of 355 and 266 nm. The probe beam needed to obtain the transient absorption signal is generated from the Oriel 350 W Xe arc lamp. Transient waveforms are digitized by the LeCroy 9420 digital oscilloscope with a bandwidth of 350 MHz at a rate of 1 point per 10. All LFP data are analyzed by Labview 5.0 software.

All transient spectra are measured in dry CH_3CN under N_2, unless otherwise stated. The samples to be photolyzed is prepared in dry CH_3CN (~150 mL) with the concentration adjusted to have an optical density between 1.5-2.0 at the excitation wavelength. The sample is photolyzed in a quartz cuvette. Fresh supply of reaction mixture from the stock solution to the cuvette is maintained by the setup of a closed flow cell under N_2 via a double-headed needle. The photolyzate is then drained from the cuvette into an Erlenmeyer flask. This setup prevents the accumulation of photoproducts and avoids the depletion of the substrate during the experiment. Waveforms are collected every 10 nm ranging from 360 – 800 nm or 270 – 800 nm depending on the excitation wavelength. Sample for quenching studies are prepared in the similar manner as above along with the quencher of any concentration

Kinetic studies are preformed in CH_3CN using static cell by replenishing the substrate solution for each quencher concentration. A stock solution of the precursor with an optical density between 1.5-2.0 is prepared in dry CH_3CN. A stock solution

of the quencher of a particular concentration (usually 1 M) is made up in CH_3CN. A 3.0 mL aliquot of the stock solution taken in a quartz cuvette containing different quencher concentration is irradiated using laser (266 or 355 nm). The quencher is added in 10 mL aliquot via a microsyringe. The pseudo-first order decay kinetics of the nitrenium ion at a particular wavelength is recorded for atleast five quencher concentrations. The second order rate of quenching is obtained as a slope by plotting the pseudo-first order decay rates as a function of the concentration of the quencher. The samples are not purged with nitrogen because no difference in behavior is observed in the presence of N_2 or O_2.

8.2 Kinetic Isotope Effect

A 50 mL stock solution of **77b** or **77c** was prepared in 50:50 CH_3CN and H_2O with an optical density between 1.5 – 2.0. A stock solution (~ 2 mL) of phenol in 50:50 CH_3CN and H_2O with a concentration around 0.6 M was also prepared. The reaction rate constant of phenol with **78b** and **78c** was measured as described above.

The reaction rate constant of deuteriated phenol was obtained by preparing reaction sample containing **77b** or **77c** and phenol in 50:50 CH_3CN and D_2O. The assumption was that shaking phenol with D_2O would deuteriate phenol.

8.3 DFT Calculations

The calculations preformed on all the compounds described in this thesis are done using the Gaussian 03 suite of programs. The geometry optimization and vibrational frequency is preformed using the density functional theory particularly utilizing the hybrid B3LYP functional that is comprised of Becke's B3 three

parameter gradient-corrected exchange functional with LYP correlation functional of Lee, Yang and Parr that was originally described by Stephens et. al.[1-4]

8.4 Synthesis of Compounds

8.4.1 *N*-(4,4'-Dichlorodiphenyl)-2,4,6-Trimethylpyridinium Tetrafluoroborate Salt (77b)

N-(4,4'-Dichlorodiphenyl)-2,4,6-trimethylpyridinium tetrafluoroborate salt (**77b**) was synthesized by coupling 1,1'-(4,4'-dichlorodiphenyl) hydrazine with 2,4,6-trimethylpyrylium tetrafluoroborate salt. Since 1,1'-(4,4'-dichlorodiphenyl) hydrazine was not available commercial, it was prepared through a series of step from 4,4'-dichlorodiphenyl amine. 4,4'-dichlorodiphenyl amine was synthesized using the Goldberg procedure by refluxing 4-chloroacetanilide with 4-bromochlorobenzene in the presence of K_2CO_3 and CuI.[5]

1.74 g (0.0073 mol) of 4,4'-dichlorodiphenyl amine was dissolved in 20 mL ethanol in a 100-mL RBF and stirred in ice-bath for 10 min. 2.1 mL of conc. HCl was added to the cold solution and again stirred for another 5 min. $NaNO_2$ (0.77g, 0.11 mol) dissolved in 8 mL H_2O was added slowly to the reaction mixture while keeping it in ice-bath. Yellow precipitate was formed. The mixture was stirred in ice-bath for an additional 45 min and then kept in the freezer overnight to maximize precipitation. The precipitate was collected the next day to yield 1.51 g of yellow powder of 4,4'-dichlorodiphenyl nitrosamine. ^{1}H NMR (400 MHz, CD_3CN) δ 7.56 (d, J = 8.9 Hz, 2H), 7.48 (d, J = 9.1 Hz, 2H), 7.39 (d, J = 9.1 Hz, 2H), 7.11 (d, J = 8.9 Hz, 2H).

4,4'-Dichlorodiphenyl nitrosamine obtained in the previous step was reduced by zinc to yield the hydrazine. A mixture of 13 mL H_2O, 13 mL acetic acid, 2 mL HCl, 15 mL THF and 6 mL ethanol was cooled in ice-bath for 10 min. 1.51g (0.0056 mol) of nitrosamine was added to the cold solution. Additional 20 mL ethanol and 10 mL THF was added to the suspension to aid solubility of the nitrosamine. After stirring for 5 min, 6 g cleaned zinc dust was added to the suspension which turned light yellow to colorless within few minutes. The suspension was stirred in ice-bath for an additional 20 min. Excess zinc was filtered off and the filtrate was neutralized using sat. $NaHCO_3$. The aqueous layer was extracted three times with CH_2Cl_2. The organic layers were combined and dried over $MgSO_4$. The solvent was then removed under reduced pressure to yield a dark oily residue. Recrystallization of the residue from 50:50 EtOH/H_2O yielded white flaky solid of 0.8878 g of pure 1,1'-(4,4'-dichlorodiphenyl) hydrazine. ^{1}H NMR (400 MHz, CD_3CN) δ 7.25 (d, J = 9.1 Hz, 4H), 7.18 (d, J = 9.1 Hz, 4H), 4.45 (br, 1H); ^{13}C NMR (400 MHz, CD_3CN) δ129.9, 129.5, 121.6, 119.6; MS (FAB) m/z (relative intensity) 252.1 (95), 236.1 (33), 201.1 (17), 155.0 (72), 119.0 (100), 85 (65), 79.0 (14).

1,1'-(4,4'-Dichlorodiphenyl) hydrazine (1.14 g, 0.0045 mol) was dissolved in 70 mL ethanol. To this solution, 0.76 g (0.0036 mol) of freshly prepared 2,4,6-trimethyl pyrylium tetrafluoroborate salt was added and refluxed for an hour. After refluxing, the reaction mixture was cooled to room temperature, and then placed in the freezer. Greenish yellow precipitate formed was collected and washed with cold ethanol and H_2O to yield 1.21 g (75 %) of pure *N*-(4,4'-dichlorodiphenyl)-2,4,6-trimethylpyridinium tetrafluoroborate salt. ^{1}H NMR (400 MHz, CD_3CN) δ 7.77 (s,

2H), 7.41 (d, *J* = 8.8 Hz, 4H), 6.95 (d, *J* = 8.8 Hz, 4H), 2.62 (s, 3H), 2.49 (s, 6H); ^{13}C NMR (400 MHz, CD_3CN) δ163.1, 158.9, 139.9, 131.2, 130.8, 120.7, 22.3, 20.5; MS-BF_4 (DEI+) m/z (relative intensity) 356.1 (5), 237.0 (100), 201 (25), 167.1 (37), 121.1 (52), 75 (14). Molar absorptivity at 355 nm is 1.15 x 10^3 $M^{-1}cm^{-1}$.

8.4.2 1-(*N*-Aminoquinoline *N*-oxide)-2,4,6-Trimethylpyridinium Tetrafluoroborate salt (120b)

The pyridinium salt was synthesized by coupling 4-hydrazinoquinoline *N*-oxide with substiochiometric amounts of 2,4,6-trimethylpyrylium BF_4 salt in methanol. The synthesis of 4-hydrazinoquinoline *N*-oxide is described elsewhere.[6] 4-hydrazinoquinoline *N*-oxide (1g, 5.7 mmol) was dissolved in 60 mL of methanol by stirring at room temperature. Approximately 95 g (4.5 mmol) of pyrylium BF_4 salt was added to the solution and stirred at room temperature. Upon addition of pyrylium salt, the solution turned to cloudy orange color. Continued stirring of the cloudy solution for 4 hours yielded a clear yellow color solution with few suspensions. The suspension was filtered off and the filtrate was concentrated under reduced pressure to yield an oily residue. The final pyridinium salt was isolated using flash chromatography by eluding with 9:1 $CHCl_3$ and methanol to yield a crystalline yellow solid in 50% yield. ^{1}H NMR (400 MHz, CD_3CN) δ 8.50 (d, *J* = 8.4 Hz, 1H), 7.81 (d, *J* = 8.4 Hz, 1H), 7.72 (t, *J* = 7.2 Hz, 1H), 7.67 (d, *J* = 7.6 Hz, 1H), 7.57 (s, 2H), 7.48 (t, *J* = 7.2 Hz, 1H), 5.00 (d, *J* = 8 Hz, 1H), 2.51 (s, 3H) 2.42 (s, 6H); ^{13}C NMR (400 MHz, CD_3CN) δ 159.2, 154.0, 152.5, 140.4, 138.7, 132.8, 128.1, 125.5, 124.7, 119.4, 115.4, 92.4, 20.8, 18.4; MS-BF_4^- (ESI) m/z:280.14569

8.4.3 1-(*N*-Aminoquinoline)-2,4,6-Trimethylpyridinium Tetrafluoroborate Salt (122b)

The pyridinium salt was prepared by coupling 4-hydrazinoquinoline with substochoimetric amounts of 2,4,6-trimethylpyrilium BF_4 salt in methanol. 4-hydrazinoquinoline was synthesized from 4-chloroquinoline *N*-oxide following the procedure in the literature.[6,7] Approximately 325 mg (2 mmol) of 4-hydrazinoquinoline was dissolved in 8 mL ethanol by stirring at room temperature. To the solution, 343 mg (1.6 mmol) of pyrilium BF_4 salt was added and stirred overnight at room temperature. The pale greenish yellow precipitate that was produced was collect by vacuum filtration to yield the final pyridinium salt in 90% yield. ^{1}H NMR (400 MHz, CD_3CN) δ 10.1 (br, 1H), 8.52 (d, *J* = 8 Hz, 1H), 7.75 (t, *J* = 8 Hz, 1 H), 7.58 (m, 4H), 7.49 (t, *J* = 8 Hz, 1H), 5.23 (d, *J* = 8 Hz, 1H), 2.52 (s, 3H) 2.45 (s, 6H; ^{13}C NMR (400 MHz, CD_3CN) δ 161.8, 154.8, 152.8, 140.1, 138.8, 133.5, 128.7, 126.0, 125.3, 119.6, 119.3, 95.3, 21.3, 19.0; MS-BF_4^- (DEI+) m/z (relative intensity) 263.1 (65), 248.1 (30), 144 (90), 121.1 (100), 79 (20), 77 (20), 39 (15).

8.5 Product Analysis

8.5.1 Photolysis of 77b and 77c with NaCl

Approximately 50 mg of the pyridinium salt was dissolved in 5 mL CH_3CN and 400 mg NaCl was dissolved in 45 mL H_2O. The two solutions were then combined and left on the lab bench for a week to be photolyzed using room light. After photolysis, the reaction mixture was shaken with equal amount of CH_2Cl_2 and and aqueous $NaHCO_3$. The organic layer was withdrawn and aqueous layer was extracted three times with CH_2Cl_2. The organic layers were combined and dried over

$MgSO_4$. Upon filtration, the solvent was removed under reduced pressure to yield a crude dark residue. The photoproducts were isolated using preparative thin layer chromatography (20 x 20 cm, 1000 microns silica gel) with mobile phase of 80:20 hexanes and ethyl acetate. The three photoproducts obtained were weighed and characterized by ^{1}H-NMR, ^{13}C-NMR and MS: *ortho* adduct (**82b** and **82c**), parent amine (**79**) and 3,6-dihalogenated carbazole (**83b** and **83c**). The halogenated carbazole (**83b** and **83c**) have been observed and characterized previously.[8-10]

Photoproducts of Dichlorodiphenyl Nitrenium Ion, **78b**: *ortho* adduct, **82b** (8.4 mg): ^{1}H NMR (400 MHz, CD_3CN). δ 7.45 (m, 1 H), 7.29 (d, J = 8.8 Hz, 2 H), 7.17 (m, 2H), 7.08 (d, J = 8.8 Hz, 2H), 6.58 (br, 1 H); ^{13}C NMR (400 MHz, CD_3CN) δ 141.7, 140.2, 130.2, 130.0, 129.9, 128.5, 127.3, 125.6, 124.0, 122.0, 119.0; MS (DEI+) m/z (relative intensity) 273.0 (100), 237.0 (14), 235.0 (12), 201.0 (60), 166.0 (11), 139.0 (9), 117.5 (12), 100.0 (7), 75.0 (9), 62.0 (5), 44.2 (4). (0.9 mg) 3,6-dichlorocarbazole, (trace amounts) **83b**: ^{1}H NMR (400 MHz, CD_3CN). δ 8.09 (d, J = 2.4 Hz, 2 H), 7.49 (d, J = 8.8 Hz, 2H), 7.41 (dd, J = 8.0, 2.4 Hz, 2H); MS (DEI+) m/z (relative intensity) 235.0 (100), 200 (40), 163.9 (22), 117.5 (20), 44.2 (25).

Photoproducts of Dibromodiphenyl Nitrenium Ion, **78c**: *ortho* adduct, **82c** (6.8 mg): ^{1}H NMR (400 MHz, CD_3CN) δ 7.57 (d, J = 2.4 Hz,1 H), 7.42 (d, J = 8.8 Hz, 2 H), 7.30 (dd, J = 8.8, 2.4 Hz, 1H), 7.13 (d, J = 8.8 Hz, 1H), 7.03 (d, J = 8.8 Hz, 2H), 6.59 (br, 1 H); ^{13}C NMR (400 MHz, CD_3CN) δ142.2, 140.6, 133.1, 133.0, 131.5, 124.4, 122.4, 119.5, 114.8, 112.5; MS (DEI+) m/z (relative intensity) 360.8 (100), 316.9 (10), 245.0 (40), 201.0 (20), 166.1 (32), 139.0 (12), 100.5 (25), 75.0 (13), 63.0 (10), 50.0 (7). 3,6-dibromocarbazole, **83c** (trace amount):^{1}H NMR (400 MHz, CD_3CN). δ

8.24 (d, *J* = 2.0 Hz, 2H), 7.53 (dd, *J* = 8.8, 2.0 Hz, 2H), 7.45 (d, *J* = 8.8, Hz, 2H); MS (DEI+) m/z (relative intensity) 324.9 (100), 322.9 (55), 280.9 (10), 245.9 (18), 244.0 (15), 163.9 (18), 82.5 (10).

8.5.2 Photolysis of 77b and 77c with 1,3,5-TMB

Approximately 50 mg of the pyridinium salt and 170 mg of 1,3,5-TMB was dissolved in 50 mL dry CH_3CN. The reaction mixture was left on the lab bench for a week to be photolyzed using room light. After photolysis, the solution was treated in a similar manner as described above. Three stable photoproducts were obtained: *N* adduct (**88b** and **88c**), *ortho* adduct (**87b** and **87c**) and the parent amine (**79**) in 2.0:2.5:1.0 mol ratio from ^{1}H-NMR. The quantity of the products was too low to obtain an accurate mass.

Photoproducts of Dichlorodiphenyl Nitrenium Ion, **78b**: *N* adduct, **88b** (12.6 mg): ^{1}H NMR (400 MHz, $CD_3C\underset{..}{N}$) δ 7.14 (d, *J* = 9.2 Hz, 4H), 6.88 (d, *J* = 8.8 Hz, 4H), 6.27 (s, 2H), 3.81 (s, 3H), 3.66 (s, 6H); ^{13}C NMR (400 MHz, CD_3CN) δ 162.5, 161.6, 159.4, 146.7, 129.5, 126.1, 122.1, 115.4, 92.4, 56.5, 56.1; MS (DEI+) m/z (relative intensity) 403.0 (25), 168.0 (100), 139.0 (65), 125.0 (20), 44.0 (12). *ortho* adduct, **87b** (12.6 mg): ^{1}H NMR (400 MHz, $CD_3C\underset{..}{N}$) δ 7.19 (d, J = 2.4 Hz, 2H), 7.13 (d, *J* = 8.8 Hz, 2 H), 7.09 (m, 1H), 6.85 (d, J = 8.8 Hz, 2H), 6.26 (s, 2H), 5.89 (br, 1H), 3.81 (s, 3H), 3.62 (s, 6H); ^{13}C NMR (400 MHz, CD_3CN) δ 162.6, 159.4, 144.1, 141.6, 133.2, 129.6, 129.1, 128.2, 126.1, 124.8, 121.2, 119.2, 107.4, 56.3, 56.0; MS (DEI+) m/z (relative intensity) 403.6 (100), 344.6 (75), 337.5 (15), 203.4 (45), 183.4 (10), 42.2 (15), 28.1 (22).

Photoproducts of Dibromodiphenyl Nitrenium Ion, **78c**: *N* adduct, **88c** (25.1 mg): ^{1}H NMR (400 MHz, $CD_3C\underset{..}{N}$) δ 7.28 (d, *J* = 9.2 Hz, 4H), 6.83 (d, *J* = 9.2 Hz, 4H), 6.27 (s, 2H), 3.81 (s, 3H), 3.65 (s, 6H); ^{13}C NMR (400 MHz, CD_3CN) δ 162.5, 161.6, 159.4, 147.1, 132.5, 122.5, 113.5, 92.4, 56.5, 56.1; MS (DEI+) m/z (relative intensity) 493.0 (50), 168.0 (100), 139 (53), 125 (26), 44 (25). *ortho* adduct, **87c** (35.4 mg): ^{1}H NMR (400 MHz, CD_3CN) δ 7.32 (dd, *J* = 8.0, 2.4 Hz, 1H), 7.26 (d, *J* = 8.8 Hz, 2 H), 7.23 (d, *J* = 2.8 Hz, 1 H), 7.16 (d, J = 8.4 Hz, 1H), 6.81 (d, *J* = 8.8 Hz, 2 H), 6.25 (s, 2H), 5.91 (br, 1H), 3.81 (s, 3H) 3.62 (s, 6H); ^{13}C NMR (400 MHz, CD_3CN) δ 162.6, 159.4, 144.4, 141.9, 136.1, 132.5, 131.1, 129.4, 121.5, 119.7, 113.5, 112.1, 107.4, 91.9, 56.3, 55.2; MS (DEI+) m/z (relative intensity) 493.0 (100), 491.0 (80), 381 (30), 338 (15), 59 (10), 44 (20).

8.5.3 Photolysis of 77b and 77c in the Absence of Trap

Approximately 50 mg of the pyridinium salt was dissolved in 50 mL distilled CH_3CN. The reaction mixture was left on the lab bench for a week to be photolyzed using room light. After photolysis, the solution was treated in a similar manner as described above. The photoproduct obtained was the hydrazine (**92**) and collidine at 1:1 mol ratio with trace amounts of parent amine (**79**) and collidine. The hydrazine products have been characterized previously. [11-15]

Photoproducts of Dichlorodiphenyl Nitrenium Ion, **78b**: hydrazine, **92b**: ^{1}H NMR (400 MHz, CD_3CN) δ 7.23 (d, *J* = 8.8 Hz, 8H), 7.02 (d, *J* = 8.8 Hz, 8H)

Photoproducts of Dibromodiphenyl Nitrenium Ion, **78c**: hydrazine, **92c**: ^{1}H NMR (400 MHz, $CD_3C\underset{..}{N}$) δ 7.35 (d, *J* = 9.2 Hz, 8H), 7.15 (d, *J* = 9.2 Hz, 8H); ^{13}C NMR

(400 MHz, CD_3CN) δ 142.7, 133.1, 120.1, 115.4; MS (FAB+) m/z (relative intensity): 651.7 (6), 571.8 (4), 325.9 (17), 164 (100), 57 (14).

8.5.4 Photolysis of 101a and 101b with $nBuN_4Cl$

Approximately 0.1 – 0.2 mmol of hydrazine (**81**) (free base) with 1 equivalent of HBF_4 (48% wt of H_2O) was taken in 5 mL dry CH_3CN in a test tube. To this solution, 0.2033 g (0.7315 mmol) of nBu_4NCl in 3 mL CH_3CN was added. The sample was purged with N_2 for 15 min and photolyzed using medium pressure Hg lamp (200 W). The photolyzate was shaken with equal volumes of CH_2Cl_2 and aqueous $NaHCO_3$. The organic layer was withdrawn and the aqueous layer was extracted three times with CH_2Cl_2. The organic layers were combined, dried over $MgSO_4$ and filtered. The filtrate was analyzed by Shimadzu Corporation GC-17 that is equipped with 15 m, 0.25 mm I.D.0.25 mm film DB-5 column. All products were confirmed by co-injecting standard samples.

8.5.5 Photolysis of 102 with TFA-Methionine

A 3 mM solution of **102** combined with 12 mM of TFA-Methionine was prepared in 80 mL dry CH_3CN. The sample was irradiated using laser (355 nm) for 40 min. The photolyzate was shaken with equal amounts of CH_2Cl_2 and aqueous $NaHCO_3$. After withdrawing the organic layer, the aqueous layer was extracted three times with CH_2Cl_2. The organic layers were combined and dried over $MgSO_4$. The filtrate obtained upon filtration was concentrated under reduced pressure to yield a brown crude residue. The products were separated using preparative thin layer chromatography (20 x 20 cm, 1000 microns silica gel) with 80:20 hexanes and ethyl acetate as the mobile phase. Photoproducts, **108**, **109** and excess methionine along

with trace amounts of dimeric methionine were isolated and characterized. Compound **108** has been observed previously.[16,17]

Reported is the characterization of **108** (1.2 mg): ^{1}H NMR (400 MHz, CD_3CN): δ 7.56 (d, *J*=6.8 Hz, 4H), 7.54 (d, *J*=6.8 Hz, 4H), 7.38 (t, *J*=6.4 Hz, 4 H), 7.26 (t, *J*=6.4 Hz, 2H), 6.89 (d, *J*=8.8 Hz, 4H), 3.07 (s, 6H); ^{13}C-NMR (400 MHz, CD_3CN) δ 149.5, 141.7, 131.8, 129.7, 128.7, 127.1, 126.8, 113.6, 34.7; MS (EI) m/z (relative intensity):364 (40), 182 (100), 152 (29), 44 (48), 42 (25): HRMS (FAB): calcd for $C_{26}H_{24}N_2$, 364.1939; found 364.1956.

8.5.6 Photolysis of 113 in CH_3CN

Approximately 50 mg (0.268 mmol) of 4-AzQO (**113**) was dissolved in 5 mL dry CH_3CN and irradiated using Xe lamp (350 W) for 5 hours. The reddish precipitate formed was collected by decanting off the supernatant. The compound was confirmed to be **116** by ^{1}H-NMR and MS. Compound **116** was observed and characterized previously. ^{1}H NMR (400 MHz, CD_3Cl) (1.3 mg): δ 9.01 (d, *J*=8.4 Hz, 2H), 8.75 (d, *J*=8.4 Hz, 2H), 8.57 (d, *J*=6.8 Hz, 2H), 7.90 (d, *J*=6.8 Hz, 2H), 7.86 (m, 4H); MS (DEI+) m/z (relative intensity):316 (25), 300 (45), 284 (65), 254 (30), 128 (100), 75 (20), 43 (20).

8.5.7 Photolysis of 113 in CH_3CN with 10% H_2SO_4

Approximately 50 mg of 4-AzQO (**113**) was dissolved in 5 mL CH_3CN with 10% H_2SO_4. The sample was irradiated using Xe lamp (350 W) for 5 hours. The reddish precipitate that was formed was collected by decanting off the supernatant. The reddish precipitate was confirmed to be **116**. The supernatant was neutralized by shaking with aqueous $NaHCO_3$ and extracted with methanol. The methanol was

removed under reduced pressure to give an oily residue. The product was confirmed to be **119** by ^{1}H-NMR and MS. The quantity was too low to obtain percent yield. The sample was too dilute to obtain ^{13}C-NMR. ^{1}H NMR (400 MHz, DMSO): δ 8.46 (d, *J*=8.4 Hz, 1H), 8.21 (d, *J*=8.4 Hz, 1H), 8.15 (d, *J*=6.8 Hz, 1H), 7.74 (t, *J*=8.4 Hz, 1H), 7.57 (t, *J*=8.4 Hz, 1H), 6.85 (br, 2H), 6.49 (d, *J*=6.8 Hz, 1H); MS (DEI+) m/z (relative intensity):160 (40), 144 (100), 117 (20), 104 (20), 89 (10).

8.6 Additional Transient Spectra of the Photolysis of 77b and 77c in Various Conditions

Figure 8.1 Transient spectra of the photolysis of (A) 77b and (B) 77c CH_3CN (O_2 purged flow cell)

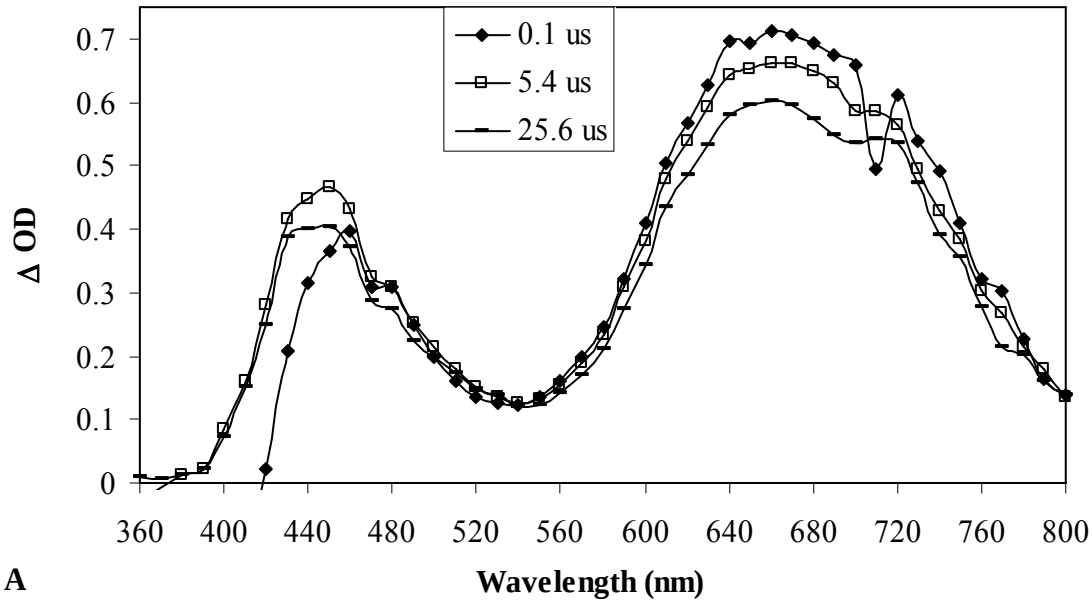

A

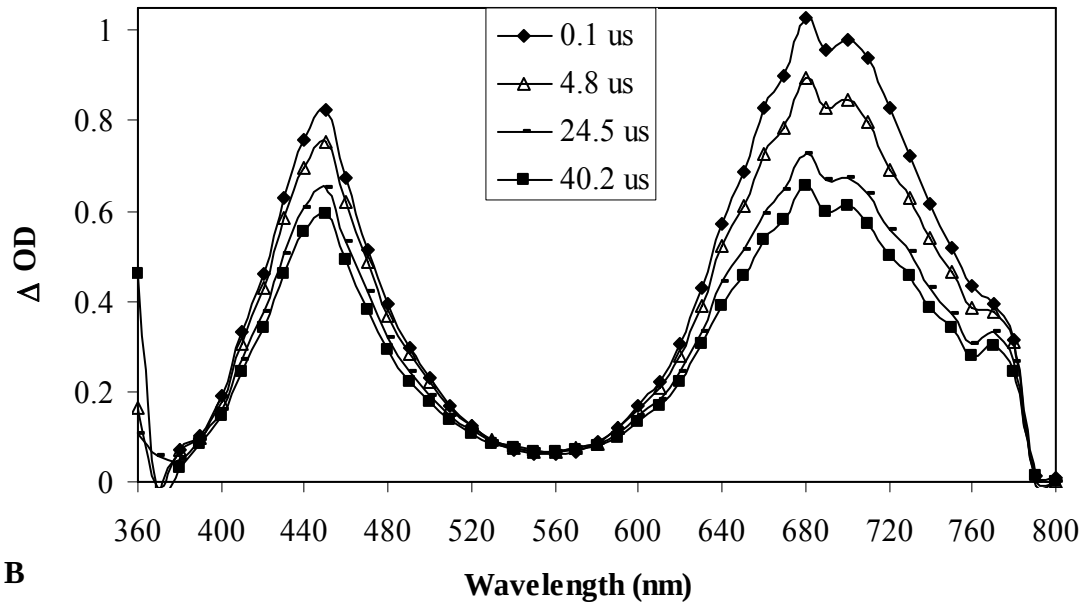

B

Figure 8.2 Transient spectra of the photolysis of (A) 77b and (B) 77c in 9:1 Buffer (25 mM, phosphate, pH 7.5) / CH_3CN

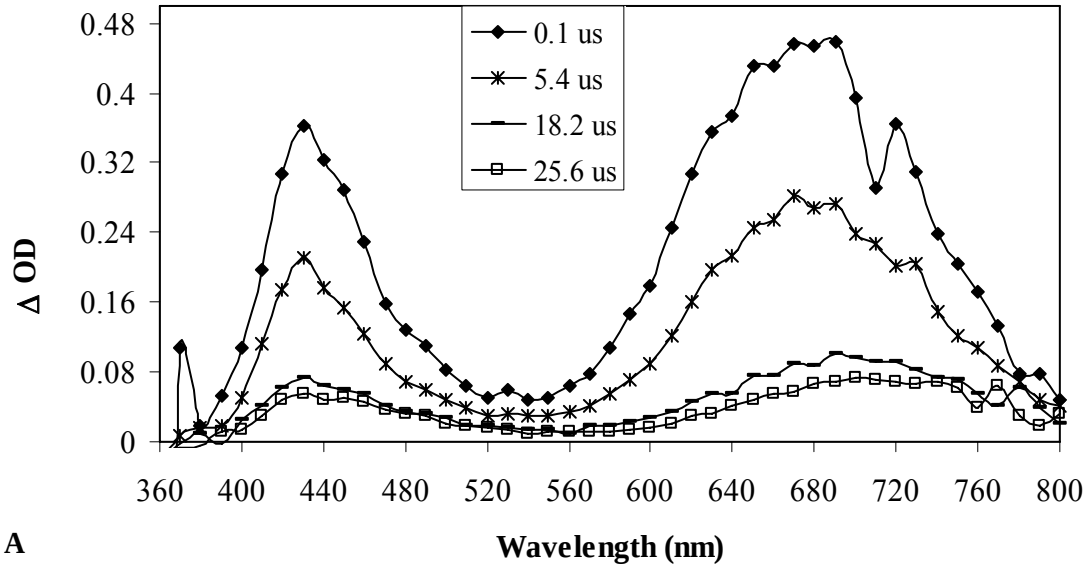

A

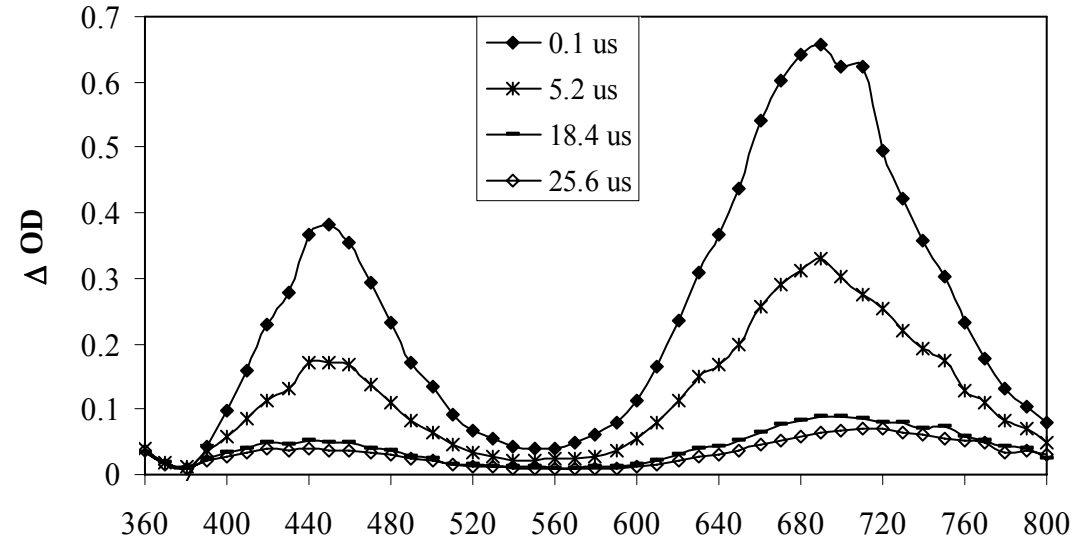

B

Figure 8.3 Transient spectra of the photolysis of 77b in CH_2Cl_2 with nBu_4NCl (~2 mM)

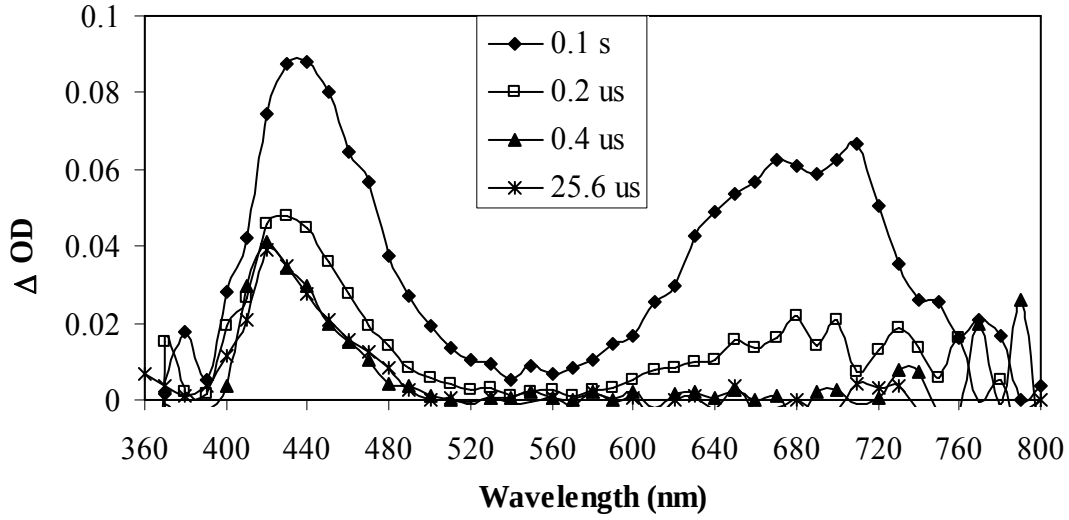

Figure 8.4 Transient spectra of the photolysis of 77b in CH_3CN with nBu_4NCl (~2 mM) in O_2 purged flow cell.

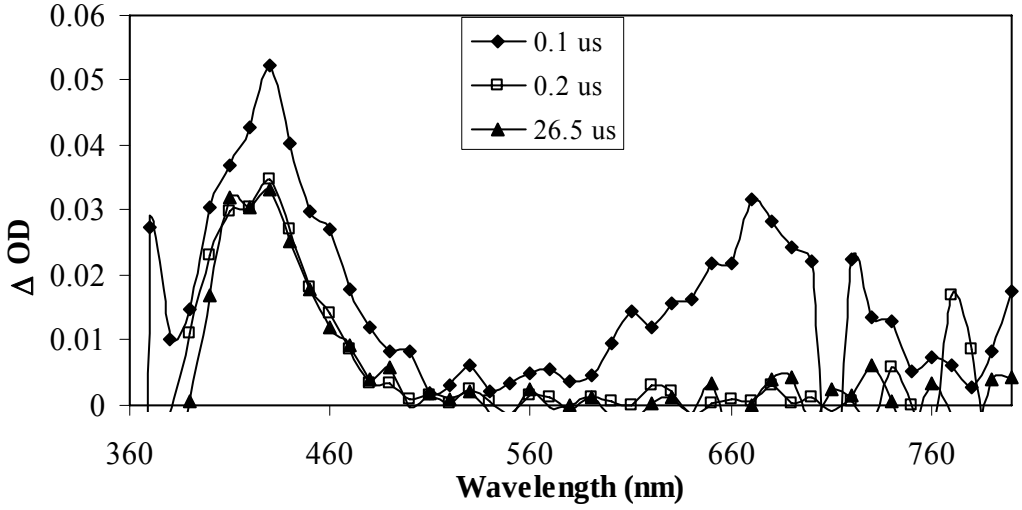

Figure 8.5 Transient spectra of the photolysis of 77b in CH_3CN with nBu_4NCl (~2 mM) at longer time scale

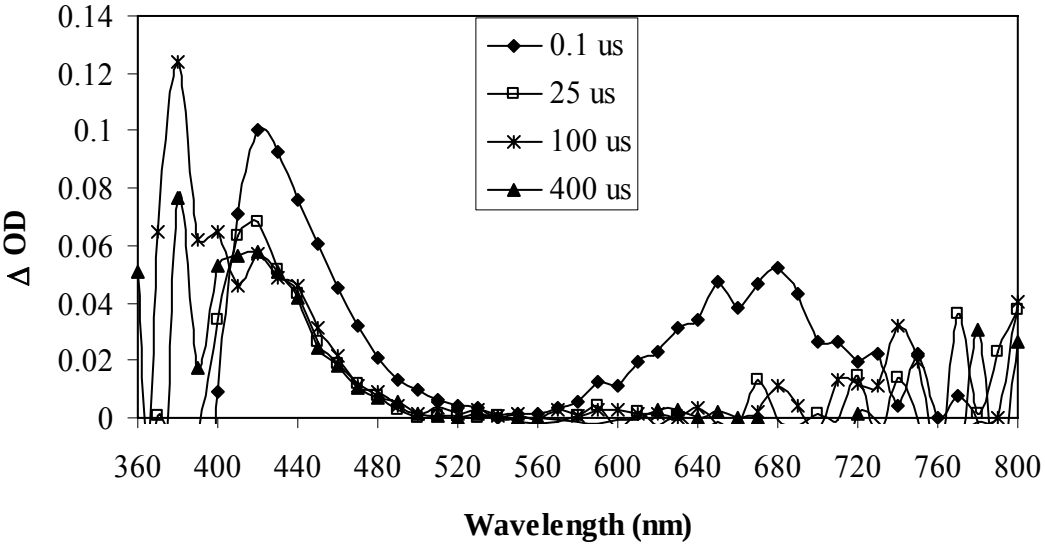

Figure 8.6 Transient spectra of the photolysis of 77b in CH_3CN with nBu_4NCl (~2 mM) and 1.23 mM pyridine

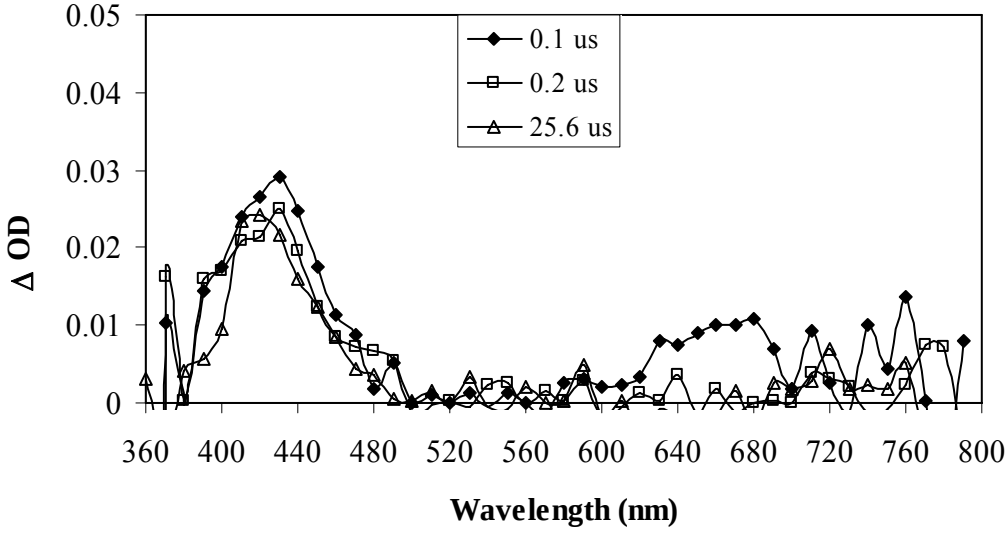

8.7 Steady State UV Spectra of the photolysis of 77b and 77c in various conditions

Figure 8.7 UV spectra of the photolysis of (A) 77b and (B) 77c in CH_2Cl_2 with no acid

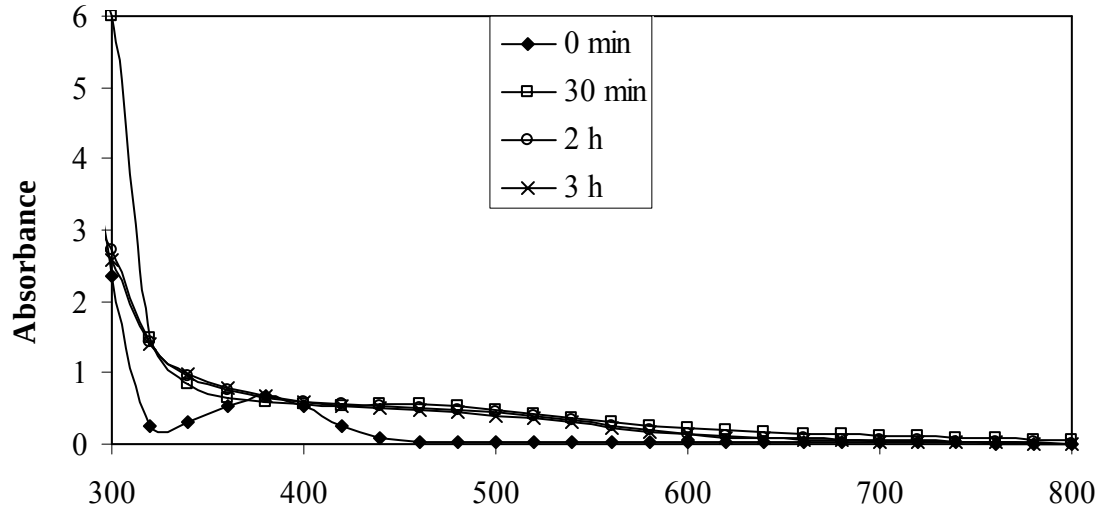

A

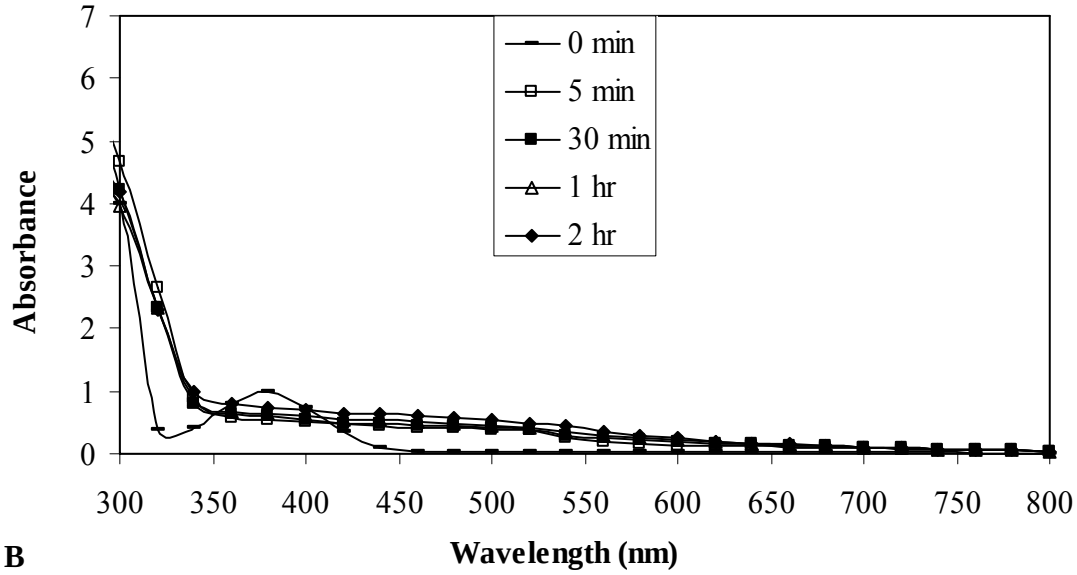

B

Figure 8.8 UV spectra of the photolysis of (A) 77b and (B) 77c in chlorobenzene with TFA

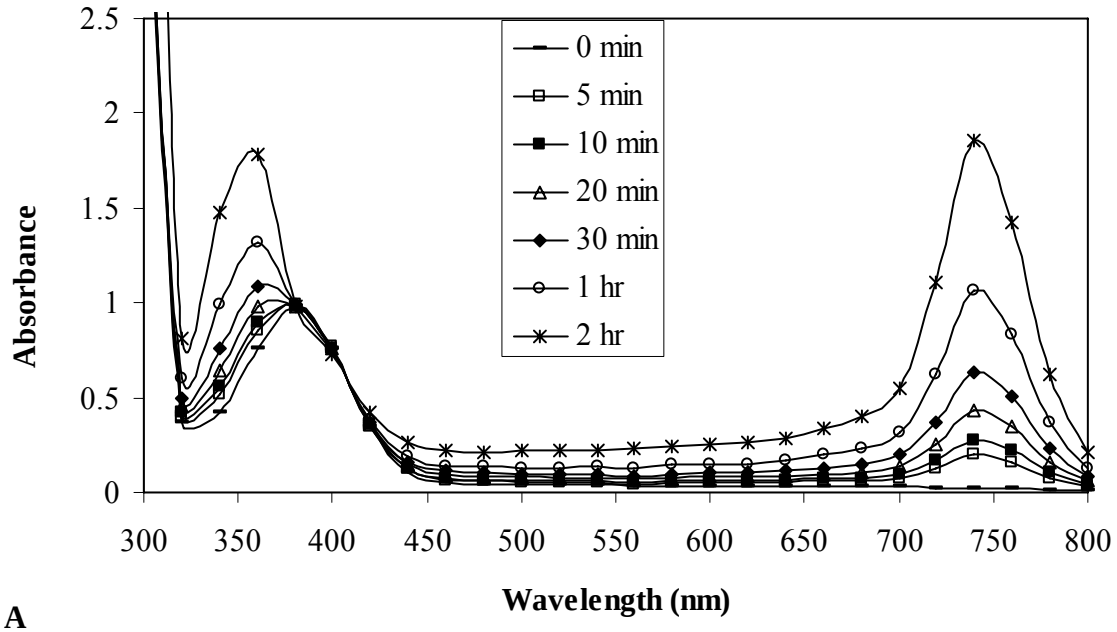

A

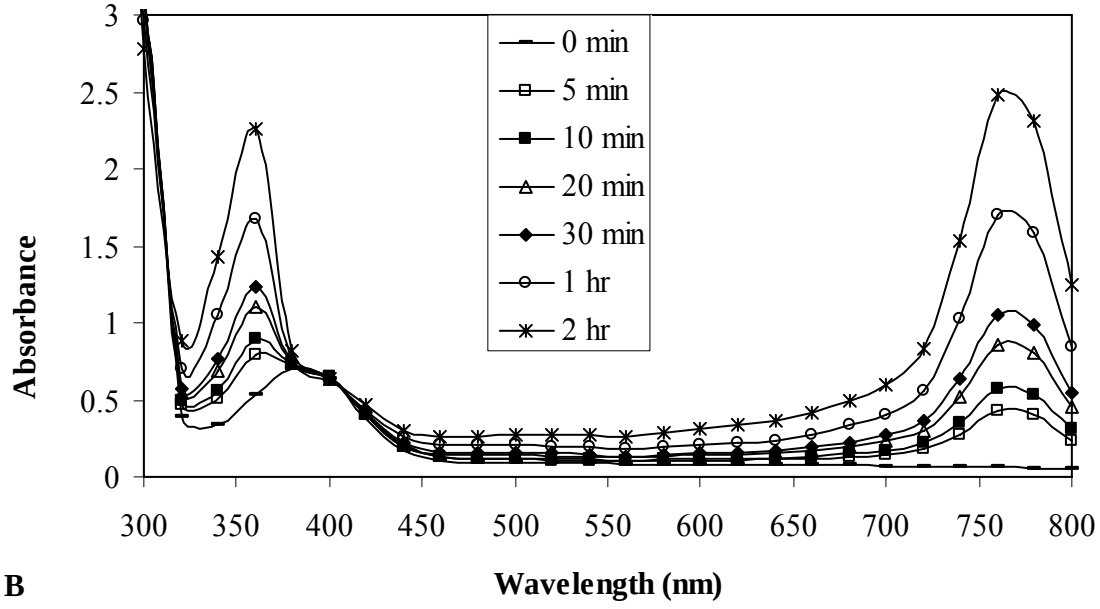

B

Figure 8.9 UV spectra of the photolysis of (A) 77b and (B) 77c in nitrobenzene with TFA

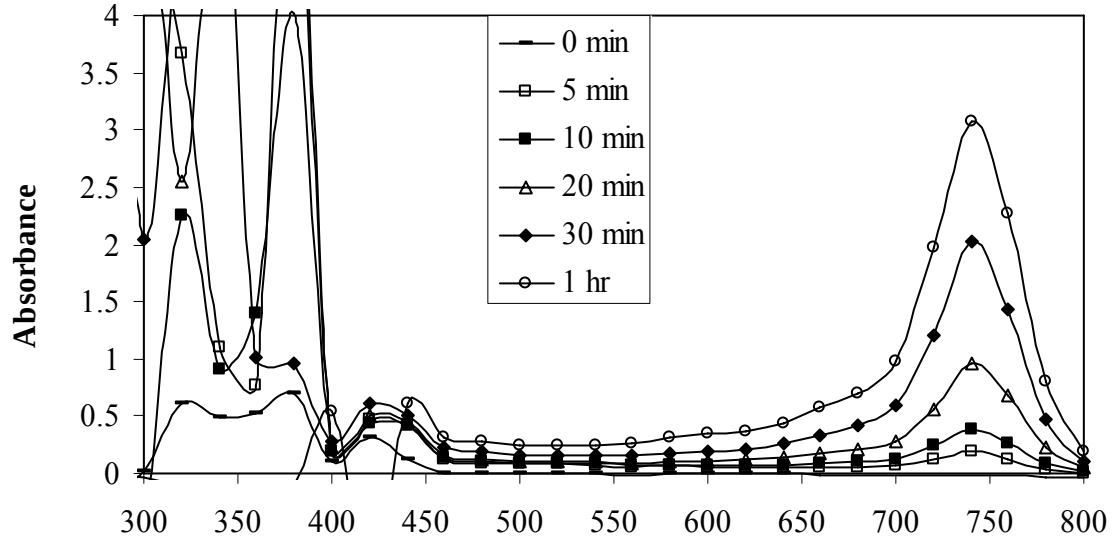

A

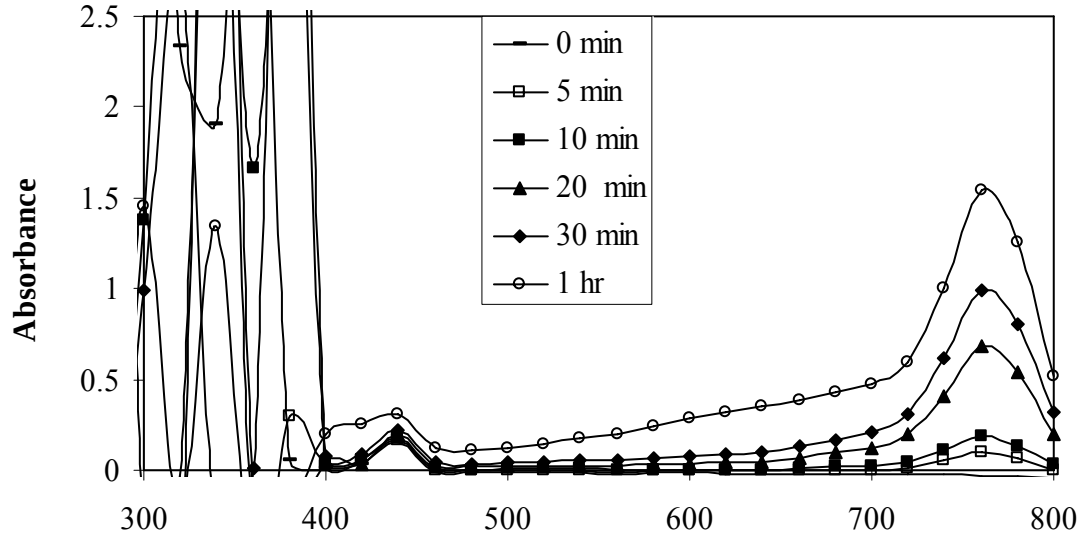

B

Figure 8.10 UV spectra of (A) 81b and (B) 81c with and without HBF_4 in CH_3CN

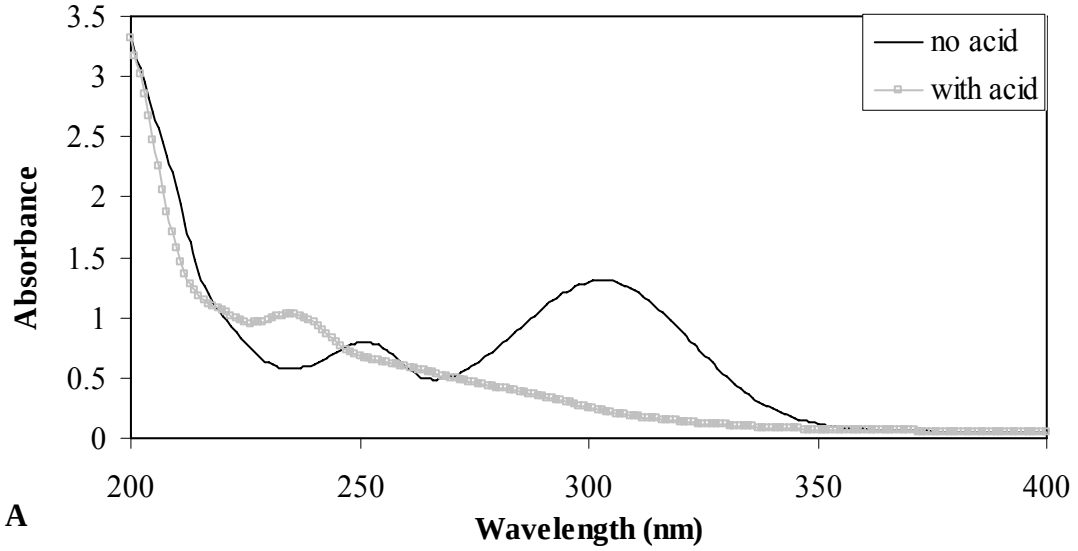

A

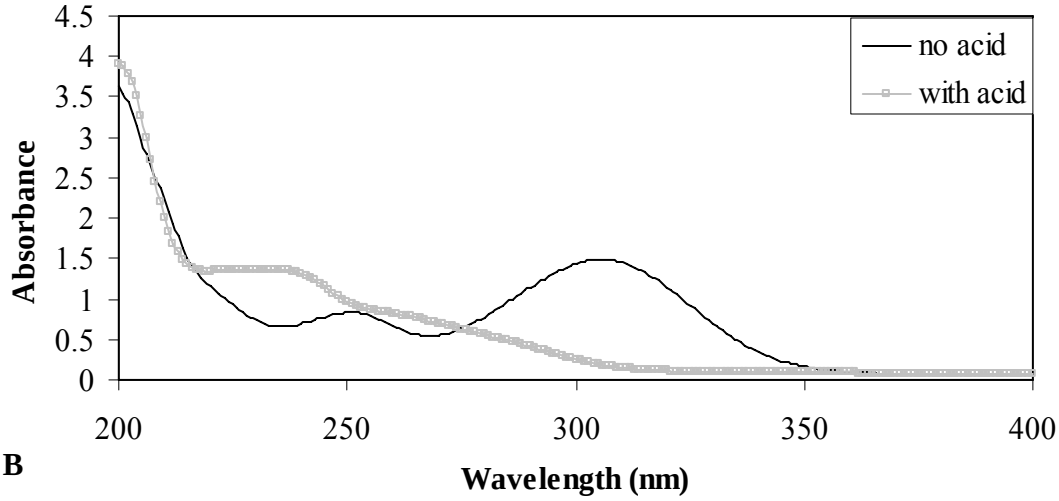

B

References

(1) Becke, A. D. *Phys. Rev. A.* **1988**, *38*, 3098-3100.

(2) Becke, A. D. *J. Chem. Phys.* **1993**, *98*, 5648-5652.

(3) Lee, C.; Yang, W.; Parr, R. G. *Phys. Rev. B* **1988**, *37*, 785-789.

(4) Stevens, P. J.; Devlin, F. J.; Chabalowski, C. F.; Frisch, M. J. *J. Phys. Chem.* **1994**, *98*, 11632-11627.

(5) Freeman, H. S.; Butler, J. R.; Freedman, L. D. *J. Org. Chem.* **1978**, *443*, 4975-4978.

(6) Itai, T.; Kamiya, S. *Chem. Pharm. Bull.* **1961**, *9*, 87-91.

(7) Ochiai, E. *J. Org. Chem.* **1953**, *18*, 534-551.

(8) Smith, K.; James, M. D.; Bye, M. R.; Faulkner, J. D. *Tetrahedron.* **1992**, *48*, 7479-7488.

(9) Chmielewski, M. J.; Charon, M.; Jurczak, J. *Org. Lett.* **2004**, *6*, 3501-3504.

(10) Rosa, M. D.; Quesada, P. A.; Dodsworth, D. J. *J. Org. Chem.* **1987**, *52*, 173-175.

(11) Neugebauer, F. A.; Fischer, H. *Chem. Ber.* **1971**, *104*, 886-889.

(12) Neugebauer, F. A.; Fischer, P. H. H. *Chem. Ber.* **1965**, *98*, 844-850.

(13) Abakumov, G. A.; Razuvaev, G. A. *Seriya Khimicheskaya* **1966**, *10*, 1744-1747.

(14) Cauquis, G.; Delhomme, H.; Serve, D. *Tetrahedron Lett.* **1971**, 4649-4652.

(15) Cauquis, G.; Delhomme, H.; Serve, D. *Electrochim. Acta* **1975**, *20*, 1019-1026.

(16) Cheng, J.-D.; Shine, H. J. *J. Org. Chem.* **1974**, *39*, 2835-2790.

(17) Cheng, J.-D.; Shine, H. J. *J. Org. Chem.* **1975**, *40*, 703-710.

References

Chapter 1

(1) McClelland, R. A. *Tetrahedron* **1996**, *52*, 6823 - 6858.

Chapter 2

(1) Bamberger, E.; Lagutt, J. *Chem. Ber.* **1898**, *31*, 1500.

(2) Heller, H. E.; Hughes, E. D.; Ingold, C. K. *Nature* **1951**, *168*, 909-910.

(3) Abramovitch, R. A.; Davis, B. A. *Chem. Rev.* **1964**, *64*, 149-185.

(4) Stieglitz, J. L., P.N. *J. Am. Chem. Soc.* **1914**, *36*, 272-301.

(5) Gassman, P. G. *Acc. Chem. Res.* **1970**, *3*, 26-33.

(6) Gassman, P. G.; Campbell, G. A. *J. Am. Chem. Soc.* **1972**, *94*, 3891 - 3896.

(7) Gassman, P. G.; Cryberg, R. L. *J. Am. Chem. Soc.* **1969**, *91*, 5176-5177.

(8) Hoffman, R. V.; Christopher, N. B. *J. Org. Chem.* **1988**, *53*, 4769-4773.

(9) Hoffman, R. V.; Kumar, A.; Buntain, G. A. *J. Am. Chem. Soc.* **1985**, *107*, 4731-4736.

(10) Claus, P.; Doppler, T.; Gakis, N.; Georgarakis, M.; Giezendanner, H.; Gilgen, P.; Heimgartner, H.; Jackson, B.; Marky, M.; Narasimhan, N. S.; Rosenkranz, H. J.; Wunderli, A.; Hansen, H. J.; Schmid, H. *Pure Appl. Chem.* **1973**, *33*, 339-361.

(11) Haley, N. F. *J. Org. Chem.* **1977**, *42*, 3929-3933.

(12) Georgarakis, E.; Schmid, H.; Hensen, H.-J. *Helv. Chim. Acta.* **1979**, *62*, 234-269.

(13) Giovanni, E.; deSousa, B. F. S. E. *Helv. Chim. Acta.* **1979**, *62*, 185-197.

(14) Giovanni, E.; deSousa, B. F. S. E. *Helv. Chim. Acta.* **1979**, *62*, 198-204.

(15) Doppler, T.; Schmid, H.; Hensen, H.-J. *Helv. Chim. Acta.* **1979**, *62*, 271-303.

(16) Doppler, T.; Schmid, H.; Hensen, H.-J. *Helv. Chim. Acta.* **1979**, *62*, 304-313.

(17) Abramovitch, R. A. J., R. *Azides and Nitrenes*: *Reactivity and Utility;* Academic: New York, 1984.

(18) Takeuchi, H. H., S; Tanahashi, T; Kobayashi,A; Adachi, T; Higuchi, D. *J. Chem. Soc., Perkin. Trans. 2* **1991**, 847-855.

(19) McClelland, R. A. *Tetrahedron* **1996**, *52*, 6823 - 6858.

(20) McClelland, R. A.; Davidse, P. A.; Hadzialic, G. *J. Am. Chem. Soc.* **1995**, *117*, 4173-4174.

(21) McClelland, R. A.; Gadosy, T. A.; Ren, D. *Can. J. Chem.* **1998**, *76*, 1327-1337.

(22) Ramlall, P.; Li, Y.; McClelland, R. A. *J. Chem. Soc., Perkin Trans. 2* **1999**, 1601-1607.

(23) McClelland, R. A.; Kahley, M. J.; Davidse, P. A.; Hadzialic, G. *J. Am. Chem. Soc.* **1996**, *118*, 4794-4803.

(24) Fishbein, J. C.; McClelland, R. A. *Can. J. Chem.* **1996**, *74*, 1321-1328.

(25) Fishbein, J. C.; McClelland, R. A. *J. Am. Chem. Soc.* **1987**, *109*, 2824-2825.

(26) Davidse, P. A.; Kahley, M. J.; McClelland, R. A.; Novak, M. *J. Am. Chem. Soc.* **1994**, *116*, 4513-4514.

(27) McClelland, R. A.; Kahley, M. J.; Davidse, P. A. *J. Phys. Org. Chem.* **1996**, *9*, 355-360.

(28) Novak, M.; Kahley, M. J.; Eigen, E.; Helmick, J. S.; Peters, H. E. *J. Am. Chem. Soc.* **1993**, *115*, 9453-9460.

(29) Anderson, G. B.; Yang, L. L.-N.; Falvey, D. E. *J. Am. Chem. Soc.* **1993**, *115*, 7254-7262.

(30) Baetzold, R. C.; Tong, L. K. J. *J. Am. Chem. Soc* **1971**, *93*, 1347.

(31) Falvey, D. E. *Organic, Physical, and Materials Photochemistry*; Ramamurthy, V. S., K.S;, Ed.; Marcel Dekker: New York, 2000; Vol. 6, pp 249-284.

(32) Falvey, D. E. *Reactive Intermediate Chemistry*; Moss, R. A., Platz, M. S., Maitland Jones, J., Eds.; Wiley-Interscience: Hoboken, 2004; Vol. 1, pp 593 - 650.

(33) Falvey, D. E. *J. Phys. Org. Chem.* **1999**, *12*, 589 - 596.

(34) Falvey, D. E.; Cramer, C. J. *Tetrahedron Lett.* **1992**, *33*, 1705-1708.

(35) Chiapperino, D.; Anderson, G. B.; Robbins, R. J.; Falvey, D. E. *J. Org. Chem.* **1996**, *61*, 3195-3199.

(36) Sullivan, M. B.; Brown, K.; Cramer, C. J.; Truhlar, D. G. *J. Am. Chem. Soc.* **1998**, *120*, 11778-11783.

(37) Srivastava, S.; Ruane, P. H.; Toscano, J. P.; Sullivan, M. B.; Cramer, C. J.; Chiapperino, D.; Reed, E. C.; Falvey, D. E. *J. Am. Chem. Soc.* **2000**, *122*, 8271-8278.

(38) Srivastava, S.; Toscano, J. P. *J. Am. Chem. Soc.* **1997**, *119*, 11552-11553.

(39) Srivastava, S.; Falvey, D. E. *J. Am. Chem. Soc.* **1995**, *117*, 10186 - 10193.

(40) Gonzalez, C.; Restrepo-Cossio, A.; Marquez, M.; Wilberg, K.; Rosa, M. D. *J. Phys. Chem. A.* **1998**, *102*, 2732-2738.

(41) Cramer, C. J.; Falvey, D. *Tetrahedron Lett.* **1997**, *38*, 1515-1518.

(42) Srivastava, S.; Kercher, M.; Falvey, D. E. *J. Org. Chem.* **1999**, *64*, 5853-5857.

(43) Robbins, R. J.; Yang, L. L.-N.; Anderson, G. B.; Falvey, D. E. *J. Am. Chem. Soc.* **1995**, *117*, 6544 - 6552.

(44) Chiapperino, D.; Falvey, D. E. *J. Phys. Org. Chem.* **1997**, *10*, 917-924.

(45) Robbins, R. J.; Yang, L. L.-N.; Anderson, G. B.; Falvey, D. E. *J. Am. Chem. Soc* **1995**, *117*, 6544-6552.

(46) Chiapperino, D.; McIlroy, S.; Falvey, D. E. *J. Am. Chem. Soc.* **2002**, *124*, 3567-3577.

(47) Kung, A. C.; McIlroy, S.; Falvey, D. E. *J. Org. Chem.* **2005**, *70*, 5283-5290.

(48) Kriek, E. *Biochim. Biophys. Acta* **1974**, *355*, 177-203.

(49) Miller, E. C.; Miller, J. A. *Pharmacol. Rev.* **1966**, *18*, 805-838.

(50) Miller, E. C.; Lotlikar, P. D.; Miller, J. A.; Butler, B. W.; Irving, C. C.; Hill, J. T. *Mol. Pharmacol.* **1968**, *4*, 147-154.

(51) Miller, J. A.; Miller, E. C. *Physico-Chemical Mechanisms of Carcinogenesis, Jerusalem Symposia on Quantum Chemistry and Biochemistry. The Israel Academy of Sciences and Humanities,*; Bergmann, E. D., Pullman, B., Eds.: Jerusalem, 1969; Vol. 1, pp 237-261.

(52) Poirier, L. A. M., J. A.; Miller, E.C.; Sato, K *Cancer Res.* **1967**, *27*, 1600-1613.

(53) Cramer, J. W.; Miller, J. A.; Miller, E. C. *J. Biol. Chem.* **1960**, *235*, 885-888.

(54) Novak, M.; Kennedy, S. A. *J. Phys. Org. Chem.* **1998**, *11*, 71-76.

(55) Novak, M.; Kennedy, S. A. *J. Am. Chem. Soc.* **1995**, *117*, 574-575.

(56) McClelland, R. A.; Ren, D.; Ghobrial, D.; Gadosy, T. A. *J. Chem. Soc., Perkin Trans. 2* **1997**, 451-.

(57) Humphreys, G. W.; Kadlubar, F. F.; Guengerich, F. P. *Proc. Natl. Acad. Sci. USA.* **1992**, *89*, 8278-8282.

(58) Kennedy, S. A.; Novak, M.; Kolb, B. A. *J. Am. Chem. Soc.* **1997**, *119*, 7654-7664.

(59) McClelland, R. A.; Ahmad, A.; Dicks, A. P.; Licence, V. E. *J. Am. Chem. Soc.* **1999**, *121*, 3303-3310.

Chapter 3

(1) Srivastava, S.; Toscano, J. P. *J. Am. Chem. Soc.* **1997**, *119*, 11552-11553.

(2) Srivastava, S.; Ruane, P. H.; Toscano, J. P.; Sullivan, M. B.; Cramer, C. J.; Chiapperino, D.; Reed, E. C.; Falvey, D. E. *J. Am. Chem. Soc.* **2000**, *122*, 8271-8278.

(3) Abramovitch, R. A.; Evertz, K.; Huttner, G.; Gibson, H. H., Jr.; Weems, H. G. *J. Chem. Soc. Chem. Commun.* **1988**, *4*, 325-327.

(4) Freeman, H. S.; Butler, J. R.; Freedman, L. D. *J. Org. Chem.* **1978**, *443*, 4975-4978.

(5) Moran, R. J. Ph. D Dissertation, University of Maryland, College Park, MD, 1997.

(6) Moran, R. J.; Falvey, D. E. *J. Am. Chem. Soc.* **1996**, *118*, 8965-8966.

(7) Falvey, D. E. In *Organic, Physical, and Materials Photochemistry*; Ramamurthy, V. S., K.S;, Ed.; Marcel Dekker, Inc: New York, 2000; Vol. 6, pp 249-284.

(8) Cramer, C. J.; Falvey, D. *Tet. Lett.* **1997**, *38*, 1515-1518.

(9) Winter, A. H.; Thomas, S. I.; Kung, A. C.; Falvey, D. E. *Org. Lett.* **2004**, *6*, 4671-4674.

(10) McIlroy, S.; Moran, R. J.; Falvey, D. E. *J. Phys. Chem.* **2000**, *104*, 11154-11158.

(11) Chiapperino, D.; Falvey, D. E. *J. Phys. Org. Chem.* **1997**, *10*, 917-924.

(12) Kung, A. C.; McIlroy, S.; Falvey, D. E. *J. Org. Chem.* **2005**, *70*, 5283-5290.

(13) Chiapperino, D.; McIlroy, S.; Falvey, D. E. *J. Am. Chem. Soc.* **2002**, *124*, 3567-3577.

(14) Shida, T. *Electronic Absorption Spectra of Radical Ions*; Elsevier: Netherlands, 1988; Vol. 34.

(15) Wagner, B. D.; Ruel, G.; Lusztyk, J. *J. Am. Chem. Soc.* **1996**, *118*, 13-19.

(16) Jonsson, M.; Wayner, D. D.; Lusztyk, J. *J. Phys. Chem.* **1996**, *100*, 17539-17543.

(17) Murov, S. L.; Charmichael, I.; Hug, G. L. *Handbook of Photochemistry*; 2 ed.; Marcel Dekker: New York, 1993.

(18) Zweig, A.; Hodgson, W. G.; Jura, W. H. *J. Am. Chem. Soc.* **1964**, *86*, 4124-4129.

(19) Rathore, R.; Kochi, J. K. *Adv. Phys. Org. Chem.* **2000**, *35*, 193-318.

(20) Sankararaman, S.; Haney, W. A.; Kochi, J. K. *J. Am. Chem. Soc.* **1987**, *109*, 7824-7838.

(21) McIlroy, S. Ph. D Dissertation, University of Maryland, College Park, MD, 2002.

(22) McIlroy, S.; Falvey, D. E. *J. Am. Chem. Soc.* **2001**, *123*, 11329-11330.

(23) Mathivanan, N.; Cozens, F.; McClelland, R. A.; Steenken, S. *J. Am. Chem. Soc.* **1992**, *114*, 2198-2203.

(24) Steenken, S.; McClelland, R. A. *J. Am. Chem. Soc.* **1990**, *112*, 9648-9649.

(25) Luo, Y.-R. *Handbook of Bond Dissociation Energies in Organic Compounds*; CRC Press: Washington, D. C, 2003.

(26) Alabugin, I. V.; Kovalenko, S. V. *J. Am. Chem. Soc.* **2002**, *124*, 9052-9053.

(27) Shono, T.; Ikeda, A.; Hayashi, J.; Hakozaki, S. *J. Am. Chem. Soc.* **1975**, *97*, 4261-4264.

(28) Grubert, L.; Jacobi, D.; Abraham, W. *J. Prakt. Chem.* **1999**, *341*, 620-630.

(29) Bordwell, F. G.; Cheng, J.-P. *J. Am. Chem. Soc.* **1991**, *113*, 1736-1743.

(30) Rosokha, Y. S.; Lindeman, S. V.; Rosokha, S. V.; Kochi, J. K. *Angew. Chem. Int. Ed. Engl.* **2004**, *43*, 4650-4652.

(31) Lenoir, D. *Angew. Chem. Int. Ed. Engl.* **2003**, *42*, 854-857.

(32) Quinonero, D.; Garau, C.; Rotger, C.; Frontera, A.; Ballester, P.; Costa, A.; Deya, P. M. *Angew. Chem. Int. Ed. Engl.* **2002**, *21*, 3389-3392.

(33) Mascal, M.; Armstrong, A.; Bartberger, M. D. *J. Am. Chem. Soc.* **2002**, *124*, 6274-6276.

(34) Gonzalez, C.; Restrepo-Cossio, A.; Marquez, M.; Wilberg, K.; Rosa, M. D. *J. Phys. Chem. A* **1998**, *102*, 2732-2738.

(35) Michalak, J.; Zhai, H. B.; Platz, M. S. *J. Phys. Chem.* **1996**, *100*, 14028-14036.

Chapter 4

(1) Novak, M.; Rajagopal, S. *Adv. Phys. Org. Chem.* **2001**, *36*, 167-254.

(2) Falvey, D. E. In *Reactive Intermediate Chemistry*; Moss, R. A., Platz, M. S., Maitland Jones, J., Eds.; Wiley-Interscience: Hoboken, 2004; Vol. 1, pp 593 - 650.

(3) Anderson, G. B.; Yang, L. L.-N.; Falvey, D. E. *J. Am. Chem. Soc.* **1993**, *115*, 7254-7262.

(4) McClelland, R. A.; Kahley, M. J.; Davidse, P. A.; Hadzialic, G. *J. Am. Chem. Soc.* **1996**, *118*, 4794-4803.

(5) Srivastava, S.; Toscano, J. P. *J. Am. Chem. Soc.* **1997**, *119*, 11552-11553.

(6) Abramovitch, R. A.; Shi, Q. *Heterocycles.* **1994**, *37*, 1463-1466.

(7) Chiapperino, D.; Anderson, G. B.; Robbins, R. J.; Falvey, D. E. *J. Org. Chem.* **1996**, *61*, 3195-3199.

(8) Falvey, D. E. In *Organic, Physical, and Materials Photochemistry*; Ramamurthy, V. S., K.S;, Ed.; Marcel Dekker, Inc: New York, 2000; Vol. 6, pp 249-284.

Chapter 5

(1) Kriek, E. *Biochim. Biophys. Acta* **1974**, *355*, 177-203.

(2) Talaska, G.; Dooley, K. L.; Kadlubar, F. F. *Carcinogenesis* **1990**, *11*, 639-646.

(3) Talaska, G.; Aljuburi, A. Z. S. S.; Kadlubar, F. F. *Proc. Natl. Acad. Sci. USA.* **1991**, *88*, 5350-5354.

(4) McClelland, R. A.; Gadosy, T. A.; Ren, D. *Can. J. Chem.* **1998**, *76*, 1327-1337.

(5) Srivastava, S.; Ruane, P. H.; Toscano, J. P.; Sullivan, M. B.; Cramer, C. J.; Chiapperino, D.; Reed, E. C.; Falvey, D. E. *J. Am. Chem. Soc.* **2000**, *122*, 8271-8278.

(6) Chiapperino, D. Ph.D Dissertation, University of Maryland, College Park, MD, 2000.

(7) Chiapperino, D.; McIlroy, S.; Falvey, D. E. *J. Am. Chem. Soc.* **2002**, *124*, 3567-3577.

(8) Kennedy, S. A.; Novak, M.; Kolb, B. A. *J. Am. Chem. Soc.* **1997**, *119*, 7654-7664.

(9) Novak, M.; Kennedy, S. A. *J. Phys. Org. Chem.* **1998**, *11*, 71-76.

(10) Miller, E. C.; Miller, J. A. *Pharmacol. Rev.* **1966**, *18*, 805-838.

(11) Miller, E. C.; Lotlikar, P. D.; Miller, J. A.; Butler, B. W.; Irving, C. C.; Hill, J. T. *Mol. Pharmacol.* **1968**, *4*, 147-154.

(12) Cramer, J. W.; Miller, J. A.; Miller, E. C. *J. Biol. Chem.* **1960**, *235*, 885-888.

(13) Scribner, J. D.; Miller, J. A.; Miller, E. C. *Biochem. Biophys. Res. Commun.* **1965**, *20*, 560-565.

(14) Poirier, L. A. M., J. A.; Miller, E.C.; Sato, K *Cancer Res.* **1967**, *27*, 1600-1613.

(15) Miller, E. C.; Miller, J. A. *Cancer* **1981**, *47*, 2327-2345.

(16) Miller, J. A. *Cancer Res.* **1970**, *30*, 559-576.

(17) Miller, J. A.; Miller, E. C. In *Physico-Chemical Mechanisms of Carcinogenesis, Jerusalem Symposia on Quantum Chemistry and Biochemistry. The Israel Academy of Sciences and Humanities,*; Bergmann, E. D., Pullman, B., Eds.: Jerusalem, 1969; Vol. 1, pp 237-261.

(18) Falvey, D. E. In *Organic, Physical, and Materials Photochemistry*; Ramamurthy, V. S., K.S;, Ed.; Marcel Dekker, Inc: New York, 2000; Vol. 6, pp 249-284.

(19) McClelland, R. A.; Kahley, M. J.; Davidse, P. A. *J. Phys. Org. Chem.* **1996**, *9*, 355-360.

(20) Novak, M.; Kennedy, S. A. *J. Am. Chem. Soc.* **1995**, *117*, 574-575.

(21) Novak, M.; Li, Y. *J. Am. Chem. Soc.* **1996**, *118*, 1302-1308.

(22) Kung, A. C.; Chiapperino, D.; Falvey, D. E. *Photochem. Photobiol. Sci.* **2003**, *2*, 1205-1208.

(23) Arcos, J. C.; Argus, M. F. *Adv. Cancer Res.* **1968**, *11*, 305-471.

(24) Davis, F. A.; Wetzel, R. B.; Devon, T. H.; Stackhouse, J. F. *J. Org. Chem.* **1971**, *36*, 799-803.

(25) Davis, F. A.; Fretz, E. R.; Horner, C. J. *J. Org. Chem.* **1973**, *38*, 690-699.

(26) McPherson, A. *Crystallization of Biological Macromolecules*; Cold Spring Harbor: New York, 1999.

(27) Brown, J. R. *Fed. Proc. Fed. Am. Soc. Exp. Biol.* **1975**, *34*, Abstract 2105.

(28) Raines, R. T. *Chem. Rev.* **1998**, *98*, 1045-1065.

(29) Smyth, D. G.; Stein, W. H.; Moore, S. *J. Biol. Chem.* **1963**, *238*, 227-234.

(30) Canfield, R. E. *J. Biol. Chem.* **1963**, *238*, 2698-2707.

(31) Ryle, A. P.; Sanger, F.; Smith, L. F.; Katai, R. *Biochem. J.* **1955**, *60*, 541.

(32) Hartley, B. S. *Nature* **1964**, *201*, 1284-1287.

Chapter 6

(1) Miller, J. A.; Miller, E. C. In *Physico-Chemical Mechanisms of Carcinogenesis, Jerusalem Symposia on Quantum Chemistry and Biochemistry. The Israel Academy of Sciences and Humanities,*; Bergmann, E. D., Pullman, B., Eds.: Jerusalem, 1969; Vol. 1, pp 237-261.

(2) Arcos, J. C.; Argus, M. F. *Adv. Cancer Res.* **1968**, *11*, 305-471.

(3) Endo, H. In *Chemistry and Biological Actions of 4-Nitroquinoline 1-Oxide*; Endo, H., Ono, T., Sugimura, T., Eds.; Springer-Verlag: Berlin, 1971, pp 32-52.

(4) Malkin, M. F.; Zahalsky, A. C. *Science* **1966**, *154*, 1665-1667.

(5) Kawazoe, Y.; Araki, M.; Nakahara, W. *Chem. Pharm. Bull.* **1969**, *17*, 544-549.

(6) Sugimutra, T.; Otake, H.; Matsushima, T. *Nature* **1968**, *218*, 392.

(7) Kohda, K.; Tada, M.; Kasai, H.; Nishimura, S.; Kawazoe, Y. *Biochem. Biophys. Res. Commun.* **1986**, *139*, 626 - 632.

(8) Bailleul, B.; Galiegue, S.; Loucheux-Lefebvre, M. H. *Cancer Res.* **1981**, *41*, 4559-4565.

(9) Kawazoe, Y.; Araki, M.; Huang, G. F.; Okamoto, T.; Tada, M.; Tada, M. *Chem. Pharm. Bull.* **1975**, *23*.

(10) Okano, T.; Takenaka, S.; Sato, Y. *Chem. Pharm. Bull.* **1968**, *16*, 556.

(11) Demeunynck, M.; Lhomme, M.-F.; Mellor, J. M.; Lhomme, J. *J. Org. Chem.* **1989**, *54*, 399-405.

(12) Demeunynck, M.; Lhomme, M.-F.; Lhomme, J. *J. Org. Chem.* **1988**, *48*, 1171-1175.

(13) McClelland, R. A.; Kahley, M. J.; Davidse, P. A.; Hadzialic, G. *J. Am. Chem. Soc.* **1996**, *118*, 4794-4803.

(14) McClelland, R. A.; Davidse, P. A.; Hadzialic, G. *J. Am. Chem. Soc.* **1995**, *117*, 4173-4174.

(15) Kamiya, S.; Sueyoshi, S.; Miyahara, M.; Yanagimachi, K.; Nakashima, T. *Chem. Pharm. Bull.* **1980**, *28*, 1485-1490.

(16) Andreev, V. P.; Ryzhakov, A. V. *Chemistry of Heterocyclic Compounds* **1993**, *29*, 1435-1440.

(17) Ramlall, P.; Li, Y.; McClelland, R. A. *J. Chem. Soc., Perkin Trans. 2* **1999**, 1601-1607.

(18) Shida, T. *Electronic Absorption Spectra of Radical Ions*; Elsevier: Netherlands, 1988; Vol. 34.

(19) Chiapperino, D.; Falvey, D. E. *J. Phys. Org. Chem.* **1997**, *10*, 917-924.

(20) Shukla, R.; Mani, R. P. *Asian J. Chem.* **1999**, *11*, 584-590.

(21) Perrin, D. D.; Dempsey, B.; Serjeant, E. P. *pKa Prediction for Organic Acids and Bases*; Chapman and Hall: New York, 1981.

(22) Itai, T.; Kamiya, S. *Chem. Pharm. Bull.* **1961**, *9*, 87-91.

Chapter 8

(1) Becke, A. D. *Phys. Rev. A.* **1988**, *38*, 3098-3100.

(2) Becke, A. D. *J. Chem. Phys.* **1993**, *98*, 5648-5652.

(3) Lee, C.; Yang, W.; Parr, R. G. *Phys. Rev. B* **1988**, *37*, 785-789.

(4) Stevens, P. J.; Devlin, F. J.; Chabalowski, C. F.; Frisch, M. J. *J. Phys. Chem.* **1994**, *98*, 11632-11627.

(5) Freeman, H. S.; Butler, J. R.; Freedman, L. D. *J. Org. Chem.* **1978**, *443*, 4975-4978.

(6) Itai, T.; Kamiya, S. *Chem. Pharm. Bull.* **1961**, *9*, 87-91.

(7) Ochiai, E. *J. Org. Chem.* **1953**, *18*, 534-551.

(8) Smith, K.; James, M. D.; Bye, M. R.; Faulkner, J. D. *Tetrahedron.* **1992**, *48*, 7479-7488.

(9) Chmielewski, M. J.; Charon, M.; Jurczak, J. *Org. Lett.* **2004**, *6*, 3501-3504.

(10) Rosa, M. D.; Quesada, P. A.; Dodsworth, D. J. *J. Org. Chem.* **1987**, *52*, 173-175.

(11) Neugebauer, F. A.; Fischer, H. *Chem. Ber.* **1971**, *104*, 886-889.

(12) Neugebauer, F. A.; Fischer, P. H. H. *Chem. Ber.* **1965**, *98*, 844-850.

(13) Abakumov, G. A.; Razuvaev, G. A. *Seriya Khimicheskaya* **1966**, *10*, 1744-1747.

(14) Cauquis, G.; Delhomme, H.; Serve, D. *Tetrahedron Lett.* **1971**, 4649-4652.

(15) Cauquis, G.; Delhomme, H.; Serve, D. *Electrochim. Acta* **1975**, *20*, 1019-1026.

(16) Cheng, J.-D.; Shine, H. J. *J. Org. Chem.* **1974**, *39*, 2835-2790.

(17) Cheng, J.-D.; Shine, H. J. *J. Org. Chem.* **1975**, *40*, 703-710.